Marine Biodiversity Hub

National Environmental Science Programme

Initial baseline survey of deepwater fish in the Ningaloo Marine Park (Commonwealth waters)

Editors:
John Keesing, Anthea Donovan, Simon Collings, Tim Langlois, Emma Lawrence, Russ Babcock

Contributors (in alphabetical order):
Charlotte Aston[1], Russ Babcock[2], Neville Barrett[3], Norm Campbell, Simon Collings[2], Craig Davey[2], Anthea Donovan[2], Karl Forcey[2], Scott Foster[2], Brooke Gibbons[1], John Keesing[2], Tim Langlois[1], Emma Lawrence[2], Margaret Miller[2], Jacquomo Monk[3], Nick Mortimer[2], Melanie Orr[2], Dirk Slawinski[2] and Mark Tonks[2]

D3 - Implementing monitoring of AMPs and the status of marine biodiversity assets on the continental shelf

Milestone 18, October 2021

[1]University of Western Australia;
[2]CSIRO;
[3]University of Tasmania

CSIRO

THE UNIVERSITY OF WESTERN AUSTRALIA

UNIVERSITY of TASMANIA | IMAS INSTITUTE FOR MARINE & ANTARCTIC STUDIES

Enquiries should be addressed to:

John Keesing
+61 8 9333 6500
john.keesing@csiro.au

Preferred Citation

Keesing J, Donovan A, Collings S, Langlois T, Lawrence E, and Babcock R (Eds) (2021) Initial baseline survey of deepwater fish in the Ningaloo Marine Park (Commonwealth waters). Report to the National Environmental Science Program, Marine Biodiversity Hub. CSIRO.

Copyright

Acknowledgement

This work was undertaken for the Marine Biodiversity Hub (Parks Australia permit number PA2019-00061-1), a collaborative partnership supported through funding from the Australian Government's National Environmental Science Program (NESP). NESP Marine Biodiversity Hub partners include the University of Tasmania; CSIRO, Geoscience Australia, Australian Institute of Marine Science, Museums Victoria, Charles Darwin University, the University of Western Australia, Integrated Marine Observing System, NSW Office of Environment and Heritage, NSW Department of Primary Industries.

Important Disclaimer

Contents

List of Figures

List of Tables

EXECUTIVE SUMMARY

This report sets out the findings of the Ningaloo Marine Park survey which was undertaken for the Marine Biodiversity Hub project '*Implementing monitoring of AMPs and the status of marine biodiversity assets on the continental shelf'.*

Background: The Ningaloo Marine Park (Commonwealth waters) (NMP) lies offshore and adjacent to the Ningaloo Marine Park (State waters) extending ~300 km along the west coast and the depth ranges from 50 to 500 m. The majority of the NMP is zoned IUCN Category IV – Recreational Use Zone and no commercial fishing is permitted. In July 2018 a new National Park Zone (NPZ) (IUCN Category II) was put place in the Point Cloates area. The NMP is one of the few Australian Marine Parks readily accessible to large numbers of recreational fishers in small vessels. In comparison with the shallow areas of Ningaloo there have been few studies on the fish of the deeper areas of the NMP including the NPZ at Point Cloates.

Project Aims: This project was established to determine the composition and abundance of fish, especially those targeted by recreational fishers, in deeper sections of the NMP. The results of the survey are intended to guide future monitoring work in the NMP.

Methods: Fish species composition, abundance and size composition were studied in 2019 using baited remote underwater stereo-videos (stereo-BRUVs). To design a rigorous sampling plan for the fish video work it was necessary to characterise and, in some cases, map parts of the NMP to determine depth and habitat features which may affect fish distribution. This work was carried out using acoustic "depth sounding" surveys of depth. The acoustic data (called sound backscatter) can also be used to infer habitat type, especially relative hardness and softness, over large areas. Smaller areas of the NMP were then surveyed with tow video to "ground truth" the habitat types inferred from the acoustic data. To contrast the fish assemblages inside the NPZ at Point Cloates with comparable sites outside the NPZ, it was sometimes necessary to sample within adjacent Ningaloo Marine Park in State waters to maintain the same depths contours.

Key findings: The habitat mapping provided new data on habitat type and distribution in the southern part of the NMP and in the new NPZ. Although much of the area has a soft sediment habitat there were large areas of sponge and soft coral gardens present. A range of deep reef features were also found.

The study recorded a total of 169 different fish species. The ten most abundant of these were Mackerel scad, Goldband Snapper, Robinson's sea bream, Red throat emperor, Long nose trevally, Frypan bream, Bludger trevally, Red eared emperor, Goldband fusilier and Yellow spotted rock cod. The fish video data enabled statistical modelling of the distribution, abundance and size composition of just one species, as only the Goldband snapper was abundant enough to be analysed on its own. The results revealed that abundance of Goldband snapper increases as water depth increases. Although this feature of Goldband snapper was already known, this study has provided a good baseline of abundance, including estimated uncertainty, to be able to monitor them into the future. The study did not reveal any major trends in size composition but did find that the Goldband Snapper was more abundant in 2019 than in surveys undertaken in the northern part of the NMP ten years before.

The results for other species of recreationally targeted fish were analysed by treating them as one group. These showed similar results with targeted fish greater than legal size being more abundant with increasing depth. But in addition, revealed their abundance also increased significantly with increasing distance from boat ramps, even allowing for the fact that water depth increases with distance from shore. The relatively remote location of the NPZ off Point Cloates, also likely explains why there are generally more fish within the NPZ than more easily accessible areas of the NMP.

Recommendations: This report recommends follow-up surveys at least every 3 years, using similar methods, but with some slight changes to sampling distribution and intensity. This would allow trends in the size and abundance of fish, especially those targeted by recreational fishers, to be identified. It is also recommended that the comparisons between fished and unfished areas are continued, given that this study has provided a baseline near to the time of the establishment of the NPZ area off Point Cloates.

1. SUMMARY OF KEY FINDINGS

1.1 Background

The Ningaloo Marine Park (Commonwealth waters; hereon referred to as NMP) lies offshore and adjacent to the Ningaloo Marine Park (state waters) (Figure 1). The NMP extends for ~300 km along the west coast and the depth ranges from 50 to 500 m. The NMP was originally proclaimed under the *National Parks and Wildlife Conservation Act 1975* in 1987 as the Ningaloo Marine Park (Commonwealth waters) and proclaimed under the *Environment Protection and Biodiversity Conservation Act 1999* (EPBC Act) on 14 December 2013 and renamed Ningaloo Marine Park in 2017.Since 2018 the NMP has been managed as part of the North-west Marine Parks Network (North-west Network Management Plan 2018).

The majority of the NMP is zoned IUCN Category IV – Recreational Use Zone and no commercial fishing is permitted. The NMP is one of the few Australian Marine Parks readily accessible to large numbers of recreational fishers (the distance from the recently enlarged Tantabiddi boat ramp to the NMP is as little as 10 km). However, in 2018, a new National Park Zone (IUCN Category II) was put in place in the Point Cloates area (Figure 1).

Little is known of the composition and abundance of demersal fish, together with the habitats they utilise in the NMP. This project aimed to determine the baseline composition and abundances of fish in the NMP. Once established, this baseline will guide future management in the marine park. This is important as an increasing number of recreational fishers are choosing to move offshore from the Ningaloo Marine Park (state waters) (Figure 2) into the deeper waters of the NMP.

1.2 Research activities undertaken

Two dedicated voyages were undertaken as part of this project. The first in March 2019 to collect acoustic bathymetry and backscatter data and towed video imagery of deep-water habitats within the new National Park Zone of the NMP, and the second in August 2019 to deploy Baited Remote Underwater Video cameras (BRUVs) to determine the composition and abundance of demersal fish in the NMP. A third field activity was the piggy-back project undertaken aboard the RV Investigator (IN2017_05) in November 2017 to swath map a transect along the 125 m depth contour of the NMP in the vicinity of what is thought to be the ancient shoreline key ecological feature.

A dedicated component of sampling design was undertaken to ensure a rigorous approach to the selection of the BRUV sites. Given the importance of deep-water habitat topographical features to the distribution of demersal fish, this design phase of the project made use of the integrated bathymetry product prepared specifically for this project to generate the Terrain Position Index (TPI) for the NMP. The sampling design, and the deployment of BRUV equipment, followed the principles outlined in the Marine Biodiversity Hub's field manuals.

The BRUVs voyage was followed up by an extensive analysis of the BRUVs imagery to extract both habitat and fish parameters which were used in the subsequent statistical

analysis of the spatial and temporal patterns in demersal fish in the NMP and the environmental factors driving those patterns.

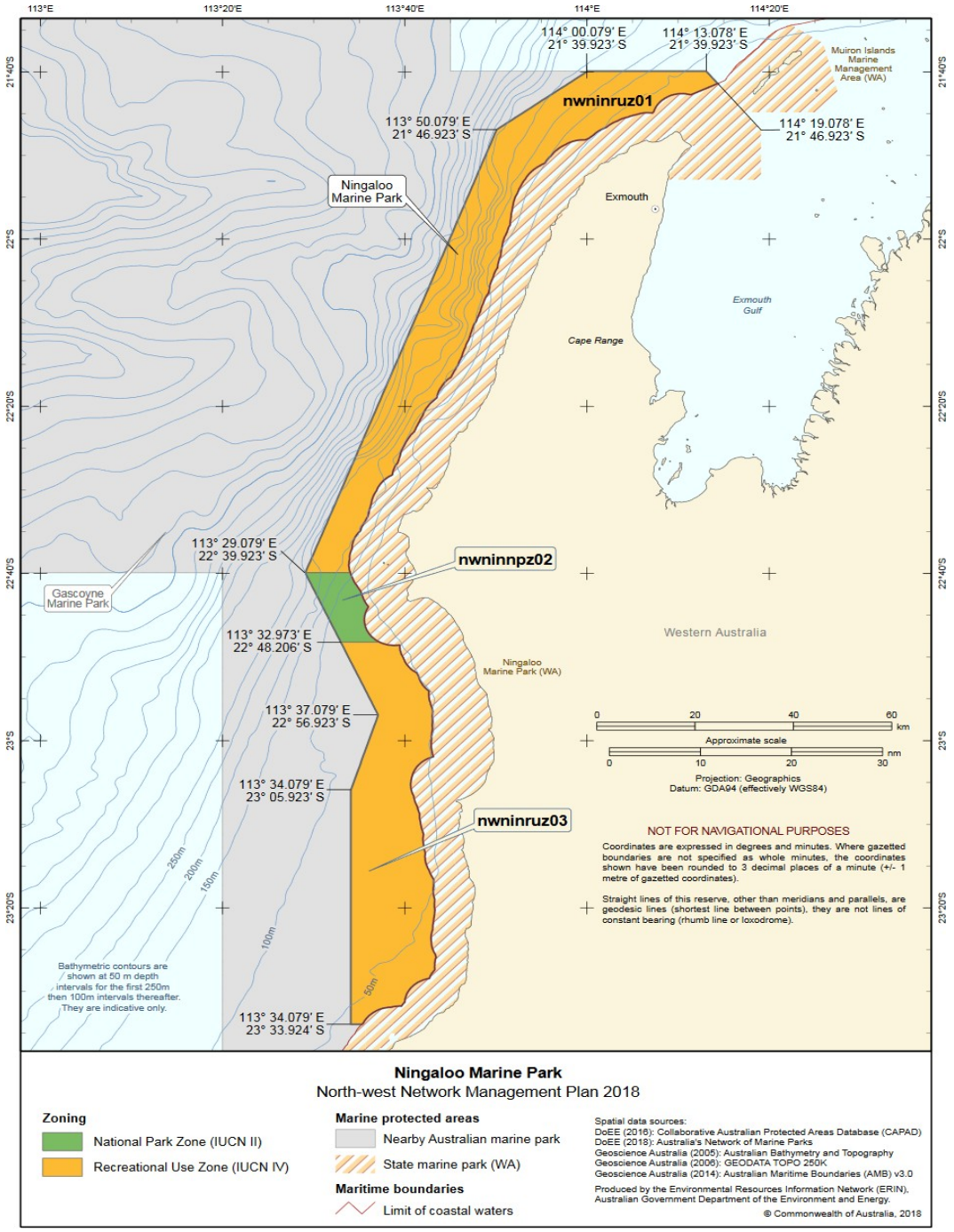

Figure 1 Location and zoning of the Ningaloo Marine Park (Commonwealth waters) in relation to the Western Australian Ningaloo Marine Park (State waters) and the regional bathymetry. (Image is from the North-west Marine Parks Network Management Plan 2018 (Director of National Parks 2018).)

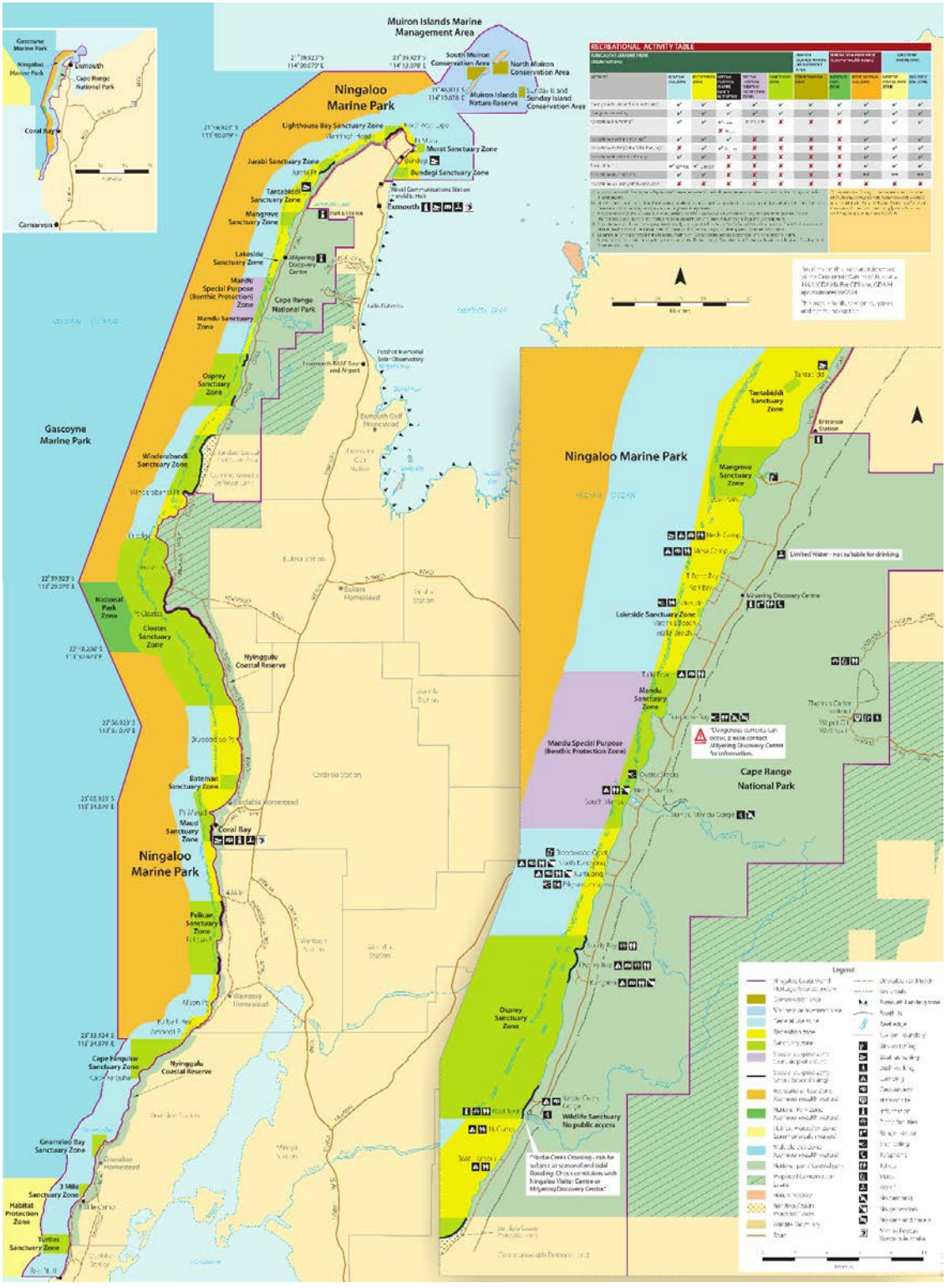

Figure 2 Map of the State and Commonwealth Ningaloo Marine Parks showing adjacent zoning. Source: Ningaloo Coast World Heritage Area map and sanctuary zones 2020. https://parks.dpaw.wa.gov.au/park/ningaloo

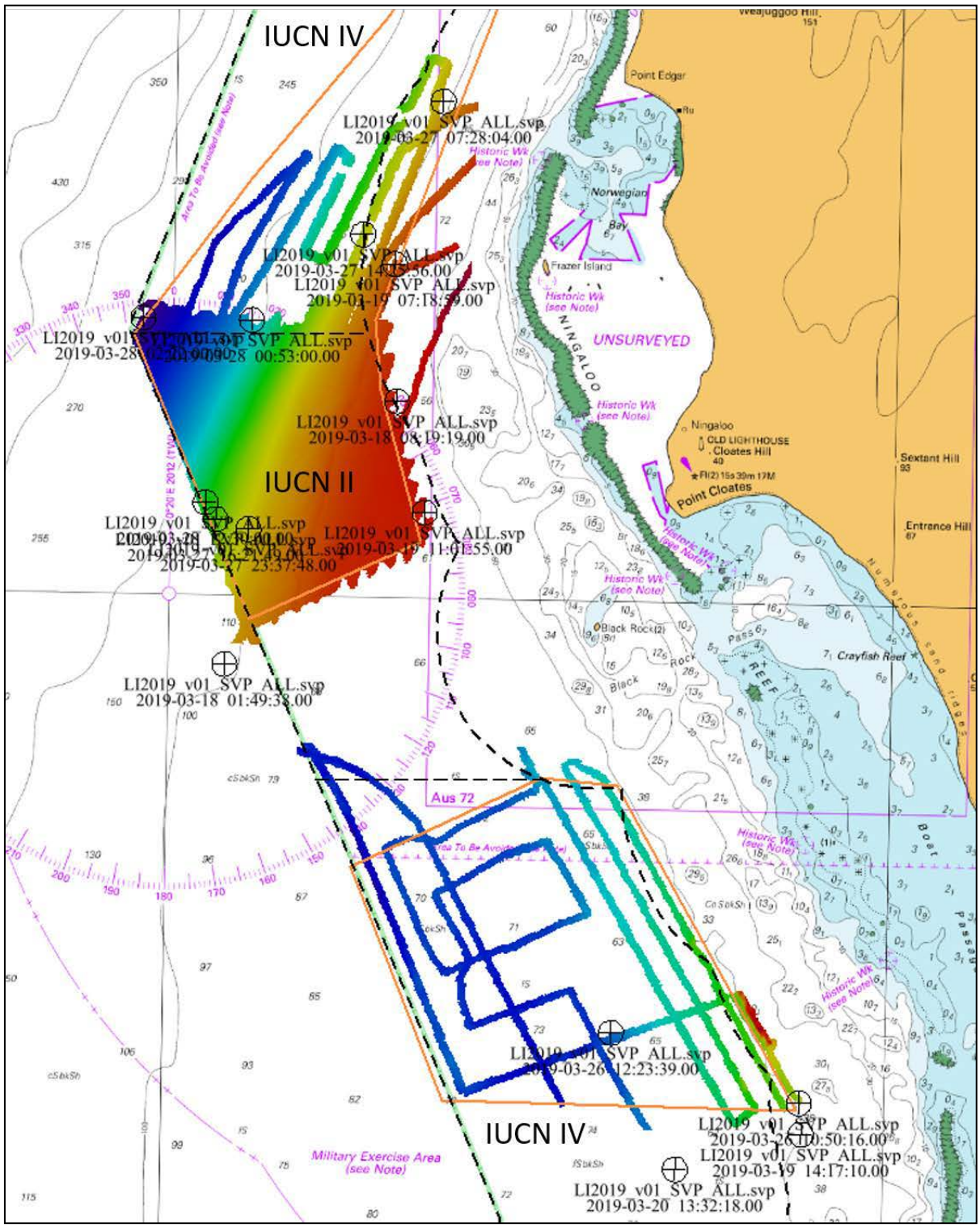

Figure 3 Location off Point Cloates of the areas surveyed for bathymetry and acoustic multibeam backscatter mapped in March 2019 (see Figure 4 and Figure 5). The NMP boundary and zonings are indicated on the map by the black dashed line.

The data from the dedicated bathymetry, acoustic backscatter voyage was developed into habitat maps and tow video imagery collected on the same voyage was analysed to describe the benthic habitats and to ground truth and assist in interpretation of the acoustic backscatter data.

In addition to the dedicated data acquisition undertaken for this project, use was also made of complementary existing datasets. These included comparable historical demersal fish data collected by BRUVs in 2006 and 2009 and the extensive set of acoustic bathymetry data previously acquired for the NMP.

1.3 Detailed summary and key findings

1.3.1 Bathymetric and tow video surveys

The voyage to map the bathymetry and acoustic backscatter of two areas west (Area 3a) and south (Area 5) of Point Cloates was undertaken in March 2019. A total of 466 km was swathed in the two areas, and video imagery of the seabed was also collected at 16 sites in these areas (Figure 3). The northern Area 3a varied in depth between 68 and 272 m (Figure 4). The seafloor slopes away from the coastline at an average gradient of less than 2% but varies across the area. Linear seafloor features are evident at two discrete depths. Around the 80–90 m contour there are seabed features that align parallel to the contour indicating a possible paleo shoreline. The features are up to 2 m above the neighbouring seafloor. Along the 185 m contour there are bedforms with general alignment perpendicular to the contour and are up to 4 m in height. The bathymetry of the southern Area 5 mapped varied in depth from 54 to 78 m (Figure 5). The seafloor slopes away from the coast at a gradient of less than 0.5%. Subtle bedforms are evident over the whole site and measure approximately 0.5 m in height. A larger feature lies just outside the park, in the south-eastern edge of the mapped area, possibly indicating a reef system. In the northern Area 3a, the four inshore tow video stations were dominated by sparse to medium density sponge gardens with gorgonians and whips also evident in two of those stations (Figure 6). The deeper stations were mostly bioturbated soft sediment habitats (burrowing animals) with areas of harder bottom featuring sponge, whip, and gorgonian habitats. In the southern Area 5, except for the shallowest station, the area was dominated by soft bottom seabed habitats, much of it bioturbated (Figure 6).

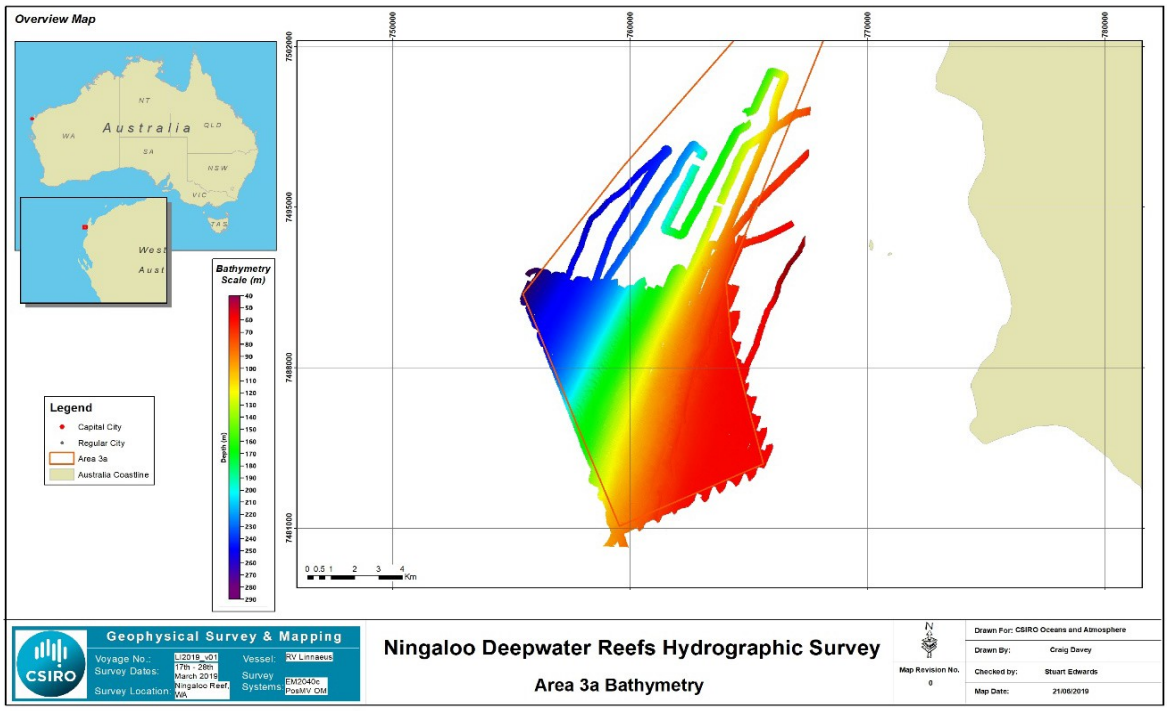

Figure 4 Bathymetry of Area 3a mapped off Point Cloates.

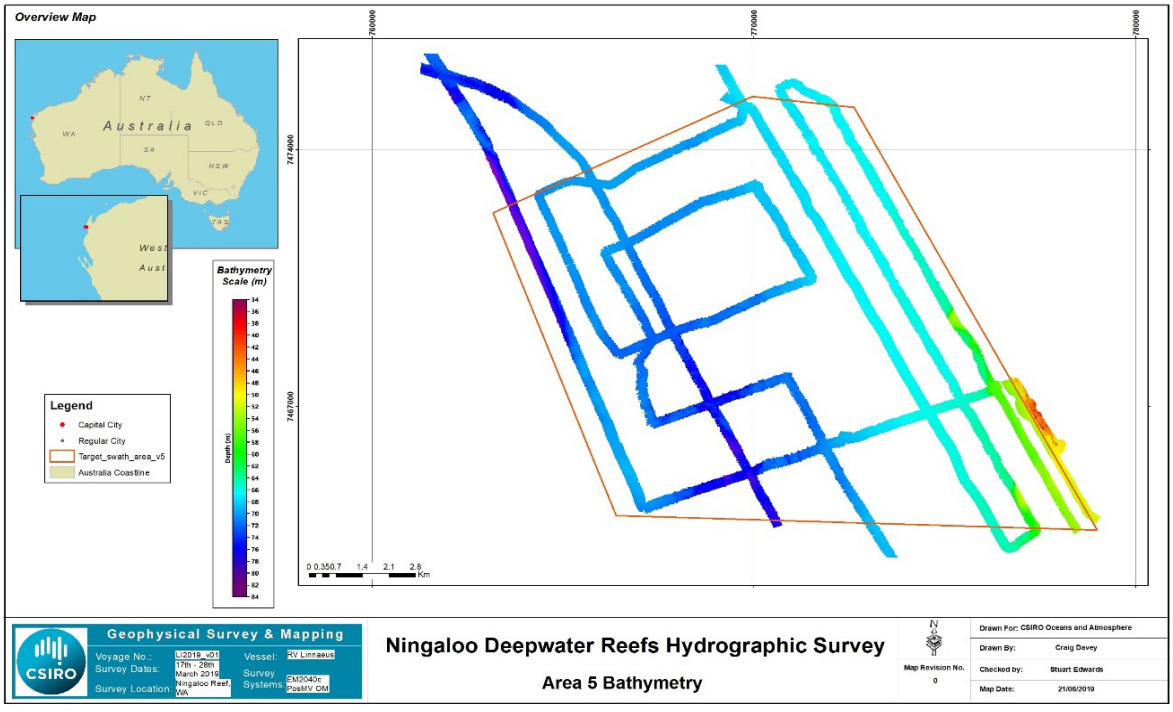

Figure 5 Bathymetry of Area 5 mapped to the south of Point Cloates.

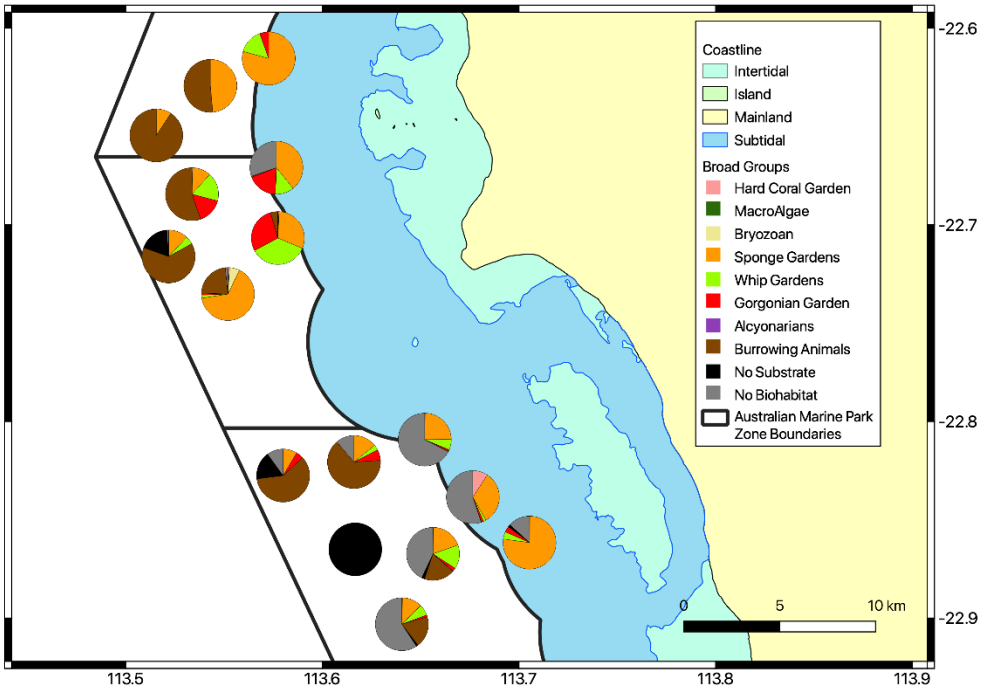

Figure 6 Benthic habitat types recorded by tow video at sites within the two survey areas. Sites in the northern cluster ranged in average depth from 74–212 m. Sites in the southern cluster range in average depth from 56–73 m. Note that the No Substrate category indicates areas over which seabed was not visible to the camera (not deep enough or orientated upwards). No Biohabitat category indicates soft seabed habitats with little or no obvious biota.

1.3.2 Deepwater benthic habitats and backscatter mapping products

Data from multibeam echosounder surveys were classified into various seafloor cover types according to their hardness, rugosity and depth. The classifications are validated with towed video ground truth where it is available. Three Areas of Interest (AOI) were classified (Figure 7), two that were explicitly part of the NESP project survey described above (Figure 8 and Figure 9) and a third transect that was acquired as a piggy back project while RV Investigator was transiting between locations in November 2017 (Figure 10). Due to the nature of the acquired data, two different approaches were taken for the classification of the multibeam backscatter (MBBS) data, the first approach used multibeam backscatter angular response curves along with rugosity as input to a maximum likelihood classifier (Hastie et al. 2001). The second approach used flattened multibeam backscatter (i.e. with the angular effects removed), along with rugosity as inputs to a Random Forest Classifier (Breiman 2001). Estimates of the accuracy of the classifiers are produced, where possible, along with area statistics for the different substratum observed in the classified maps. Given the variable quality of the data (and lack of video ground truthing in the case of the RV Investigator data), a pragmatic approach was taken to classify the seafloor into reasonable maps with a fair degree of confidence in the cover types.

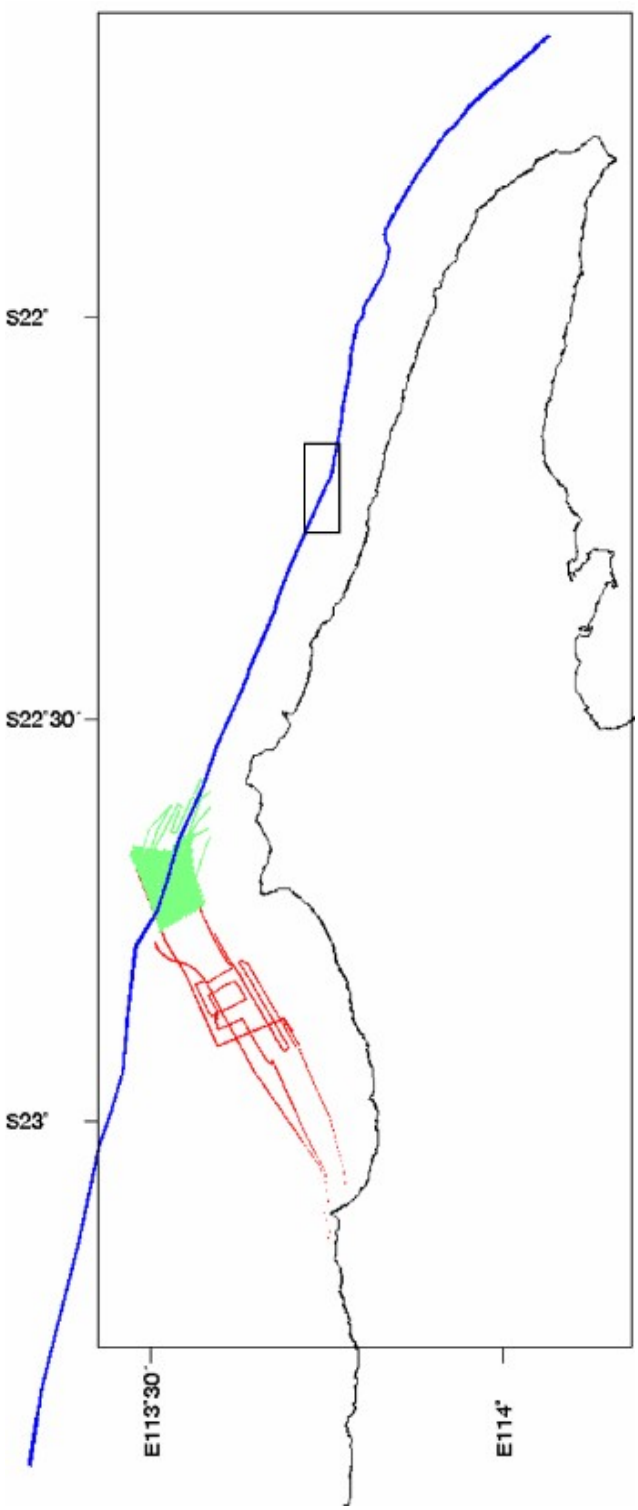

Figure 7 Locality map showing the three sets of multibeam backscatter data collected and analysed in this study. The rectangle section of the swath over the 120 m depth contour (in blue) shows the location of the detailed extract of the map given in Figure 10.

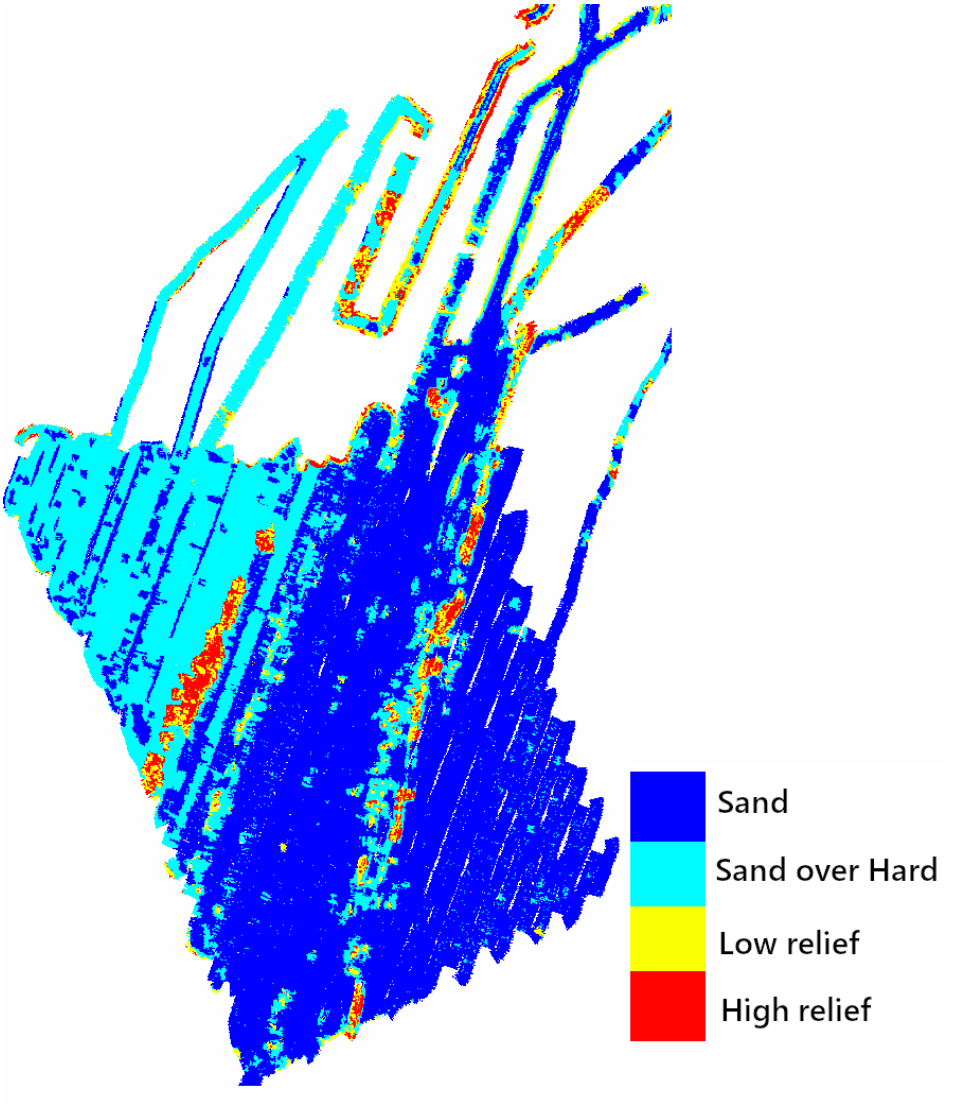

Figure 8 Four class habitat map of Area 3a, west of Point Cloates. There are some artefacts at the edge of the swaths which are explained in the text. See Figure 7 for locality map.

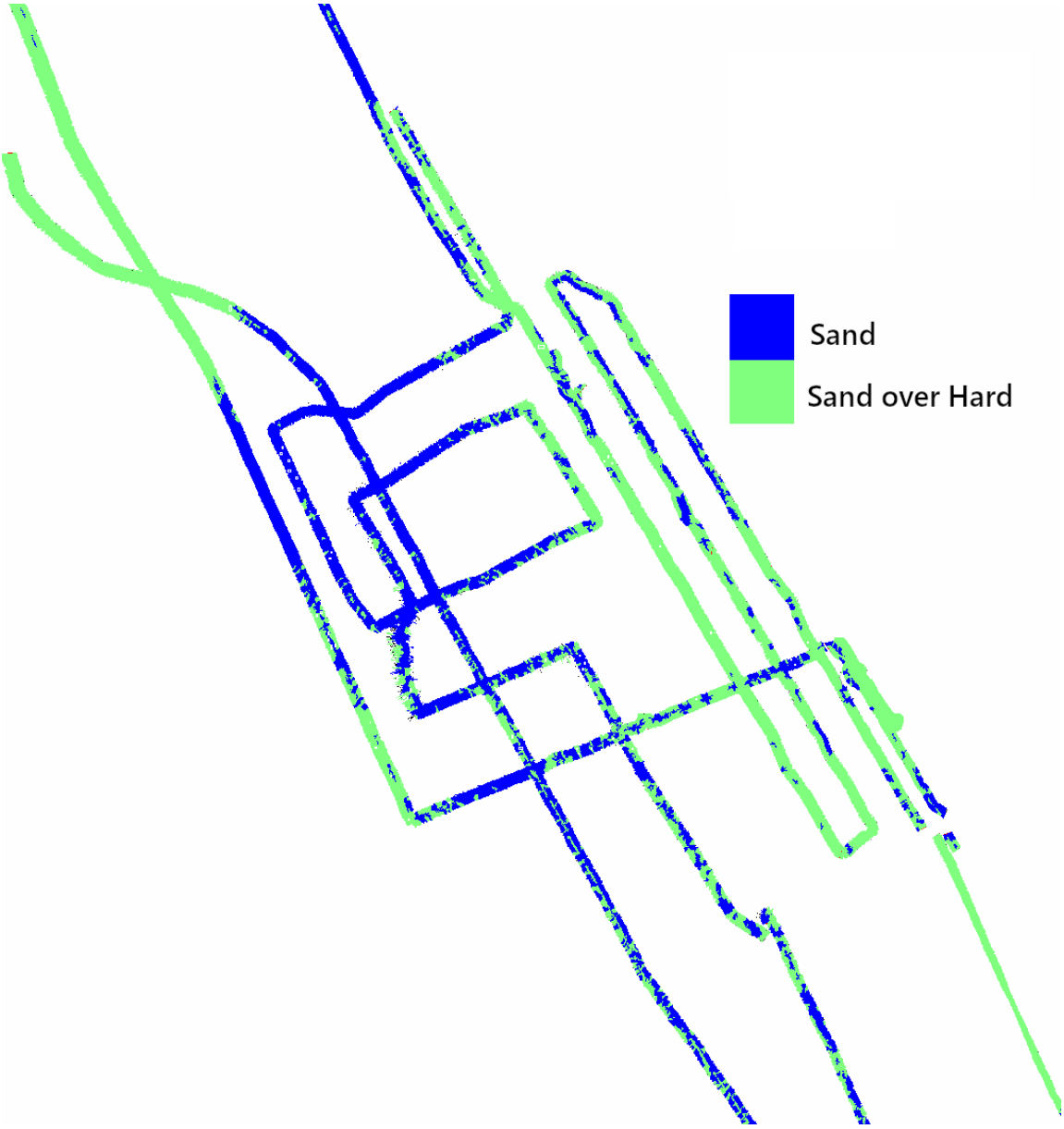

Figure 9 Two class habitat map of Area 5 south of Point Cloates. See Figure 7 for locality map.

For Area 3a, west of Point Cloates, the MBBS were not of sufficient quality to allow classification using angular response curves, so instead the flattened MBBS data were used. There was a lack of clarity in the MBBS, where normally distinct segments would be apparent in the harder areas of the seafloor. Regardless of this, it was evident that there is a harder region in the west of this area, and this is visible in the backscatter (Figure 8). There are artefacts in the classification, in particular in the “Sand over Hard” region in the west, consisting of between-swath lines of only “Sand” class and blocks of sand class running along the tracks. These are unlikely to be real; instead they represent regions where the observed backscatter is not representative of its class due to extraneous effects. The highly textured areas of the image (i.e. high rugosity) are thought to be sections of deep reef, but further investigation would be required to confirm their full extent.

The area mapped to the south of Point Cloates (Area 5) contained superior MBBS data, so the angular response curves were incorporated into the classification. This allows the shape of the curve to be used as part of our characterisation of the seafloor. There were no direct observations of rocky reef in the ground truth video for this area and no clear indications from the rugosity that such areas exist in the region. Therefore, we chose to map the area into just the two classes observed in the ground truth video (Figure 9).

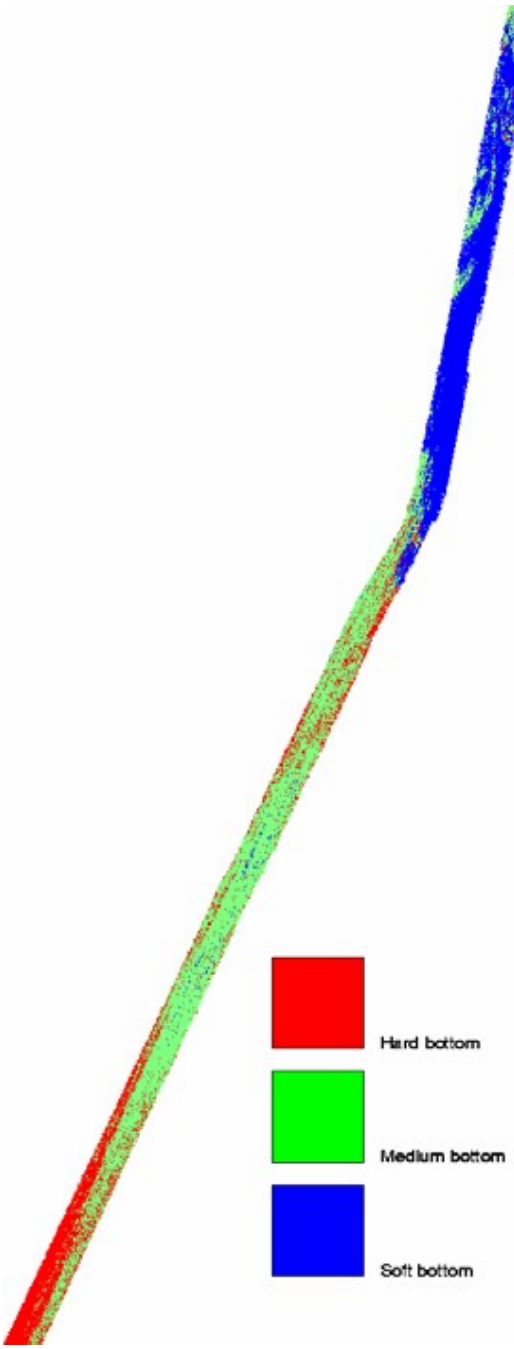

Figure 10 Three class habitat map for a small section of the total length of the 120 m depth contour swath through the Ningaloo Marine Park. See Figure 7 for locality map. Red = hard bottom; green = medium bottom; blue = soft bottom.

1.3.3 Spatial and temporal patterns in demersal fish abundance and size

The goals of the Baited Remote Underwater Video (BRUVs) survey undertaken in August 2019 were to:

1. provide baseline data to establish/quantify biodiversity content within the NMP
2. provide a baseline for the recently established IUCN II area, and for controls in nearby areas, and
3. leverage historical data to try and gain some understanding of the changes in recent history throughout the area.

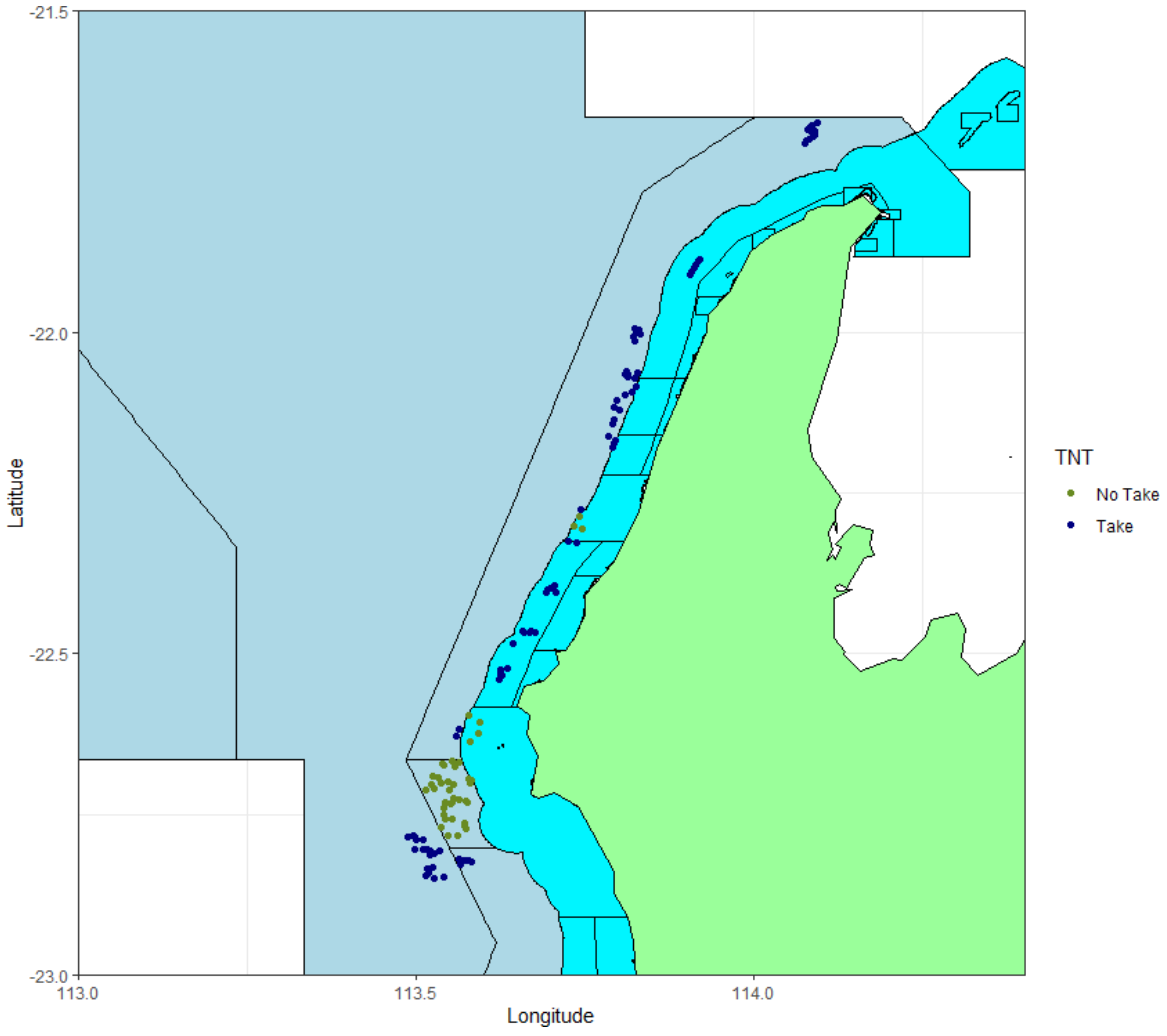

Figure 11 Map of BRUV locations sampled during the 2019 field trip. No Take (DARK GREEN): areas closed to fishing, Take (DARK BLUE): areas that may be fished. 42 BRUVs were deployed in No Take areas and 88 BRUVs were deployed in Take areas.

The sampling was spread across the northern Ningaloo MPs (state and commonwealth) and Gascoyne MP region to straddle management zone boundaries as well as variations in fishing pressure – from the new No Take zone in the south to the highly fished areas in the north (Figure 11). Emphasis was also given to previously sampled sites in order to provide the potential to detect any trends in fish abundance or biomass that have developed in the 10 years since the first surveys. A total of 130 BRUV drops were analysed, 42 of these in No Take zones.

Table 1 Top ten species by counts from 130 BRUV drops.

Species	**Common name**	**Family**
Decapterus spp	Mackerel scad	Carangidae
Pristipomoides multidens	Goldband snapper	Lutjanidae
Gymnocranius grandoculis	Robinson's sea bream	Lethrinidae
Lethrinus miniatus	Red throat emperor	Lethrinidae
Carangoides chrysophrys	Longnose trevally	Carangidae
Argyrops spinifer	Frypan bream	Sparidae
Carangoides gymnostethus	Bludger trevally	Carangidae
Lethrinus rubrioperculatus	Red eared emperor	Lethrinidae
Pterocaesio chrysozona	Goldband fusilier	Caesionidae
Epinephelus areolatus	Yellow spotted rock cod	Serranidae

A total of 169 different species were recorded across the 130 BRUV drops, of which 140 species were in Take areas and 114 in No Take areas. Table 1 provides a listing of the 10 most abundant species. Small Mackeral scads (*Decapterus* spp.) were the most abundant by far, followed by the important target species Goldband snapper *Pristipomoides multidens*, Robinson's sea bream *Gymnocranius grandoculis* and the Red throat emperor, *Lethrinus miniatus*. While the Caesionidae family were only captured on BRUV footage at a small number of sites, their counts were the highest (>30). Other families, like Lethrindae, were seen more often but in smaller numbers, with a couple of counts greater than ten.

The mean MaxN (maximum number seen on a BRUV drop) was calculated for each species by Take/No Take area. A comprehensive analysis and statistical modelling exercise was undertaken for the most abundant target species, Goldband snapper (*P. multidens*) and an analysis of the total count of all of the other targeted fished species combined (i.e. excluding *P. multidens*). These species were *Loxodon macrorhinus, Lethrinus minatus, Carcharhinus albimarginatus, Lethrinus nebulosus, Gymnocranius grandoculsis, Lethrinus olivaceus, Lethrinus punctulatus, Pristipomoides filatmentosus, Lutjanus sebae, Symphorus nematophorus, Aprion virescens, Genicanthus Lamarck, Scomberomorus commerson, Epinephelus rivulatus, Epinephelus multinotatus, Variola louti,* and *Chysophyrs auratus*.

Pristipomoides multidens were recorded on more than half of the BRUV drops. While many drops recorded one individual, several recorded 10 or more (Figure 12).

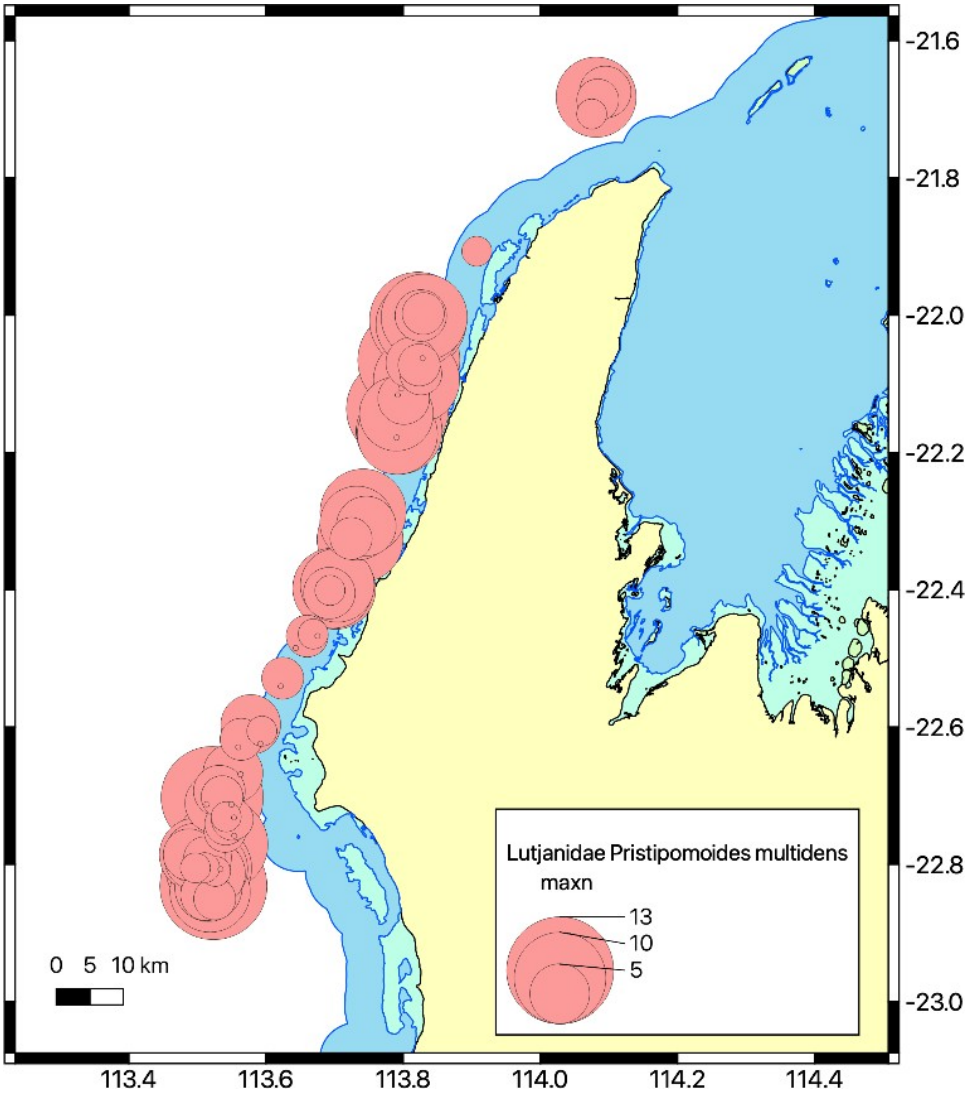

Figure 12 Map of study area displaying the MaxN value at all sites that *Pristipomoides multidens* (Goldband snapper) were observed.

Analysis included all variables that were used for the design in the analysis, regardless of whether they are significant in the statistical model. For the Ningaloo 2019 design, those variables were TPI (rugosity) and site type (whether the site was a legacy site—included in previous years' surveys) and also included whether the sites sampled were as dictated by the premeditated design or additional opportunistic sites at which drops were made.

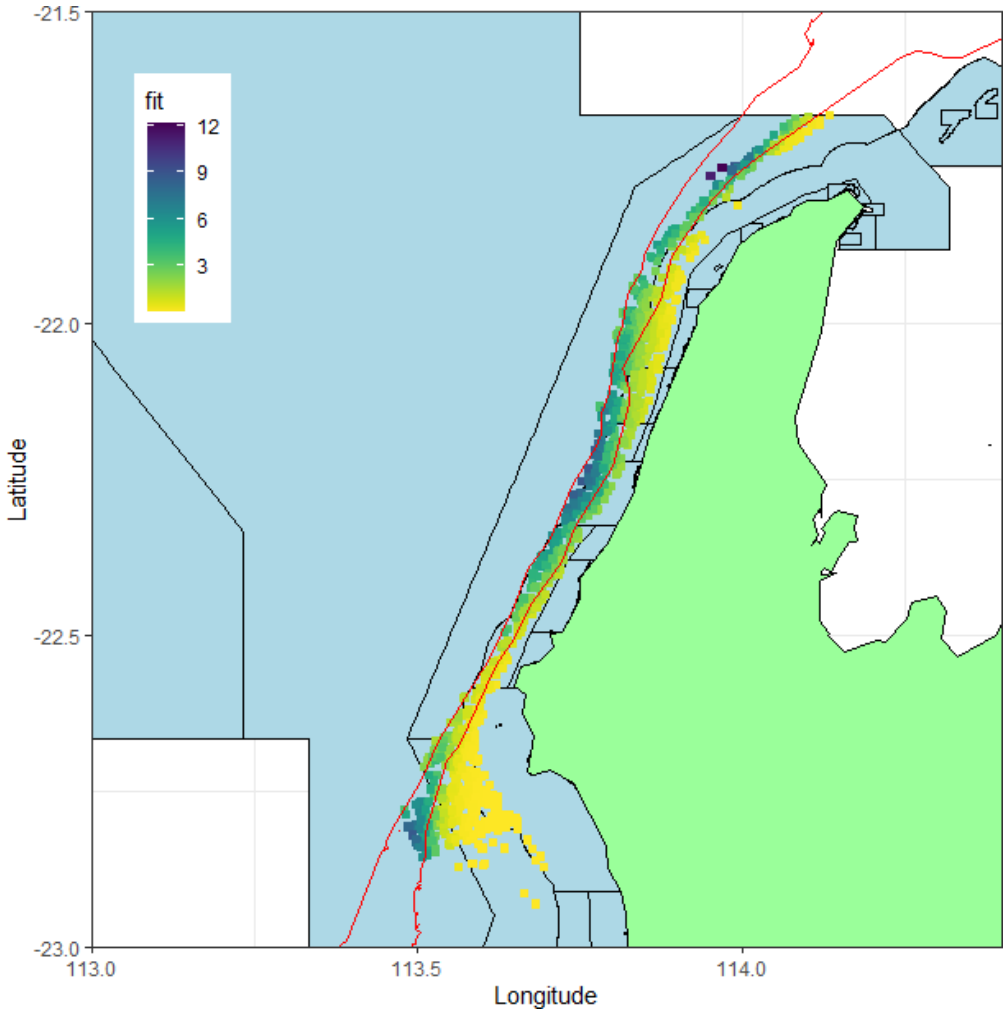

Figure 13 Predicted values of *Pristipomoides multidens* based on the model selected. Darker colours indicate increasing predictions. Red lines indicate the 100 m and 200 m contour lines.

The statistical model for *P. multidens* included terms for site type, TPI, bathymetry, distance to boat ramp and spatial location as a random factor. The latter measures the relationship between sites that are close to each other as these are expected to be more similar, but in this study it also reveals important long-shore gradients. Spatial location was significant (p=0.0006), indicating a high degree of site to site variability. The only other significant predictor of *P. multidens* abundance was depth (p=0.0332). The abundance of *P. multidens* is known to be greater in deeper water (Figure 13), however the predicted abundance also increases as distance from boat ramp increases. This was not significant (p=0.0637) but given the very low p- value and the management importance of this parameter (and as it was found to be significant when the historical data was considered- see below), it should be noted and re-evaluated periodically. TPI (rugosity) was not significant (p=0.9913). Targeted species were observed on most BRUV drops with one drop recording more than 30 targeted fish. Examples for the spatial distributions of counts for other common species including some targeted taxa are shown in Figure 14.

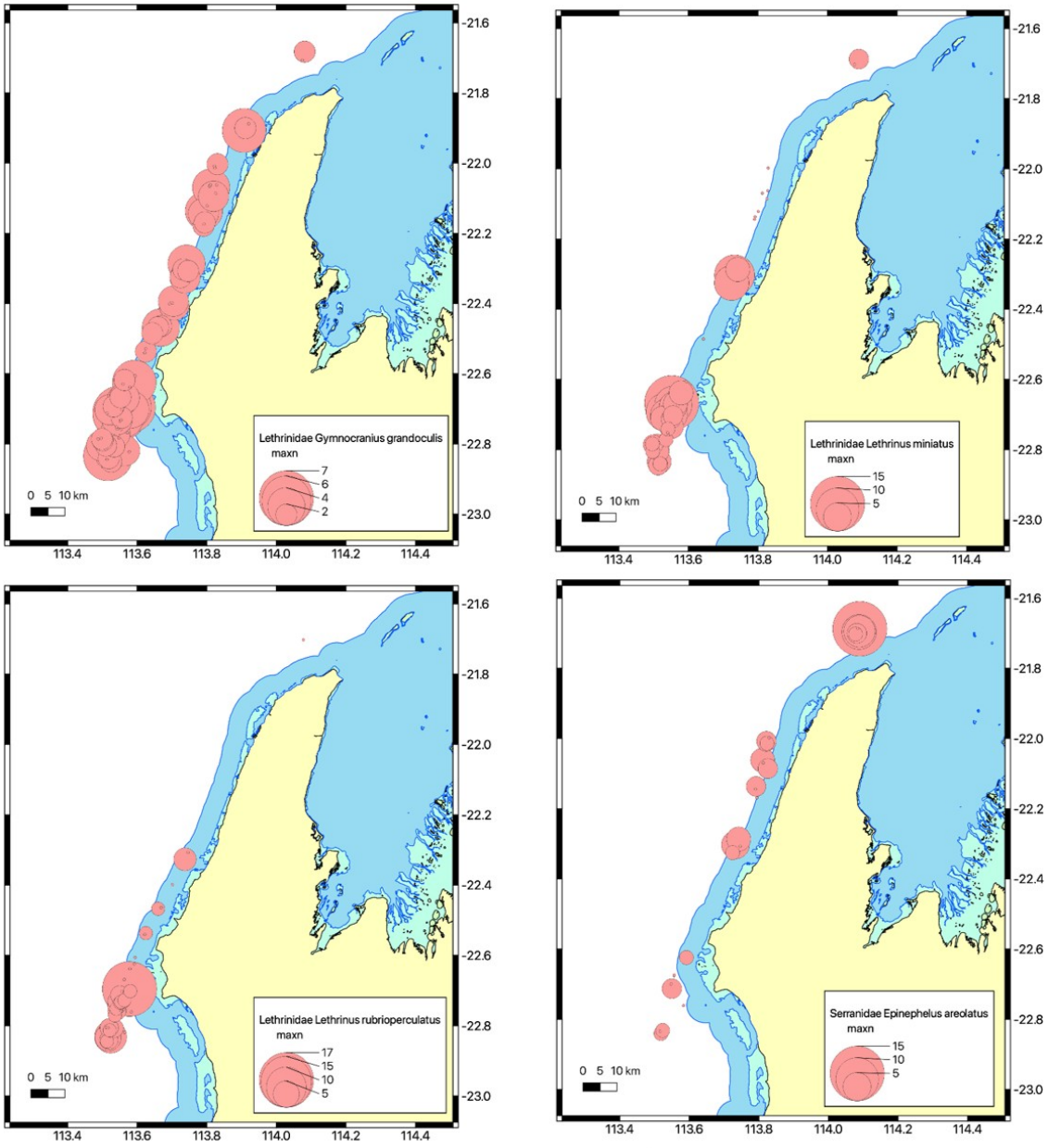

Figure 14 Map of study area displaying the MaxN value at all sites for four of the more common species observed: *Gymnocranius grandoculsis* (Robinson's sea bream), *Lethrinus minatus* (Red throat emperor), *Lethrinus rubrioperculatus* (Red eared emperor) and *Epinephalus areolatus* (Yellow spotted rock cod).

Statistical modelling for other targeted species similar to that described above for *P. multidens*, showed that spatial location (p=0.0047) was significant, this time indicating a significant long-shore gradient, and that both bathymetry (more fish in shallower water, p<0.0001) and distance from boat ramp (more fish further from boat ramps, p=0.0012) were both significant predicters of targeted fish abundance (Figure 15). Again, TPI (rugosity) was not significant (p=0.7610).

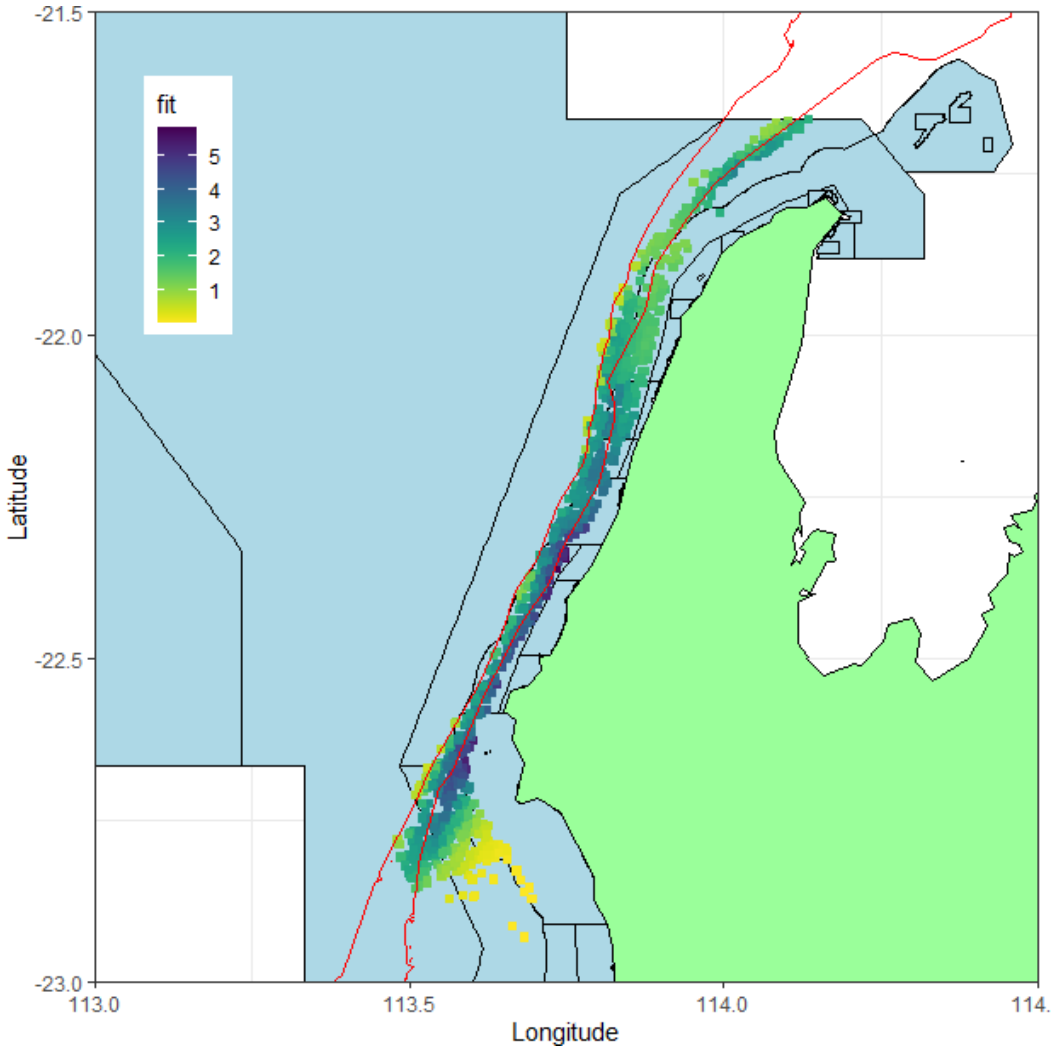

Figure 15 Predicted values of MaxN of target species based on the model selected. Darker colours indicate increasing predictions. Red lines indicate the 100 m and 200 m contour lines.

The influence of Take and No Take zones was also examined. The size distribution of targeted fish was very similar between the two although there was some evidence of greater numbers of fish >600 mm in the No Take areas (Figure 16). There was also no difference in abundance of target fish species between Take and No Take zones (p=0.5615). An analysis of the impact of Take and No Take zones for *P. multidens* showed a significant difference with more fish in No Take zones (p=0.0016). It needs to be noted that National Park Zoning off Point Cloates in the NMP only came into effect in July 2018. Analysis of the historical data from 2006 and 2009 when compared with 2019 revealed that *P. multidens* was more abundant in 2019 than in 2006 and 2009. Of particular note was that when the 2006 and 2009 data was included in the analyses, the effect of distance from boat ramp was highly significant (p=0.0002).

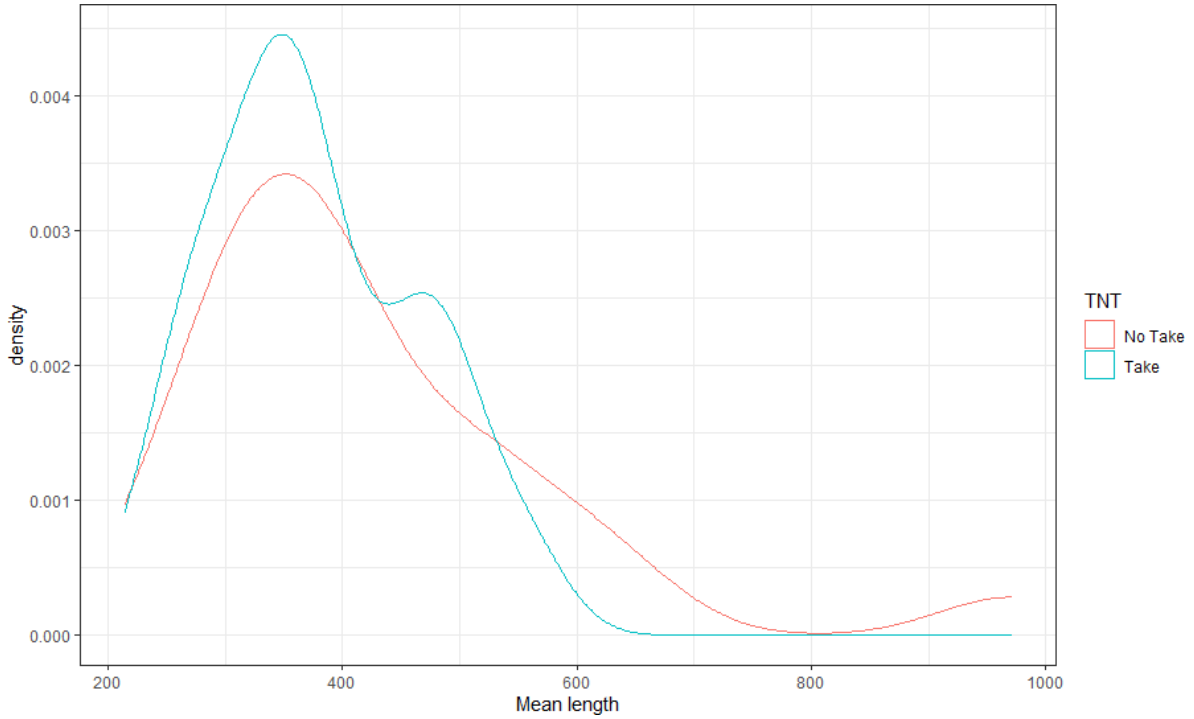

Figure 16 Plot of mean length of target fish species per BRUV drop in Take (BLUE) vs No Take (RED) zones.

1.3.4 Implications for marine park management and recommendations

The project provides an important baseline for targeted fish abundance in the NMP. In addition, it has added to the spatial coverage of habitat maps for the NMP. The project has reinforced the importance of No Take zones to the suite of conservation measures in place in the Ningaloo MP. While this report focused attention in the NMP, the findings regarding the importance of No Take zones and the increased abundance of targeted fish with increasing distance from boat ramps will also be relevant to species that co-occur in the adjacent Ningaloo MP (state waters). The project has also shown that the abundance of at least one species, *P. multidens*, can change significantly between periods of assessment highlighting the need for frequent repeat surveys, probably at least every 3 years. This survey revealed that despite the sampling effort undertaken (130 BRUV drops), for most species there was insufficient data for individual species assessments (except for the Goldband snapper, *P. multidens*). This points to the need for greater sampling effort in future surveys. Lastly, the project reinforced the importance of a robust, premeditated statistical design to avoid biases in sampling.

1.4 Project outputs, communication products, data archives and resources

The various outputs for this project are as follows:

- Post survey report describing data acquired on the survey and preliminary interpretations:
  - A report on the development of the BRUVs sampling design is given in Chapter 2.
  - A report on the BRUVs sampling voyage from August 2019 is given in Chapter 3.
  - A report on the swath mapping (bathymetry and backscatter) from March 2019 is given in Chapter 4.
  - A report on the underwater towed videography voyage from March 2019 is given in Chapter 5.
- High resolution bathymetry and acoustic backscatter data and maps for deepwater reefs within NMP:
  - These maps for the area mapped off Point Cloates in March 2019 are included in the report given in Chapter 6. This report also includes analysis of the bathymetry and backscatter data collected along the 125 m contour within the NMP in October 2017 and the work done to calculate the TPI across the NMP.
  - The acoustic backscatter data is archived on the CSIRO Data Access Portal (see https://doi.org/10.25919/kssa-5b46; https://doi.org/10.25919/8m65-7k26; https://doi.org/10.25919/kttc-x397)
  - The information (data and code) needed to reproduce the survey design aspect of the NESP Marine Biodiversity Hub Project D3's BRUV survey of Ningaloo Reef (http://hdl.handle.net/102.100.100/389900?index=1).
- Underwater images (video and still) of benthic communities and demersal fish assemblages can be viewed:
  - In the CSIRO Data Access Portal (see https://doi.org/10.25919/b9r3-x356; https://doi.org/10.25919/aa15-7296; https://doi.org/10.25919/sr5t-wh22; https://doi.org/10.25919/6ny5-7m28; https://doi.org/10.25919/kt1v-7s12)
  - In the Global Archive (see https://globalarchive.shinyapps.io/FishNClips/)
- BRUV data from 133 sites to provide initial baseline data on fish assemblages of shelf-break habitats in the eastern NMP:
  - A report on the analysis of the BRUVs imagery to determine composition and abundance of demersal fish in the NMP is given in Chapter 7. This report includes a representation of the spatial distribution and abundance of key fish species.

  - A report on the statistical analysis of the BRUVs fish data to compare spatial and temporal trends in the abundance and size composition of demersal fish in the NMP is given in Chapter 8.
  - The BRUV annotations data has also been lodged as an open-access dataset on GlobalArchive.org. (https://globalarchive.org/geodata/data/campaign/get/986)
  - A thesis based on the data collected on this voyage is in Appendix A.
- Publications in peer reviewed literature:
  - At the time of reporting, no scientific papers had been published from the report, however this report provides the content for planned papers on demersal fish composition and abundance in the NMP.
- Communication products highlighting submerged reefs and deep-water fish communities.
  - *Pictures uncover diverse marine life at Ningaloo Reef*
    - Lead: Tim Langlois MBH / Russ Babcock MBH
    - Story: Fish biodiversity surveys from Ningaloo Marine Park (Commonwealth)
    - Release: Pictures uncover diverse marine life at Ningaloo Reef
    - Youtube clips: https://www.youtube.com/watch?v=C5RVL0aklA4&feature=emb_logo
    - Youtube clips: https://www.youtube.com/watch?v=Le6ZlnaBrA4&feature=emb_logo
    - NESP MBH website: https://www.nespmarine.edu.au/news/ningaloo-survey-finds-deep-treasures-worth-protecting
  - *Fish Frenzy: marine parks for biodiversity and society*
    - Lead: Tim Langlois MBH / Peter Barnes from DBCA / Darren Phillips from PA
    - Public talk (in collaboration with DBCA and Parks Australia): at Whale Bone Pub Exmouth (~170 attendees)
    - Release: Public talk - Science of marine parks (flyer)
  - *Say cheese …. we're off to film fish communities at Ningaloo Marine Park*
    - Lead: Russ Babcock MBH / Tim Langlois MBH
    - Story: BRUV surveys from Ningaloo Marine Park (Commonwealth)
    - Parks Australia website: https://parksaustralia.gov.au/marine/news/fish-filming-at-ningaloo-marine-park/
  - *Nice one BRUV! Counting deep-water fish at Ningaloo Reef*
    - CSIRO Blog article: 13 August 2019:
    - Release: https://blog.csiro.au/nice-one-bruv-counting-deep-water-fish-at-ningaloo-reef/

2. GENERATING THE SAMPLING PLAN FOR THE NINGALOO MARINE PARK SURVEY

Authors: Scott Foster, Russ Babcock, Tim Langlois, Nick Mortimer, Jacquomo Monk, Neville Barrett

Date: 16 August 2019

2.1 Purpose of document

The intention of this document is to describe the genesis of the sample design. This is important for those that want to re-use the data in future in order to know about any potential intentional bias, so that they can adjust for it during data re-use. Also, if future surveys are conducted in the area, then this information can be useful in its design for temporal signals.

2.2 Sample area

The area under study is the northern part of the NMP (See Figure 17). From just south of the IUCN II area off Point Cloates to the northern most extent off Exmouth. This area contains a newly established IUCN II area, and due to this (see Section 2.3) the NMP area has been expanded for survey. A comparable section in state-managed waters to the north and one in the Gascoyne MP to the south have been added. Both these areas have similar depths and similar linear reef structures, and both have IUCN VI status.

Previous data in the region include high resolution bathymetry data (from multibeam acoustics), which is not available throughout the whole study area. Elevated risk of gear loss / breakages during the current survey dictates that new sampling sites will not be chosen outside of these mapped areas resulting in a reduced sampling frame. Additionally, there has been a significant amount of biological sampling in the area through BRUVs surveys. These were performed in 2006, 2009, 2013, 2014 and 2015 (with most effort in 2009). These historical deployments are not spread throughout our study region however, nor are they inter-dispersed with each other (see Figure 18).

2.3 Survey goals

The goals of the current survey were to:

1. Provide base-line data to establish/quantify fish biodiversity content within NMP
2. Provide a base-line for the recently established IUCN II area, and for controls in nearby areas
3. Leverage historical data to try and gain some understanding of the changes in recent history throughout the area.

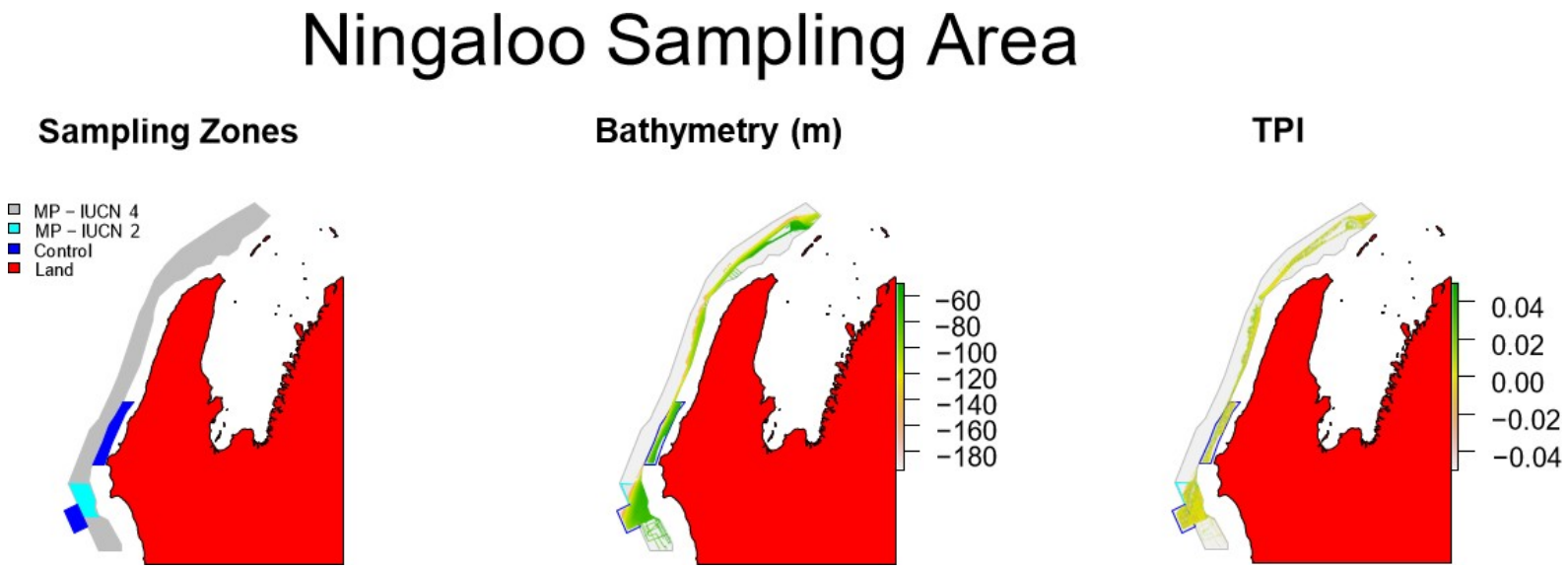

Figure 17 Ningaloo MP study area. *Left Panel:* The boundaries of the MP – IUCN IV (grey) and IUCN II (cyan) – with the control areas (IUCN VI) to north and south of the IUCN II zone (control in blue). *Middle Panel:* Study area with available bathymetry overlayed. *Right Panel:* Study Area with available TPI (Weiss, 2001) overlayed. The full extent of available (and robust) high-resolution bathymetry in any of the areas is presented, subject to depth constraints (50 m – 190 m depth).

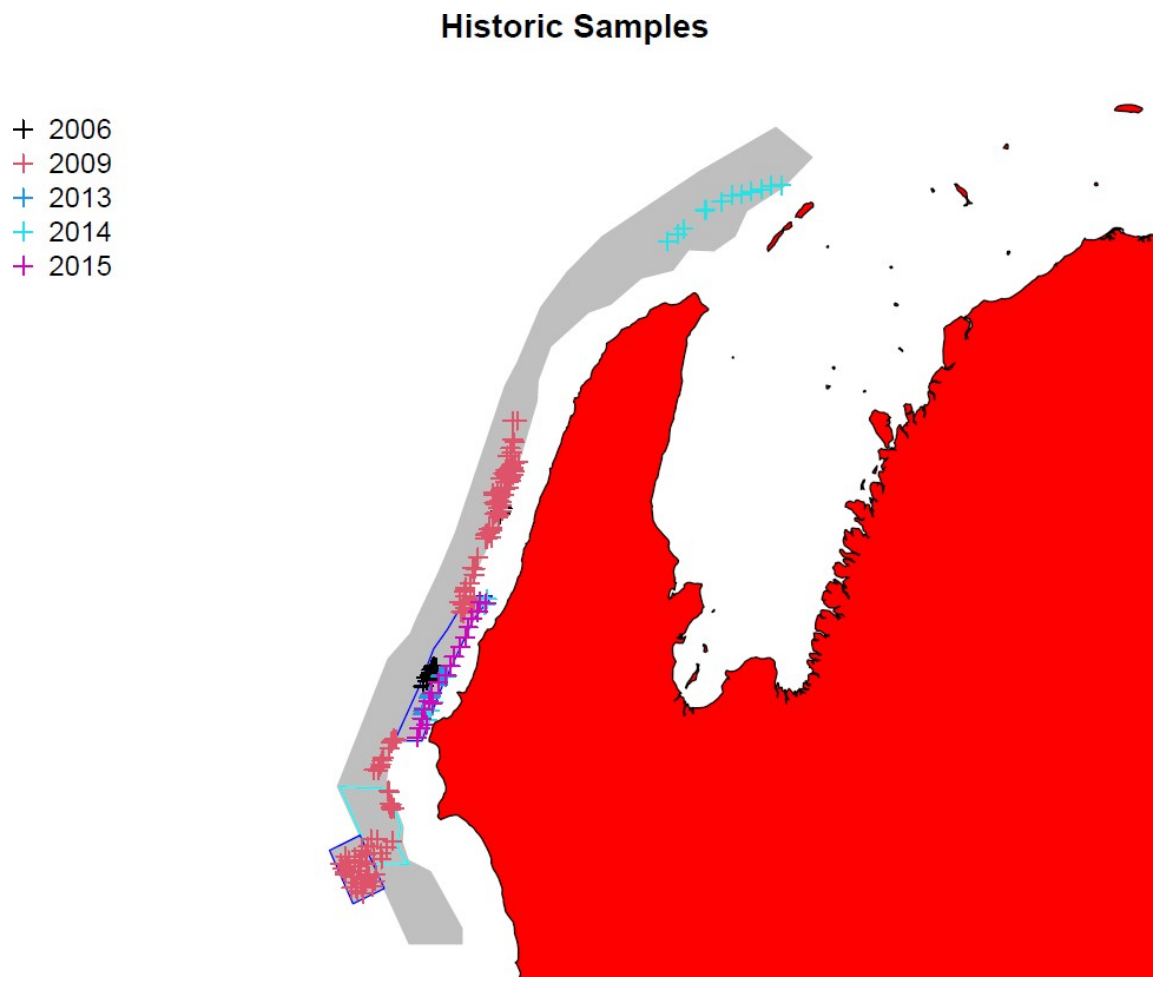

Figure 18 Historic BRUV Deployments within study area. Locations of previous BRUV drops. Colours represent the year (survey) that drop was taken. There are 18 drops in 2006, 132 in 2009, 17 in 2013, 17 in 2014, and 19 in 2015.

2.4 Outline of process

The strategy used to design the survey was based on that outlined in Przeslawski and Foster (2018), albeit with a few BRUV-specific alterations. The important parts of this approach are: randomisation, and spatial balance. Randomisation helps to relate the observed data to the survey area, and spatial balance makes sure that sampling sites are well spread out in space. Spreading samples out in space decreases spatial auto-correlation whilst simultaneously increasing balance on spatially-smooth covariates.

Another strategy to increase efficiency is to increase the chance of sampling sites that are more likely to have measurements with higher variance. In ecology, where variance increases with mean (Taylor, 1961, e.g.), this usually means increasing those environments where high abundances of fish are likely to occur. This is achieved through upweighting the *inclusion probabilities* (e.g. see Thompson, 2012; Przeslawski and Foster, 2018). In this region we expect higher abundances of fish to be associated with locally-elevated features, and so increase inclusion probabilities (for sampling new sites) based upon the terrain position index (TPI Weiss, 2001) – see Figure 17.

To provide temporal inference, it is best to revisit individual sites (e.g. Urquhart and Kincaid, 1999). This minimises the potential confounding between variance in temporal signal with variance in spatial signal. We note that for many organisms the relatively slight spatial misalignment will not matter overly much (Perkins et al., 2015), especially for baited sampling gear. The revisit approach assumes that the sites to revisit are randomly chosen themselves, which we have assumed to be so (the 2009 samples were at least). This helps the revisit panel to be representative (in both status and trend) of the survey area. In this design, we re-visit previous sampling locations. In future studies, some thought will need to be given as to what kind of temporal replication is warranted – fixed revisit plan, rotating panel, etc. See Urquhart and Kincaid (1999) for some discussion.

For the present study, up to a quarter of deployments in each of the different zones (IUCN II, IUCN IV, North Control and South Control) were revisits. This was done by randomly sampling the historic sites. However, some zones did not have that many historic sites to revisit and so there is less than a quarter. The legacy-site inclusion probabilities for historic site selection were not uniform, for two reasons: most of the historic sites were previously sampled only in 2009, and some of the historic sites formed large 'clumps' which do not need revisiting in equal density. To avoid sampling only 2009, the legacy-site inclusion probabilities were adjusted so that equal numbers of each of the 5 sampling periods are expected. Additionally, and because 2006 is the earliest sampling time, we substantially upweighted the chance of choosing 2006 sites for legacy/reference sites. To avoid choosing legacy sites that formed similar 'clumps' to the un-sampled locations, we further alter legacy-site inclusion probabilities so that historic samples in higher-density areas are down-weighted.

For the new sites, which form at least three-quarters of sampling locations, we define the inclusion probabilities solely on the TPI for the survey area. It is not adjusted for the spatial locations of legacy sites (see Foster et al., 2017) as it is desired that the new sample is independent of the legacy sites. To get the inclusion probability surface we first categorise the TPI surface into 8 different classes using the 80th, 90th, 92.5th, 95th, and 97.5th percentiles. We then assign inclusion probabilities so that we expect the same number of samples within each category.

Additionally, and perhaps more importantly, we choose the inclusion probabilities so that we expect 50 samples in the IUCN II zone, 25 in each of the control zones, and 100 in the IUCN IV zone. The resultant inclusion probabilities are presented (as the background data) in Figure 19. The inclusion probabilities accentuate the high TPI areas.

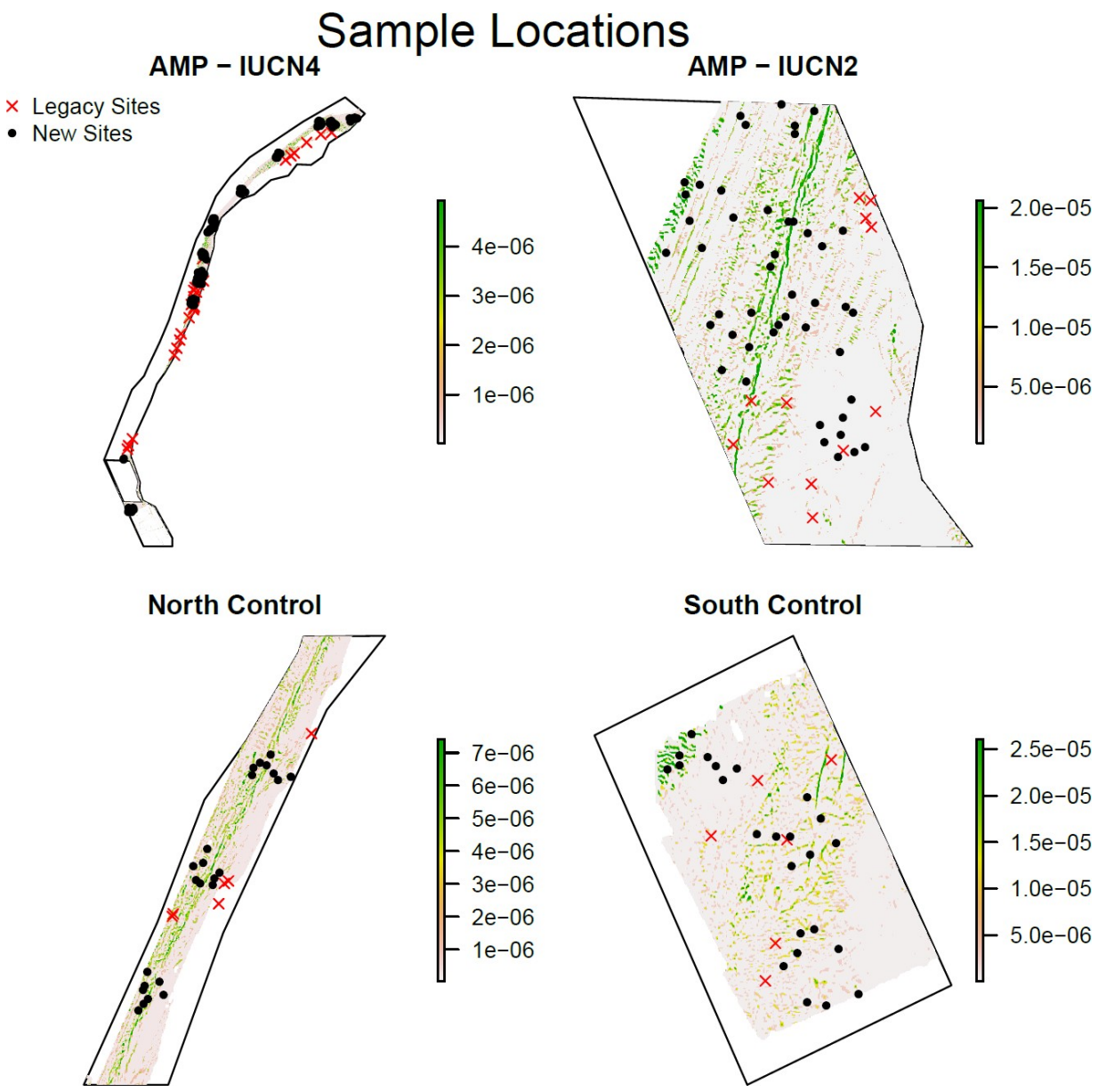

Figure 19 Summary of BRUV design, by study area. The background data is the inclusion probabilities, described in Section 4. The red crosses are the locations of the legacy sites chosen for revisit (a random subset of those in Figure 18). The black dots are the clustered locations of the 'new' sampling sites that are to be visited.

This is a BRUV survey, which need some time to soak, and it is preferential to have multiple BRUVs soaking concurrently. Since there are six BRUV units on board, we chose to sample using spatial clusters and cluster them close enough that there is not too much time lost to excessive travel or waiting for soak time. To achieve this, we first chose cluster centres (based on a coarsening of the inclusion probability grid, to 100 m), using spatially balanced sampling with non-even inclusion probabilities, and then sample within a radius of 1500 m from this location to get the cluster sample. The two-step randomisation process will not respect the inclusion probabilities if both steps use the un-altered inclusion probabilities. Rather, we use the square root of this surface for both steps. This will provide the correct inclusion probabilities *if the clusters do not*

overlap. Unfortunately, this is not the case and so the observed inclusion probabilities will not match those specified. It is thought that the observed inclusion probabilities will over-sample the high TPI areas. This is not an issue for a model-based analysis – as we recommend (see Section 5).

It is the nature of spatially balanced samples that they are spread out in space. However, this does not mean that they are equi-distant – far from it. In reality, some survey locations can be quite close together – especially when inclusion probabilities pick out small, localised features. This is not acceptable for BRUV samples, whose bait plume may spread a hundred metres. Our solution is to sample eight locations within each cluster and then discard one of any pair that is too close spatially as well as those samples numbered 7 or 8. This is a little bit ad-hoc, but it will work and if the scientists-in-the-field choose the sites based only on pair-wise distances, then there should be no inherent bias in this step. Of course, if the scientists-in-the-field consistently choose sites that may have higher biodiversity values, then a bias is likely to arise.

Since the locations of the legacy sites may be close to the locations of the clustered samples, it makes sense to try and incorporate these into the daily sampling plan. This may mean incorporating a legacy site into a cluster for sampling purposes – and dropping one of the new sites. This is OK. Preference should be given to dropping the new site that has the highest ordering but just as long as there isn't consistent bias in this choice, then all should work out well.

2.4.1 The design

A summary of the design is given in Figure 19 and Figure 20.

2.5 Analysis considerations

In adjusting the simple randomisation approach (non-equal inclusion probabilities and cluster sampling), we created a number of considerations that need to be accounted for in any statistical analysis. In particular, we need to condition on TPI to adjust for the bias incorporated by targeting locally elevated structures (e.g. Gelman et al., 2013), and also account for localised spatial-autocorrelation induced from the cluster sampling. Note explicitly that taking means of all the data is not appropriate (see Thompson, 2012, for example) and will produce biased estimates.

Both these issues can be over-come (usually) easily in a model-based framework. All that is required is a covariate effect for TPI and a spatial auto-correlation term (or a random effect for cluster is almost as good).

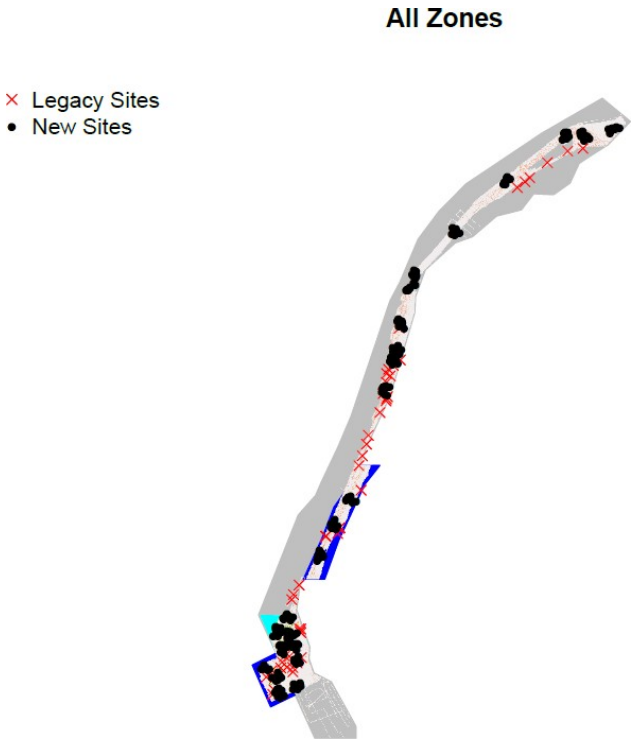

Figure 20 Summary of BRUV sampling design, for all zones. The red crosses are the locations of the legacy sites chosen for revisit (a random subset of those in Figure 18). The black dots are the clustered locations of the 'new' sampling sites that are to be visited.

2.6 Data and code

All of the data and code used to generate this design is available via request from the CSIRO Data Access Portal (http://hdl.handle.net/102.100.100/389900?index=1).

2.7 References

Foster, S. D., G. R. Hosack, E. Lawrence, R. Przeslawski, P. Hedge, M. J. Caley, N. S. Barrett, A. Williams, J. Li, T. Lynch, J. M. Dambacher, H. P. Sweatman, and K. R. Hayes (2017). Spatially balanced designs that incorporate legacy sites. *Methods in Ecology and Evolution 8*(11), 1433–1442.

Gelman, A., J. Carlin, H. Stern, D. Dunson, A. Vehtari, and D. Rubin (2013). *Bayesian Data Analysis, Third Edition*. Chapman & Hall/CRC Texts in Statistical Science. Taylor & Francis.

Perkins, N. R., N. A. Hill, S. D. Foster, and N. S. Barrett (2015). Altered niche of an ecologically significant urchin species, *Centrostephanus rodgersii*, in its extended range revealed using an autonomous underwater vehicle. *Estuarine, Coastal and Shelf Science 155*(0), 56 – 65.

Przeslawski, R. and S. D. Foster (Eds.) (2018). *Field Manuals for Marine Sampling to Monitor Australian Waters, Version 1.* Report to the National Environmental Science Programme. Marine Biodiversity Hub. http://dx.doi.org/10.11636/9781925297669.

Taylor, L. (1961). Aggregation, variance and the mean. *Nature 189*(4766), 732–735.

Thompson, S. (2012). *Sampling*. Wiley.

Urquhart, N. and T. Kincaid (1999). Designs for detecting trend from repeated surveys of ecological resources. *Journal of Agricultural, Biological, and Environmental Statistics 4*(4), 404–414.

Weiss, A. (2001). Topographic positions and landforms analysis (poster). ESRI International User Conference, July 2001. San Diego, CA: ESRI.

3. AUGUST 2019 BRUV FIELD TRIP REPORT

Authors: Anthea Donovan, Russ Babcock, Mark Tonks, Tim Langlois

Date: 30 September 2019

3.1 Field trip details

Field trip scientific personnel:

- Anthea Donovan (CSIRO)
- Mark Tonks (CSIRO)
- Tim Langlois (UWA)
- Brooke Gibbons (UWA)

Departure date: 11/8/19

Return date: 18/8/19

Duration of field trip: 8 days (1 mobilisation day, 6 days field work, 1 demobilisation day)

Vessel: Keshi Mer II

3.2 Objectives of the field trip

This research trip was conducted by CSIRO and the University of Western Australia. The aim was to deploy BRUVs (Baited Remote Underwater Videos) at up to 200 pre-determined sites (Figure 21) within Ningaloo Marine Park (Commonwealth waters) to sample deep water fish assemblages living along the coast between Coral Bay and the Muiron Islands. As well as fish species and abundances, the habitat at each of the sites was also sampled. The depths of the sites sampled typically ranged from 60–190 m.

The sampling spreads across the Northern Ningaloo Marine Park (Commonwealth waters) Region to straddle management zone boundaries as well as variations in fishing pressure—from the new (July 2018) no-take zone in the south to the highly fished areas in the north. In addition, emphasis was given to previously sampled sites where this was consistent with the above two objectives. This was in order to provide the potential to detect any trends in fish abundance or biomass that have developed in the 10 years since the first surveys in these waters.

3.3 Methods

In addition to information on park boundaries and previous sampling effort, a single layer of bathymetry compiled from all existing data from the region was used to develop a GIS layer representing sea floor roughness at a 2 m scale, in order to up-weight sampling for high rugosity habitat areas. BRUV deployments were conducted using standard BRUV systems according to standard BRUV practices.

BRUVS were deployed in sets of six, in 60 min drops separated by 0.5–2 km in order to efficiently use available time (minimise steaming and non-sampling time). Typically, 3–4 sites of six drops could be conducted each day, depending on weather, water depth, weather conditions, distance between sites and available light. Because of the time of year, sufficient daylight hours for operations (BRUV retrieval) and navigation in and out of reef anchorages were limited, restricting the number of sites to an unexpected degree. Ultimately 133 sites were sampled (Figure 22).

3.4 Site maps

3.4.1 All proposed sites

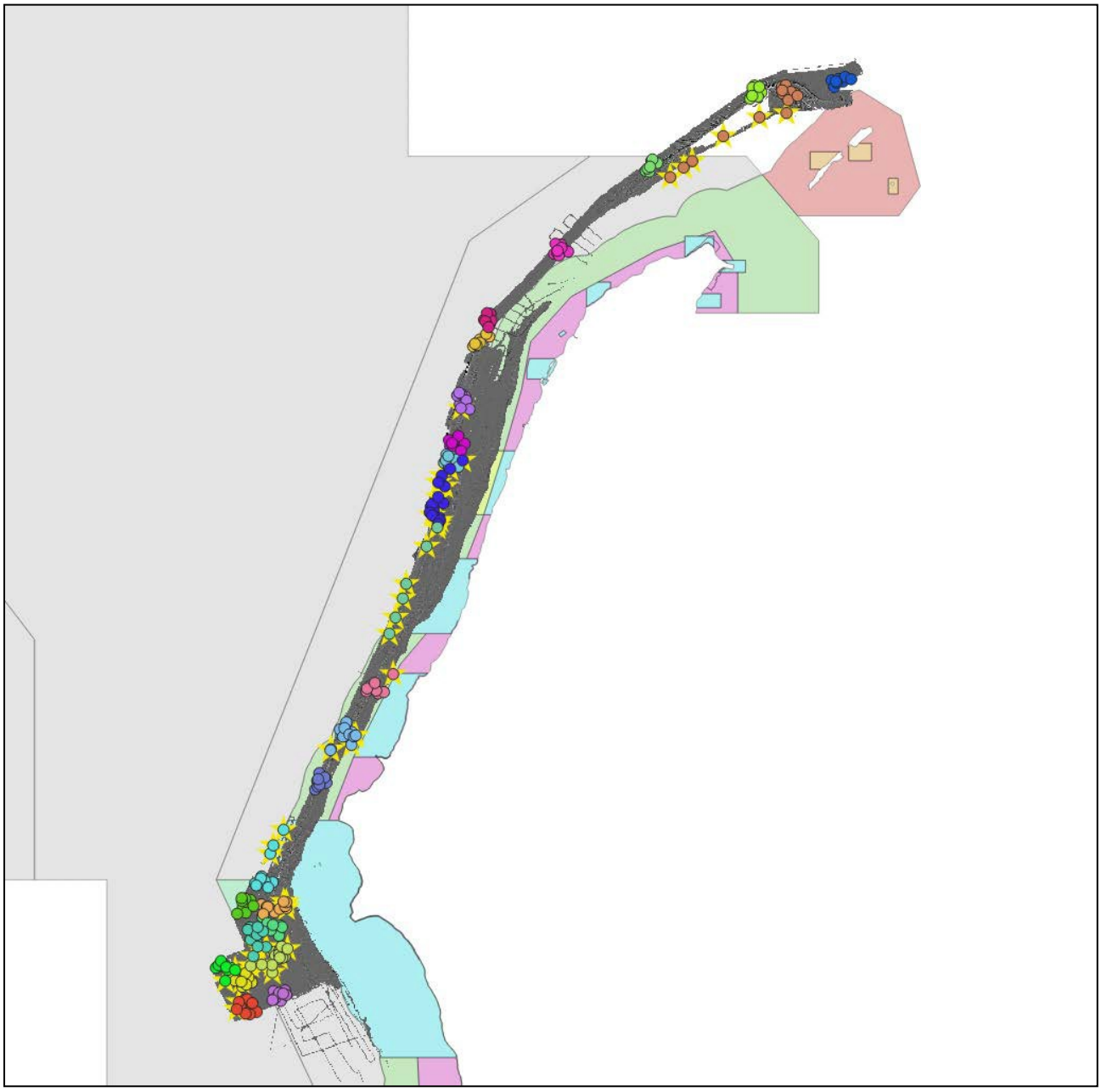

Figure 21. Map of all proposed sites. Each different coloured circle is a different “group” of sites. Six BRUV sites were selected from each “group”. Background colours refer to different zonings: light blue = various sanctuary zones; green = General Use Zone; pink = Recreation Zone; aqua = National Park Zone; orange = Muiron Islands Marine Management Area; light grey = Commonwealth Waters; dark grey = areas with swath mapping data available. See Figure 2 for more details on zonings.

3.4.2 Sites sampled

Figure 22 Map of all sites sampled. Legacy sites are blue circles, new sites are pink circles and ad hoc sites (those selected during the field trip) are orange circles. Background colours refer to different zonings: light blue = various sanctuary zones; green = General Use Zone; pink = Recreation Zone; aqua = National Park Zone; orange = Muiron Islands Marine Management Area; light grey = Commonwealth Waters; dark grey = areas with swath mapping data available. See Figure 2 for more details on zonings.

3.5 Daily summary of field trip

11 AUGUST 2019

Scientific staff arrive at Learmonth Airport at 14:30 and get transported via shuttle bus to Coral Bay where they board the vessel at approximately 16:30.

Vessel safety induction is conducted.

Travel the short distance to Point Cloates where the vessel anchors for the night.

Began setting up all the gear (assembling BRUV frames, installing housings, charging batteries, etc.)

12 AUGUST 2019

Depart from Point Cloates at 07:00 and travel to first site.

Continued setting up the gear (formatting cameras, attaching appropriate ropes to frames, attaching weights to frames, etc.).

Sites sampled:

Site	Type	Latitude	Longitude	Time in	Time out
1.01	new	113.5405	-22.8478	9:23:00	10:33:00
1.02	new	113.5253	-22.8502	9:35:00	10:50:00
1.03	legacy	113.513	-22.8444	9:43:00	10:59:00
1.04	new	113.5184	-22.8403	9:51:00	11:13:00
1.05	legacy	113.516	-22.8342	9:58:00	11:20:00
1.06	new	113.5234	-22.8315	10:06:00	11:31:00
2.07	new	113.564	-22.8191	12:24:00	13:43:00
2.06	new	113.5716	-22.8216	12:18:00	13:35:00
2.05	new	113.5771	-22.8226	12:12:00	13:25:00
2.04	new	113.5816	-22.8244	12:05:00	13:15:00
2.03	new	113.5659	-22.829	11:57:00	13:04:00
2.02	new	113.5626	-22.8315	11:47:00	12:55:00
3.06	new	113.5106	-22.8046	14:25:00	15:43:00
3.05	new	113.5163	-22.8053	14:21:00	15:37:00
3.04	legacy	113.5194	-22.8061	14:17:00	15:30:00
3.01	new	113.5208	-22.8131	14:12:00	15:21:00
3.02	new	113.5262	-22.8102	14:07:00	15:13:00
3.03	new	113.5338	-22.8069	14:00:00	15:05:00

Return to Point Cloates for anchorage.

13 AUGUST 2019

Depart from Point Cloates and travel to first site.

Sites sampled:

Site	Type	Latitude	Longitude	Time in	Time out
4.01	legacy	113.4971	-22.805	8:05:00	9:16:00
4.03	new	113.5006	-22.7899	8:24:00	9:37:00
4.02	legacy	113.5108	-22.79	8:15:00	9:25:00
4.12	new	113.4878	-22.7858	8:56:00	10:03:00
4.08	new	113.4984	-22.786	8:29:00	9:44:00
4.11	new	113.4961	-22.7837	8:33:00	9:57:00
9.01	new	113.536	-22.7014	11:16:00	12:51:00
9.05	new	113.5248	-22.6915	11:05:00	12:28:00
9.06	new	113.5319	-22.6931	11:10:00	12:40:00
9.07	new	113.5255	-22.7108	10:52:00	12:05:00
9.02	new	113.5215	-22.7025	11:00:00	12:14:00
9.08	new	113.5136	-22.7122	10:45:00	11:55:00
6.03	legacy	113.5419	-22.7575	13:25:00	14:53:00
6.02	legacy	113.5537	-22.7582	13:31:00	15:09:00
6.01	legacy	113.536	-22.7709	13:41:00	15:22:00
6.04	new	113.5403	-22.7518	13:21:00	14:42:00
6.05	new	113.5412	-22.7412	13:15:00	14:31:00
6.12	new	113.5419	-22.7306	13:11:00	14:16:00
5.13	legacy	113.5832	-22.7608	16:11:00	17:24:00
5.11	new	113.5723	-22.7628	16:05:00	17:16:00
5.08	new	113.5716	-22.7681	15:53:00	17:08:00
5.07	new	113.5725	-22.7728	15:49:00	17:00:00
5.03	legacy	113.5619	-22.783	15:42:00	16:50:00
5.02	legacy	113.5476	-22.7825	15:37:00	16:40:00

Steam to Norwegian Bay for anchorage.

14 AUGUST 2019

Depart from Norwegian Bay and travel to first site

Sites sampled:

Site	Type	Latitude	Longitude	Time in	Time out
7.08	new	113.5757	-22.7306	8:03:00	9:06:00
7.05	new	113.5733	-22.7288	8:08:00	9:15:00
7.04	new	113.5631	-22.7276	8:13:00	9:22:00
7.03	new	113.5555	-22.7251	8:16:00	9:29:00
7.02	new	113.5533	-22.7317	8:21:00	9:38:00
7.01	new	113.5509	-22.7343	8:24:00	9:44:00
8.01	new	113.5498	-22.7127	10:00:00	11:02:00
8.02	new	113.5559	-22.7028	10:06:00	11:12:00
8.12	new	113.5474	-22.6993	10:11:00	11:22:00
8.07	legacy	113.5778	-22.6954	10:23:00	11:38:00
8.06	legacy	113.5816	-22.6962	10:27:00	11:45:00
8.05	legacy	113.5799	-22.7017	10:31:00	11:52:00
10.01	new	113.5564	-22.6759	12:13:00	13:15:00
10.02	new	113.5564	-22.6733	12:19:00	13:23:00
10.03	new	113.5628	-22.6687	12:24:00	13:31:00
10.04	new	113.5519	-22.6669	12:33:00	13:42:00
10.07	new	113.54	-22.6731	12:40:00	13:55:00
10.08	new	113.5384	-22.6704	12:46:00	14:05:00
10.09	legacy	113.5594	-22.6292	14:34:00	16:05:00
10.11	legacy	113.5636	-22.6177	14:41:00	15:52:00
10.13	ad hoc	113.579	-22.638	14:53:00	16:24:00
10.14	ad hoc	113.5917	-22.624	15:02:00	16:36:00
10.15	ad hoc	113.594	-22.6058	15:10:00	16:47:00
10.12	legacy	113.5778	-22.5962	15:20:00	16:58:00

Steam to Yardie Creek for anchorage.

15 AUGUST 2019

Depart from Yardie Creek and travel to first site.

Sites sampled:

Site	Type	Latitude	Longitude	Time in	Time out
11.01	new	113.6215	-22.5404	8:06:00	9:12:00
11.02	new	113.6248	-22.5365	8:11:00	9:18:00
11.03	new	113.6274	-22.5338	8:15:00	9:24:00
11.04	new	113.6244	-22.5287	8:19:00	9:32:00
11.05	new	113.6255	-22.5262	8:25:00	9:39:00
11.06	new	113.6346	-22.5239	8:31:00	9:47:00
12.11	legacy	113.6433	-22.4848	10:14:00	11:23:00
12.06	new	113.6574	-22.4655	10:25:00	11:35:00
12.05	new	113.66	-22.4673	10:29:00	11:43:00
12.02	legacy	113.675	-22.4672	10:37:00	12:02:00
12.03	new	113.6678	-22.4682	10:44:00	11:49:00
12.04	new	113.6688	-22.4643	10:48:00	11:56:00
13.02	new	113.7058	-22.4039	12:32:00	13:40:00
13.06	new	113.6923	-22.4048	12:39:00	13:56:00
13.05	new	113.6932	-22.4009	12:43:00	14:03:00
13.04	new	113.6973	-22.3977	12:48:00	14:10:00
13.03	new	113.7013	-22.399	12:52:00	13:46:00
13.08	new	113.7039	-22.3933	12:56:00	14:16:00
14.01	legacy	113.7241	-22.3252	14:46:00	15:49:00
14.11	new	113.7372	-22.3267	14:53:00	15:58:00
14.12	new	113.746	-22.3072	15:05:00	16:08:00
14.02	legacy	113.7325	-22.3028	15:12:00	16:21:00
14.13	new	113.7417	-22.2867	15:20:00	16:32:00
14.03	legacy	113.7427	-22.2765	15:25:00	16:39:00

Steam to Tantabiddi for anchorage.

16 AUGUST 2019

Depart from Tantabiddi and travel to first site.

Sites sampled:

Site	Type	Latitude	Longitude	Time in	Time out
14.06	legacy	113.7905	-22.1783	8:12:00	9:16:00
15.01	legacy	113.7915	-22.1734	8:16:00	9:23:00
15.02	legacy	113.7941	-22.1688	8:20:00	9:30:00
15.05	legacy	113.7834	-22.1617	8:27:00	9:39:00
15.12	new	113.7899	-22.1438	8:39:00	9:53:00
15.07	legacy	113.7916	-22.1364	8:43:00	10:03:00
16.01	legacy	113.8007	-22.1216	10:22:00	11:28:00
16.02	legacy	113.7919	-22.1162	10:28:00	11:37:00
16.03	legacy	113.7967	-22.1067	10:39:00	11:48:00
16.04	legacy	113.8081	-22.0974	10:48:00	12:04:00
17.08	new	113.8194	-22.0944	10:53:00	12:15:00
16.05	legacy	113.8256	-22.0856	11:00:00	12:23:00
18.01	new	113.8123	-22.0695	12:33:00	13:35:00
18.02	new	113.812	-22.0652	12:38:00	13:42:00
18.03	new	113.8082	-22.0656	12:46:00	13:53:00
18.04	new	113.8106	-22.0617	12:50:00	14:01:00
18.07	new	113.8282	-22.0626	12:54:00	14:10:00
18.08	new	113.8232	-22.0725	12:58:00	14:16:00
19.01	legacy	113.8229	-22.0135	14:42:00	15:44:00
19.02	new	113.8215	-22.0079	14:44:00	15:53:00
19.04	new	113.8256	-22.0006	14:49:00	15:59:00
19.03	new	113.8306	-22.0029	14:55:00	16:07:00
19.05	new	113.8291	-21.9976	14:59:00	16:15:00
19.08	new	113.8234	-21.9941	15:03:00	16:22:00

Steam to Tantabiddi for anchorage.

17 AUGUST 2019

Depart from Tantabiddi and travel to first site. Weather quite rough. Attempted to sample the sites in the "20" group but it was too exposed. Also wanted to sample in site groups 24 (new sites only) and 25, but travel time to these sites in the rougher conditions was too long. Site groups 30 and 31 were added instead.

Sites sampled:

Site	Type	Latitude	Longitude	Time in	Time out
30.01	ad hoc	113.9041	-21.9112	10:04:00	11:12:00
30.02	ad hoc	113.9072	-21.9069	10:08:00	11:19:00
30.03	ad hoc	113.9108	-21.9	10:13:00	11:28:00
30.04	ad hoc	113.9142	-21.8951	10:16:00	11:36:00
30.05	ad hoc	113.918	-21.8898	10:20:00	11:44:00
30.06	ad hoc	113.9202	-21.8876	10:23:00	11:49:00
23.09	ad hoc	114.0747	-21.7069	13:13:00	14:24:00
23.01	new	114.0836	-21.6865	13:22:00	14:40:00
23.02	new	114.0786	-21.6856	13:28:00	14:48:00
23.03	new	114.0812	-21.6823	13:31:00	14:54:00
23.04	new	114.0845	-21.6798	13:35:00	15:01:00
23.06	new	114.0945	-21.6748	13:46:00	15:09:00
31.01	ad hoc	114.0899	-21.6873	15:25:00	16:31:00
31.02	ad hoc	114.09	-21.692	15:29:00	16:36:00
31.03	ad hoc	114.0888	-21.6945	15:31:00	16:41:00
31.04	ad hoc	114.0878	-21.6964	15:34:00	16:47:00
31.05	ad hoc	114.0814	-21.7005	15:39:00	16:52:00
31.06	ad hoc	114.0775	-21.7025	15:45:00	16:58:00

Steam to Exmouth Marina.

Disassemble all the gear.

18 AUGUST 2019

At 08:00, unload all the gear from the vessel onto a WA Parks and Wildlife truck. At the Parks and Wildlife facility, all BRUVs gears is loaded onto pallets to be returned to UWA.

Scientific staff leave Learmonth Airport at 15:20.

3.6 Communications

13 August 2019: CSIRO Blog article https://blog.csiro.au/nice-one-bruv-counting-deep-water-fish-at-ningaloo-reef/

15 August 2019: GWN7 News article https://www.gwn7.com.au/news/10714-deep-sea-explorers

4. NINGALOO DEEPWATER REEFS HYDROGRAPHIC SURVEY

Author: Craig Davey

Date: 11 July 2019

4.1 Executive summary

The CSIRO's Oceans & Atmosphere Shallow Survey Facility (SSF) was contracted to conduct a multibeam survey of areas adjacent to the Ningaloo Reef system, Western Australia for CSIRO Oceans and Atmosphere.

Three areas were outlined to be surveyed (see Table 2 and Figure 23).

Table 2 Proposed Survey Areas.

Name	Total Area (km²)	Area Surveyed (km²)
Area 3a	345.4	88.5
Area 4	237.1	0
Area 5	120.3	N/A

The survey prioritised Area 3a and the southern end of this area was completed with full coverage along with a number of expeditionary lines. Area 5 was surveyed in a larger grid pattern to get a general overview of the area. These lines in Area 5 where generally run while transiting from anchorage at Coral Bay to Area 3a. All transit lines were surveyed.

The vessel RV Linnaeus was mobilised at Hillarys Boat Harbour, Perth WA from the 8th March 2019 to the 14th March 2019. The vessel was lifted out of the water on the 8th March and transducer and speed of sound probe installed on the hull. Topside equipment was installed and tested on the 11th and 12th March. Patch test/sea trials scheduled for the 14th March were not undertaken. The vessel departed Hillarys on the 15th March transiting to Coral Bay via Geraldton and Carnarvon arriving onsite on the 17th March. On the 18th March a patch test and GAMS calibration were conducted and surveying commenced. Weather conditions were not ideal for multibeam operations with the data being affected by a 3 m swell and 20–25 knot winds up until the 20th March. The 21st March was a weather standby day with conditions deemed too rough to survey.

With the approach of Tropical Cyclone Veronica the decision was made to postpone the survey and send the vessel south and away from any danger.

Survey was recommenced on the 26th March 2019 and survey operations completed on the 28th March and thereafter towed camera operations commenced. On the 29th March the PosMV motion sensor was demobilised and shipped back to the supplier terminating the hire contract. The remainder of the GSM topside multibeam equipment was removed in Exmouth in conjunction with the demobilisation of the towed camera system.

Survey speed was dictated by weather conditions with an average speed of 6-8 knots maintained. On the 27th March 2019 the speed of sound at the transducer head stopped working. Being subsea it could not be repaired or replaced. Survey data collected on the 27th and 28th used the sound velocity profile for beam steering.

The soundings and map products have been reduced to the Australian Height Datum (AHD) and the horizontal datum and projection the data is reduced to is WGS84 and UTM Zone 49S respectively. The survey covered approximately 724 line kilometres (or 390 nautical miles), including transits.

4.1.1 Summary of the survey details

Table 3 Summary of the survey details.

CATEGORY	DETAILS
Survey Area(s)	Area 3a and Area 5, Ningaloo Reef, WA.
Survey Dates	18th March to 29th March 2019
Survey Vessel	MV Linnaeus (CSIRO)
Survey Personnel	Craig Davey (CSIRO)
MBES System	Kongsberg EM2040c
Real Time Positioning System	POS MV V5 (aided with Fugro G4+ Marinestar signal). *Accuracy: 0.10 m (Horizontal) & 0.15 m (Vertical) @ 95%.*
Real Time Motion & Gyro System	POS MV V5 *Accuracy: 0.02° (Heading), 0.02° (Roll/Pitch), 5 cm or 5% (Heave) & 2 cm or 2% (TrueHeave)*
Sound Velocity	Valeport MiniSVS (Head) & Monitor SVP (Water Column)
Horizontal Datum & Projection (Processed)	WGS84, UTM Zone 49S
Reduced Vertical Datum (Processed)	AHD (Australian Height Datum) using AUSGeoid09
Survey Standard (Processed)	Not applicable

4.1.2 Summary of the data acquired

Table 4 Raw data collected by instrument.

INSTRUMENT	DATA TYPE	RAW DATA SIZE	NUMBER OF FILES
EM2040C	Multibeam Echosounder Bathymetry & Backscatter (.ALL)	211 Gb	211
EM2040C	Multibeam Echosounder Water Column Data (.WCD)	178 Gb	103
POS MV	RAW GNSS & IMU (000 file)	6.88Gb	65
SVP Casts	Sound Velocity Profile	189 Kb	17

4.1.3 Summary of bathymetry results

Table 5 Bathymetry results.

SITE	MINIMUM DEPTH	MAXIMUM DEPTH	COMMENTS
Area 3a	~68 m	~272 m	Seabed topography slopes west away from the coast at an average slope of less than 2%. Possible palaeoshorelines (~2m) evident on the 80-90m contour and bedforms (~4m) on the ~185m contour.
Area 5	~54m	~78m	Not a uniform dataset. Single transit lines only. Seabed slopes away from the coast at a gradient of less than 0.5%. Subtle bedforms with a height of ~0.5m evident in all depth ranges.

4.1.4 Summary of backscatter results

Table 6 Backscatter features noted.

SITE	SIGNIFICANT FEATURES
Area 3a	➢ Backscatter Intensity values are increasing with depth indicating harder, coarser sediments in the deeper water and finer, softer sediments in the shallower water. ➢ Bedforms identified in the bathymetry on the 80m and 180m contour do not show as a strong backscatter contrast/signature but are detectable.
Area 5	➢ Some transit lines show varying backscatter intensity values which indicate varying bottom type. These backscatter variations align with the subtle bedforms noted in the bathymetry.

4.2 Site location

4.2.1 Site location overview

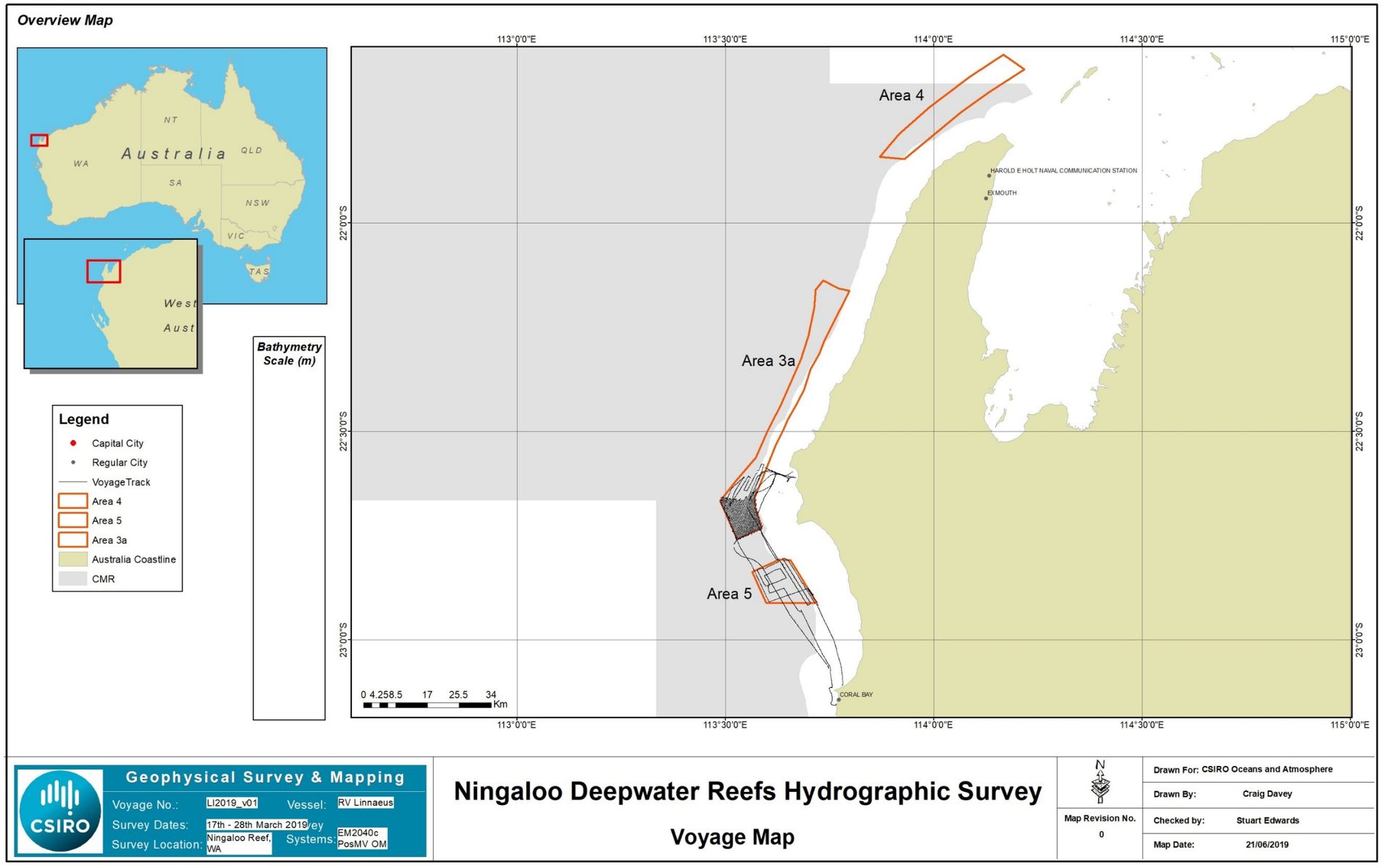

Figure 23 General site locality map.

4.3 Results

The bathymetry and backscatter data is presented together with a brief description/interpretation for the site in the following sections of the report. The data provided is presented in the WGS84, UTM Zone 49S projected horizontal datum, and the vertical datum is referenced to the Australian Height Datum (AHD).

Backscatter data is derived from the amplitude strength of the returning sound from the MBES, and is useful in that it can give an indication of seafloor characterisation. Greyscale mosaics have been produced from the backscatter data and are presented, along with the bathymetry, in the sections below. It should be noted that the greyscale imagery of the mosaics has been displayed in a manner that highlights finer sediments with a darker tonal range, while coarser sediments present as lighter tones in the maps shown.

The data is presented at a 2.0 m resolution for bathymetry and 2.0 m resolution for backscatter. This adequately highlights both larger scale seafloor features as well as more subtle, smaller-scale geomorphology. Many of the subtle tonal changes from the backscatter data (inferring different sediment classifications), when combined with the bathymetry, can provide a good indication of both the overall seafloor geomorphology and its composition.

4.3.1 Ningaloo deep reefs Western Australia

AREA 3A

The bathymetry and backscatter data for survey Area 3a are presented in Figure 24 to Figure 28.

The Bathymetry within the survey area varies in depth from around 68 m to 272 m depth (AHD). The seafloor slopes away from the coastline at an average gradient of less than 2% but this varies across the area. Linear seafloor features are evident around the 80 m to 90 m contour and 185 m contour.

The seabed features that exist on the 80 m to 90 m contour align parallel to the contour indicating a possible palaeoshoreline and are up to 2 m in height above the neighbouring seafloor. The bedforms existing on the 185 m contour have a general alignment perpendicular to the contour and are up to 4 m in height.

The backscatter for the Area 3a shows no areas of high backscatter contrast. The backscatter intensity increases with depth indicating coarser/harder sediments at depth and finer/softer sediments in the shallower areas.

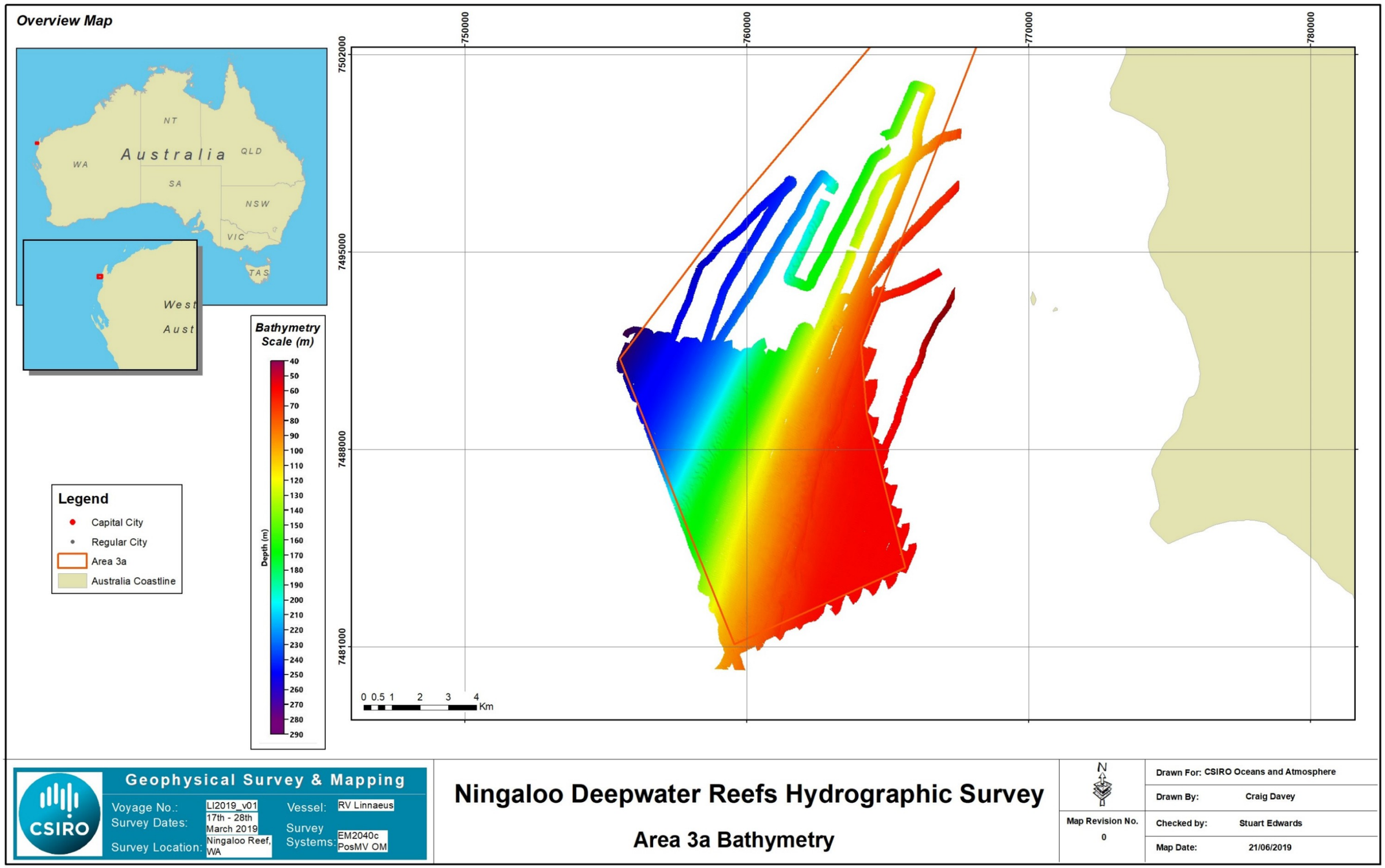

Figure 24 Area 3a Bathymetry overview.

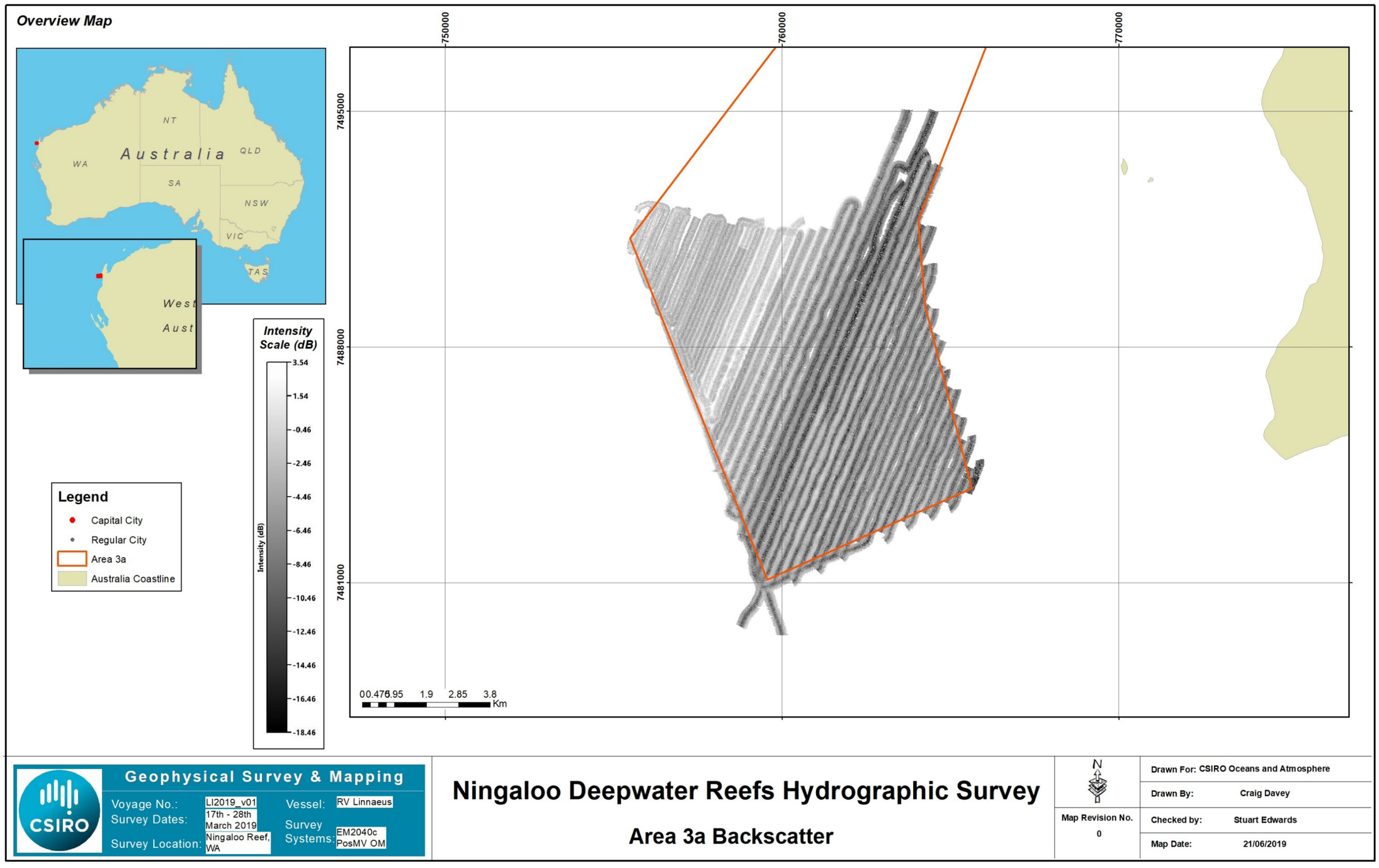

Figure 25 Area 3a Backscatter overview.

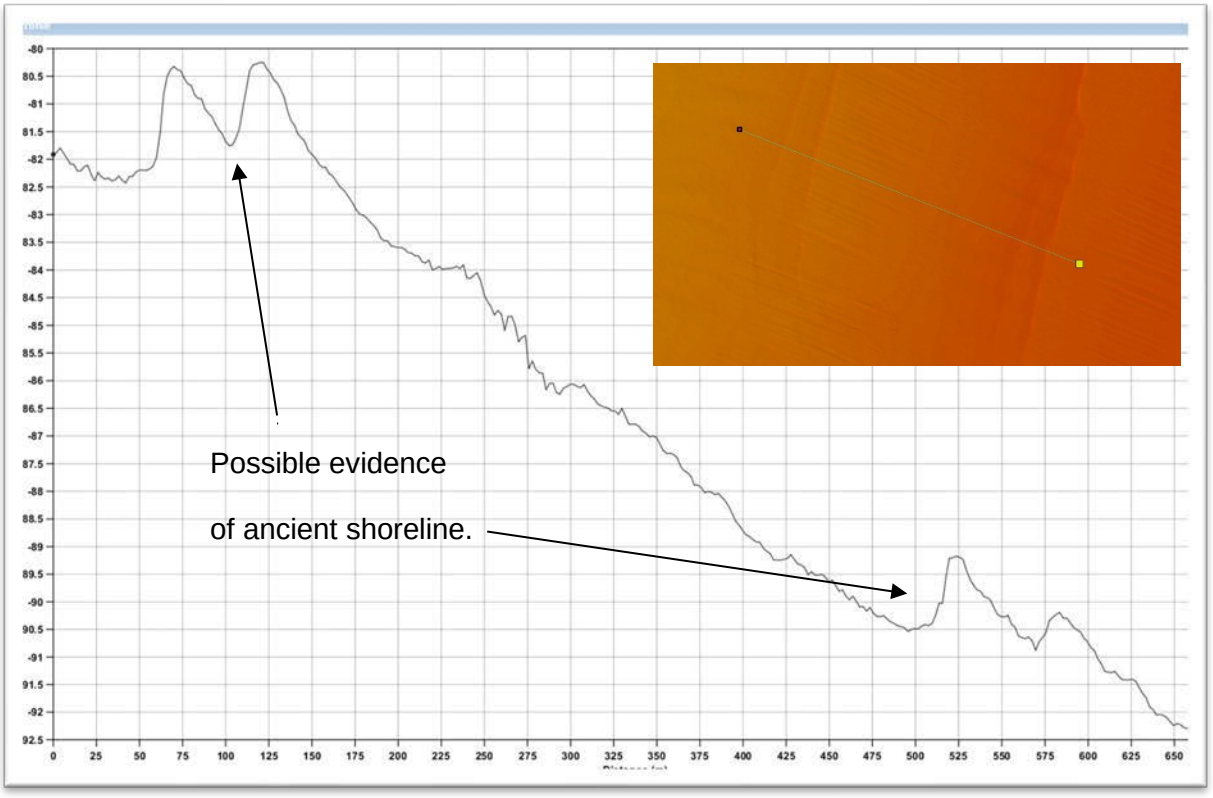

Figure 26 Seabed features on the 80 m – 90 m contour, Area 3a.

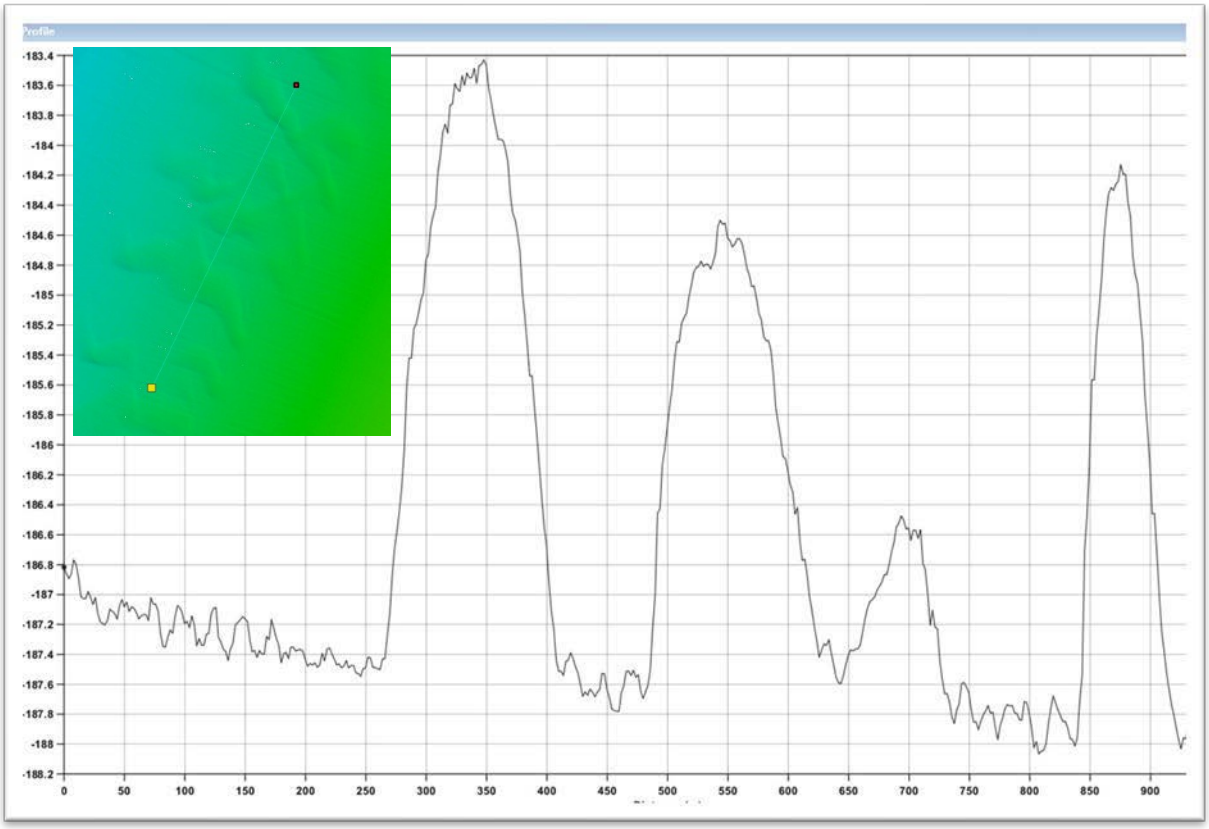

Figure 27 Bedforms on the 185 m contour, Area 3a.

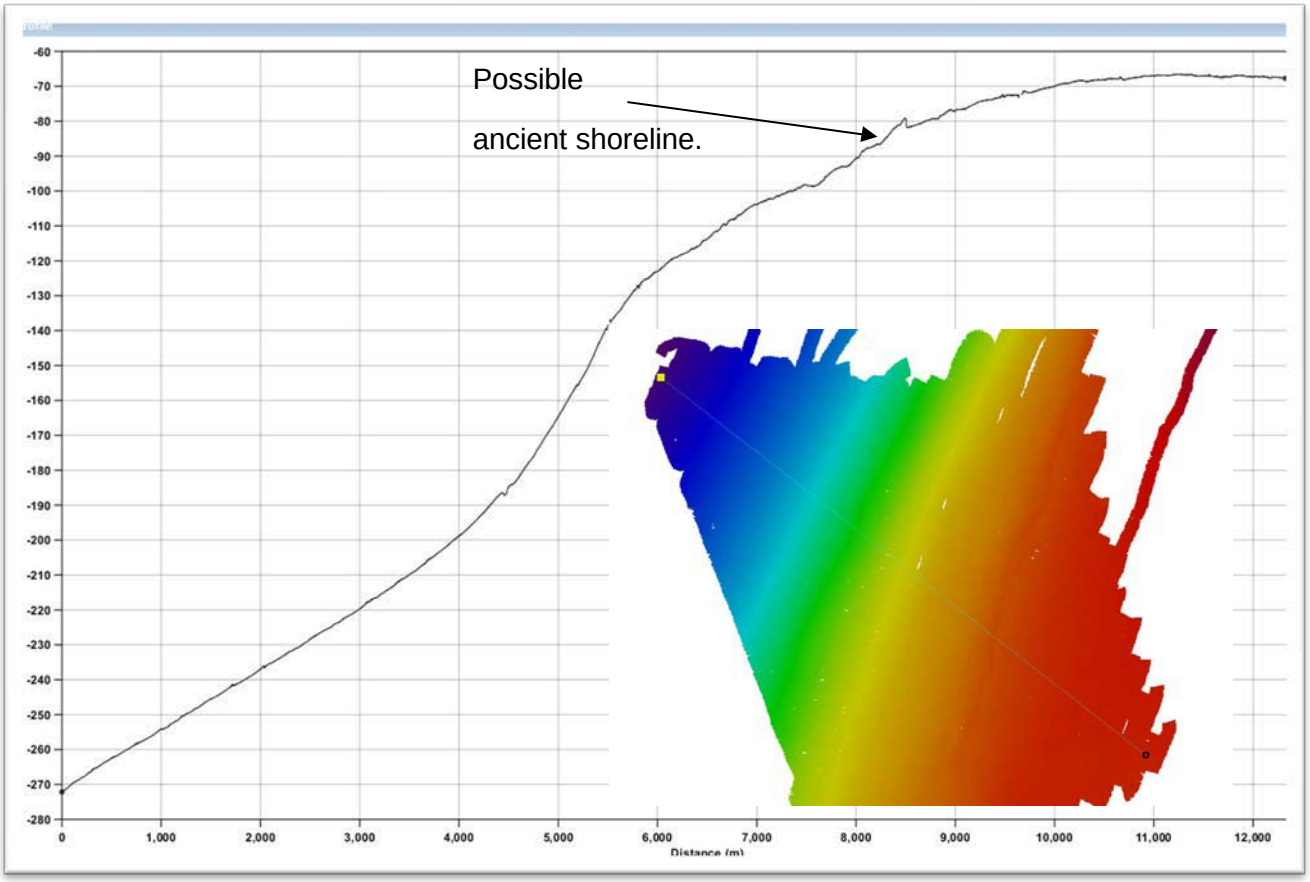

Figure 28 Area 3a Depth profile.

AREA 5

The bathymetry and backscatter data for survey Area 5 are presented in Figure 29 and Figure 30.

The bathymetry within the survey area varies in depth from 54 m to 78 m. The seafloor slopes away from the coast at a gradient less than 0.5%. Subtle bedforms are evident over the whole site and measure ~0.5 m in height. A larger feature lies just outside the eastern edge of boundary, possibly a reef system.

The backscatter mosaic identifies neighbouring areas of varying backscatter intensities. Lighter grey scale suggests or interprets to be harder/coarser sediments with darker tones indicating finer/softer sediments.

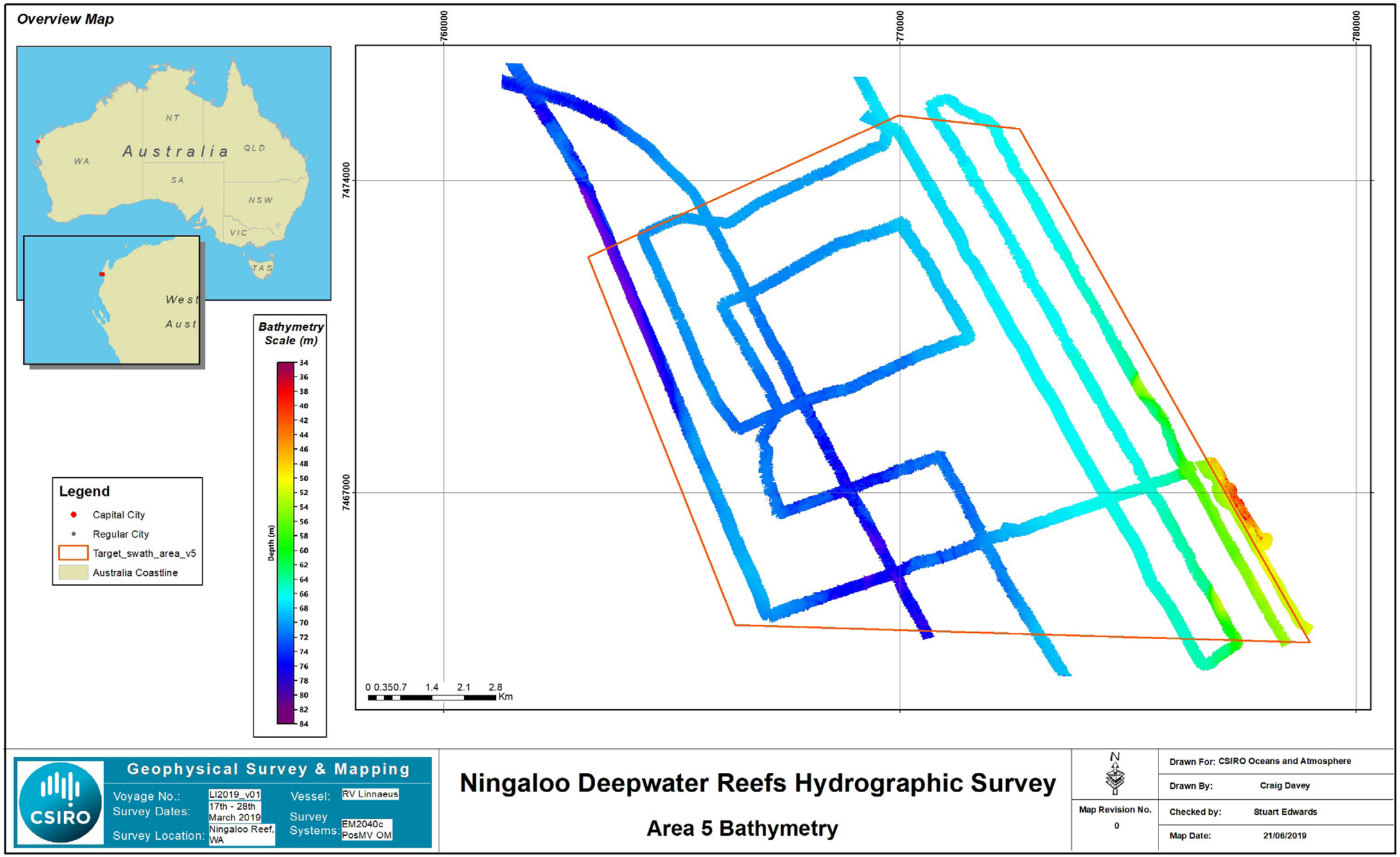

Figure 29 Area 5 Bathymetry overview

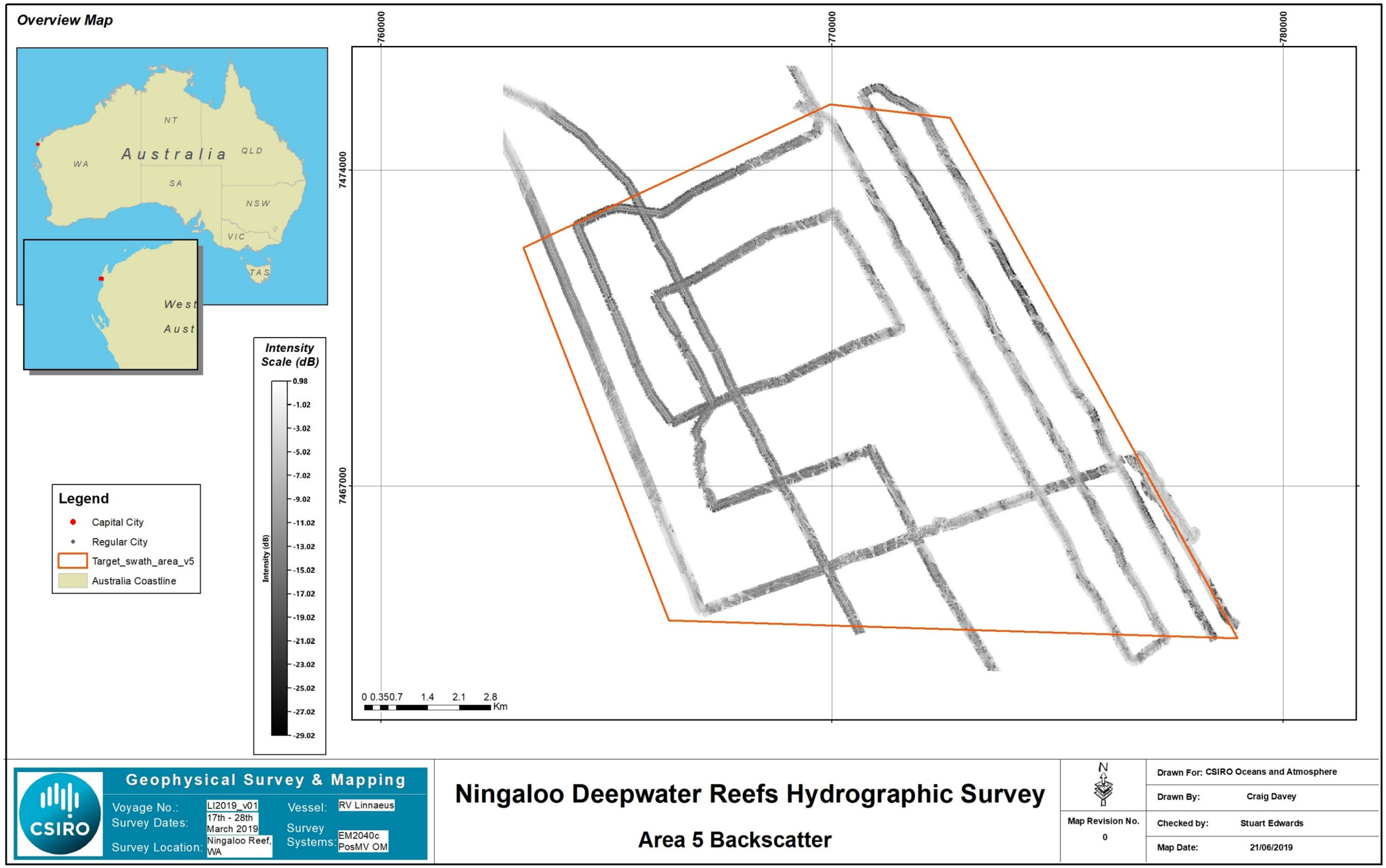

Figure 30 Area 5 Backscatter overview.

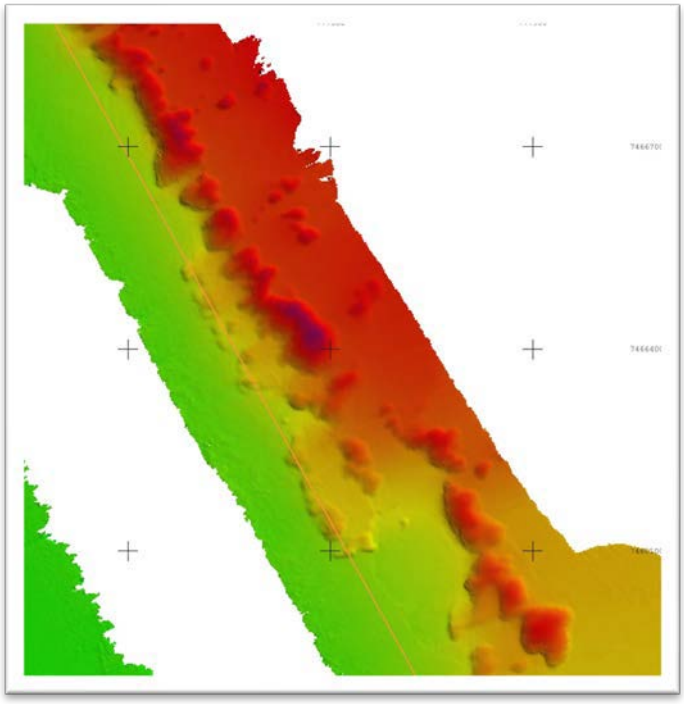

Figure 31 Reef feature on eastern boundary, Area 5. Orange line is marine park boundary.

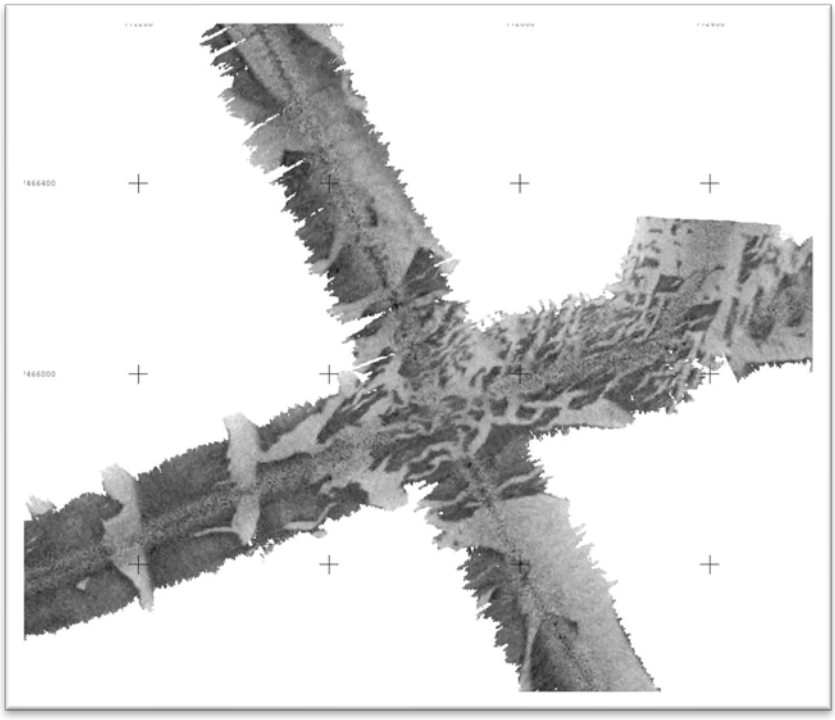

Figure 32 Backscatter patterns in Area 5.

4.4 Survey & processing details

4.4.1 Vessel & equipment

VESSEL

The CSIRO Oceans and Atmosphere operated vessel, *RV Linnaeus,* was used for the survey operations.

Figure 33 RV Linnaeus.

SURVEY HARDWARE

The following survey equipment, owned and installed by CSIRO, was used for the survey operations.

Table 7 Survey equipment (Source: CSIRO).

ITEM	MANUFACTURER	MODEL	SERIAL NO.
Acquisition Computer	Dell	Workstation	-
Ancillary Computer	Dell	Latitude	-
MBES (PU, Master)	Kongsberg (Norway)	EM2040C slim PU	20087
MBES Transducer	Kongsberg (Norway)	EM2040C	1403
Motion Reference System	Applanix	POS MV Oceanmaster	8438
Inertial Measurement Unit (IMU)	Applanix	Type 65	-
SV Sensor (MBES Tx)	Valeport UK	miniSVS	38339
SV Sensor - Profiler	Valeport UK	Monitor SVP	38500

SURVEY SOFTWARE

The following CSIRO processing software was used on board the vessel.

Table 8 Survey software (Source: CSIRO).

ITEM	VENDOR	SOFTWARE	VERSION
Data Acquisition	Kongsberg	SIS	4.3.2
Motion Reference Unit	Applanix	POS MV FW	9.29
Sound Velocity	Valeport UK	Datalog X2	V1.0
MBES Data Processing	CARIS	HIPS & SIPS	10.4
Backscatter Data Processing	CARIS	HIPS & SIPS	10.4

4.4.2 Acquisition

GENERAL DATA ACQUISITION INFORMATION

Survey acquisition was undertaken according to the following criteria:

- A Kongsberg EM2040C MBES (with a 1.3° x 1.3° beamwidth) was used to acquire all data. Auxiliary sensors included an Applanix POS MV for position and motion information (aided with a Fugro Marinestar GNSS G4+ subscription signal), a Valeport MiniSVS for sound velocity at the transducer and a Valeport Monitor SVP for water column sound velocity profiles.
- The MBES system was installed and calibrated by CSIRO.
- The bathymetry data was acquiring using Kongsberg's SIS (Seafloor Information System) software.
- Reference Position (RP) was chosen to be the Acoustic Centre of EM2040c transducer.
- Dual Swath mode (fixed setting) was utilised throughout the survey to increase the along track resolution.
- A sonar frequency of 200 kHz was selected.
- A FM pulse was used.
- A sector coverage of 65° (Port) and 65° (Starboard) were applied and line spacing adjusted to ensure data overlap.
- Angular coverage mode was set to Auto and Beam Spacing was set to High Density Equidistant.
- Vessel speed was 6-8 knots
- Seventeen sound velocity profiles were taken throughout the survey campaign.

SURFACE POSITIONING

An Applanix POS MV was used to provide real time surface positioning aided with a Fugro Marinestar GNSS G4+ correction signal. The POS MV combines the Inertial Measurement Unit (IMU) and Global Navigation Satellite System (GNSS) data into an integrated navigation solution.

Real time position information was output to the EM2040C processing unit (PU) via RS232 at a frequency of 100 Hertz. Lever arm offsets were entered in to the Applanix POSMV to reduce the position information to an arbitrary location (RP) on the vessel. The reference position was chosen to be the acoustic centre of the EM2040c transducer.

HEADING AND MOTION DATA

An Applanix POS MV was used to provide heading and motion data in real time. Motion and heading data were output to PU via RS232 at a frequency of 100 Hertz.

Applanix 000 files were recorded via ethernet logging for application of TrueHeave and/or for post processing an SBET (smoothed best estimate of trajectory) solution.

MULTIBEAM BATHYMETRY

Bathymetry was acquired using a Kongsberg EM2040C multibeam echosounder operating in single head/dual swath mode. Position data was input directly to the PU via a NMEA GGA string at 1 Hertz. Time information was input directly to the PU via a NMEA ZDA string in conjunction with a 1PPS input via RS232 from the POS MV. Velocity information was input directly via an Ethernet real time output packet at 100 Hertz. Motion and heading data was input directly to the PU via an EM3000 string at 100 Hertz.

Sound velocity at the transducer was interfaced to the EM2040C acquisition computer at 1 Hertz. Multibeam bathymetry was corrected for position, motion and sound velocity in real time and recorded in Kongsberg's standard datagram format with the .all extension. Multibeam bathymetry data was monitored for quality throughout the survey through the Seafloor Information System (SIS) software provided by Kongsberg.

4.4.3 Processing

MULTIBEAM BATHYMETRY DATA

Multibeam data was logged in the Kongsberg's proprietary *.all format and was converted to be processed within CARIS HIPS and SIPS version 10.4.

An AHD GPS tide was calculated based on GNSS derived ellipsoidal heights reduced via an Ausgeoid09 file (AUSGeoid09_GDA94_49K.txt). The GPS tide was smoothed at 120sec and applied to the data during the merge process in CARIS.

Cube surfaces were created at a 2 m resolution.

NAVIGATION, MOTION AND TIME DATA

The real-time position and attitude solution was used for the processing of this multibeam data.

An SBET solution was not calculated.

BACKSCATTER DATA

Backscatter information was extracted from the raw .all using the CARIS HIPS and SIPS. Backscatter mosaics were created at a 2 m resolution.

The linear greyscale image displays data with a lower reflectivity (e.g. finer sediments) as a darker appearance, and data with a higher reflectivity (e.g. coarser sediments or rock) as a lighter appearance.

WATER COLUMN DATA

Water column data (.wcd format) was acquired for the survey site as an additional dataset. The processing and reporting of these datasets is beyond the scope of this report, and a separate project request would be required to process these data and provide associated products.

SOUND VELOCITY CORRECTION

The Valeport Monitor SVP was hand deployed to provide sound velocity profiles for the EM2040c. Only 100 m of rope was available for deployment. The profile data was downloaded using Valeport's DataLog Express software. Profiles were extended and saved into the Kongsberg .asvp format using Ifremer DORIS software.

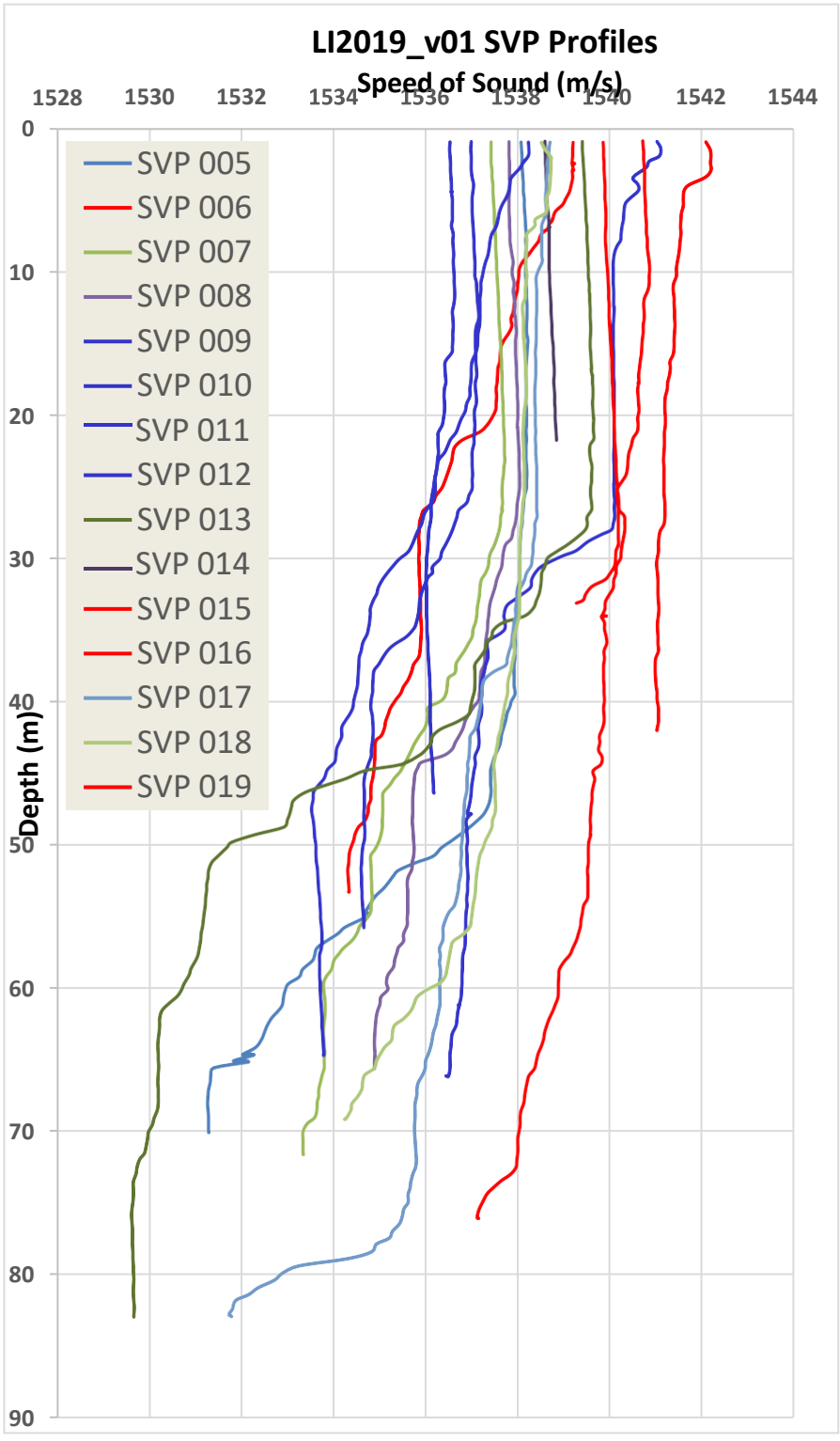

Figure 34 Sound Velocity Casts.

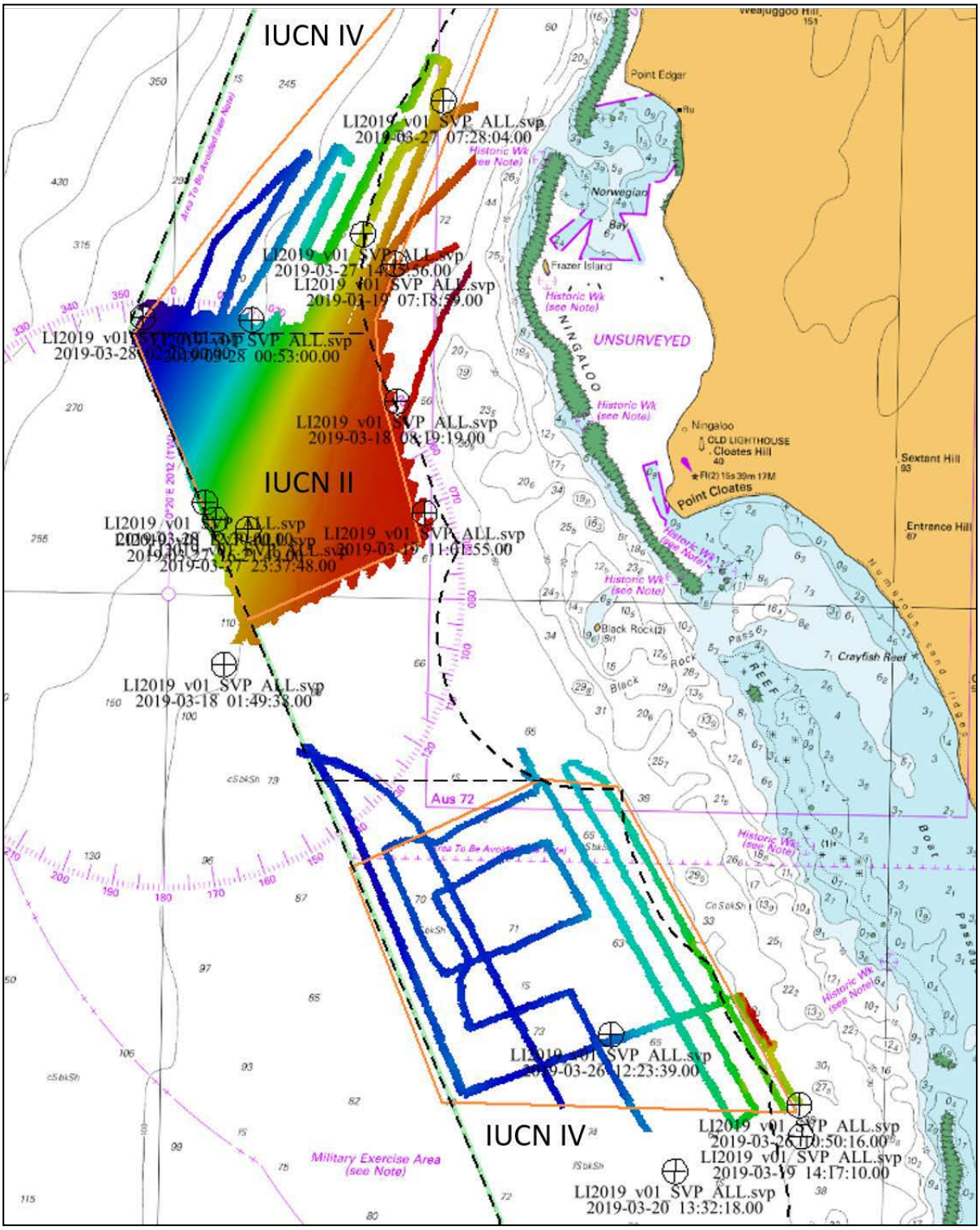

Figure 35 Sound Velocity Profile locations.

TIDAL DATA PROCESSING

Tidal reduction of acquired data was performed by calculating a GPS tide in CARIS HIPS and SIPS based on the Applanix PosMV and Marinestar G4+ ellipsoidal height. A text file containing Ausgeoid09 values (AUSGeoid09_GDA94_49K.txt) was applied to bring the ellipsoidal height to the AHD datum.

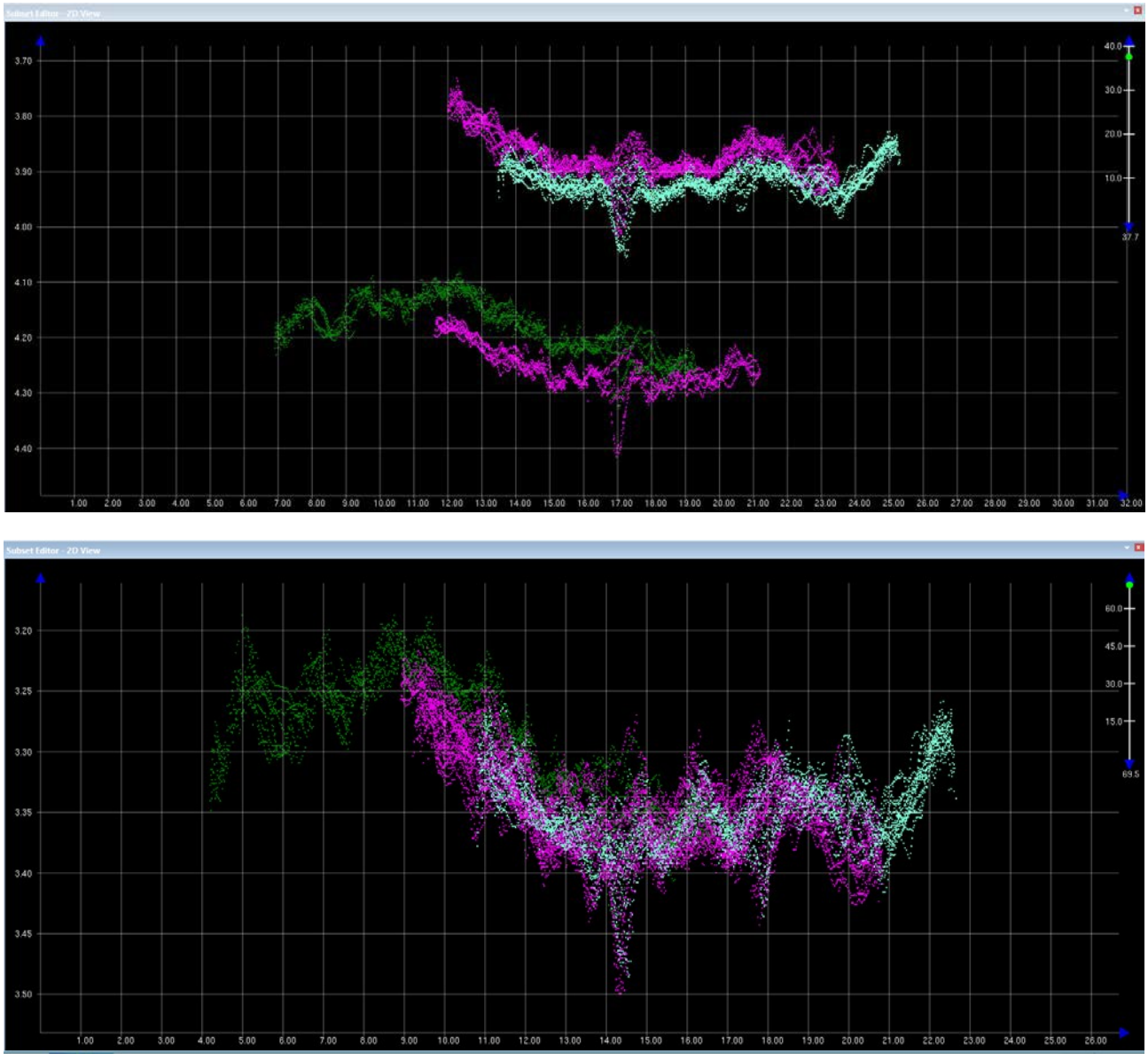

Figure 36 Before and after application of GPS Tide on transit data into Coral Bay.

WATERLINE

Waterline measurement used with reference to the sonar setup, was determined to be -1.23 m. This value is based on measurements taken alongside at Hillarys Boat Harbour prior to departure.

4.5 Vessel configuration

4.5.1 Sensor offsets

Sensor offsets on-board (online) the RV Linnaeus are summarised in Table 9. The offsets are derived from measurements taken during the dimensional survey conducted by McMullenNolan Group in 2012 and outlined in the document "Linnaeus Vessel Multibeam System Parameters".

Table 9 Sensor Offsets (as per POS MV sign convention).

SENSOR	X OFFSET FORWARD +VE (M)	Y OFFSET STARBOARD +VE (M)	Z OFFSET +VE DOWN (M)
Sonar Head 1 – EM2040c	0.000	0.000	0.000
Ref to IMU	-0.001	-0.008	-1.562†
Ref to Primary Antenna (Port)	2.175	-1.408	-5.881‡
Ref to Centre of Rotation	0.000	0.000	-1.227
Waterline			-1.23

**Please note that the offsets between the RP, IMU and the primary GNSS antenna are reduced by the POS MV before being sent to the EM2040C PU. With the RP set as the EM2040C Transducer acoustic centre offset values of 0,0,0 were entered into the SIS acquisition software for Sonar head location.*

†Reference to IMU value derived from li2017_v18 survey report. The value 1.457m from this report uses the Seapath MRU5+ IMU, not the Applanix PosMV Type 65 IMU, and a RP located at the IMU.

‡Reference to Primary Antenna Z offset used the L2 Phase centre value of 0.066m above the ARP (antenna reference plane).

4.6 Calibrations and checks

4.6.1 Pre-survey calibrations

POS MV

The POS MV was calibrated by 18th March 2019. The calibration, called a GAMS calibration, required manoeuvring of the vessel to induce velocities in the IMU. As such figure of eight style manoeuvres were conducted by the vessel while logging data. The calibration converged in real time and produced a baseline vector between the primary and secondary antennas as shown in Table 10.

Table 10 POS MV GAMS Calibration Values.

CALIBRATION	X VECTOR (M)	Y VECTOR (M)	Z VECTOR (M)
GAMS (Pri to Sec GNSS)	0.027	2.701	-0.027

PATCH TEST CALIBRATION

The patch test calibration of the EM2040C multibeam was conducted on 18th March 2019 over a feature off the reef edge just outside Bateman Bay. The position of the patch test calibration was: 23°03.91 S 113°44.79' E

The water depth range was between 15m and 32m.

Some underwater features were noticed while transiting from Coral Bay to Area 5 that may provide a more suitable patch location for future surveys in the area.

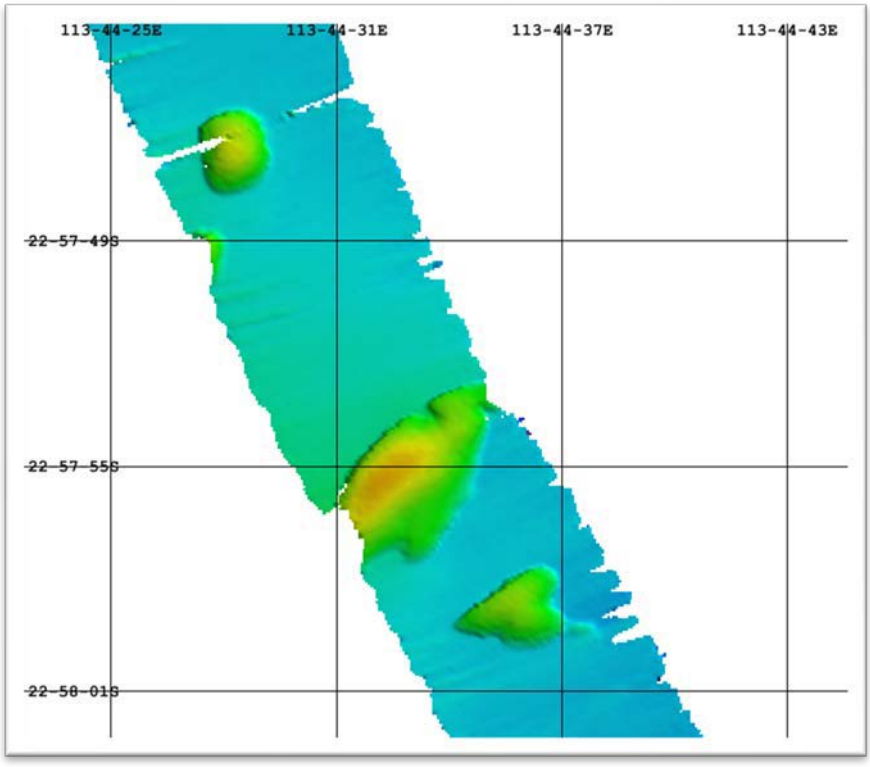

Figure 37 Future Patch Test Location.

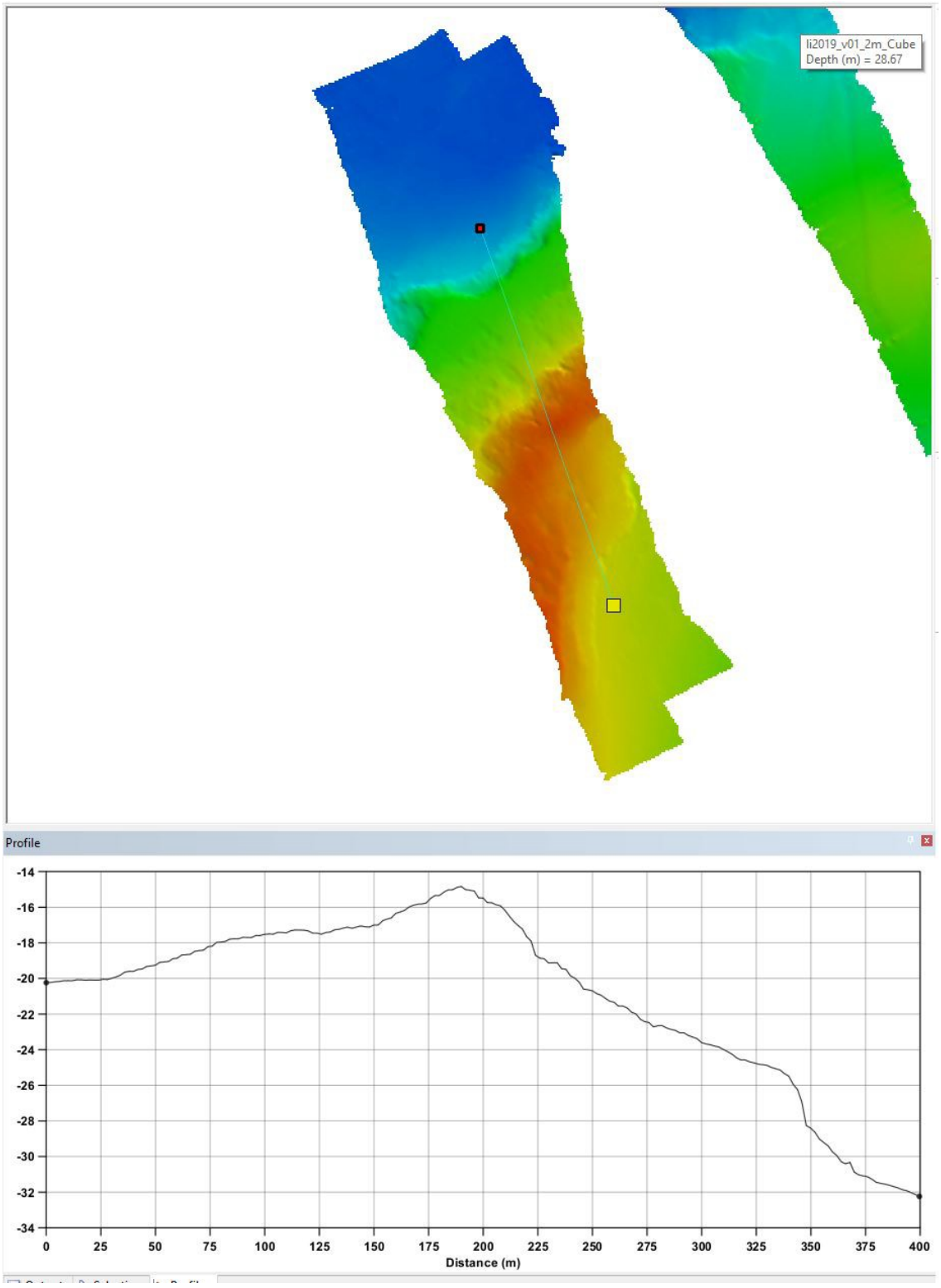

Figure 38 Chosen Patch Test Location

Table 11 Patch Test Calibration Values.

SENSOR	PITCH (°)	ROLL (°)	YAW (°)
EM2040c	0.58	-0.90	0.55

The angular offsets in SIS were left as 0,0,0 and the patch test values were added into the CARIS vessel file and applied to .all files upon import into CARIS HIPS and SIPS.

POSPAC CONFIRMATION OF LEVER ARMS AND GAMS VALUES

GAMS calibration and lever arm values were confirmed by post-processing the POS MV "000" data in POSPac MMS 8.3. The 000 files chosen for processing were from the 18th March. This POSPac processing confirmed the GAMS calibration and the X and Y offset for the Primary Antenna Lever Arm, it also highlighted a difference of 0.149 m in the entered and processed value of the Primary Antenna Z value offset that would need further investigation. The post processed offsets are presented in Table 12 and Table 13. Because of their magnitude the post-processed offsets were not applied to the data via the SBET.

Table 12 POSPac derived Offsets.

SENSOR	X OFFSET FORWARD +VE (M)	Y OFFSET STARBOARD +VE (M)	Z OFFSET +VE DOWN (M)
*Port GNSS Antennae (Pri)	2.173	-1.411	-6.030

Table 13 POSPac derived Heading Vector.

CALIBRATION	X VECTOR (M)	Y VECTOR (M)	Z VECTOR (M)
GAMS (Pri to Sec GNSS)	0.033	2.699	-0.022

DEPTH CHECKS

Depth checks were performed alongside in the Hillarys berth to test depth values from the multibeam against a dip tape value. The results are summarised in Table 14.

Table 14 Depth Checks alongside Hillarys Boat Harbour.

Date	Line #	EM2040C Depth (m)	Dipped/Tapped Depth (m)	Difference
12/03/2019	0001	6.82	6.81	0.01
12/03/2019	0003	6.70	6.80	-0.10
13/03/2019	0004	6.65	6.67	-0.02
14/03/2019	0006	6.53	6.55	-0.02

WATER LEVEL CHECKS

While alongside in the Hillarys berth, water level checks were performed. The water level checks involve the logging of multibeam data (GPS Height) and comparing this to the water level readings from the Hillarys Tide Gauge. This check confirms the vertical measurements for the GPS antenna offset and the waterline offset.

Table 15 Water Level checks, Hillary's Boat Harbour.

Date	Line	Time (UTC)	CARIS GPS TIDE (AHD)	HILLARY'S GAUGE (LAT)*	DIFFERENCE LAT to AHD†
12/03/2019	0001	04:20	0.41	1.05	0.64
12/03/2019	0002	06:02	0.39	0.98	0.59
12/03/2019	0003	06:10	0.42	1.00	0.58
13/03/2019	0004	02:28	0.24	0.90	0.66
13/03/2019	0005	07:50	0.27	0.91	0.64
14/03/2019	0006	01:55	0.33	0.83	0.50
				Average	0.60
				Standard Deviation	0.06

**Tide gauge data adjusted by +0.06m based on tide board readings taken at Hillary's Boat Harbour tide board.*

†AusTides 2019 quotes LAT 0.56m below MSL.

The Hillarys Station (ANTT=62237, BoM=009265) is a continuously recording tide gauge operating as part of the Australian Baseline Sea Level Monitoring Project. The six minute tide data was supplied by the Bureau National Operations Centre (BNOC). The water level checks are summarised in the Table 15.

4.7 Geodetic parameters

The differential corrections supplied to the POS MV were referenced to the International Terrestrial Reference Frame (ITRF2014). The Global Positioning System (GPS) is referenced to the World Geodetic System 1984 (WGS84). Many providers of satellite positioning services however have receivers which output referenced to the International Terrestrial Reference Frame (ITRF). Due to continual refinement annually of the WGS84 reference frame, the WGS84 and ITRF2014 reference frame are considered to be the same.

4.7.1 ITRF2014 datum and projection

Table 16 ITRF2014 Datum Description.

DATUM DESCRIPTION	
Datum	ITRF2014 (Epoch 2010.0)
Ellipsoid	Geodetic Reference System 1980 (GRS80)
Semi-major Axis (a)	6 378 137.000m
Semi-minor Axis (b)	6 356 752.314m
Eccentricity Squared (e^2)	0.006 694 380
Flattening (1/f)	298.257 222 101
Projection Type	Universal Transverse Mercator (UTM)
UTM Zone	49 S
Central Meridian	111° East
Scale Factor at CM	0.9996
False Easting	500 000m
False Northing	10 000 000m
Latitude of Origin	0° (Equator)

5. IMAGERY FIELD TRIP REPORT

Authors: Anthea Donovan, John Keesing, Dirk Slawinski, Nick Mortimer, Melanie Orr, Karl Forcey, Craig Davey and Russ Babcock

Date: 31 May 2020

5.1 Field trip details

CSIRO field trip scientific personnel:

- Russ Babcock – PI
- Karl Forcey Field – Instrumentation
- Nick Mortimer – Data Management
- Craig Davey – Team Swath

Departure date: 15/3/19 (after mobilisation at Hillary's Boat Harbour, Perth)

Return date: 5/4/19 (with demobilisation at Exmouth)

Vessel: RV Linnaeus

Outline of trip:

CSIRO component

- 18th–20th March: Bathymetry and back-scatter
- 21st–25th March: No work due to TC Veronica
- 26th–28th March: Bathymetry and back-scatter
- 28th–30th March: Towed camera
- 30th March–1st April: Starbug AUV

University of Sydney component

- 2nd–4th April: Sirius AUV

This report covers the work done on the second half of the CSIRO field trip with the imagery acquisition (towed camera and Starbug work conducted by CSIRO), as well as the Autonomous Underwater Video (AUV) work conducted by USyd and Russ Babcock using Sirius. The bathymetric and back-scatter work has been already covered in a field trip report written by Craig Davey.

5.2 Objectives of the field trip

The aim of this component of the research trip was to deploy the towed camera system (Hobart Shallow Video) and the Starbug at pre-determined sites within Ningaloo Marine Park (Commonwealth Waters).

Following this leg of the trip, the University of Sydney came onboard with the AUV Sirius. Sites previously sampled 5 and 10 years ago were revisited.

5.3 Onboard methods

Table 17 Start and end date time and position of each of the Towed Camera sites visited.

Site	Start time	End time	Start position	End position	Mean Depth (m)
2818	28/03/2019 12:57	28/03/2019 13:14	22.7089S; 113.5104E	22.7031S; 113.5072E	185.5
2803	28/03/2019 14:21	28/03/2019 14:43	22.8183S; 113.6368E	22.8273S; 113.6409E	67.3
2812	28/03/2019 15:01	28/03/2019 15:23	22.8471S; 113.6635E	22.8572S; 113.6698E	65.4
2905	29/03/2019 8:33	29/03/2019 8:47	22.8777S; 113.6408E	22.8843S; 113.6444E	70.2
2907	29/03/2019 9:06	29/03/2019 9:24	22.889S; 113.6248E	22.8968S; 113.6306E	73.2
2909	29/03/2019 10:00	29/03/2019 10:25	22.8319S; 113.6216E	22.8373S; 113.6102E	71.0
2910	29/03/2019 10:43	29/03/2019 10:59	22.8379S; 113.5789E	22.8445S; 113.5814E	68.0
2906	29/03/2019 11:23	29/03/2019 11:39	22.8764S; 113.6039E	22.8817S; 113.6039E	68.5
2904	29/03/2019 12:23	29/03/2019 12:42	22.8714S; 113.6914E	22.8796S; 113.6941E	56.3
3014	29/03/2019 7:37	29/03/2019 7:58	22.6868S; 113.5661E	22.6818S; 113.5604E	74.9
3015	30/03/2019 8:20	30/03/2019 8:43	22.7264S; 113.5369E	22.7167S; 113.5408E	93.3
3019	30/03/2019 9:11	30/03/2019 9:32	22.7248S; 113.563E	22.7157S; 113.5653E	66.5
3023	30/03/2019 9:56	30/03/2019 10:14	22.6966S; 113.519E	22.6922S; 113.5215E	171.2
3020	30/03/2019 10:34	30/03/2019 10:54	22.671S; 113.5013E	22.6644S; 113.5031E	211.7
3017	30/03/2019 11:16	30/03/2019 11:36	22.6458S; 113.5312E	22.6396S; 113.535E	210.5
3016	30/03/2019 11:52	30/03/2019 12:15	22.6326S; 113.5572E	22.6248S; 113.5614E	155.2

5.3.1 Towed camera

The camera system used to obtain video images of the seafloor was the Hobart Shallow Towed Video system. It is comprised of a Global Bionic Optics 1080HD video camera and a Canon EOS 700D DSLR with a Canon EF 24mm f1.4L USM lens and two Quantum strobes. The system was connected to an onboard computer by a single mode sea cable. The vessel's hydraulic pump was used to power the winch which controlled the retrieval and deployment of the camera system.

Sixteen sites were towed (Table 17) with a maximum of 245 m depth. They were approximately 20–30 mins in duration.

As the camera system was being towed and the live imagery recorded on the onboard computer via the optical fibre in the sea cable, video footage was being scored using Tappity.

5.3.2 Starbug

Starbug-X is a relatively small, lightweight, actively propelled AUV system. Its primary function is its vision system (housing 2 pairs of cameras), yet it is also equipped with oceanographic quality sensors. A 360fly camera was mounted onto Starbug and recorded video footage on 6 of the 18 missions (Table 18).

At the completion of each mission, the Starbug laptop was plugged in to the AUV's network port, and all the data and pictures were retrieved. Once this was done, the next mission file was loaded, the network cable disconnected and Starbug was redeployed. Images were analysed back in the lab after the completion of the field trip.

5.3.3 Sirius

At the conclusion of the CSIRO field trip, Russ Babcock stayed onboard while the other scientific staff disembarked. USyd staff boarded along with their AUV Sirius (http://marine.acfr.usyd.edu.au/systems/auv-sirius/).

Two deployments were made on the 2nd of April offshore of Tantabiddi and Multires, another was made on the 3rd off Yardie Creek and the final deployment was off Torpedo Bay. Data from this trip has been loaded onto the AODN and can be found here: https://auv.aodn.org.au/auv/ (under Ningaloo201904).

Table 18 Start and end date time and position of each of the Starbug missions. * indicates the 360fly camera was operational during that mission. ** indicates no images were obtained.

Mission No.	Start time	Finish time	Start position	End position
mu02	30/03/2019 16:53	30/03/2019 17:29	22.1025S; 113.8726E	22.097S; 113.8729E
mu02-2**	31/03/2019 8:16	31/03/2019 8:45		
mu023rd*	31/03/2019 9:20	31/03/2019 9:46	22.1024S; 113.8718E	22.1004S; 113.8697E
mu03	31/03/2019 10:09	31/03/2019 10:43	22.0758S; 113.8805E	22.0757S; 113.8765E
mg04*	31/03/2019 11:22	31/03/2019 11:56	21.984S; 113.908E	21.9852S; 113.9051E
mg01	31/03/2019 12:11	31/03/2019 13:01	21.9531S; 113.9141E	21.9527S; 113.9071E
mg01r*	31/03/2019 13:40	31/03/2019 14:30	21.9522S; 113.9108E	21.9496S; 113.9066E
tb02	31/03/2019 15:16	31/03/2019 15:50	21.9175S; 113.9227E	21.9151S; 113.9202E
tb04	31/03/2019 16:03	31/03/2019 16:58	21.9113S; 113.9287E	21.907S; 113.9238E
tb04_2*	31/03/2019 17:20	31/03/2019 17:47	21.9075S; 113.9257E	21.907S; 113.9238E
tb01*	1/04/2019 8:00	1/04/2019 8:40	21.8832S; 113.9486E	21.8794S; 113.9468E
hb01*	1/04/2019 9:18	1/04/2019 9:48	21.8274S; 114.0175E	21.8265S; 114.0148E
hb02	1/04/2019 9:57	1/04/2019 10:17	21.8196S; 114.0092E	21.8173S; 114.0115E
hb02_2**	1/04/2019 10:33	1/04/2019 11:02		
hb06	1/04/2019 11:22	1/04/2019 11:49	21.8157S; 114.0183E	21.8135S; 114.018E
hb06_02	1/04/2019 12:40	1/04/2019 13:32	21.8157S; 114.0187E	21.812S; 114.0168E
hb03	1/04/2019 13:55	1/04/2019 14:58	21.805S; 114.0306E	21.802S; 114.0258E
hb05**	1/04/2019 15:18	1/04/2019 16:06		

5.4 Site maps

5.4.1 Towed camera

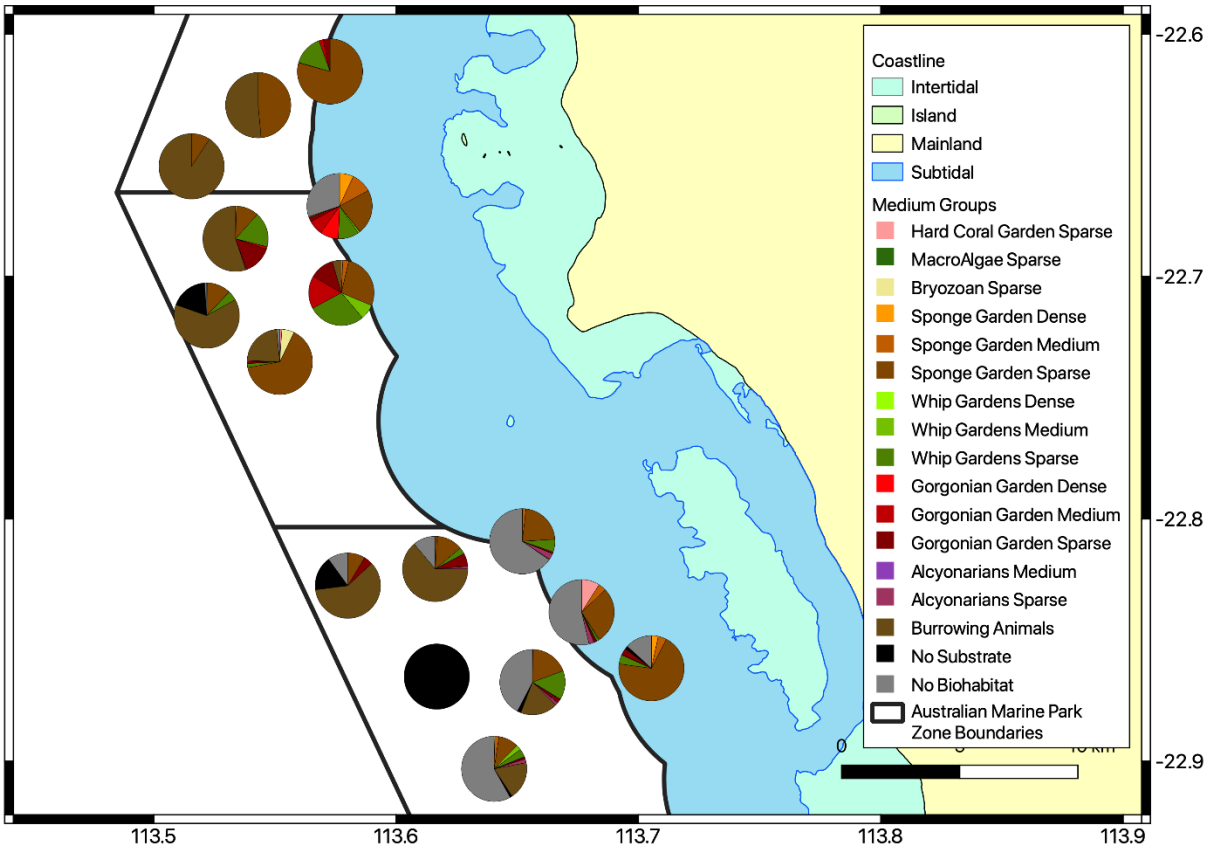

Figure 39 Map of southern Ningaloo showing midpoint location of each camera tow along with proportional breakdown of habitat observed along that transect. “No substrate” is defined when the camera is tilted upwards and the seafloor cannot be seen on the footage.

5.4.2 Starbug

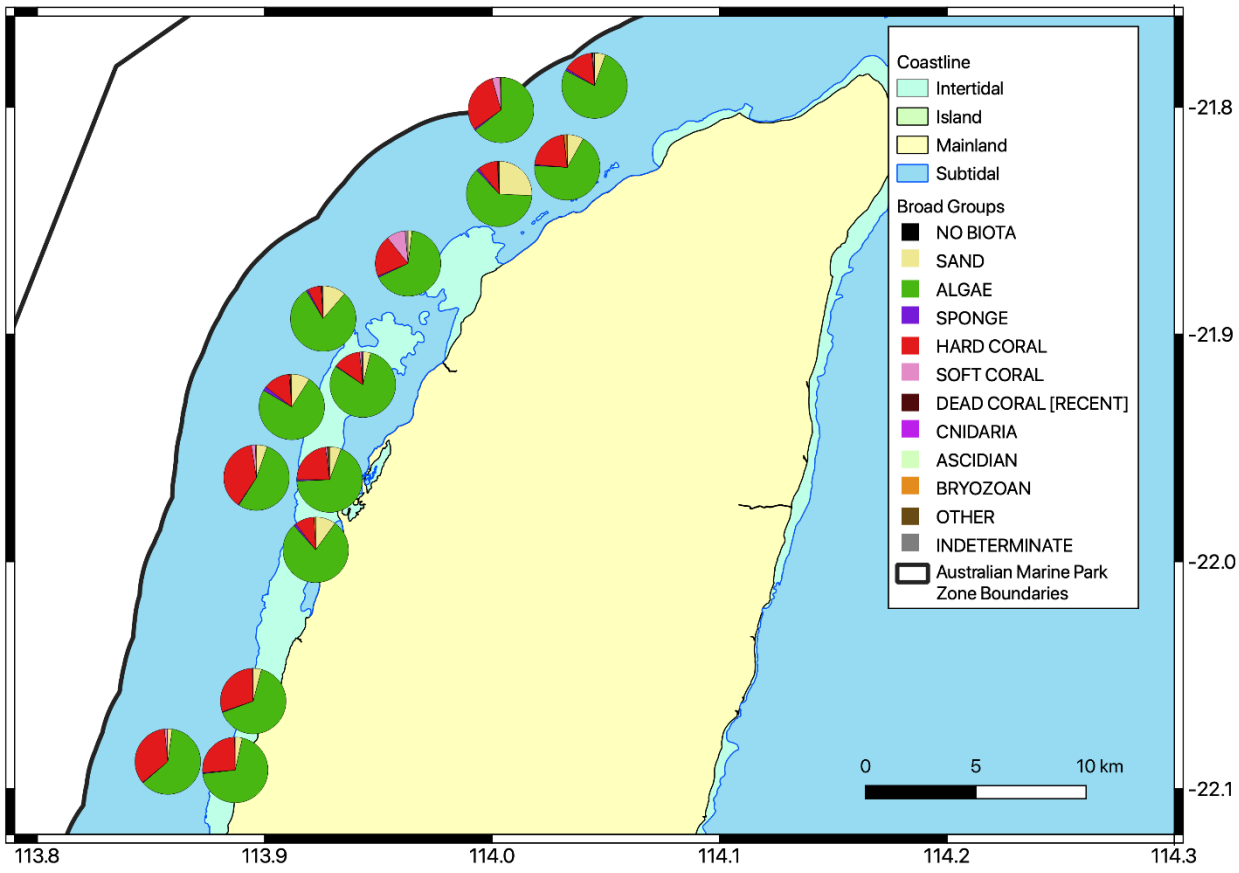

Figure 40 Map of northern Ningaloo showing midpoint location of each Starbug mission along with proportional breakdown of habitat observed along that transect.

5.4.3 Sirius

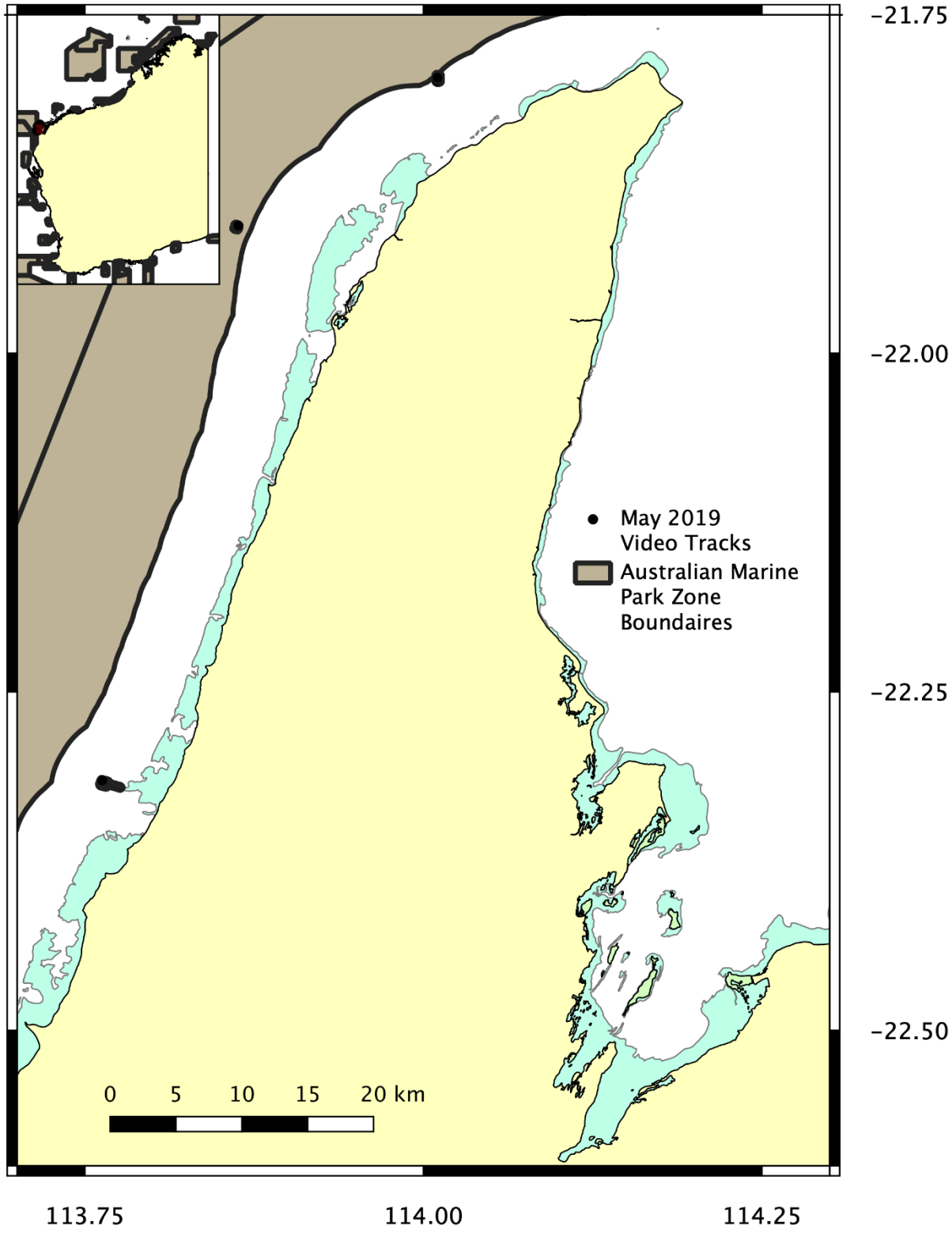

Figure 41 Map of Sirius sites sampled during the University of Sydney component of the field trip.

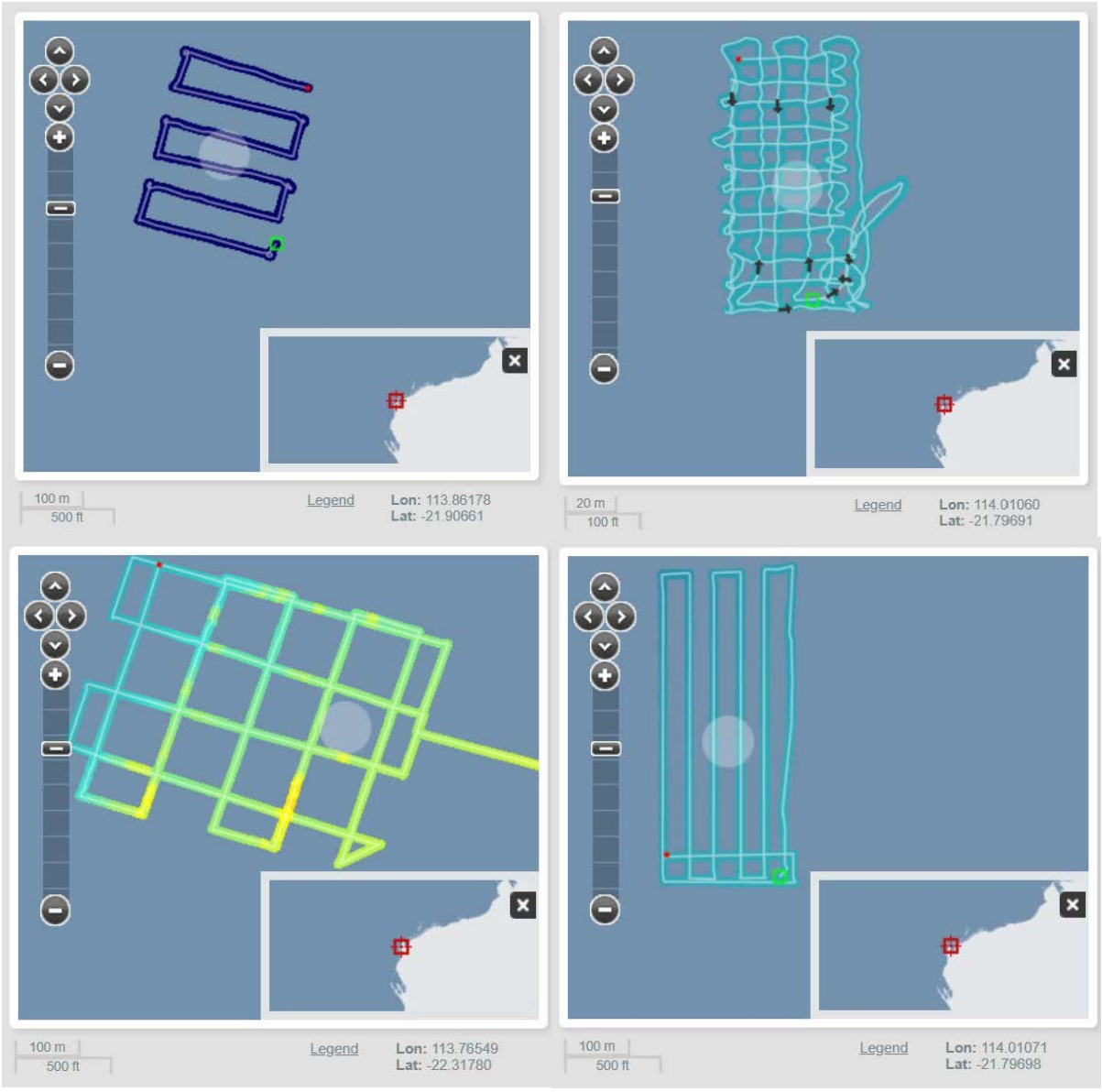

Figure 42 Tracks from the Sirius AUV captured off Tantabiddi (upper left panel),Multires (upper right panel), Yardie Creek (lower left panel) and Torpedo Bay (lower right panel).

6. CLASSIFYING DEEP REEF SUBSTRATA AT NINGALOO MARINE PARK

Authors: Simon Collings, Norm Campbell, Mark Tonks, Anthea Donovan and John Keesing

Date: 31 January 2021

6.1 Abstract

Data from multibeam echosounder surveys taken as part of the Ningaloo Outlook project are classified into various seafloor cover types according to their hardness, rugosity and depth. The classifications are validated with towed video ground truth where it is available. Three AOIs are classified, two that were explicitly part of the Ningaloo Outlook Deep Reefs project and a third transect that was acquired incidentally while RV Investigator was transiting between locations. Due to the nature of the acquired data, two different approaches were taken for the classification, the first approach used multibeam backscatter angular response curves along with rugosity as input to a maximum likelihood classifier. The second approach used flattened multibeam backscatter (i.e. with the angular effects removed), along with rugosity as inputs to a Random Forest Classifier. Estimates of the accuracy of the classifiers are produced, where possible, along with area statistics for the different substratum observed in the classified maps.

6.2 Introduction

This report details the methods used to form classified underwater substrate maps. The maps will be useful for ecological assessments and to form baselines to assess any environmental damage that may occur in the reefs as a result of human activity, such as tourism, fishing or transport through the region.

6.3 Study areas

Figure 43 shows the locations of the three AOIs relative to the Northwest Cape in Western Australia.

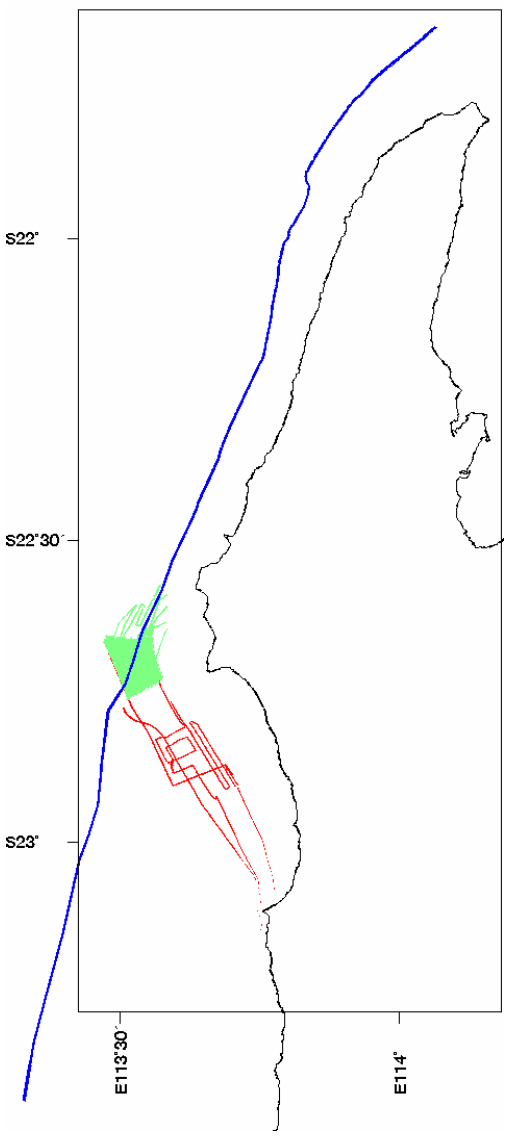

Figure 43 Three AOIs: Area 3A (green), Area 5 (red) and the 120 m transect (blue). Boundaries for the marine park can be seen in Figure 2.

6.3.1 Area 3A

Area 3A consists of densely acquired multibeam swaths over a portion of the Ningaloo reef. The water depth was between approximately 40 and 250 m.

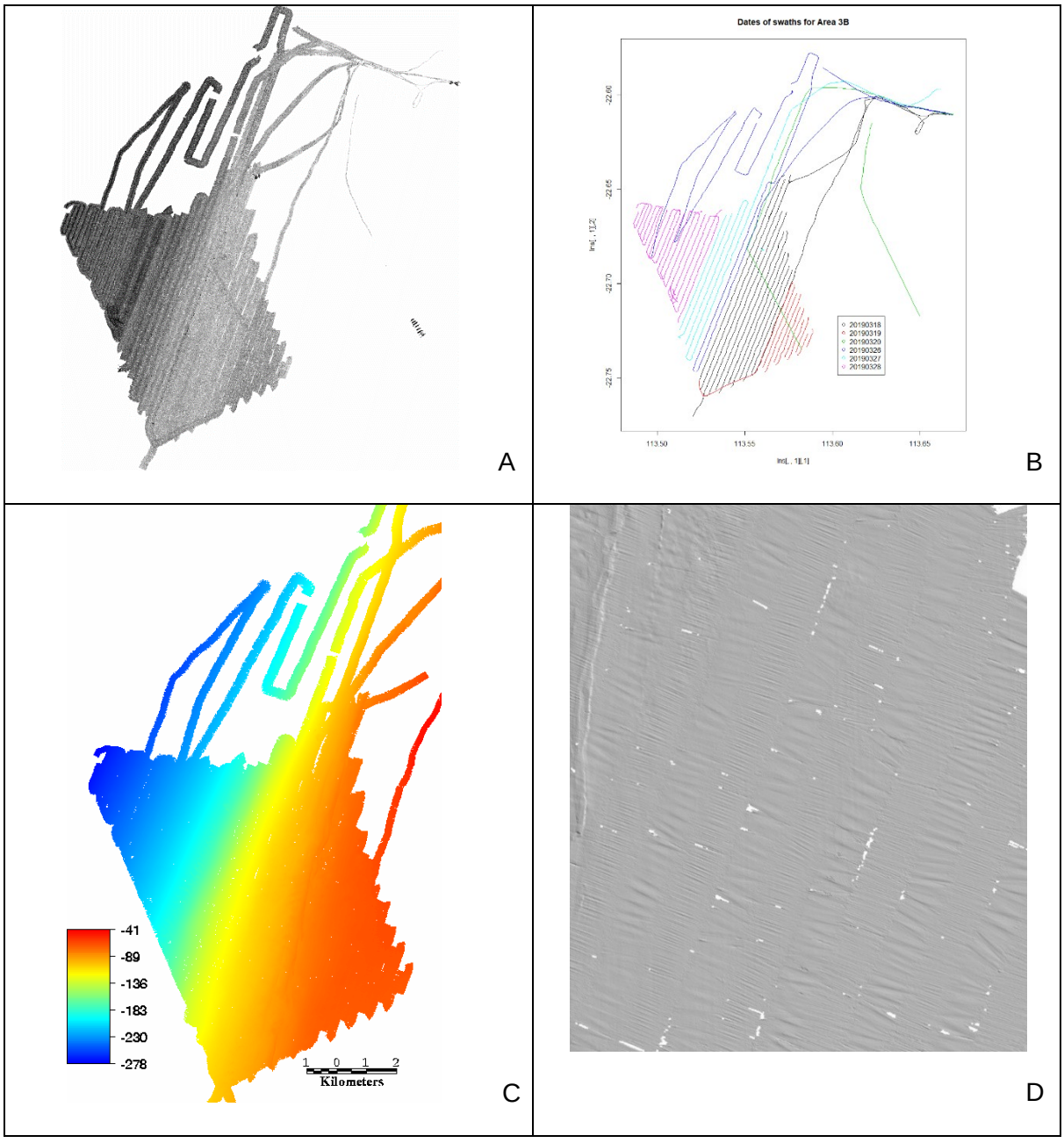

Figure 44 A. Multibeam backscatter image from Area 3A. B. The dates of that the swaths were acquired. C. Bathymetry from Area 3A. D. Relief image of the bathymetry shows patterning according to the ship motion.

Note that the weather was sub-cyclonic, so there was difficulty processing the depth and we are left with artefacts, especially in swath directions with following seas. The depth, weather and settings on the instrument made the angular response curves of the backscatter unsuitable for classification, so only the depth and texture/rugosity, along with the “flattened” backscatter was used for the classification.

Figure 44 shows a collection of input data for Area 3A.

6.3.2 Area 5

This area is immediately to the south of Area 3A. The depth in this region is predominantly between 40 and 80 m. There is incomplete swathing of this area compared to 3A.

The weather was comparatively calm, so backscatter maps are reasonably good. Figure 45 shows backscatter from Area 5.

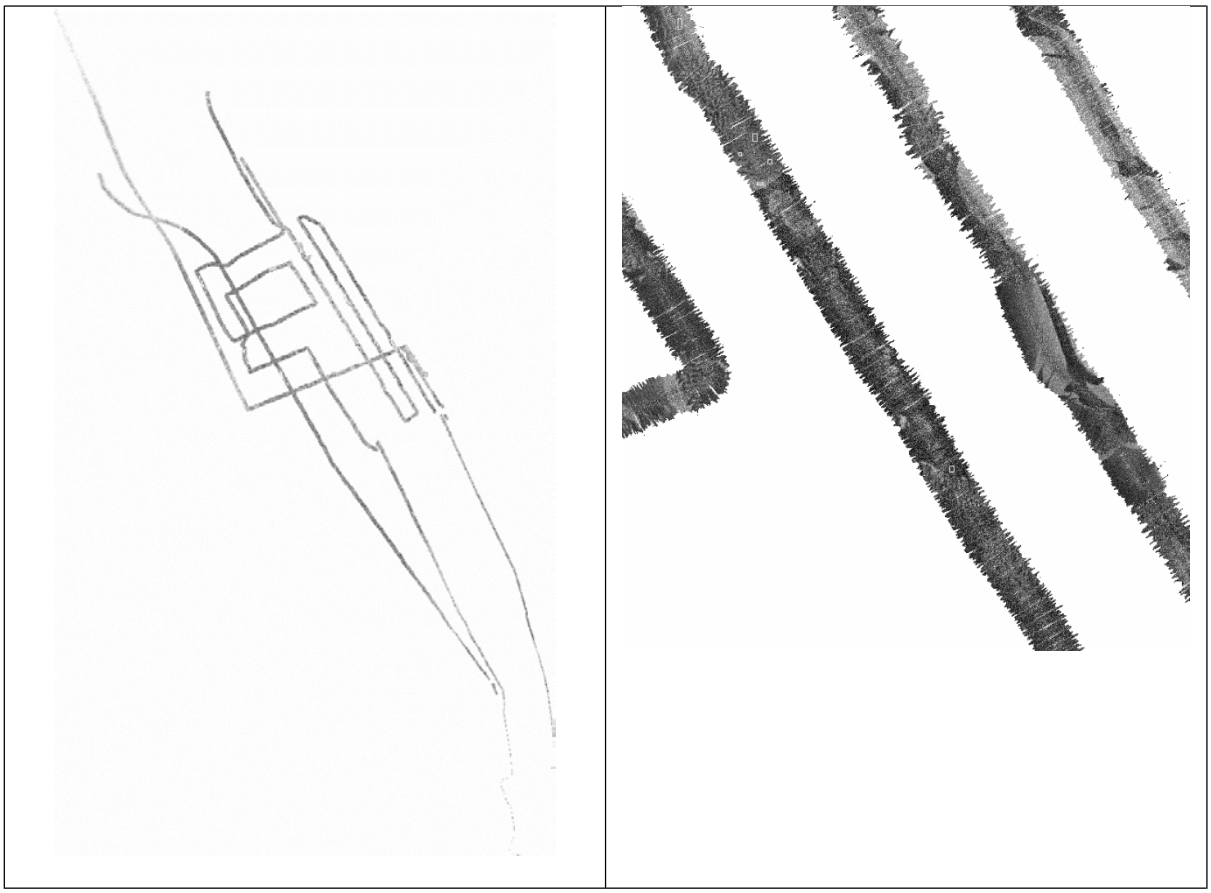

Figure 45 A. An overview of Area 5 backscatter. B. Detail of Area 5 backscatter.

6.3.3 120 m transect

This transect was opportunistically acquired in the study when RV Investigator was transiting past on another mission in 2017. The transect roughly follows the 120 m bathymetric contour, and this takes it through the middle of Area 3A. The data consists of "flattened" backscatter and depth, from which we have calculated several different resolutions of rugosity. Figure 46 shows a small segment of the bathymetry (it's around 120 m depth) and the backscatter for this transect.

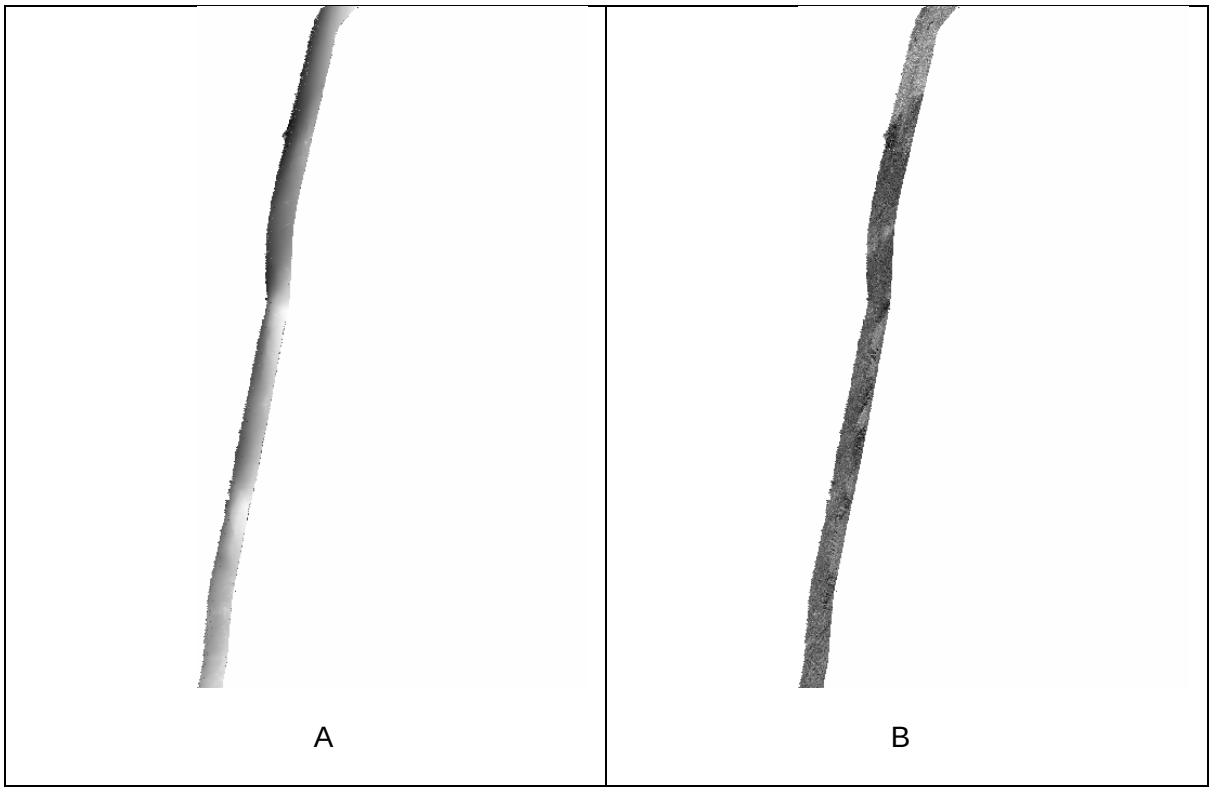

Figure 46 A. Extract of the 120 m transect bathymetry. B. Extract of the 120 m transect backscatter.

6.4 Methods

6.4.1 Towed video ground truth

Ground truth for the substrate mapping was in the form of towed video. The camera system used was the Hobart Shallow Towed Video system. It is comprised of a Global Bionic Optics 1080HD video camera and a Canon EOS 700D DSLR with a Canon EF 24 mm f1.4L USM lens and two Quantum strobes. The towed video was interpreted by benthic habitat experts and this was used to provide labels for pixels so that classifiers could be trained and validated in Area 3A and Area 5 (see Appendix – Ground Truthing). Figure 47 shows some example images of the towed video.

There was no ground truth available for the 120 m transect, except where it overlaps with Area 3A.

Figure 47 Example images from the towed video.

6.4.2 Flattened backscatter

For the classifications of Area 3A and the 120 m transect, a “flattened” (i.e. with angular effects removed) backscatter image was employed. Using QPS FMGT software, the MBES backscatter image was normalised to the values at 40 degrees off nadir and the individual swaths were feathered and adjusted to give a coherent result.

6.4.3 Slope-corrected roughness (rugosity)

Slope-corrected roughness is a measure of local standard deviation over an NxN window, with the background slope removed, so that only the surface roughness contributes to the result. If the slope is not removed, the standard deviation over such a window may be high because the slope is quite steep, although the surface itself is smooth. By removing the slope effect, we can estimate the roughness separately from the slope.

To create the slope corrected roughness at each point, an NxN window centred at the point was selected. For each row and column of the window, the median depth was calculated. For every row of the window we subtract the row median depth. For every column of the window we subtract the column median depth. After this, we calculate the standard deviation of the window as the roughness value.

6.4.4 Random forest classifiers

To classify the substrata types in the Area 3A and the 120 m transect AOIs, the random forest classification technique (Breiman 2001; Cutler et al. 2012) was employed. Random forest classification is based on an ensemble (forest) of decision trees, which are each created by randomly sampling the training samples, creating a set of independent classifiers for each of the randomly selected training sets. To classify a new pixel (i.e. not in the training set), it is classified according to each of the trees in the ensemble and the one class with the most votes becomes the random forest classification. If probability estimates for each class are required, then the proportion of votes for each class are used.

The random forest classifier is able to intrinsically estimate the classification error for a given training sample, by considering the trees that were trained on subsets that did not include that sample, however this estimate is often optimistic (i.e. the estimated accuracy is higher than reality). For this reason, we have separately split the ground data into training and validation sites, to allow an independent estimate of the error.

6.4.5 MLC applied to backscatter angular response curves

For Area 5, the backscatter was deemed to be of sufficient quality that the methods from our previous Ningaloo reef work could be employed. This is briefly outlined below.

Angular response curves

The premise behind the use of backscatter-incidence-angle response curves is that the AR curves are an "*intrinsic property*" of the seafloor (Fonseca et al. 2009, Hamilton and Parnum 2011), and therefore there is information regarding the observed substratum embedded within the multivariate data of the response curves. This means that the shape of the curves as well as the overall level of the returned value provides statistical information on the bottom substratum.

To standardise the backscatter curves and remove noise, they are linearly interpolated to 200 equal size beam angles, mean-smoothed across the track with a moving window of size 11.

Maximum likelihood

In the well-known technique of maximum likelihood classification (MLC; Hastie et al. 2001), KK classes of interest are selected from the NN-dimensional input data, using expert knowledge and ground truth. The classes are assumed to be multivariate Gaussian (at least for the key input variables).

While MLC is reasonably robust to non-Gaussian distributions, it is crucial that the distribution of the sites is at least unimodal, otherwise the output can be nonsensical as their mean may lie between two or more modes of the distribution and be unrepresentative.

The training sites are used to estimate the assumed Gaussian distribution of each of the $kk = 1, \dots, KK$ classes by forming the covariance matrices Σ_{kk} (need a hat) and rendering the explicit formula for the likelihood:

$$LL_{kk}(XX) = \frac{1}{(2\pi)^{nn/2}\left|\Sigma_{kk}\right|^{1/2}} \exp\left[-\frac{1}{2}(XX - \mu_{kk})\Sigma_{kk}^{-1}(XX - \mu_{kk})\right],$$

where XX is the vector of inputs, $\hat{\mu}_{kk}$ the estimated class means, $\hat{\Sigma}_{kk}$ the estimated class covariance matrices and NN the number of input variables. In the classical technique, each new data point to be classified is then evaluated for each likelihood for each class. By normalising these values, we obtain the posterior probabilities of class membership. If no further information is available, classes can then be assigned to whichever has the greatest posterior probability. Additionally, a calculation using the chi-squared or F distribution provides the *typicality* of that class assignment, which is the probability that an object of that class is to be found at that distance from the class centre (Campbell 1984, deJong and van der Meer 2007). When the maximum likelihoods for a large number of pixels have low typicalities, this indicates that additional training classes may be needed to describe the data in the map.

With the training sites derived using the methods from the previous section, we can use MLC with any choice of variables that we wish. To produce a result comparable to Hamilton and Parnum 2011, we can classify half or whole pings into their various classes, or we can take a moving window (of any size) from the angular response curves and classify the centre beam angle of the window.

To incorporate rugosity into the classification, the moving window values are augmented with the mean rugosity over that window.

6.4.6 Markov Random Field updating

To account for the spatial relations and cohesiveness of the substrata classes, the technique of Markov Random Field updating is employed (Besag 1986, Berthod et al. 1996, Benedek et al. 2015). To do this, we consider each pixel to be classified in turn and look at the posterior probabilities that have been assigned to its neighbours. We want to weight the posterior probability of the centre pixel with the local prior information that comes from the neighbouring pixels. One possible approach is as follows. For each neighbour that has been classified as class *i*, the posterior probability of the centre pixel being class *i* is increased by a factor of $\beta\beta$, weighted by the inverse distance of the neighbour to the pixel. The new probabilities are stored, and then all of the labels are simultaneously updated.

After several iterations of this process, the labels converge to a "smoother" set of labels, with more coherent groups of classes. Setting the parameters ($\beta\beta$, the number of iterations and the size of the neighbourhood) is done by trial and error.

6.4.7 Validation

For Area 3A and Area 5, validation sites are randomly picked from the ground truth sites.

6.4.8 Morphological filtering

To remove fragments of cover that are likely to be spurious artefacts, the results can be filtered so that only connected segments of seafloor types above a certain area are left. The small fragments are removed and then the holes are filled with a modal filter. This filter was applied to remove segments of pixels that were less than 500 m in area for non-reef classes in the each of the AOIs. This made a significant difference to the appearance of the maps as many small fragments of cover were cleaned up.

6.5 Results

6.5.1 Area 3A

The map for Area 3A was classified with the Random Forrest algorithm, using a combination of flattened multibeam backscatter (MBBS), bathymetry and rugosity as described above for N=7, N=21, N=41 and N=101 (Figure 48). The processing was completed on a 2 m grid.

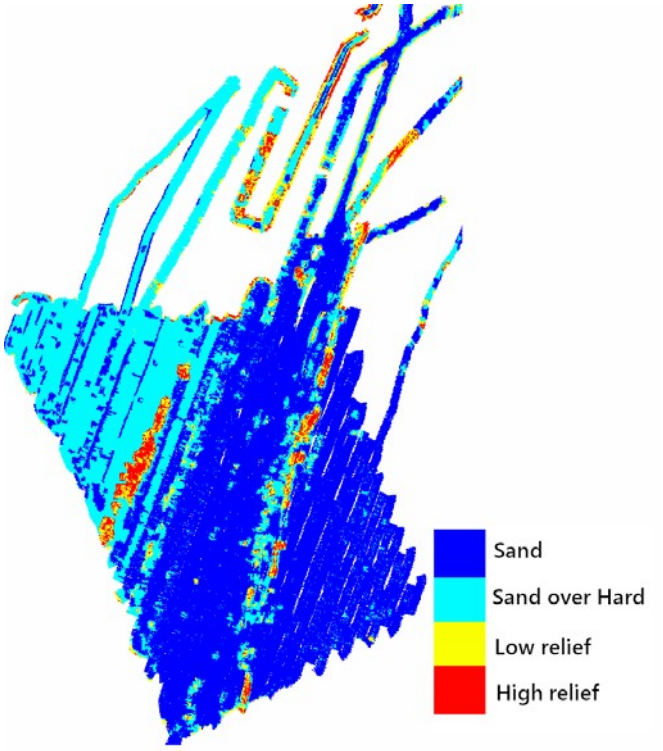

Figure 48 Area 3A classified into 4 classes.

For this region, there were some highly textured areas of the bathymetry that were deemed to be relevant to the substrate classification, so these were included as classes although they were not observed in the ground truth video. If it is desirable to remove these classes so that the integrity of the ground truth is observed, they should be relabelled to the “Sand over Hard” class. The maps were cleaned up using morphological filtering to remove small fragments of non-reef classes.

Table 19 shows the confusion matrix for the Area 3A classification, while Table 20 shows the summary statistics for each of the substrata.

Table 19 Confusion matrix for Area 3A classification.

		Predicted			
		Sand	**Sand over Hard**	**Low relief**	**High relief**
Observed	**Sand**	1363	108	0	0
	Sand over Hard	53	227	0	0
	Low relief	0	1	377	253
	High relief	0	35	47	426

Table 20 Total areas of each class in Area 3A.

Substratum	Area (square kilometres)
Sand	58.7
Sand over Hard	30.5
Low relief	5.7
High relief	3.3
Total	**98.1**

6.5.2 Area 5

There were only two main classes identified in the ground truth video for Area 5: Sand and Sand over Hard. None-the-less, an effort was made to extract an additional, intermediate class from the data, with mixed results. Figure 49 and Figure 50 show the results of these two efforts.

Table 21 shows the 2-class confusion matrix for the Area 5 classification, while Table 22 shows the summary statistics for each of the substrata. The 3-class confusion matrix for this area is shown in Table 23.

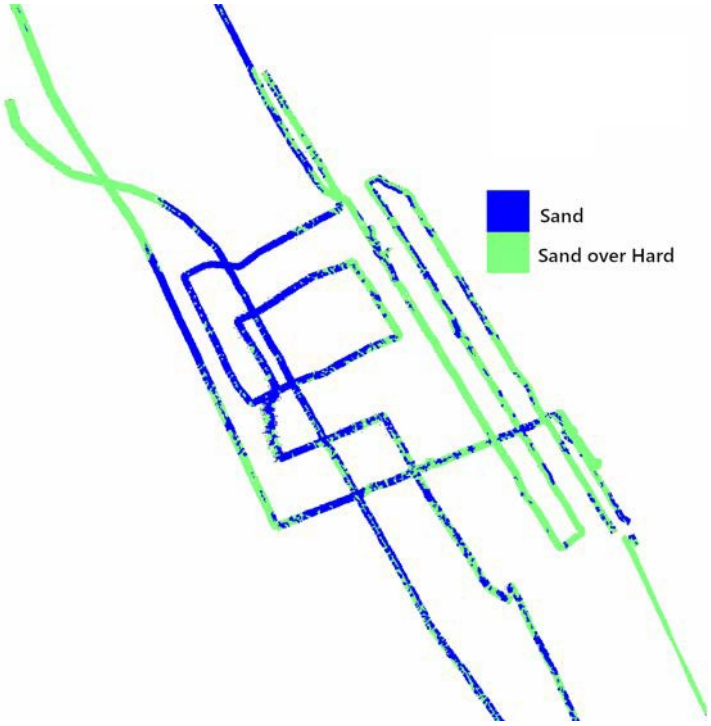

Figure 49 2- class classification of Area 5.

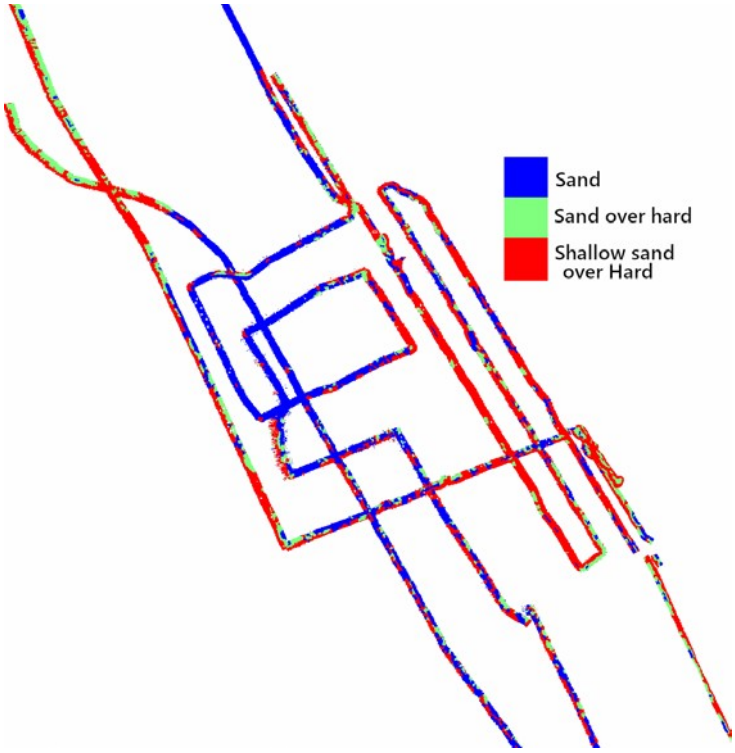

Figure 50 3-class classification of Area 5.

Table 21 Confusion matrix for 2-class classification of Area 5.

		Actual	
		Sand	**Sand over Hard**
Observed	**Sand**	168	0
	Sand over Hard	14	125

Table 22 Total areas of each class for Area 5.

Substratum	**Area (square kilometres)**
Sand	20.7
Sand Over Hard	33.8
Total	**54.5**

Table 23 Confusion matrix for 3-class classification of Area 5.

		Actual		
		Sand	**Sand over Hard**	**Shallow sand over Hard**
Observed	**Sand**	136	19	13
	Sand over Hard	13	55	71
	Shallow sand over Hard	0	30	123

6.5.3 120 m transect

Figure 51 shows the classifed 120 m transect.

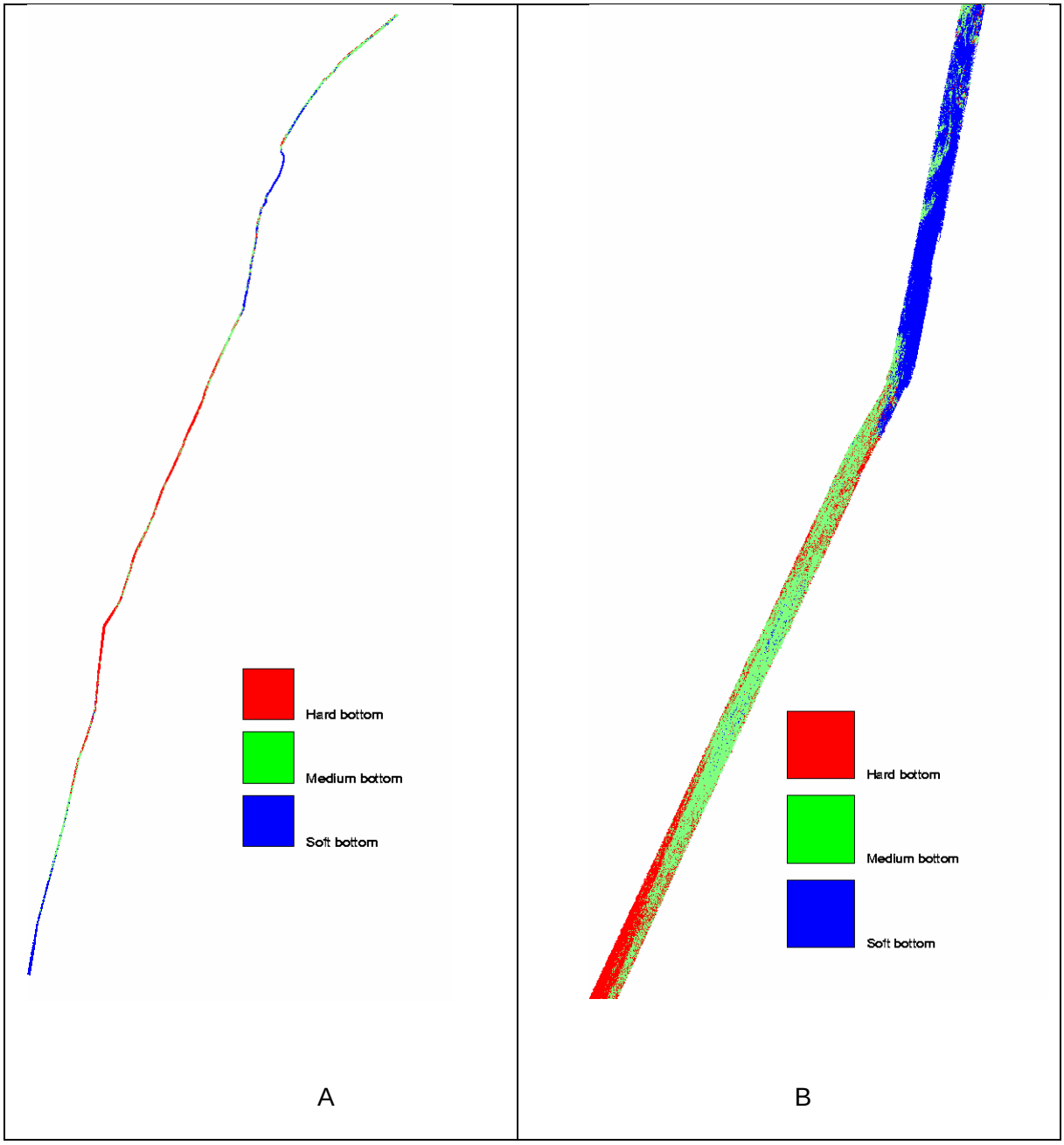

Figure 51 A. The classified 120 m Transect. B. Extract from the classified 120 m Transect.

Since there were no ground truth available for this AOI we are unable to estimate the accuracy of the classification. Table 24 shows the areas of each.

Table 24 Summary of the areas of each substratum type for the 120m transect.

Substratum	Area (square kilometres)
Soft Bottom	26.1
Medium Bottom	42.6
Hard Bottom	37.6
Total	**106.3**

6.6 Conclusion

With limited and noisy data, a pragmatic approach was taken to classify the seafloor into reasonable maps with a fair degree of confidence in the cover types.

For Area 3A the MBBS were not of sufficient quality to allow classification using angular response curves, so instead the flattened MBBS data were used. There was a lack of clarity in the MBBS, where normally distinct segments would be apparent in the harder areas of the seafloor. Regardless of this, it was apparent that there is a harder region in the west of this area, and this is visible in the backscatter. There are artefacts in the classification, in particular in the “Sand over Hard” region in the west, consisting of between-swath lines of only “Sand” class and blocks of sand class running along the tracks. These are unlikely to be real; instead they represent regions where the observed backscatter is not representative of its class due to extraneous effects. The highly textured areas of the image (i.e. high rugosity) were not photographed by the ground truth video, but are unlikely to be sand, which cannot settle over a certain steepness. It is speculated that these are sections of deep reef, but further investigation would be required to confirm this.

The Area 5 region contained superior MBBS, so the angular response curves were incorporated into the classification. This allows the shape of the curve to be used as part of our characterisation of the seafloor. Similarly to Area 3A, there were no direct observations of rocky reef in the ground truth video, but unlike Area 3A there were no clear indications from the rugosity that such areas exist in the region. Therefore, it makes sense to stick to the two classes observed in the ground truth video, rather that speculate about the existence of a third substratum. An effort was made to pick out an intermediate class based on the MBBS, but the results weren’t too convincing. One thing that stood out in the MBBS was the differences between the signals on either side of nadir, which necessitated training separately for each side. While every effort was made to choose appropriate representatives from the port and starboard sides, the result still shows some artefacts of this effect.

The 120 m transect presented some difficulties due to the lack of any ground truth at all. Therefore, pragmatic choices had to be made about what and how many classes could be gleaned from the data. This was performed by observing the different textures and hardness that were apparent in the MBBS and rugosity images. Ultimately the three classes must be validated to improve confidence in their labels and locations.

Bathymetric data from these analyses were used, in part, for the development of the sampling design of the NESP offshore Ningaloo baited remote underwater video study which

was conducted in August 2019. Details of how this data was used can be seen in Appendix – Developing bathymetry and topographic position index.

6.7 Appendix – Ground truthing

NB Some of the original content from this report has been removed.

Linnaeus EM2040c – interpretation of video stills Ningaloo March 2019

Mark Tonks and Anthea Donovan, CSIRO O&A St Lucia Qld

Norm Campbell, Perth WA,

in collaboration with

John Keesing, CSIRO O&A Nedlands WA

Simon Collings, CSIRO Data61 Perth WA

Overview and summary

Section 1.1 shows the multibeam tracks. Google Earth (GE) screen captures of the backscatter images are also shown. These are followed by a list of the mappings from the video files to the JSON log and tappity files to the multibeam tracks.

Section 1.2 shows images extracted from the videos for the tracks listed in Section 1.

Section 1.3 provides details of the interpretation for some of the tracks in area 3A. An edited email trail is included, to show how the interpretation proceeded.

Section 1.4 provides details of the interpretation for some of the tracks in Area 5. An edited email trail is included.

Section 1.5 provides a summary of the interpretation.

1.1 EM2040c multibeam backscatter tracks and images

The following images show the multibeam tracks for the two areas, 3A (left) and Area 5 (right), off Ningaloo.

The following images show the multibeam backscatter for the two areas, 3A (left) and Area 5 (right), off Ningaloo. The locations and numbering of the JSON files and video tracks are also indicated.

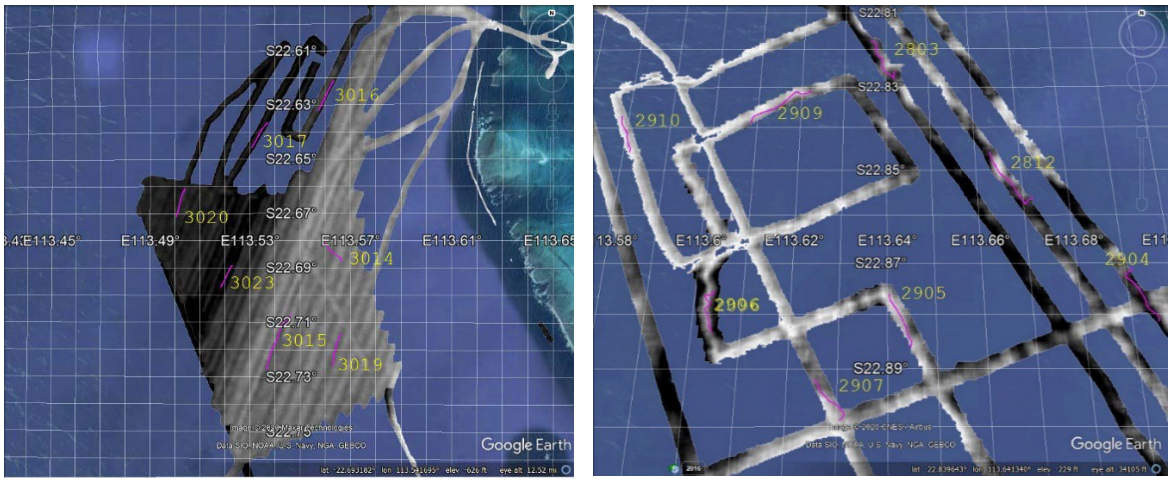

The following lists the mappings from the video files to the JSON log and tappity files to the multibeam tracks.

3A:

video file name (including tappity code)	central lat lon	EM2040c
HSV_SVY_LI2019_V05_3020_014_20190330T022853Z_0001.mp4	-22.667865 113.502145	0508, 0706
HSV_SVY_LI2019_V05_3023_013_20190330T015014Z_0001.mp4	-22.694307 113.520328	0701
HSV_SVY_LI2019_V05_2818_001_20190328T045144Z_0001.mp4	-22.706360 113.508212	0717 (crosses 0702)
HSV_SVY_LI2019_V05_3017_015_20190330T031057Z_0001.mp4	-22.642582 113.533127	0510
HSV_SVY_LI2019_V05_3016_016_20190330T034823Z_0001.mp4	-22.628533 113.559452	0512
HSV_SVY_LI2019_V05_3015_011_20190330T001655Z_0001.mp4	-22.718928 113.539780	0203, 0114
HSV_SVY_LI2019_V05_3019_012_20190330T010738Z_0001.mp4	-22.720285 113.563902	0125, 0126
HSV_SVY_LI2019_V05_3014_010_20190329T233352Z_0001.mp4	-22.684480 113.562962	crosses 0116, 0117
-- sponge gardens at	-22.684598 113.563127	

Area 5:

video file name (including tappity code)	central lat lon	EM2040c
HSV_SVY_LI2019_V05_2910_007_20190329T024121Z_0001.mp4	-22.841150 113.580230	0308
HSV_SVY_LI2019_V05_2904_009_20190329T042058Z_0001.mp4	-22.875237 113.692067	0221 (crosses 0504)
HSV_SVY_LI2019_V05_2907_005_20190329T010305Z_0001.mp4	-22.889333 113.624937	0108
HSV_SVY_LI2019_V05_2909_006_20190329T015656Z_0001.mp4	-22.834237 113.616155	0306, 0307
HSV_SVY_LI2019_V05_2812_003_20190328T065851Z_0001.mp4	-22.852363 113.666765	0721, 0218
HSV_SVY_LI2019_V05_2803_002_20190328T061850Z_0001.mp4	-22.823128 113.638933	0216
HSV_SVY_LI2019_V05_2905_004_20190329T002833Z_0001.mp4	-22.880635 113.642777	0304
HSV_SVY_LI2019_V05_2906_008_20190329T032009Z_0001.mp4	-22.878532 113.603258	0305

1.2 Extracted video stills – Area 3A and Area 5

The images in this Section are extracted from the videos for the tracks listed above.

JSON-video 3023_013_20190330T015014Z_0001 EM2040c 0701

JSON-video 3020_014_20190330T022853Z_0001 EM2040c 0508, 0706

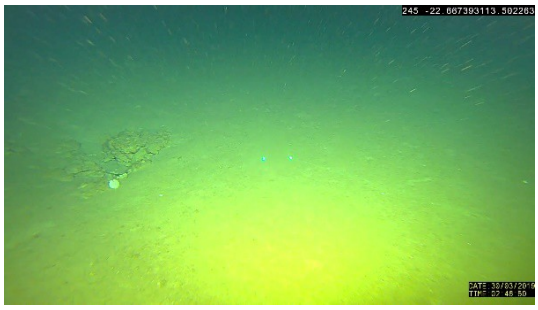

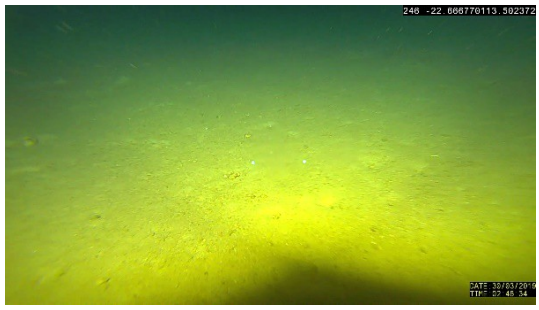

JSON-video 2818_001_20190328T045144Z_0001 EM2040c 0717

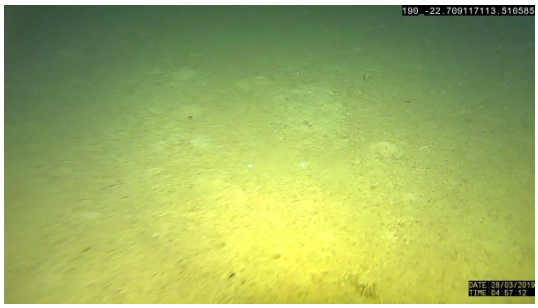

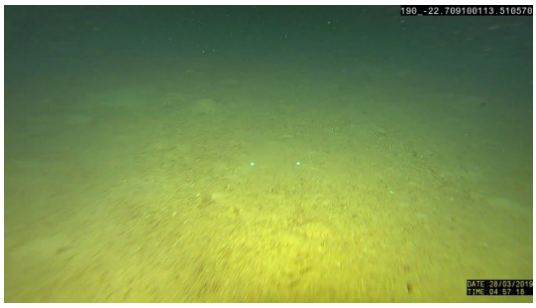

JSON-video 3015_011_20190330T001655Z_0001 EM2040c 0203, 0114

JSON-video 3019_012_20190330T010738Z_0001 EM2040c 0125, 0126

JSON-video 3017_015_20190330T031057Z_0001 EM2040c 0510

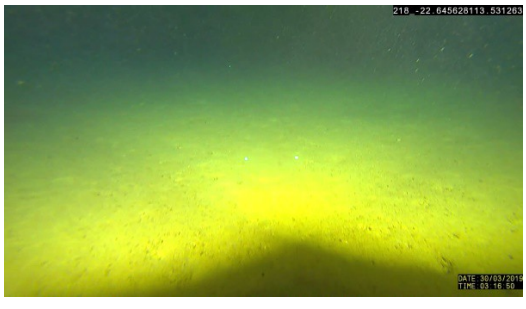

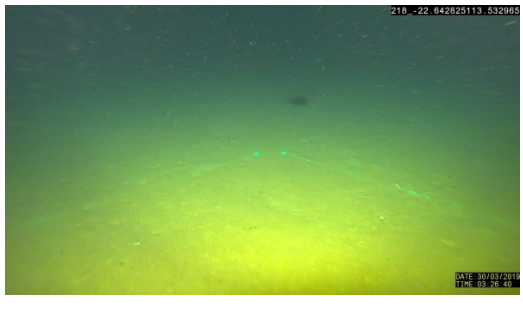

JSON-video 3016_016_20190330T034823Z_0001 EM2040c 0512

JSON-video 2910_007_20190329T024121Z_0001 EM2040c 0308

JSON-video 2904_009_20190329T042058Z_0001 EM2040c 0221

(crosses 0504)

JSON-video 2907_005_20190329T010305Z_0001 EM2040c 0108

JSON-video 2909_006_20190329T015656Z_0001 EM2040c 0306, 0307

JSON-video 2812_003_20190328T065851Z_0001 EM2040c 0721, 0218

JSON-video 2803_002_20190328T061850Z_0001 EM2040c 0216

JSON-video 2905_004_20190329T002833Z_0001 EM2040c 0304

JSON-video 2906_008_20190329T032009Z_0001 EM2040c 0305

1.3 Notes from email conversations used when interpreting video stills for area 3A

- To provide a bit of QA, all images and scores were checked by 2 staff to identify any discrepancies and to add further comments if needed.
- Transect 3023 (track #0701) looks to be qualitatively different from the other four – lots of sponge gardens and other cover, and a different surface. Track 0701 shows a lot of fine-scale detail on the backscatter images and is arguably harder than the rest.
- Looking at 2818 (#0717) and 3020 (#0508) relative to 3015 (#0203) and 3019 (#0125):
  The first two seem to me to be pretty much devoid of vegetative cover; this agrees with your classification.
  The latter two show reasonably sparse cover, though it looks as though the density of the cover is reasonably consistent. You note vegetative cover, which you classify as sparse.
  It seems that the sparseness of the cover for 2818 and 3020 is qualitatively different from that for 3015 and 3019.
  RESPONSE: We agree with the observation about the two groups of transects. Note that between the last pair, 3019 has considerably more biohabitat than 3015.
- Looking at 3017 and 3016. Could you please classify the frame grabs for these transects, and see whether you would rate them as being similar to 3023, or to 2818 and 3020, or to 3015 and 3019.
  REPSONSE: 3017 is very similar to 2818 and 3020, while 3016 is very similar to 3023.
- Do you see any differences in the surface material for 2818 and 3020, compared with 3015 and 3019. Are they all simply silty / sand? Can you see anything about the former two (apart from the relative lack of vegetative cover) that would allow you to distinguish those frame grabs from those for the latter two?
  RESPONSE: The surface material between transects 2818 and 3020 differ from 3015 and 3019. While the covering sand (with silt) appears quite similar for all four transects, the underlying substrate which is exposed at times is different. For 2818 and 3020, there is an underlying shell grit or fine rubble material. In contrast, 3015 and 3019 have coarser rubble material and occasional rocks exposed. In addition, 3019 has some exposed consolidated rubble. Therefore, we would expect that the substrate for these transects is harder than for 3015 and 3019.

1.4 Notes from one email conversation used when interpreting video stills for Area 5

- The number of images available (for some tracks) and their quality wasn't as good as the tracks previously examined in the 3A Area.

1.5 Interpretation of video stills for areas 3A and Area 5

The following Table was compiled by Mark Tonks and Anthea Donovan, to compare their scoring from video images with a previous classification from frame grabs in the Task Report.

	Transect	Video images	Frame grabs from report	Agreement
3B	2818	Sand (with silt), coarser shell grit or other material below sand surface; very sparse (<2%) biohabitat cover – consistent along transect.	Hard bottom	No? Uncertain as top sand/silt cover is consistent without exposing harder substrate
	3020	Sand (with silt), coarser shell grit or other material below sand surface; very sparse (<2%) biohabitat cover – consistent along transect. Like 2818.	Hard bottom	No? Uncertain as top sand/silt cover is consistent without exposing harder substrate
	3017	Sand (with silt); very sparse (<2% cover) biohabitat cover – consistent along transect. Like 2818 and 3020.	Hard bottom	No? Uncertain as top sand/silt cover is consistent without exposing harder substrate
	3015	Sand (with silt); coarse rubble under sand surface with occasional exposed rock; sparse (<5%) biohabitat cover with sponges, hydroids, soft coral but more than 2818 and 3020.	Sand over hard bottom	Yes
	3019	Sand (with silt), very coarse rubble under sand cover with occasional exposed rubble piles and consolidated rubble; sparse (<30%) biohabitat cover with whips, sponges, gorgonians; more biohabitat than 3015.	Sand over hard bottom	Yes
	3023	Silty sand over consolidated rubble with regular exposed rock and occasional consolidated rubble pavement; sparse (<30%) biohabitat cover with whips, sponges, gorgonians	Hard bottom	Yes
	3016	Silty sand over consolidated rubble with regular exposed rock and occasional consolidated rubble pavement; sparse (<30%) biohabitat cover with whips, sponges, gorgonians. Like 3023	Hard bottom to sand over hard bottom	Yes
Area 5	2904	Sand over consolidated rubble and loose small/ medium sized rubble; very sparse (<5%) biohabitat cover with whips, sponges, hydroids.	Sand over hard bottom to sand bottom	Yes
	2905	Sand (with silt), coarser shell grit or other material below sand surface; very sparse (<2%) biohabitat cover – consistent along transect. Like 2818, 3020, 3017.	Sandy bottom and sand over hard	Mostly yes Sand bottom for majority of track. Not mush evidence of underlying hard substrate
	2906	Sand (with silt); small amount of consolidated rubble; very sparse (<2%) biohabitat cover with sponges, hydroids. Few images to view (6).	Sandy bottom	Mostly yes Sand bottom for majority of track and then underlying consolidated rubble towards end (last image).
	2907	Sand (with silt); coarse shell grit under sand/ silt surface with occasional exposed rubble/ rock; very sparse (<2%) biohabitat cover with sponges, hydroids. Very few images to view (3).	Sandy bottom	No Looks more compact than a sandy bottom but note only very few images available to make this assessment
	2909	Sand (with silt); mostly sand with occasional coarse shell grit and exposed rock – inconsistent along transect; very sparse (<2%) biohabitat cover with sponges, hydroids. Few images to view (5).	Sandy bottom and sand over hard	Yes More sandy bottom than sand over hard
	2910	Sand; very sparse (<2% cover) biohabitat cover – consistent along transect.	Sandy bottom	Yes
	2812	Sand (with silt); shell grit under sand ripple surface with occasional exposed rubble - inconsistent along transect; sparse (<5%) biohabitat cover with sponges, hydroids, whips.	Sandy bottom and sand over hard	Yes
	2803	Sand (with silt); shell grit under sand/silt surface; very sparse (<2%) biohabitat cover. Few images to view (5).	Sand over hard bottom to sand bottom	No? Uncertain as entirely sand/silt substrate and not much evidence of hard bottom underneath.

1.6 Supplementary material

Extraction of seabed stills from seabed videos

A number of programs allow the extraction of still photos from seabed videos.

Free-Video-to-JPG-Converter is easy to use. The user simply loads the file and sets the extraction rate by frames or seconds. The program is available at:

https://www.dvdvideosoft.com/products/dvd/Free-Video-to-JPG-Converter.htm

Typical seabed stills from seabed videos

The following set of images is, in my experience, quite representative.

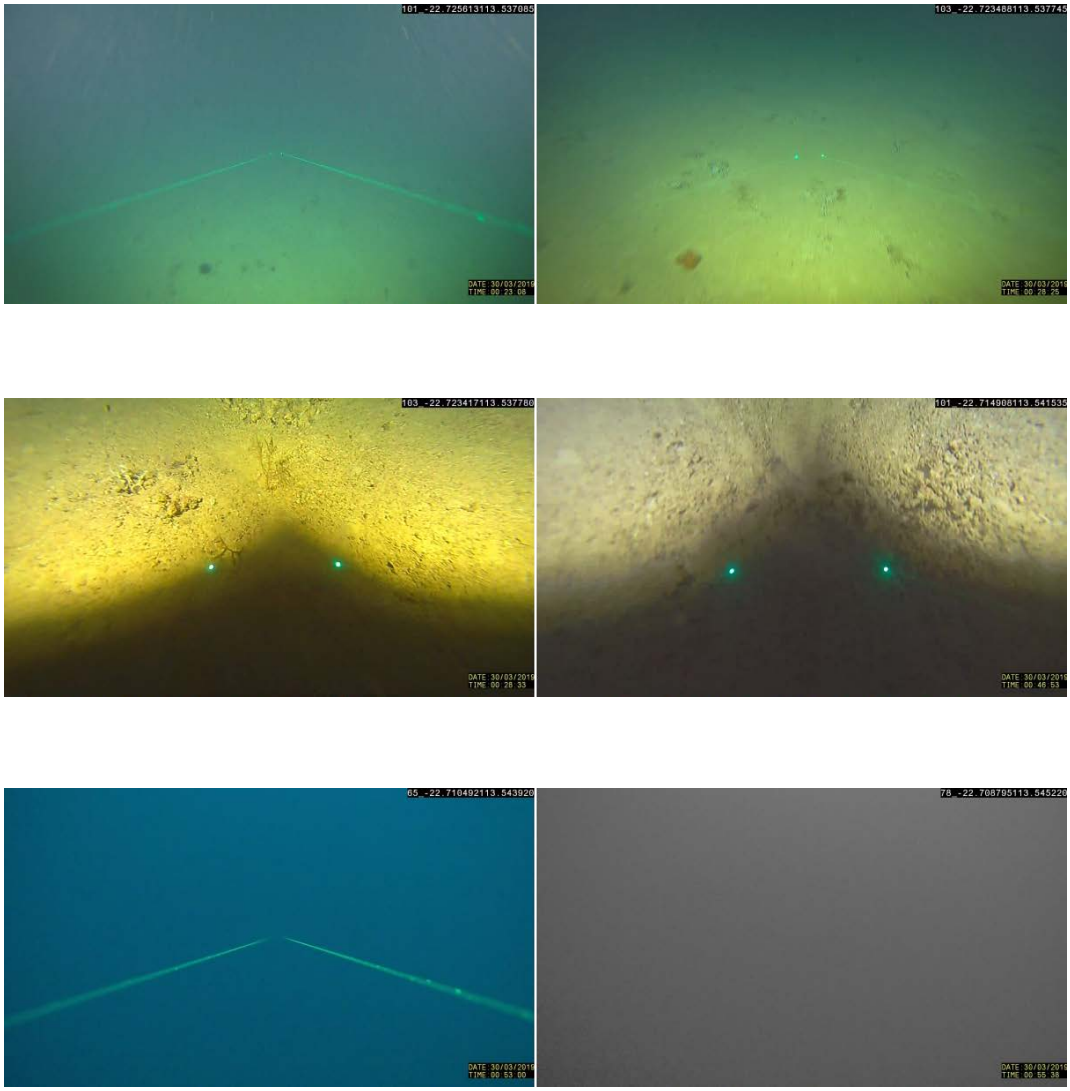

The challenge is to identify those photos, such as the first four and the last two, which do not show any seabed features; and delete them.

Identifying discriminating values

Due to the differential illumination of the seabed, the images are typically relatively brighter in the lower part.

The images are 1020 L x 1980 P.

For a preliminary analysis, the R G B values were extracted on a 3 x 2 grid located at lines {700, 800, 900} x pixels {600, 800}.

The set of 300 images were sorted roughly by illumination – for example, duller illumination (image 7 above); medium illumination (image 5 above); brighter illumination (image 6 above); dark wedge (images 9, 10 above); water column (images 4, 11 above); and set-up and finish (images 1, 2, 3, 12 above).

A discriminant-based analysis was then applied to the resulting R G B grid values, based on small contiguous group sizes of 5.

Canonical variate analysis (CVA) based on the extracted values

The following figure shows the resulting CV1 (upper plot) and CV2 (lower plot) scores plotted against the roughly ordered photo or image number.

Images 1 – 50 represent duller illumination; 51 - 120 medium illumination; 121 – 154 brighter illumination; 155 - 162 dark wedges; 163 – 279 water column; and 280 - 300 set-up and finish images.

There are obvious differences in the levels of the CV trace plots from the photos of the seabed, to those from the water column and the set-up photos.

There are also more subtle increases in CV1 level within the former, as the degree of illumination becomes more obvious.

This differentiation offers the potential for a simple but effective screening of the photos:

1. calculate the CV1 and CV2 scores for a photo
2. if CV1 < 2, mark the file for deletion
3. if CV1 > 2 and CV2 > say 2.25, mark the file for possible deletion.

A comment

The extraction of values to characterise the variation across an image is somewhat simplistic, especially with the modern trend to deep learning for identifying features in images.

The selection of discriminating values could no doubt be refined, perhaps by considering a larger grid and / or a greater separation between the pixel locations across the image.

The current grid size and location was chosen in part to avoid the confounding impact of the laser dots. The positions of the dots could be located, and a larger grid could be employed, with the modification that nearby R G B values are extracted if the grid position falls too near to a laser dot.

6.8 Appendix – Developing bathymetry and topographic position index

A topographic position index (TPI) map was developed as an input for statistical selection of baited remote underwater video cameras (BRUVs) sites. The first step of developing a TPI map is to produce an accurate bathymetry for the area of interest. CSIRO's GSM team provided as much raw data a possible from previous swath mapping voyages from Southern Surveyor, Investigator, Linnaeus and gridded products from NESP. This resulted in a large volume of data that had to be processed. In order to do this efficiently, data were transferred to CSIRO's high-performance computer center for processing. All of the input files were converted to parquet format to allow for parallel processing. Position data was decimated to a fixed UTM grid at a spacing of 5 meters. Point data were binned, averaged and interpolated onto two grids of 5 and 25 m. The input data ranged from the centimeter scale up to 50 m gridded products, so in areas of high-density data more texture can be observed than in areas of low data density. Interpolation distances were also restricted to prevent the generation of spurious data. Examples of the bathymetry can be seen in Figure A2.1.

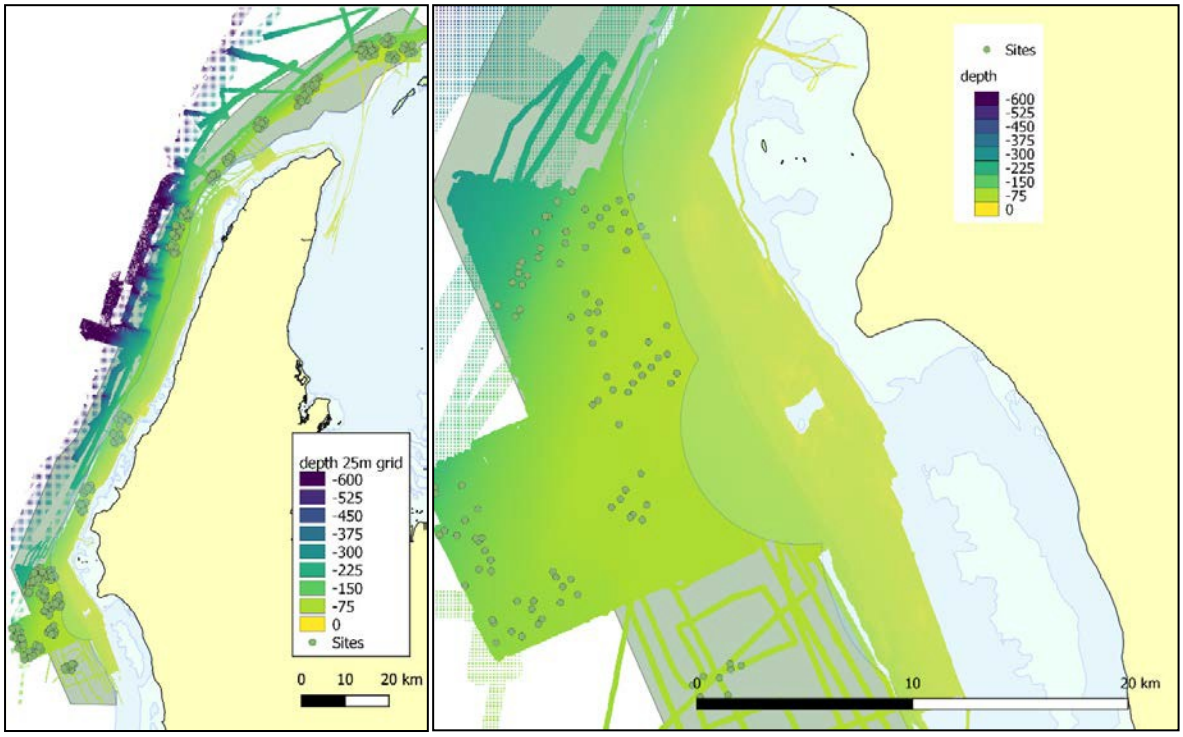

Figure A2.1 Examples of combined (left panel) and resampled (right panel) bathymetry from the study area of Ningaloo.

TPI is defined as the difference between the value of a cell and the mean value of its eight surrounding cells. This computation is most efficiently done using a kernel matrix with the following values:

$$\begin{matrix} -0.125 & -0.125 & -0.125 \\ -0.125 & 1 & -0.125 \\ -0.125 & -0.125 & -0.125 \end{matrix}$$

The mean of the surrounding cells is subtracted from the center cell.

The resulting image highlights areas of changing bathymetry and features of interest. Figure A2.2, displaying TPI output, highlights a ridge around the 80 m contour which is present across multiple surveys, along with artifacts from vessel movement.

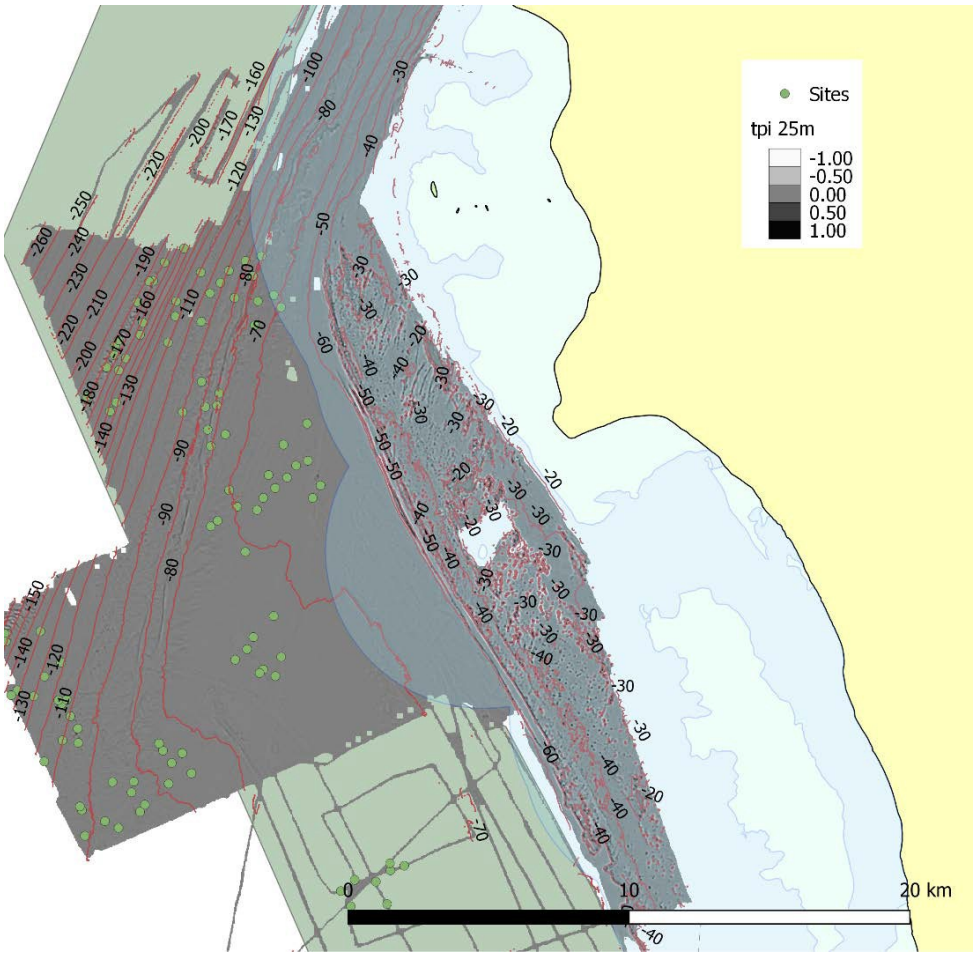

Figure A2.2 TPI output highlighting smaller, important features of the bathymetry.

6.9 References

Benedek C, Shadaydeh M, Kato Z, Szirányi T and Zerubia J (2015) Multilayer Markov Random Field models for change detection in optical remote sensing images.

Besag J (1986) On the statistical analysis of dirty pictures. J. Roy. Statis. Soc. B. 68: 259–302.

Breiman L (2001) Random Forests. Machine Learning 45(1): 5–32.

Campbell NA (1984) Some aspects of allocation and discrimination. In: van Vark GN and Howells WW (eds.) Multivariate Statistical Methods in Physical Anthropology. Dordrecht, Reidel, pp 177–192.

Cutler A, Cutler DR and Stevens JR (2012) Random Forests. In: Zhang C and Ma YQ (eds.) Ensemble Machine Learning. Springer, New York, pp 157–175. http://dx.doi.org/10.1007/978-1-4419-9326-7_5

De Jong SM and van der Meer F (2007) Remote Sensing and Image Analysis. Springer Science and Business Media.

Fonseca L, Brown C, Calder B, Mayer L and Rzhanov Y (2009) Angular range analysis of acoustic themes from Stanton Banks Ireland: a link between visual interpretation and multibeam echosounder angular signatures. Appl Acoust 70(10):1289–1304.

Hamilton LJ and Parnum I (2011). Acoustic seabed segmentation from direct statistical clustering of entire multibeam sonar backscatter curves. Continental Shelf Research 31: 138–148.

Hastie T, Tibshirani R and Friedman J (2001) The Elements of Statistical Learning. Springer.

7. SUMMARY OF BRUV FISH AND HABITAT DISTRIBUTION DATA

Authors: Dirk Slawinski, Anthea Donovan, Tim Langlois, Brooke Gibbons

Date: 31 January 2021

7.1 Methods

Each Baited Remote Underwater Video (BRUV) unit consisted of a stereo pair of calibrated Cannon 4K HF25 cameras in water-proof housings. The housings were mounted on a metal frame along with a rear-facing GoPro camera pre-set to take one photo every 60 s. A mesh bait bag containing pilchards was attached to the front of the unit.

BRUV units were deployed in sets of six, in proximate 60 min drops separated by 0.5–2 km in order to efficiently use available time (minimise steaming and non-sampling time). Typically, 3–4 sites of six drops could be conducted each day, depending on weather, water depth, weather conditions, distance between sites and available light. Because of the time of year, sufficient daylight hours for operations (BRUV retrieval) and navigation in and out of reef anchorages were limited, restricting the number of sites to an unexpected degree.

7.1.1 Fish data

Fish video analysis was carried out in EventMeasure (https://www.seagis.com.au/event.html). Fish were identified to their lowest taxonomic level and recorded in the software. The allowed an estimate of maximum abundance (using MaxN – the maximum number of individuals of a given species observed in a single frame) to be determined. In addition, fork length of fish was also recorded.

7.1.2 Habitat data

Habitat data was taken from images obtained from both the forward and backward BRUV cameras and analysed using TransectMeasure (https://www.seagis.com.au/transect.html). Methods for recording the habitat data are outlined in Langlois et al. (2020).

A 4x5 grid was superimposed over each image and the habitat type with the largest proportion in each cell was classified using the CATAMI classification scheme (Althaus et al. 2015). Grid cells covering open water excluded from further analysis. A percent cover of reef or sand was determined for each site. These values were then summed for the forwards and backwards images from each stereo-BRUV and an overall percent cover habitat type was calculated.

Table 25 Relief values and their associated descriptor. Distinct categories have been adapted from Wilson et al. (2006).

Relief Value	Descriptor
0	Flat substrate, sandy, rubble with few features. ~0 substrate slope.
1	Some relief features amongst mostly flat substrate/sand/rubble. <45 degree substrate slope.
2	Mostly relief features amongst some flat substrate or rubble. ~45 degree substrate slope.
3	Good relief structure with some overhangs. >45 substrate slope.
4	High structural complexity, fissures and caves. Vertical wall. ~90 substrate slope.
5	Exceptional structural complexity, numerous large holes and caves. Vertical wall. ~90 substrate slope.

Relief for each cell was also assessed using a 0–5 scale (Table 25, as described in Langlois et al. (2020)). For each BRUV drop, the values for relief in each cell from both forwards and backwards camera images were averaged and the standard deviation was calculated.

7.2 Results

7.2.1 Fish data

Table 26 The most common species of fish observed on the BRUV footage.

Species	Family	Total of MaxN
Decapterus spp	Carangidae	901
Pristipomoides multidens	Lutjanidae	358
Gymnocranius grandoculis	Lethrinidae	178
Lethrinus miniatus	Lethrinidae	133
Carangoides chrysophrys	Carangidae	130
Argyrops spinifer	Sparidae	103
Carangoides gymnostethus	Carangidae	100
Lethrinus rubrioperculatus	Lethrinidae	92
Pterocaesio chrysozona	Caesionidae	84
Epinephelus areolatus	Serranidae	79

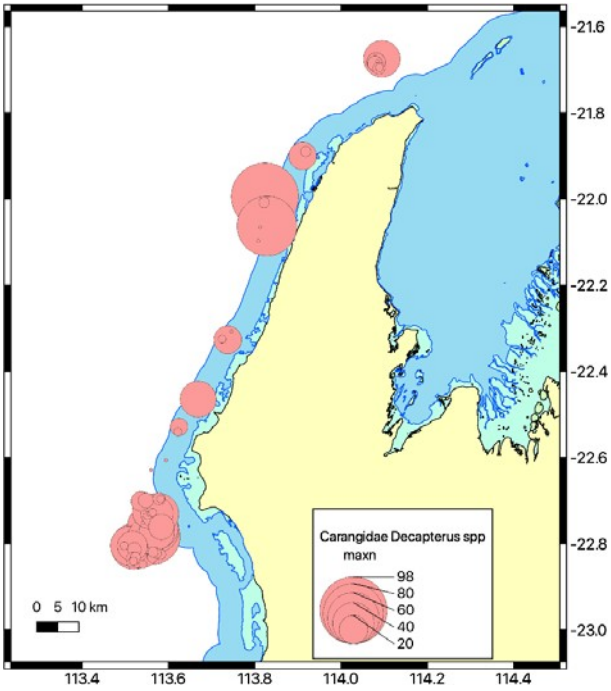

Figure 52 Map of study area displaying the MaxN value at all sites that *Decapterus* spp (the most abundant species) were observed.

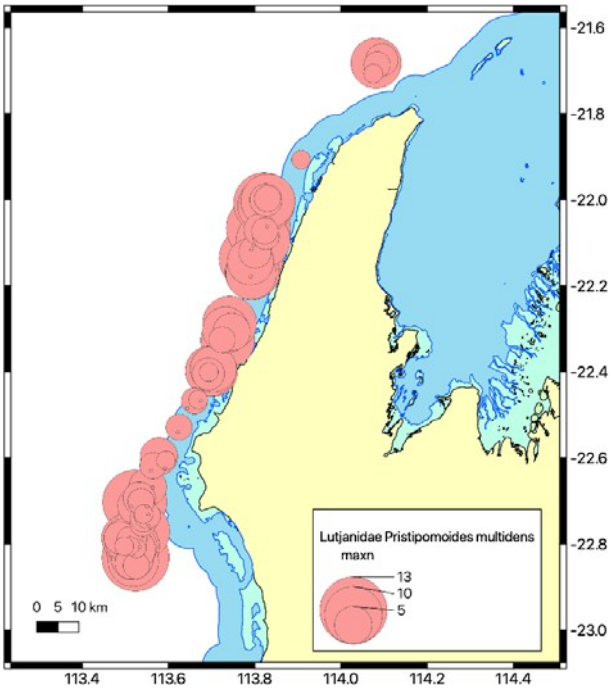

Figure 53 Map of study area displaying the MaxN value at all sites that *Pristipomoides multidens* (the second most abundant species) were observed.

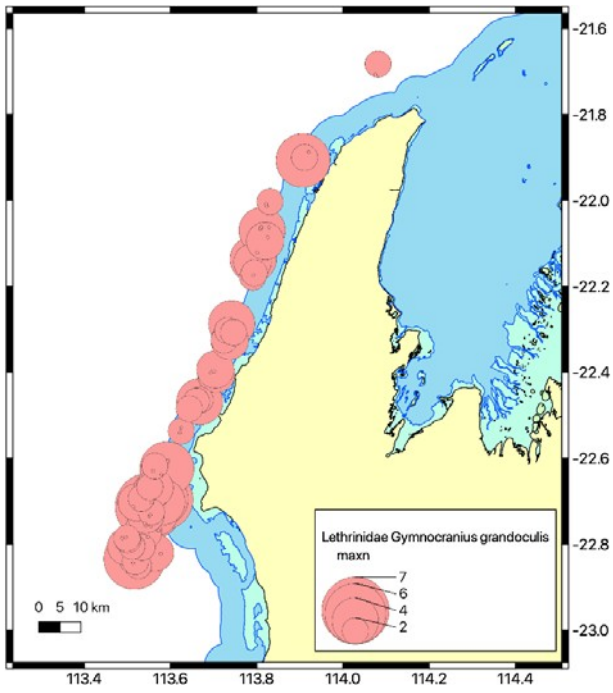

Figure 54 Map of study area displaying the MaxN value at all sites that *Gymnocranius grandoculis* (the third most abundant species) were observed.

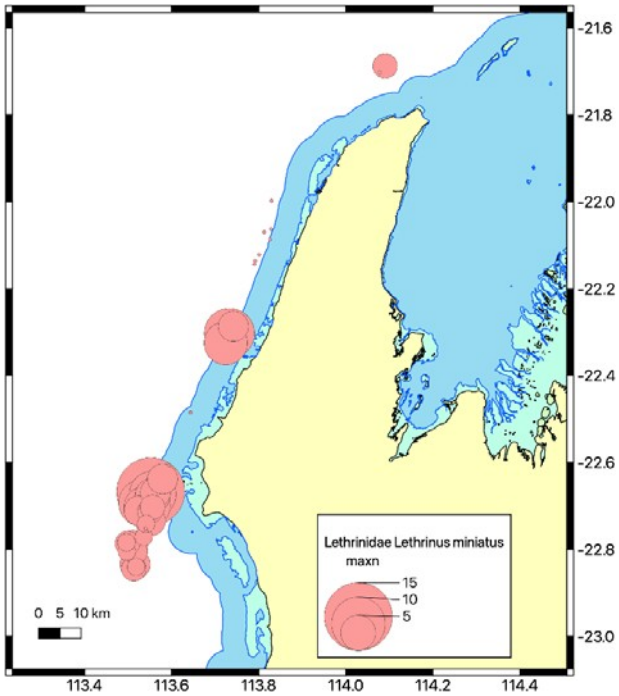

Figure 55 Map of study area displaying the MaxN value at all sites that *Lethrinus miniatus* (the fourth most abundant species) were observed.

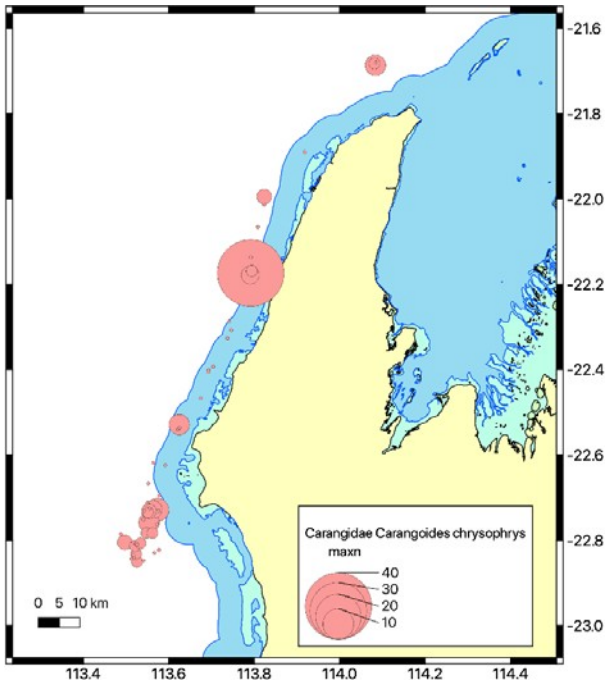

Figure 56 Map of study area displaying the MaxN value at all sites that *Carangoides chrysophrys* (the fifth most abundant species) were observed.

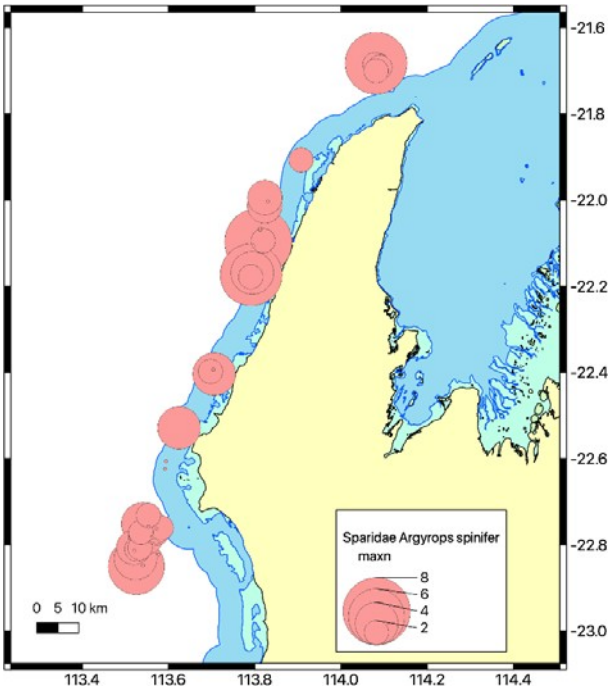

Figure 57 Map of study area displaying the MaxN value at all sites that *Argyrops spinifer* (the sixth most abundant species) were observed.

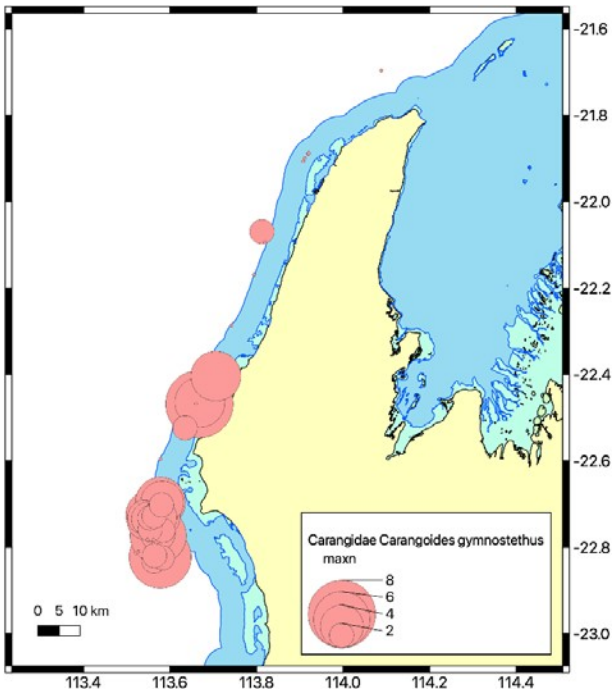

Figure 58 Map of study area displaying the MaxN value at all sites that *Carangoides gymnostethus* (the seventh most abundant species) were observed.

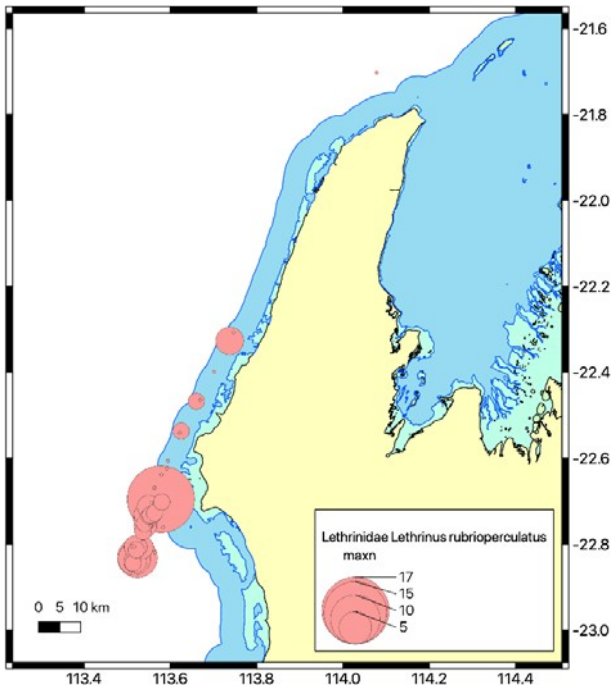

Figure 59 Map of study area displaying the MaxN value at all sites that *Lethrinus rubrioperculatus* (the eighth most abundant species) were observed.

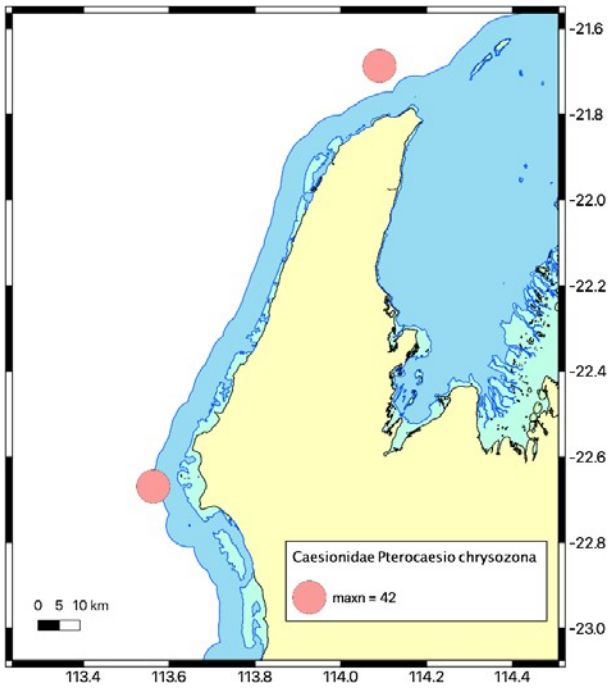

Figure 60 Map of study area displaying the MaxN value at all sites that *Pterocaesio chrysozona* (the ninth most abundant species) were observed.

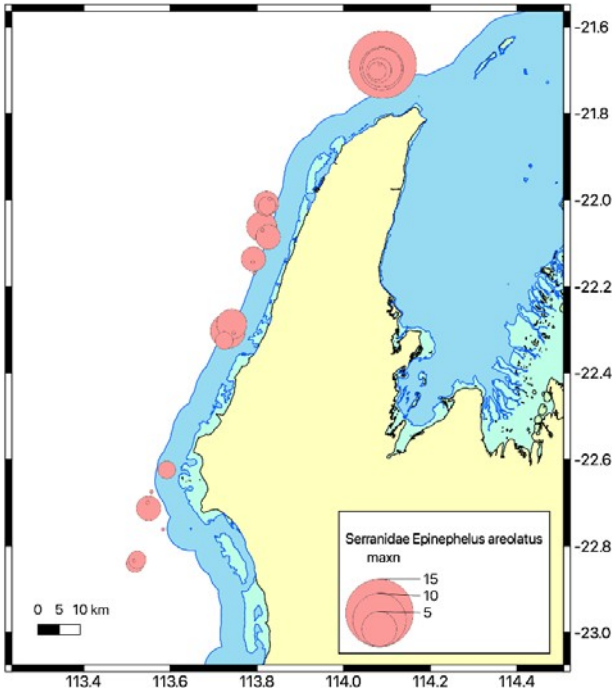

Figure 61 Map of study area displaying the MaxN value at all sites that *Epinephelus areolatus* (the tenth most abundant species) were observed.

7.2.2 Habitat data

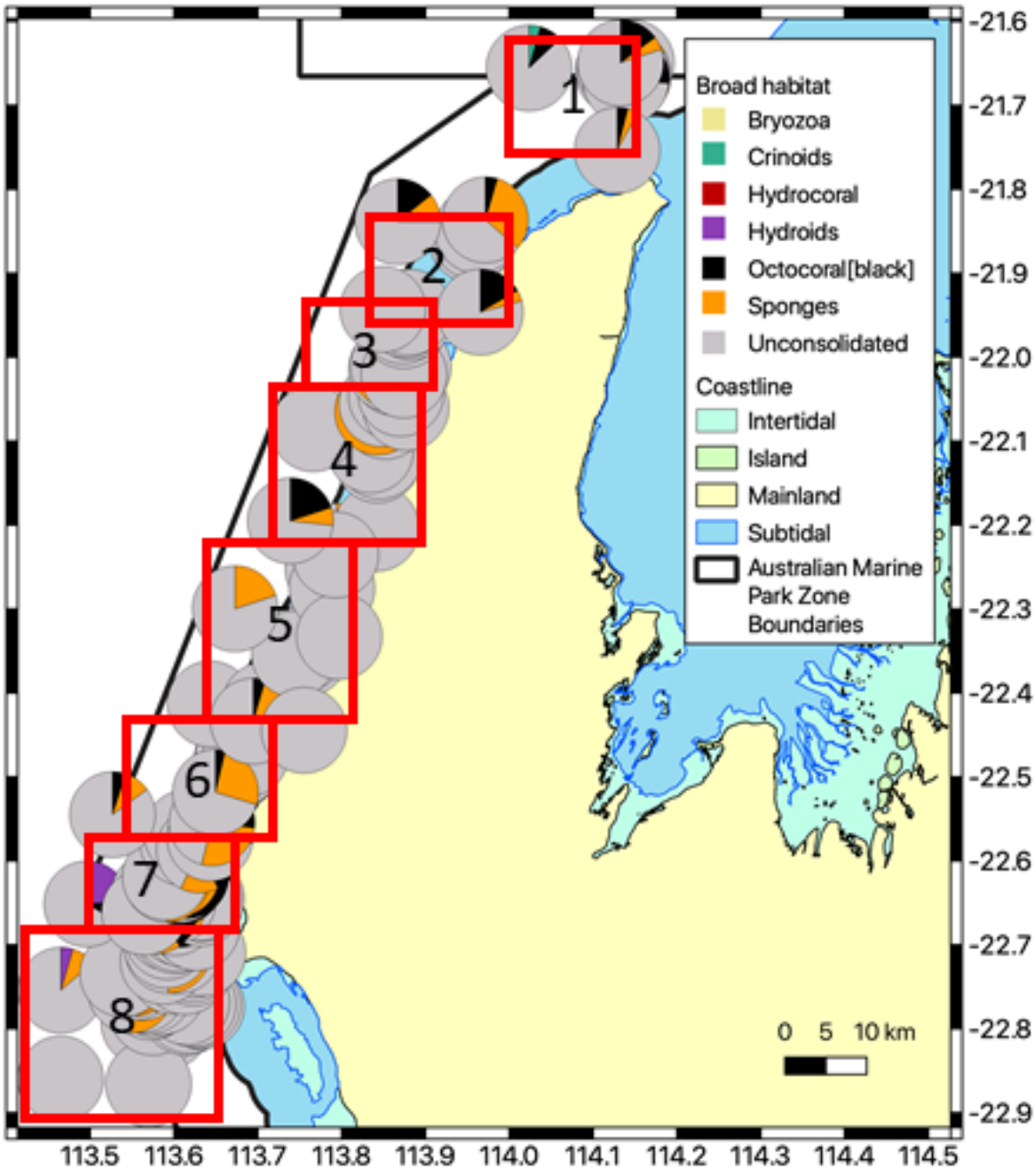

Figure 62 Map of study area showing locations of BRUV sets. Pie charts display the mean habitat type within the set of BRUVs (6 drops). “Unconsolidated” is a substrate type which is not reef but is usually sand or a mix of sand and rubble. Each numbered region is displayed in more detail in the following figures.

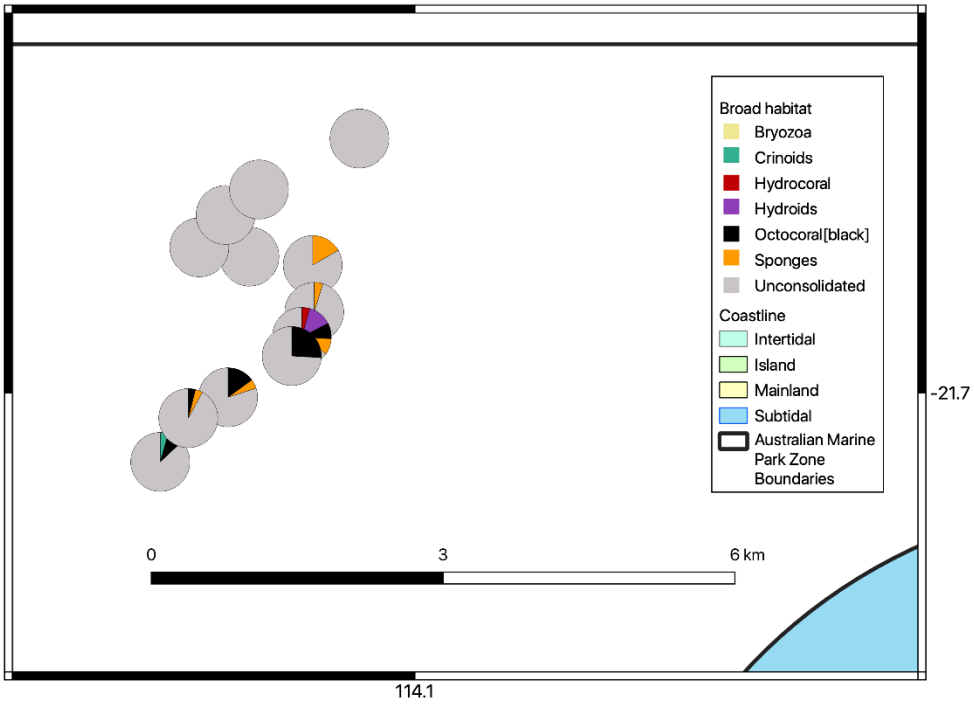

Figure 63 Map of Region 1 (from Figure 62) showing locations of BRUV sets. Pie charts display the mean habitat type within the set of BRUVs (6 drops). “Unconsolidated” is a substrate type which is not reef but is usually sand or a mix of sand and rubble.

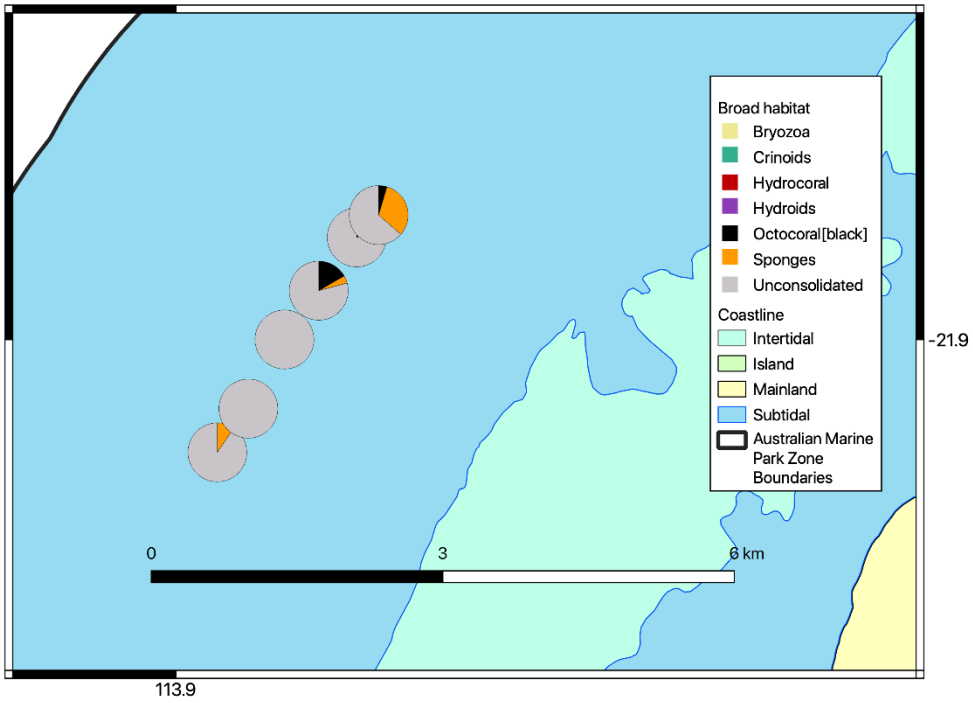

Figure 64 Map of Region 2 (from Figure 62) showing locations of BRUV sets. Pie charts display the mean habitat type within the set of BRUVs (6 drops). “Unconsolidated” is a substrate type which is not reef but is usually sand or a mix of sand and rubble.

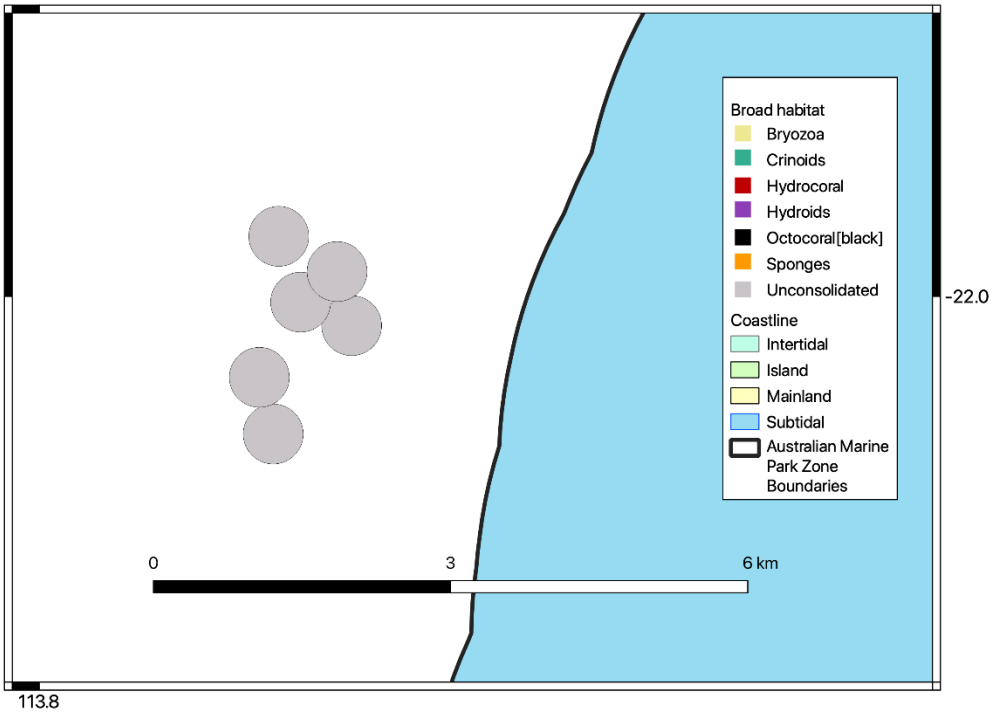

Figure 65 Map of Region 3 (from Figure 62) showing locations of BRUV sets. Pie charts display the mean habitat type within the set of BRUVs (6 drops). “Unconsolidated” is a substrate type which is not reef but is usually sand or a mix of sand and rubble.

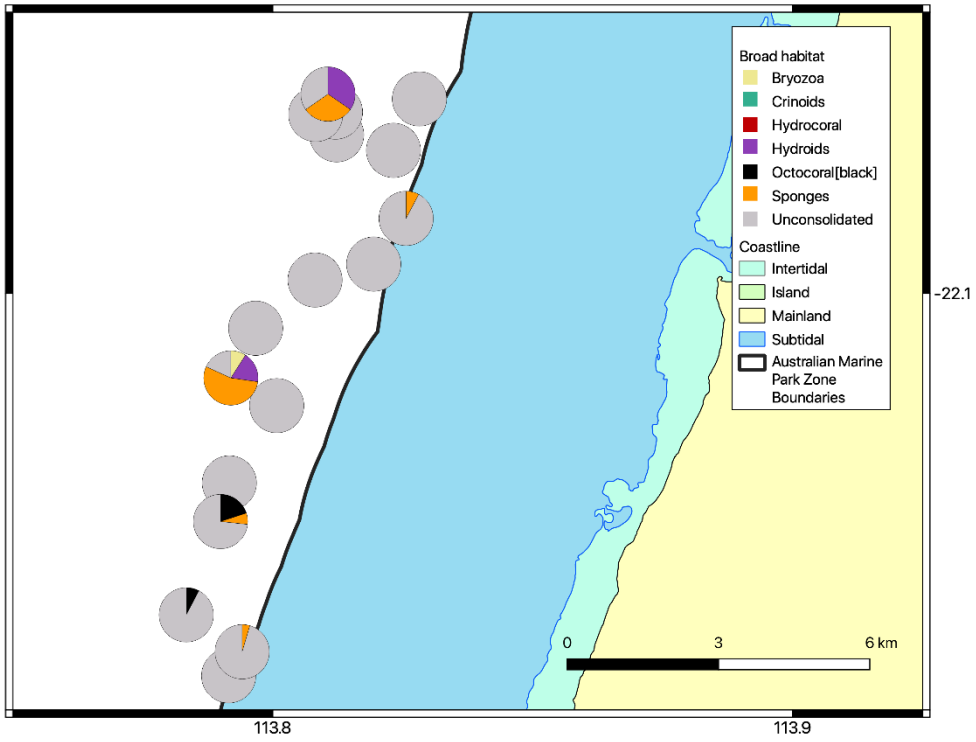

Figure 66 Map of Region 4 (from Figure 62) showing locations of BRUV sets. Pie charts display the mean habitat type within the set of BRUVs (6 drops). “Unconsolidated” is a substrate type which is not reef but is usually sand or a mix of sand and rubble.

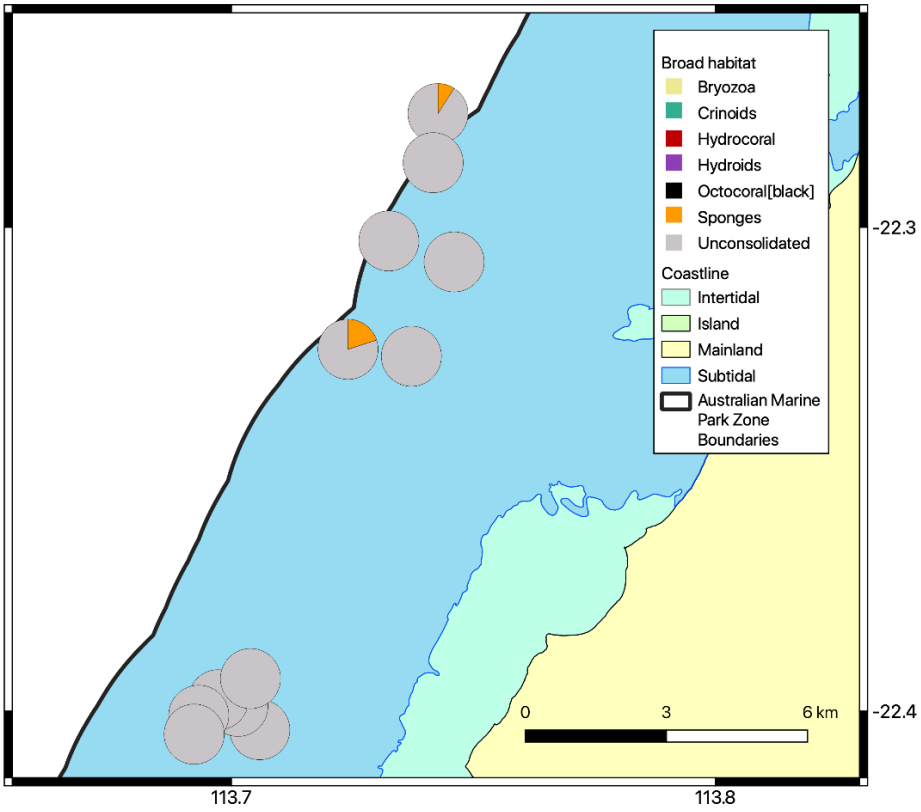

Figure 67 Map of Region 5 (from Figure 62) showing locations of BRUV sets. Pie charts display the mean habitat type within the set of BRUVs (6 drops). “Unconsolidated” is a substrate type which is not reef but is usually sand or a mix of sand and rubble.

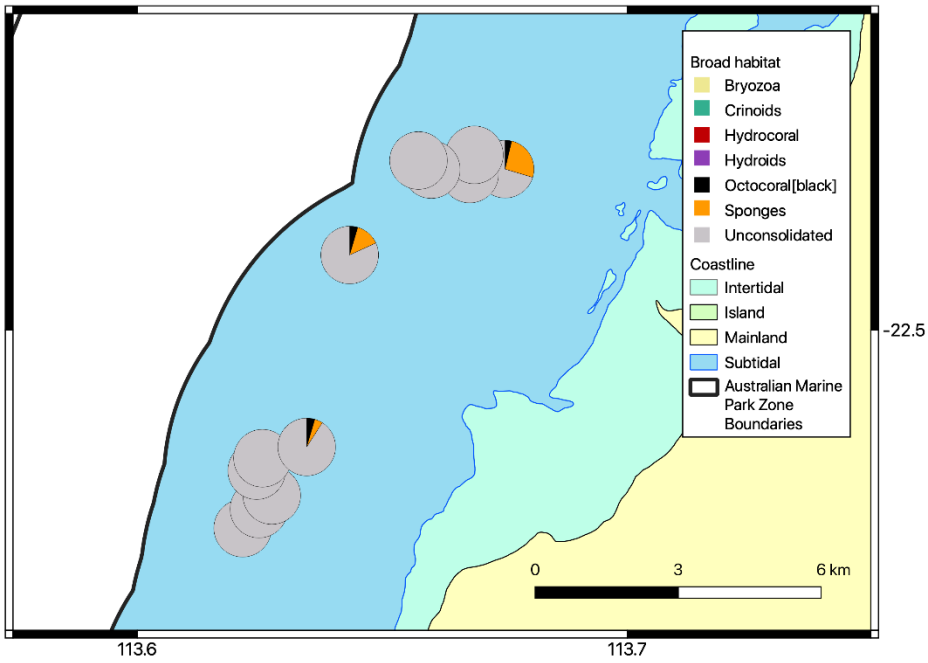

Figure 68 Map of Region 6 (from Figure 62) showing locations of BRUV sets. Pie charts display the mean habitat type within the set of BRUVs (6 drops). “Unconsolidated” is a substrate type which is not reef but is usually sand or a mix of sand and rubble.

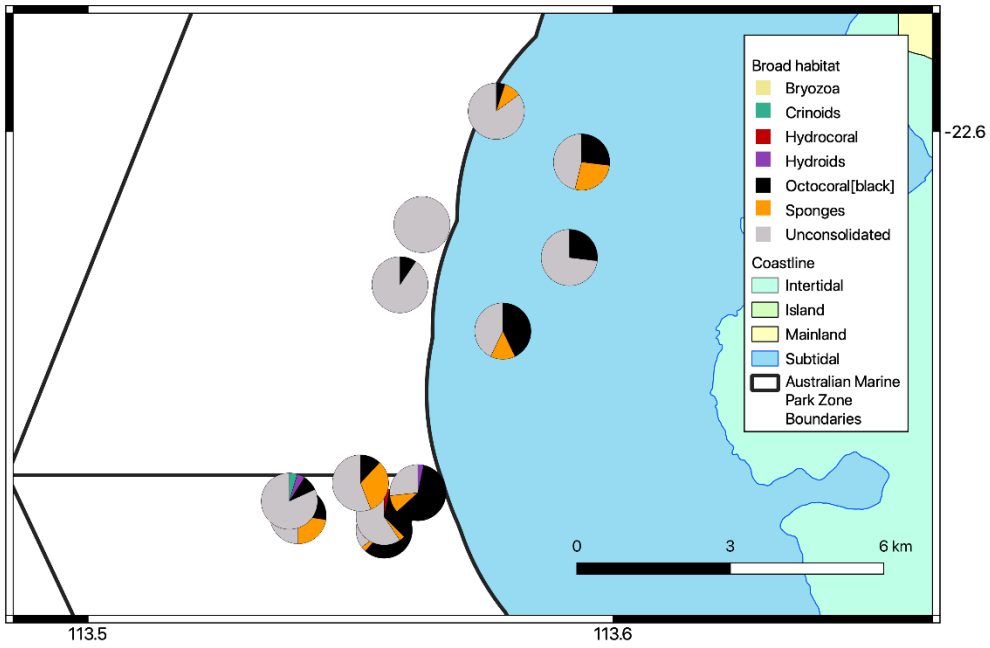

Figure 69 Map of Region 7 (from Figure 62) showing locations of BRUV sets. Pie charts display the mean habitat type within the set of BRUVs (6 drops). “Unconsolidated” is a substrate type which is not reef but is usually sand or a mix of sand and rubble.

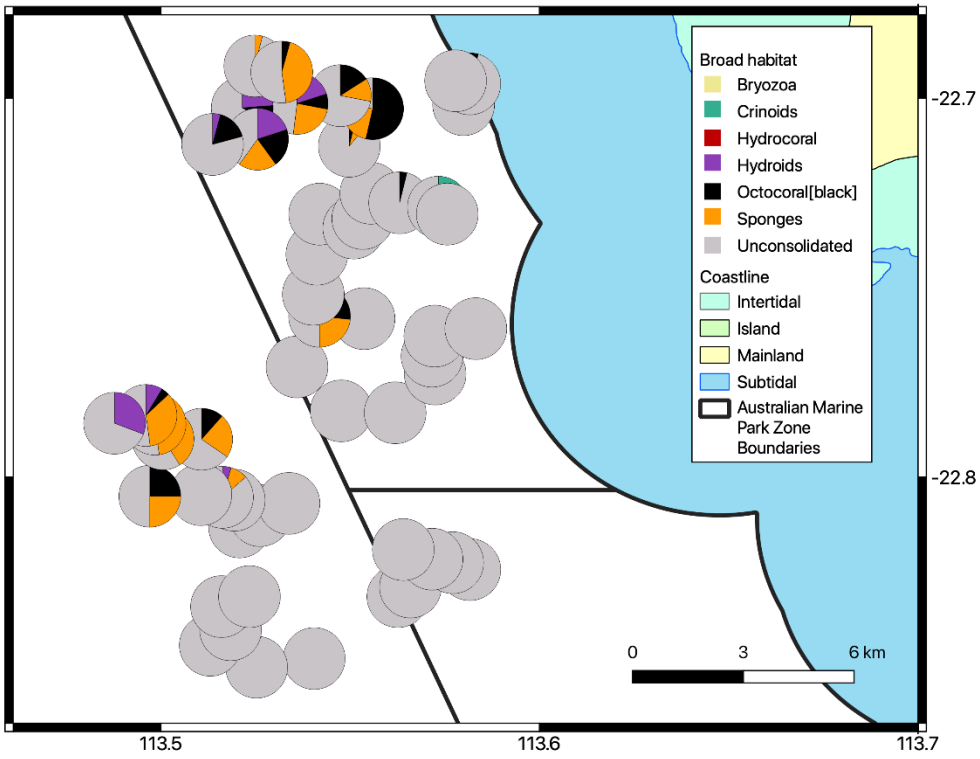

Figure 70 Map of Region 8 (from Figure 62) showing locations of BRUV sets. Pie charts display the mean habitat type within the set of BRUVs (6 drops). “Unconsolidated” is a substrate type which is not reef but is usually sand or a mix of sand and rubble.

7.3 References

Althaus F, Hill N, Ferrari R, Edwards L, Przeslawski R, Schönberg CHL, Stuart-Smith R, Barrett N, Edgar G, Colquhoun J, Tran M, Jordan A, Rees T, Gowlett-Holmes K (2015). A standardised vocabulary for identifying benthic biota and substrata from underwater imagery: The CATAMI classification scheme. PLoS ONE, 10, e0141039. https://doi.org/10.1371/journal.pone.0141039

Langlois T, Goetze J, Bond T, Monk J, Abesamis RA, Asher J, Barrett N, Bernard ATF, Bouchet PJ, Birt MJ, Cappo M, Currey-Randall LM, Driessen D, Fairclough DV, Fullwood LAF, Gibbons BA, Harasti D, Heupel MR, Hicks J, Holmes TH, Huveneers C, Ierodiaconou D, Jordan A, Knott NA, Lindfield S, Malcolm HA, McLean D, Meekan M, Miller D, Mitchell PJ, Newman SJ, Radford B, Rolim FA, Saunders BJ, Stowar M, Smith ANH, Travers MJ, Wakefield CB, Whitmarsh SK, Williams J, Harvey ES (2020). A field and video annotation guide for baited remote underwater stereo-video surveys of demersal fish assemblages. Methods in Ecology and Evolution 11: 1401– 1409.

Wilson SK, Graham NAJ, Polunin NVC (2006). Appraisal of Visual Assessments of Habitat Complexity and Benthic Composition on Coral Reefs. Marine Biology 151 (3): 1069–76.

7.4 Appendix – Raw Ningaloo habitat data

sample	mean. relief	sd. relief	Fieldof view. limited	Fieldof view. open	broad. bryozoa	broad. crinoids	broad. Hydro coral	broad. hydroids	broad. Octocoral .black	broad. sponges	broad. Unconsolidated
1.01	0.421053	0.507257	0	100	0	0	0	0	0	0	100
1.02	0.88	0.331662	0	100	0	0	0	0	0	0	100
1.03	1	0	0	100	0	0	0	0	0	0	100
1.04	0.44	0.506623	0	100	0	0	0	0	0	0	100
1.05	1	0	0	100	0	0	0	0	0	0	100
1.06	0.44	0.506623	0	100	0	0	0	0	0	0	100
10.01	3.352941	1.574077	37.5	62.5	0	0	0	0	61.76	2.94	35.29
10.02	2.25	1.04727	0	100	0	0	3.12	0	34.38	3.12	59.38
10.03	3.233333	1.633345	0	100	0	0	0	3.33	60	10	26.67
10.04	3.24	1.16476	0	100	0	0	0	0	12	32	56
10.07	3	1.023533	0	100	0	0	0	4.55	22.73	22.73	50
10.08	1.5	0.511766	0	100	0	4.55	0	4.55	9.09	0	81.82
10.09	0.904762	0.436436	0	100	0	0	0	0	9.52	0	90.48
10.11	1.157895	0.374634	0	100	0	0	0	0	0	0	100
10.12	1.7	0.864505	0	100	0	0	0	0	5	10	85
10.13	2.514286	0.853072	0	100	0	0	0	0	42.86	14.29	42.86
10.14	1.192308	0.491466	0	100	0	0	0	0	26.92	0	73.08
10.15	2.192308	1.059027	0	100	0	0	0	0	26.92	26.92	46.15
11.01	0.96	0.2	0	100	0	0	0	0	0	0	100
11.02	1.916667	1.017955	0	100	0	0	0	0	16.67	0	83.33
11.03	1.2	0.615587	0	100	0	0	0	0	0	0	100
11.04	0.96	0.2	0	100	0	0	0	0	0	0	100
11.05	0.590909	0.503236	0	100	0	0	0	0	0	0	100
11.06	1.045455	0.72225	0	100	0	0	0	0	4.55	4.55	90.91
12.02	2.333333	1.270978	0	100	0	0	0	0	3.7	25.93	70.37
12.03	1	0	0	100	0	0	0	0	0	0	100
12.04	0.6	0.5	0	100	0	0	0	0	0	0	100
12.05	0.76	0.522813	0	100	0	0	0	0	0	0	100
12.06	1	0	0	100	0	0	0	0	0	0	100
12.11	2.090909	1.019294	0	100	0	0	0	0	4.55	13.64	81.82
13.02	0.423077	0.503831	0	100	0	0	0	0	0	0	100
13.03	1.5	0.511766	0	100	0	0	0	0	0	0	100
13.04	1.08	0.276887	0	100	0	0	0	0	0	0	100
13.05	0.809524	0.402374	0	100	0	0	0	0	0	0	100
13.06	1	0	0	100	0	0	0	0	0	0	100
13.08	1	0	0	100	0	0	0	0	0	0	100
14.01	0.88	0.781025	0	100	0	0	0	0	0	20	80
14.02	1.15	1.089423	0	100	0	0	0	0	0	0	100
14.03	1	0.308607	0	100	0	0	0	0	0	9.09	90.91
14.06	0.73913	0.448978	0	100	0	0	0	0	0	0	100
14.11	0.84	0.6245	0	100	0	0	0	0	0	0	100

sample	mean. relief	sd. relief	Fieldof view. limited	Fieldof view. open	broad. bryozoa	broad. crinoids	broad. Hydro coral	broad. hydroids	broad. Octocoral .black	broad. sponges	broad. Unconsolidated
14.12	0.6	0.5	0	100	0	0	0	0	0	0	100
14.13	1	0	0	100	0	0	0	0	0	0	100
15.01	1	0	0	100	0	0	0	0	0	0	100
15.02	0.909091	0.294245	0	100	0	0	0	0	0	4.55	95.45
15.05	1.115385	0.325813	0	100	0	0	0	0	7.69	0	92.31
15.07	1.3	0.470162	0	100	0	0	0	0	0	0	100
15.12	1.866667	0.351866	0	100	0	0	0	0	20	6.67	73.33
16.01	0.7	0.470162	0	100	0	0	0	0	0	0	100
16.02	3.818182	0.501081	0	100	9.09	0	0	18.18	0	54.55	18.18
16.03	1	0	0	100	0	0	0	0	0	0	100
16.04	1	0	0	100	0	0	0	0	0	0	100
16.05	1.846154	0.612686	0	100	0	0	0	0	0	7.69	92.31
17.08	0.590909	0.590326	0	100	0	0	0	0	0	0	100
18.01	0.583333	0.50361	0	100	0	0	0	0	0	0	100
18.02	0.555556	0.50637	0	100	0	0	0	0	0	0	100
18.03	2	0.748331	0	100	0	0	0	0	26.92	0	73.08
18.04	2.384615	0.852147	0	100	0	0	0	34.62	0	30.77	34.62
18.07	1.130435	1.01374	0	100	0	0	0	0	0	0	100
18.08	0.5	0.512989	0	100	0	0	0	0	0	0	100
19.01	1	0	0	100	0	0	0	0	0	0	100
19.02	1.4	0.502625	0	100	0	0	0	0	0	0	100
19.03	0.909091	0.294245	0	100	0	0	0	0	0	0	100
19.04	1.086957	0.514609	0	100	0	0	0	0	0	0	100
19.05	0	0	0	100	0	0	0	0	0	0	100
19.08	1	0	0	100	0	0	0	0	0	0	100
2.02	0.904762	0.300793	0	100	0	0	0	0	0	0	100
2.03	1	0	0	100	0	0	0	0	0	0	100
2.04	0.769231	0.429669	0	100	0	0	0	0	0	0	100
2.05	1	0	0	100	0	0	0	0	0	0	100
2.06	0.961538	0.196116	0	100	0	0	0	0	0	0	100
2.07	1.153846	0.784465	0	100	0	0	0	0	0	0	100
23.01	1.666667	0.617213	0	100	0	0	0	0	0	0	100
23.02	1	0	0	100	0	0	0	0	0	0	100
23.03	0.666667	0.48795	0	100	0	0	0	0	0	0	100
23.04	1	0	0	100	0	0	0	0	0	0	100
23.06	0.5	0.512989	0	100	0	0	0	0	0	0	100
23.09	0.304348	0.470472	0	100	0	4.35	0	0	8.7	0	86.96
3.01	1	0	0	100	0	0	0	0	0	0	100
3.02	1	0	0	100	0	0	0	0	0	0	100
3.03	0.884615	0.431455	0	100	0	0	0	0	0	0	100
3.04	0.95	0.510418	0	100	0	0	0	0	0	0	100
3.05	1.272727	0.827032	0	100	0	0	0	4.55	0	9.09	86.36
3.06	0.347826	0.831685	0	100	0	0	0	0	0	0	100

sample	mean. relief	sd. relief	Fieldof view. limited	Fieldof view. open	broad. bryozoa	broad. crinoids	broad. Hydro coral	broad. hydroids	broad. Octocoral .black	broad. sponges	broad. Unconsolidated
30.01	0.333333	0.658281	0	100	0	0	0	0	0	9.52	90.48
30.02	0	0	0	100	0	0	0	0	0	0	100
30.03	0.052632	0.229416	0	100	0	0	0	0	0	0	100
30.04	1	0.978019	0	100	0	0	0	0	16.67	4.17	79.17
30.05	1.428571	0.790151	0	100	0	0	0	0	14.29	10.71	75
30.06	2	1.112697	0	100	0	0	0	0	4.55	31.82	63.64
31.01	1.541667	0.931533	0	100	0	0	0	0	0	16.67	83.33
31.02	0.571429	0.507093	0	100	0	0	0	0	0	4.76	95.24
31.03	1.26087	0.448978	7.5	92.5	0	0	4.35	13.04	8.7	8.7	65.22
31.04	0.730769	0.533494	0	100	0	0	0	0	25.93	0	74.07
31.05	0.55	0.510418	0	100	0	0	0	0	15	5	80
31.06	0.52	0.585947	0	100	0	0	0	0	4	4	92
4.01	2.277778	1.363626	0	100	0	0	0	0	25	25	50
4.02	1.807692	1.16685	0	100	0	0	0	0	11.54	23.08	65.38
4.03	2.590909	1.501082	0	100	0	0	0	0	4.55	36.36	59.09
4.08	2.173913	1.029217	0	100	0	0	0	0	8.7	39.13	52.17
4.11	2.391304	0.940944	0	100	0	0	0	8.7	4.35	34.78	52.17
4.12	1.5	1.104536	0	100	0	0	0	30.77	0	0	69.23
5.02	1	0	0	100	0	0	0	0	0	0	100
5.03	1	0	0	100	0	0	0	0	0	0	100
5.07	1	0	0	100	0	0	0	0	0	0	100
5.08	0.92	0.276887	0	100	0	0	0	0	0	0	100
5.11	1	0	0	100	0	0	0	0	0	0	100
5.13	1	0	0	100	0	0	0	0	0	0	100
6.01	0.142857	0.358569	0	100	0	0	0	0	0	0	100
6.02	0.96	0.2	0	100	0	0	0	0	0	0	100
6.03	2.533333	1.431983	7.5	92.5	0	0	0	0	26.67	23.33	50
6.04	0.48	0.509902	0	100	0	0	0	0	0	0	100
6.05	0.76	0.43589	0	100	0	0	0	0	0	0	100
6.12	1	0	0	100	0	0	0	0	0	0	100
7.01	1	0	0	100	0	0	0	0	0	0	100
7.02	1	0	0	100	0	0	0	0	0	0	100
7.03	1	0	0	100	0	0	0	0	0	0	100
7.04	1	0	0	100	0	0	0	0	3.85	0	96.15
7.05	1	0	0	100	0	13.04	0	0	0	0	86.96
7.08	0.95	0.223607	0	100	0	0	0	0	0	0	100
8.01	1.074074	0.54954	0	100	0	0	0	0	3.7	7.41	88.89
8.02	3.892857	1.342725	2.5	97.5	0	0	0	0	53.57	25	21.43
8.05	0.952381	0.218218	2.5	97.5	0	0	0	0	0	0	100
8.06	1.045455	0.213201	0	100	0	0	0	0	4.55	0	95.45
8.07	1	0	0	100	0	0	0	0	0	0	100
8.12	1.6	1.080123	0	100	0	0	0	0	16	12	72
9.01	2.16	0.943398	0	100	0	0	0	20	8	24	48

sample	mean. relief	sd. relief	Fieldof view. limited	Fieldof view. open	broad. bryozoa	broad. crinoids	broad. Hydro coral	broad. hydroids	broad. Octocoral .black	broad. sponges	broad. Unconsolidated
9.02	1.619048	0.740013	0	100	0	0	0	23.81	9.52	0	66.67
9.05	1.04	0.2	0	100	0	0	0	0	0	4	96
9.06	2.217391	0.795243	0	100	0	0	0	0	4.35	43.48	52.17
9.07	2.8	0.763763	0	100	0	0	0	20	20	20	40
9.08	0.708333	0.550033	0	100	0	0	0	4.17	16.67	0	79.17

8. NINGALOO BRUV FISH ANALYSIS

Author: Emma Lawrence

Date: 10 December 2020

8.1 Background

The 2019 sampling spreads across the Northern Ningaloo Marine Park (Commonwealth Waters) Region to straddle management zone boundaries as well as variations in fishing pressure – from the new no-take zone in the south to the highly fished areas in the north. Emphasis was also given to previously sampled sites in order to provide the potential to detect any trends in fish abundance or biomass that have developed in the 10 years since the first surveys.

8.2 Survey objectives

The goals of the current survey were to:

1. Provide baseline data to establish/quantify biodiversity content within the AMP

2. Provide a baseline for the recently established IUCN II area, and for controls in nearby areas

3. Leverage historical data to try and gain some understanding of the changes in recent history throughout the area.

8.3 Sample design

The strategy used to design the survey was based on that outlined in Przeslawski and Foster (2018) with some alterations to make it more efficient for BRUV deployment (minimise steaming and non-sampling time). The key attributes of the sample design were randomness and spatial balance but with an increased probability of selection given to sites with a high terrain position index (as these are likely to be associated with higher fish abundances) and those that had been previously sampled in 2006 and 2009. The BRUV drops were also clustered to improve efficiency (see Appendix A of main report for full details).

8.4 Data collected

BRUVS were deployed in sets of six proximate 60 min drops, separated by 0.5–2 km. Typically, 3–4 sites of six drops could be conducted each day, depending on water depth, weather conditions, distance between sites and available light. Because of the time of year, sufficient daylight hours for operations (BRUV retrieval) and navigation in and out of reef anchorages were limited, restricting the number of sites to an unexpected degree, particularly to the north. We have BRUV data analysed from 130 sites (Figure 11), this includes some sites that were selected preferentially in the field rather than visiting the planned sites further to the north (Figure 72).

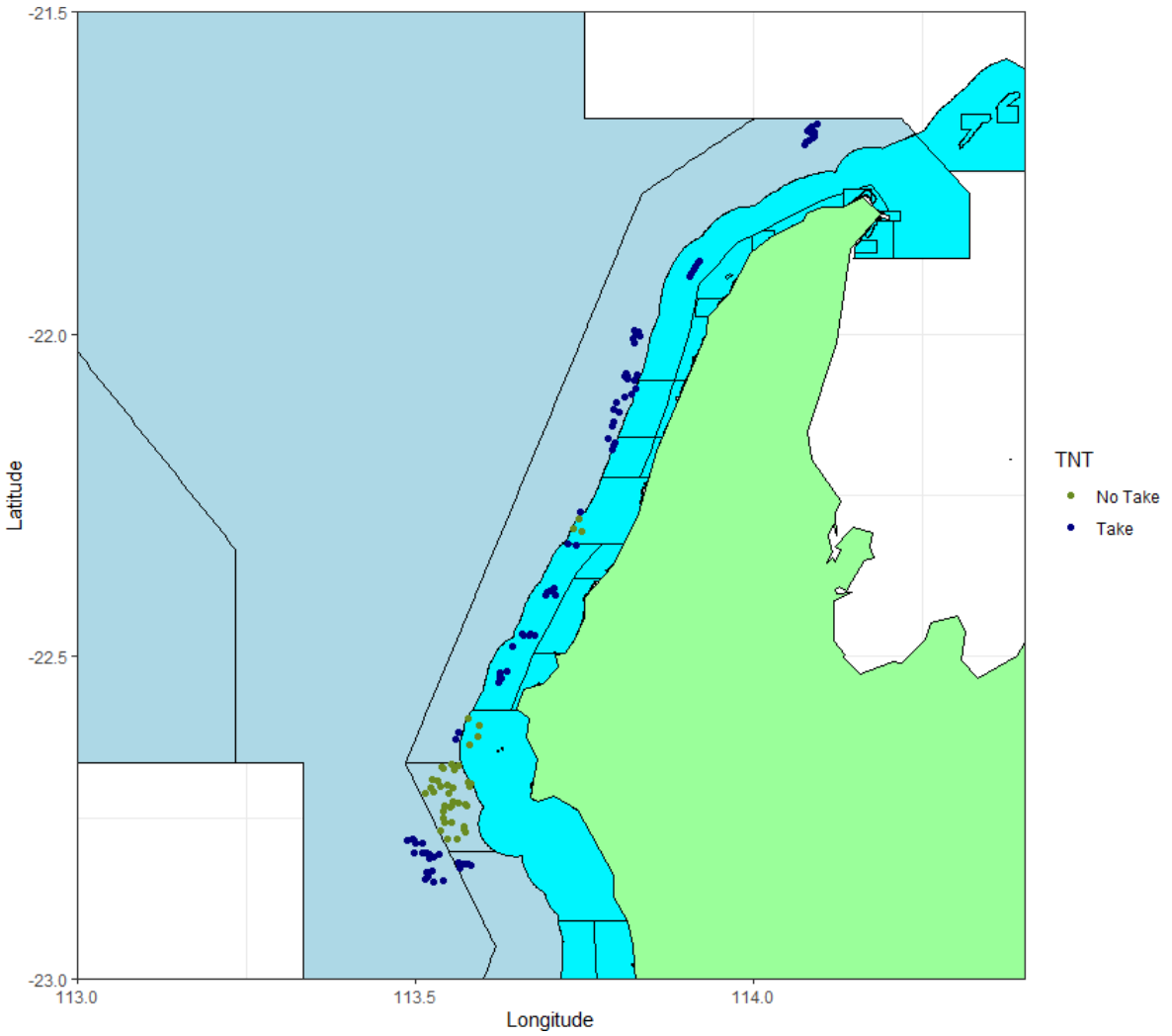

Figure 71 Map of BRUV locations sampled during the 2019 field trip. No take (DARK GREEN): areas closed to fishing, Take (DARK BLUE): areas that may be fished. 42 BRUVs were deployed in No Take areas and 88 BRUVs were deployed in Take areas.

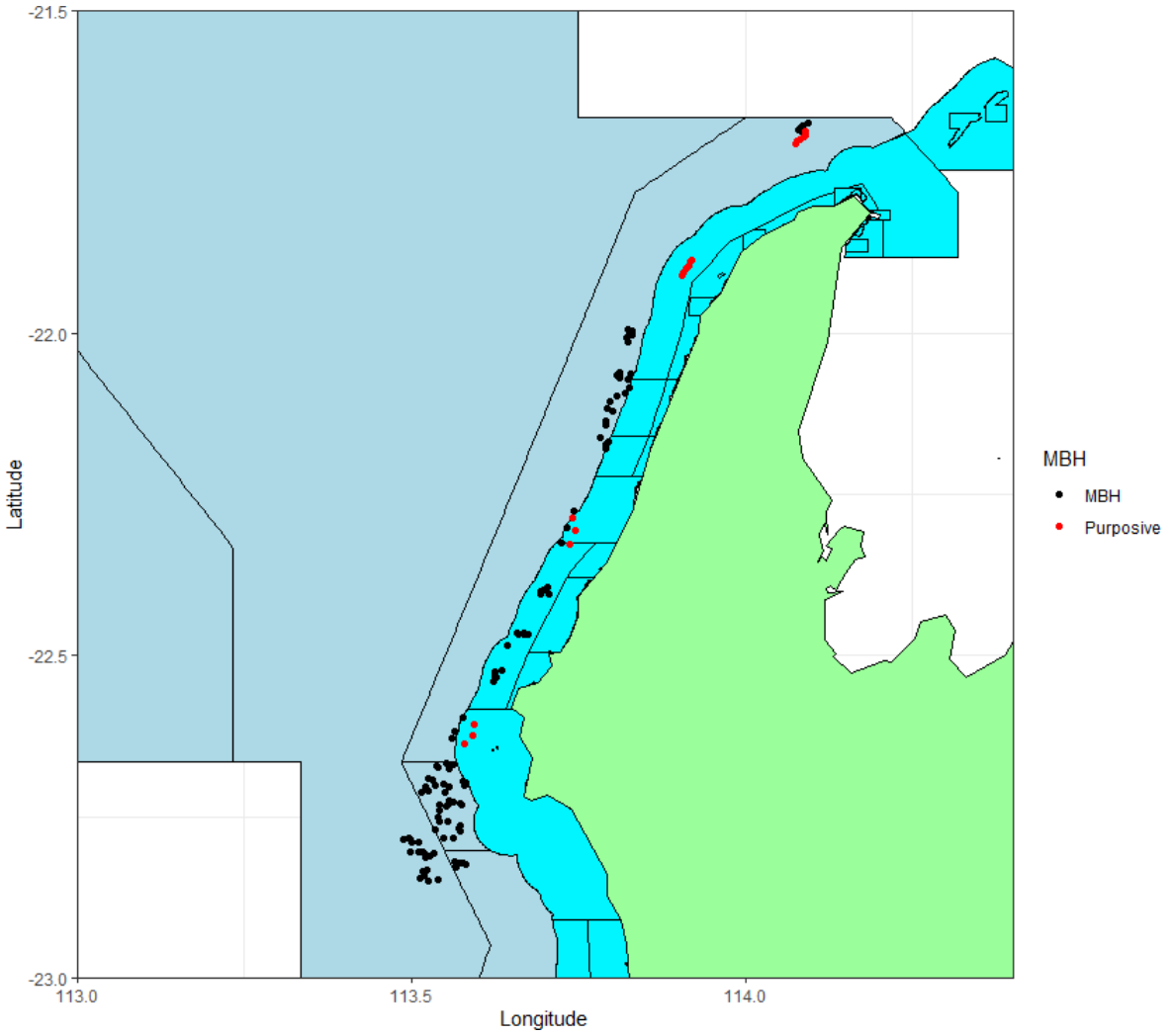

Figure 72 Map of planned BRUV drops (MBH) vs those selected in the field (Purposive).

8.5 Data analysis

A total of 169 different species were recorded across the 130 BRUV drops, of which 140 species were in Take areas and 114 in No Take areas. We looked at the sum of the MaxN by Take/No Take of the fished species. The fished species seen in the highest total numbers (not highest number of sites) are shown in Figure 73. While the Caesionidae family were only captured on BRUV footage at a small number of sites, their counts were the highest (>30). Other families, like Lethrindae, were seen more often but in smaller numbers, with a couple of counts greater than ten.

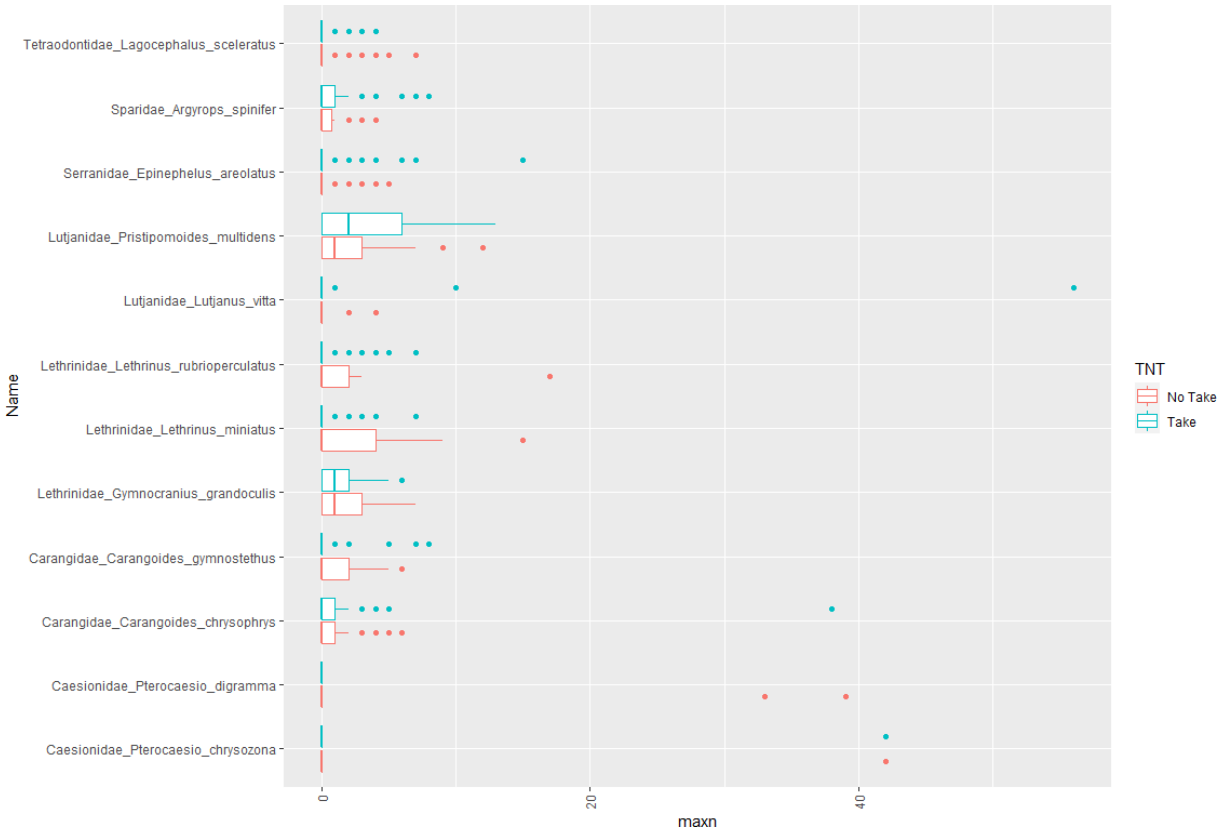

Figure 73 Boxplot of MaxN for the fished species seen in the highest numbers in total.

For most of the species identified there is insufficient data to perform any modelling but we have calculated the Mean MaxN for each species by Take/No Take area (see Appendix). We were however, able to undertake a more comprehensive modelling exercise for *Pristipomoides multidens* and for the total count of all of the targeted fished species combined, excluding *P. multidens*, *Loxodon macrorhinus, Carcharhinus albimarginatus, Lethrinus bebulosus, Gymnocranius grandoculsis, Lethrinus olivaceus, Lethrinus punctulatus, Pristipomoides filatmentosus, Lutjanus sebae, Symphorus nematophorus, Aprion virescens, Genicanthus Lamarck, Scomberomorus commerson, Epinephelus rivulatus, Epinephelus multinotatus, Variola louti, Chysophyrs auratus*.

8.5.1 Abundance of *P. multidens*

P. multidens were recorded on more than half of the BRUV drops. While many drops recorded one individual, several recorded 10 or more (Figure 74 and Figure 75). We analysed the effects of protection and habitat *on P. multidens* using generalised additive models (GAM) with a negative binomial error distribution. We also considered the Tweedie and Poisson distributions, however the model checks of the residual versus fitted plots revealed the negative binomial provided the best fit. The variables included for consideration were drop location (Easting and Northing), Site (BRUV drops close together belong to the same Site), tpi (terrain position index), aspect, slope, roughness, bathymetry, distance to nearest boat ramp, MBH (indicating whether the drops were part of the sample plan vs selected in field) and TNT (Take vs No Take area). The initial model fits showed that there were several observations where the covariates indicated that the environment was extremely different at these few sites compared to the remainder, these observations were

subsequently removed so as not to overly influence the GAM fits. Following this process there were still several observations with a very high tpi value that heavily drove the GAM fit to this covariate and so these values were reduced to a tpi value of 0.1 (variable with capped tpi at 0.1 was renamed tpi2). Slope and roughness were highly collinear with tpi and so they were dropped from the analysis.

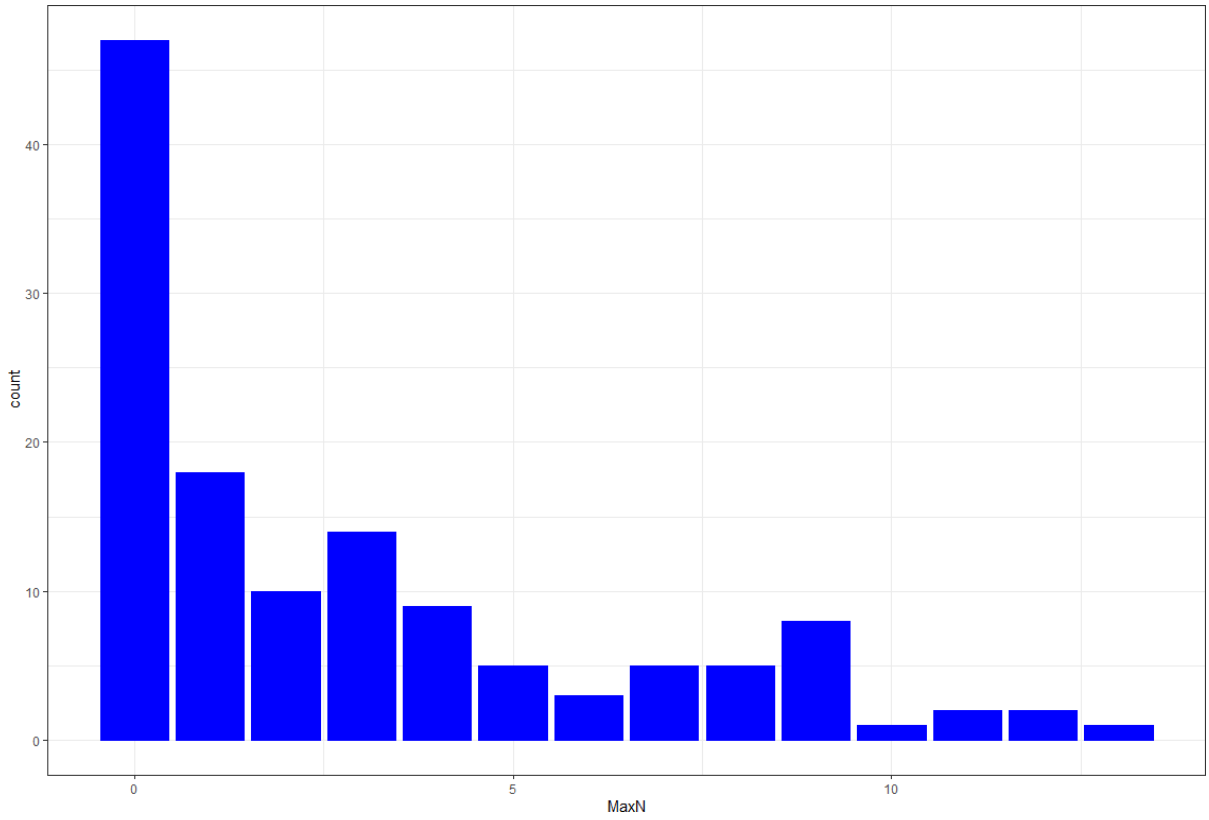

Figure 74 Histogram of *P. multidens* MaxN counts.

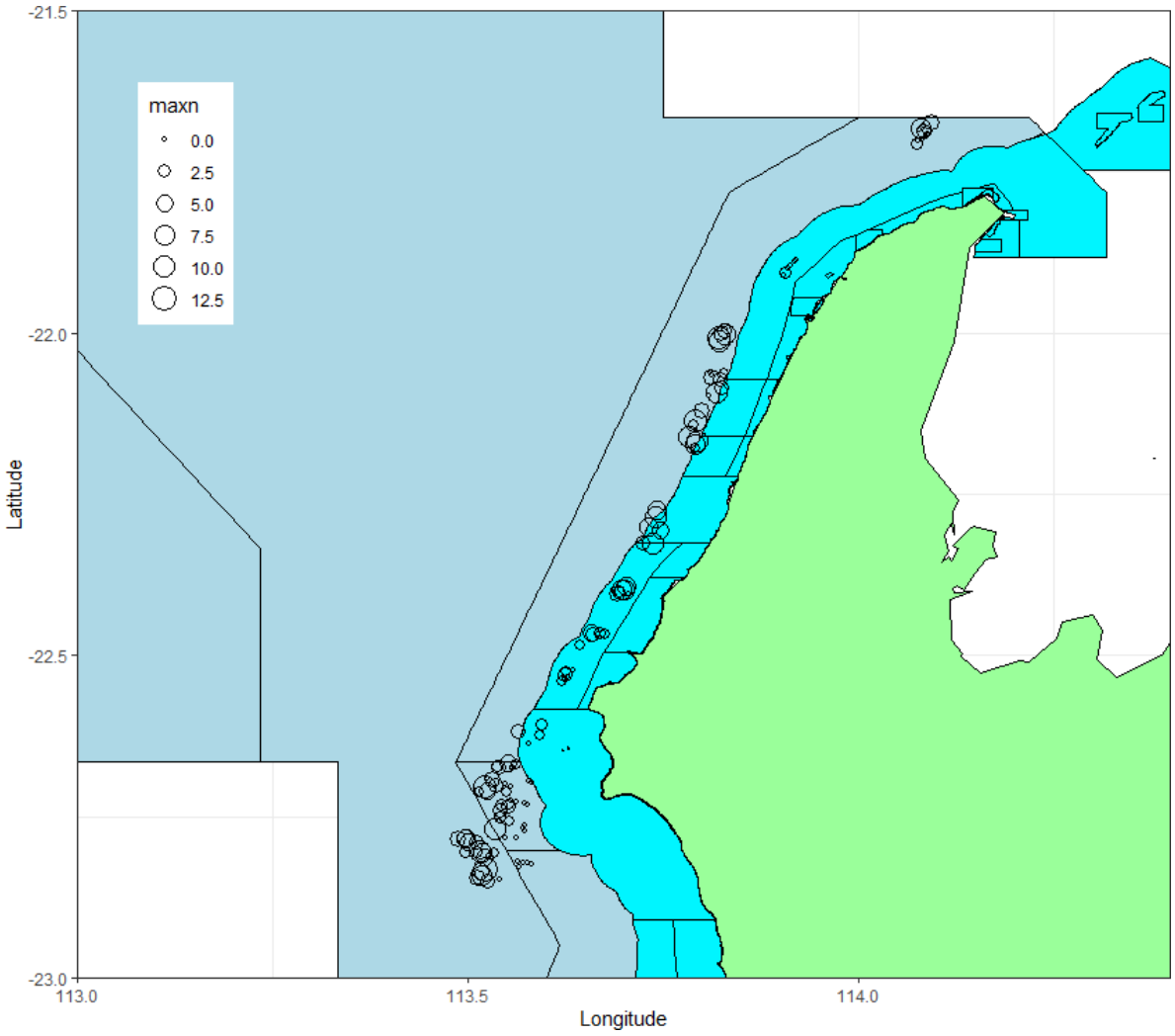

Figure 75 Distribution of observed MaxN values for *P. multidens*. The larger the circle, the higher the observed value.

When analysing data collected under a sampling design it is important to account for (include) all variables that were used for the design in the analysis, regardless of whether they are significant in the model. For the Ningaloo 2019 design, those variables were tpi and site type (whether the site was a legacy site - included in previous years' surveys). We included the interaction of TNT and MBH to determine whether the sites selected in the field were different to those selected as part of the initial sample design. The interaction was not significant and so it was dropped. Our model included main effects for TNT, MBH and site Type, a tensor smooth (Easting, Northing) to account for any spatial autocorrelation (sites close to each other are likely to be more similar than those further apart) and spline smooth terms for tpi, distance to boat ramp, bathymetry and aspect. The models were fitted using the mgcv package in R 3-4.0.3 (Wood, 2017). We used the diagnostic information from the gam.check function to determine the whether the basis spline dimension choices were adequate. Model terms (other than those considered essential due to the design) were dropped on the basis of significance, AIC and deviance explained.

The final model for *P. multidens* included terms for site type, tpi, bathymetry, distance to boat ramp and spatial location and is summarised in Table 27.

Table 27 Summary of final model for *P. multidens* using 2019 survey data. Deviance explained = 47.7%, AIC= 491.36, number of observations = 124.

	Estimate	**p-value**
(Intercept)	0.533382	0.0232
Type: New	0.002792	0.9913
	edf (estimated degrees of freedom)	**p-value**
s(tpi2)	1.000	0.9973
s(bathy)	1.972	0.0332
s(Distance to ramp)	1.000	0.0637
te(x,y)	7.284	0.0006

The only significant (α=0.05) variables in the model are bathymetry and the spatial term. However, distance to boat ramp is bordering on significance. The relationship between the smoothed covariates is shown in Figure 76. While the abundance of *P. multidens* is predicted to be greater in deeper water, the predicted abundance increases as distance from boat ramp increases.

We created and stacked rasters using the raster package in R to allow the prediction of the model onto the broader region (including unsampled areas). The large amount of data caused some computing problems and so the spatial locations were subsampled from the full raster to produce a map. Where there are gaps in the map it is due to missing covariates (namely bathymetry). The highest predicted values are spatially clustered (Figure 13 Predicted values of *Pristipomoides multidens* based on the model selected. Darker colours indicate increasing predictions.), namely further off the coast and furthest from boat ramp. Note that the few locations with very high predicted values (MaxN ~12) also have the highest standard errors (Figure 78), as is typical with count data.

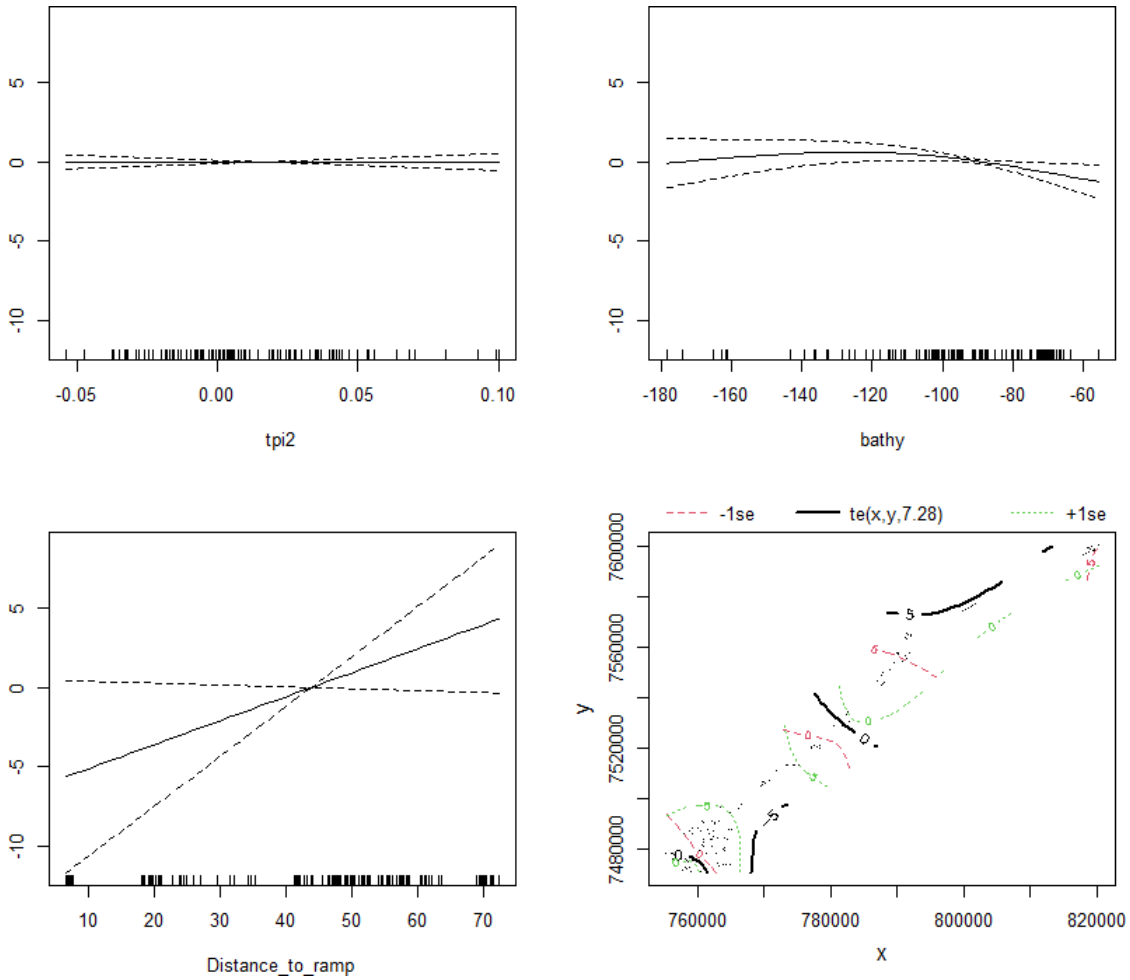

Figure 76 The solid line shows the model fit to each of the smoothed covariates, and the dotted lines show +/- two standard errors. Notwithstanding the influence of other covariates, these plots can be used to interpret the influence of each covariate on the observed abundance of *P. multidens*.

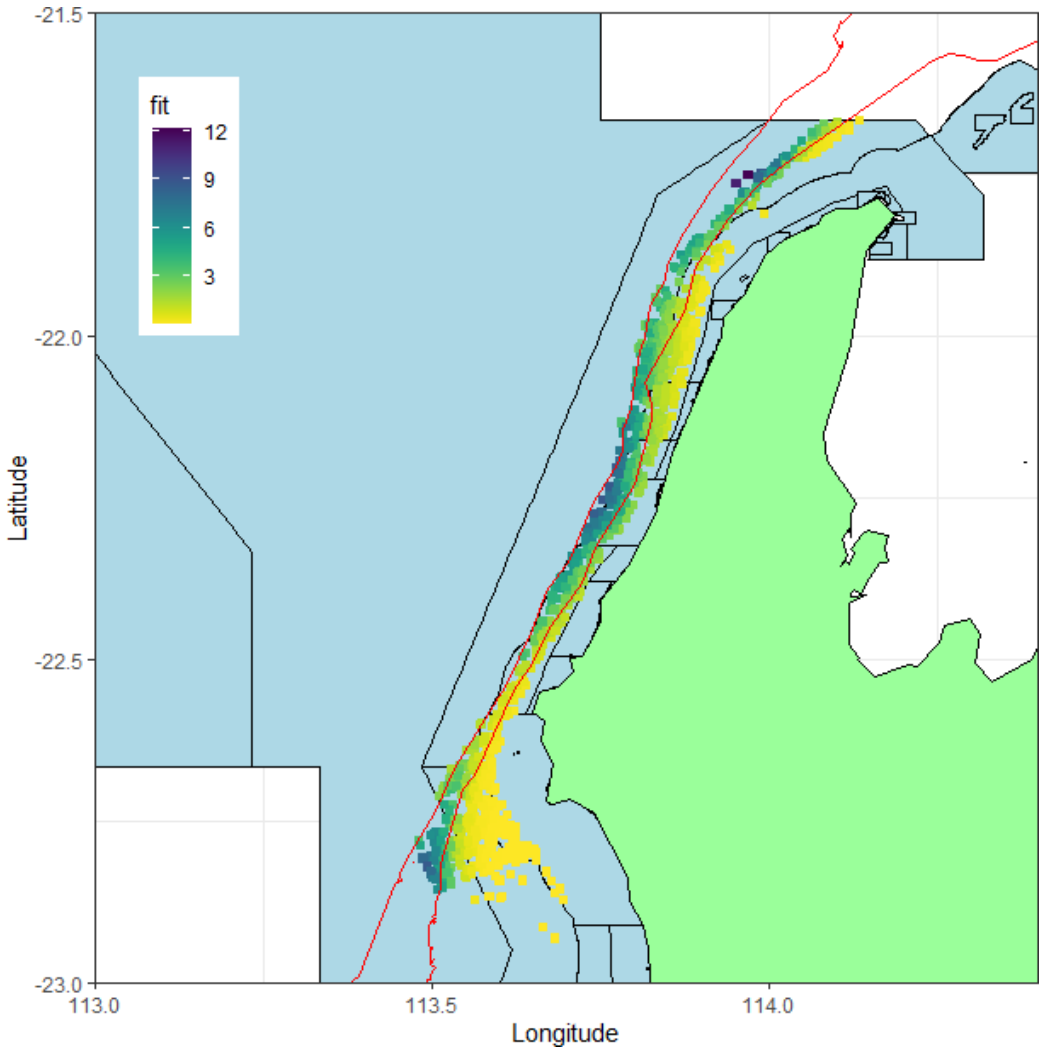

Figure 77 Predicted values of *P. multidens* based on the model selected. Darker colours indicate increasing predictions. Red lines indicate the 100 m and 200 m contour lines.

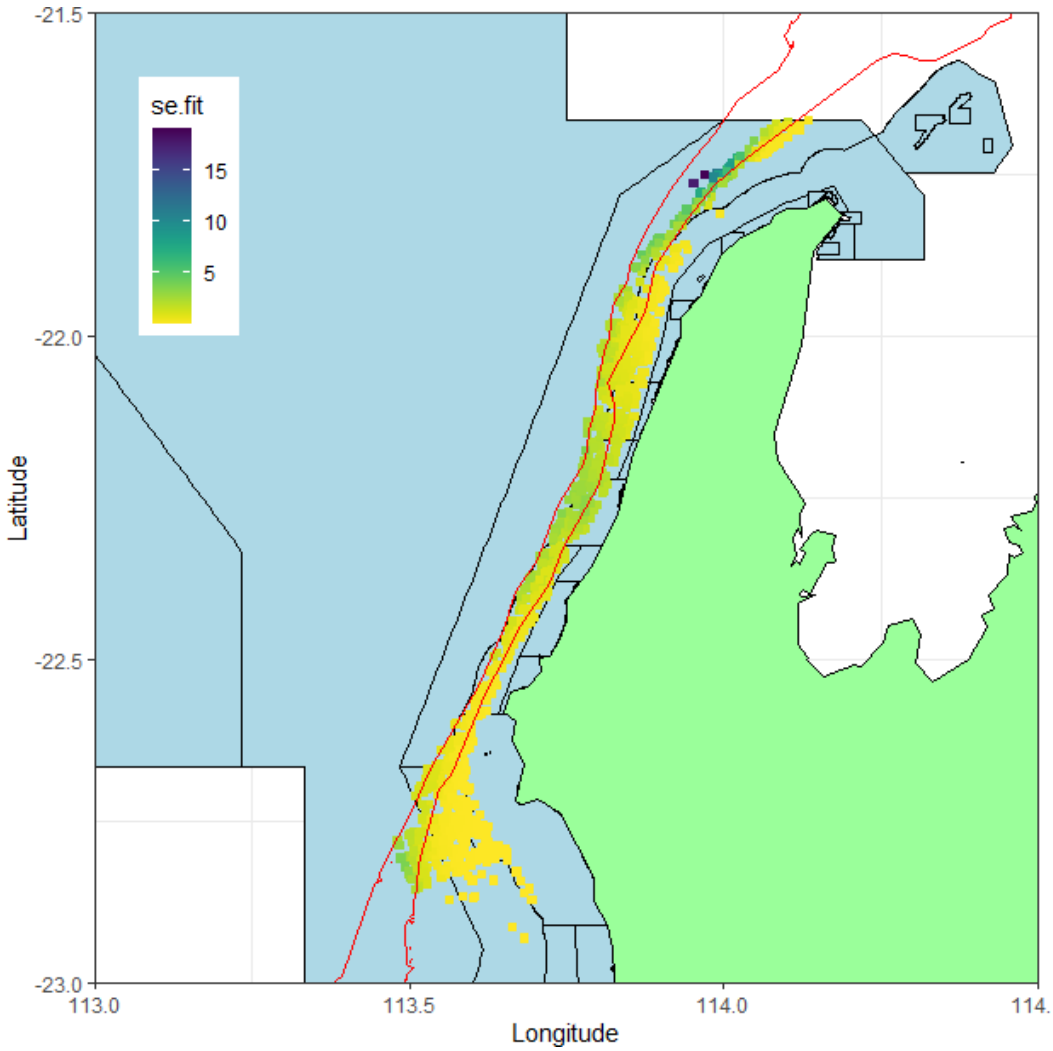

Figure 78 Predicted standard errors of *P. multidens*. Darker colours indicate higher standard errors. Red lines indicate the 100 m and 200 m contour lines.

8.5.2 Abundance of targeted species (excluding *P. multidens*)

Targeted species were observed on most BRUV drops with one drop recording more than 30 targeted fish (Figure 79). We analysed the effects of protection and habitat combined targeted species using generalised additive models (GAM) with a negative binomial error distribution. We also considered the Poisson distribution, however the model checks of the residual versus fitted plots revealed the negative binomial provided the best fit. The variables considered and the model fitting process were the same as for the *P. multidens* model.

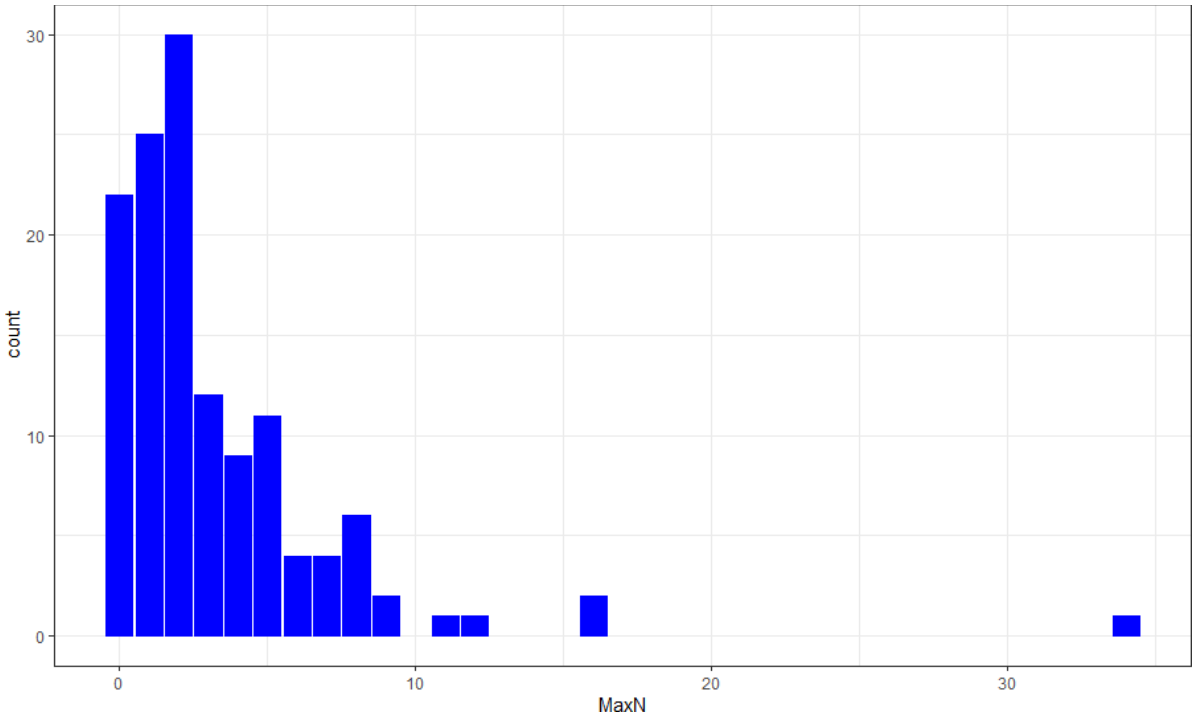

Figure 79 Histogram of sum of MaxN of targeted species observed per BRUV drop.

Table 28 Summary of final model for total MaxN for target fish species using 2019 survey data. Deviance explained = 32.5%, AIC= 567.09, number of observations = 126.

	Estimate	**p-value**
(Intercept)	1.0259	<0.0001
MBH: Purposive	0.9496	0.0008
Type: New	-0.2421	0.2624
	edf (estimated degrees of freedom)	**p-value**
s(tpi2)	1.142	0.7610
s(bathy)	1.972	<0.0001
s(Distance to ramp)	1.924	0.0012
te(x,y)	3.441	0.0047

Again, the model contains terms for legacy vs new sites (Type) and tpi despite their lack of significance, as these variables were used during the design process (Table 28). The significant (α=0.05) terms in the model are MBH (indicating more target species were observed at the sites selected in the field vs the planned sites), bathymetry, distance to boat ramp and the spatial term. The relationship between the smoothed covariates is shown in Figure 80. While the abundance of targets species is predicted to be greater in shallower water (the opposite of the *P. multidens* result), the predicted abundance again increases as

distance from boat ramp increases. The spatial term (bottom right) shows a very strong spatial gradient along the coastline.

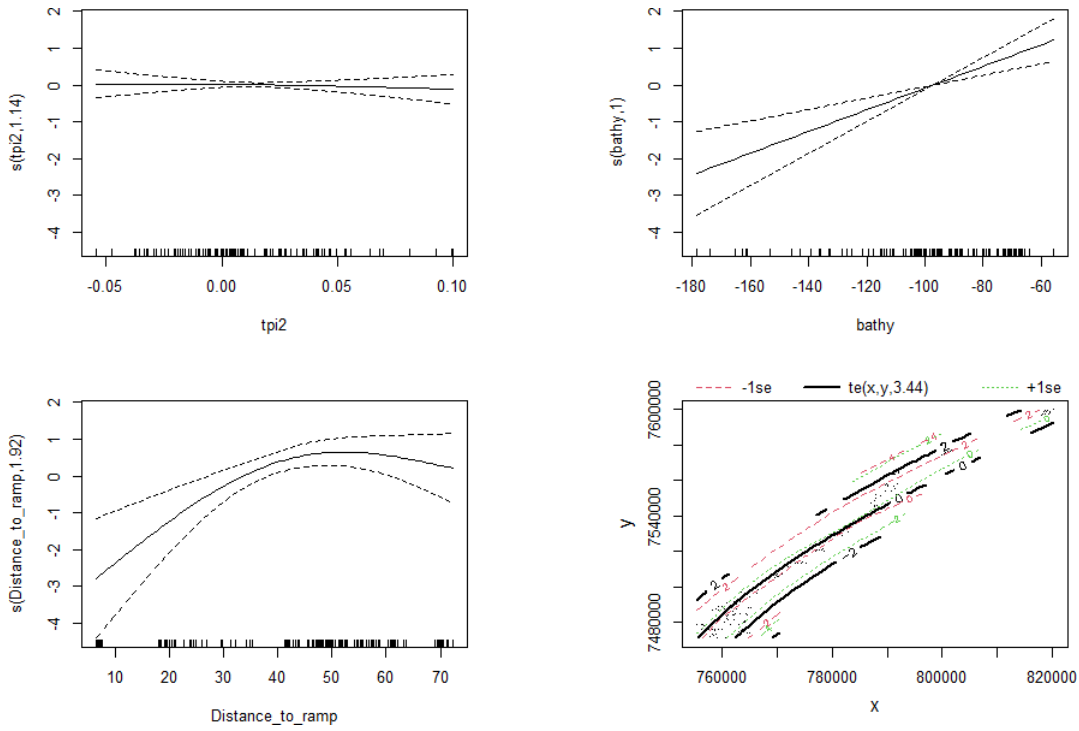

Figure 80 The solid line shows the model fit to each of the smoothed covariates, and the dotted lines show +/- two standard errors. Notwithstanding the influence of other covariates, these plots can be used to interpret the influence of each covariate on the observed values of total maxN of target species.

We predicted the total abundance of fished species across the broader region using the raster created previously. We set all sites to be 'MBH' to account for the increased counts observed at the sites selected in the field. The limited predictions and associated standard errors show, as is standard with count data, the highest counts are associated with the greatest error (Figure 82). It may be beneficial to direct extra sampling to these areas of high predicted abundance in the future to reduce the associated errors.

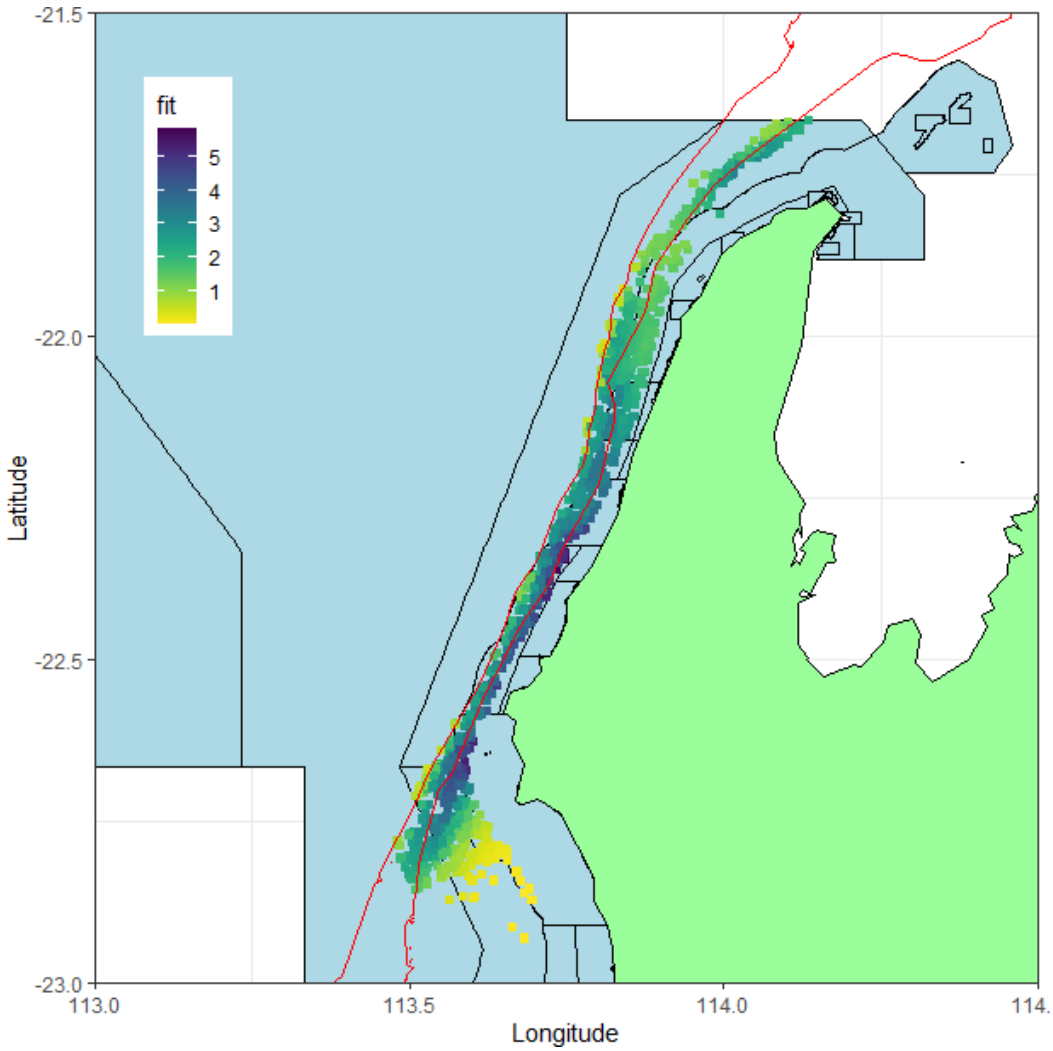

Figure 81 Predicted values of MaxN of target species based on the model selected. Darker colours indicate increasing predictions. Red lines indicate the 100 m and 200 m contour lines.

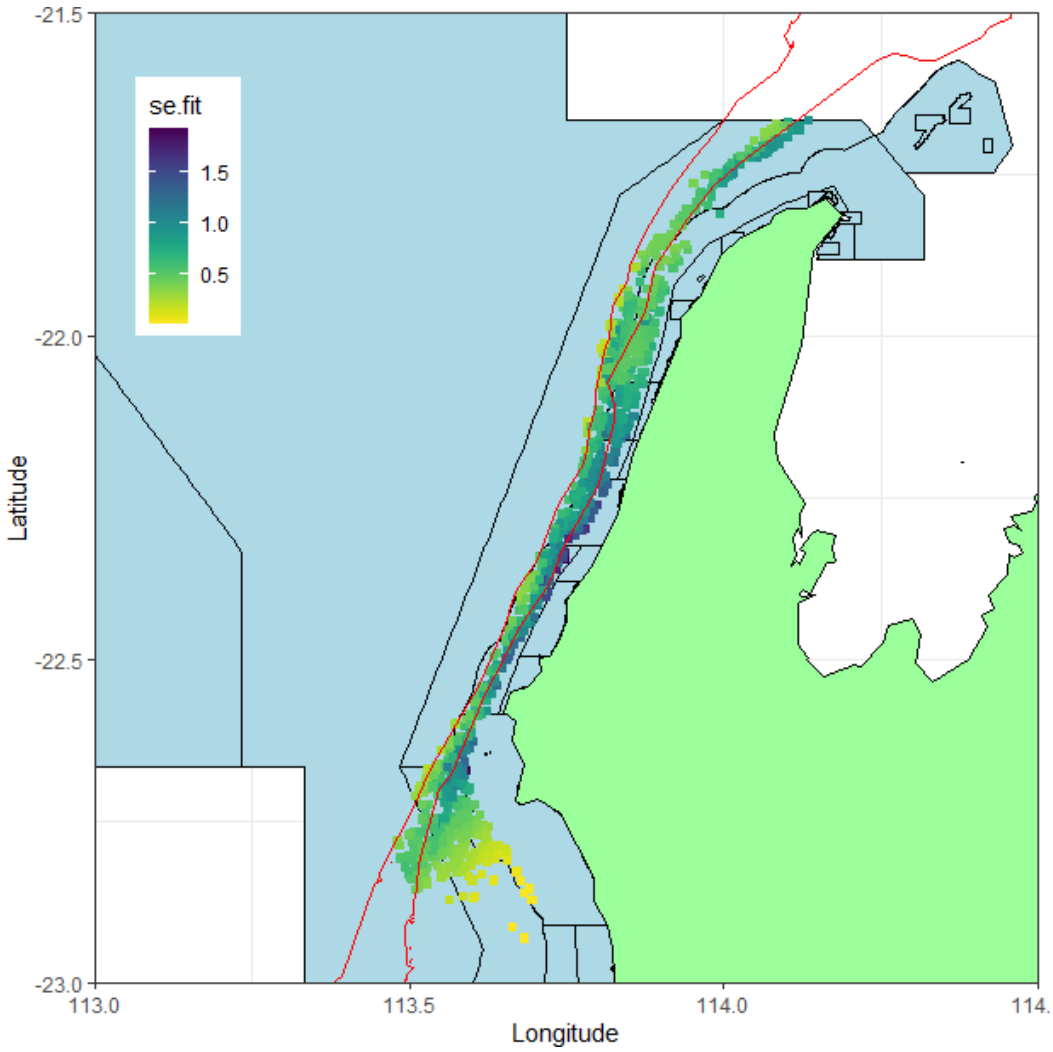

Figure 82 Predicted standard errors of MaxN of target species model. Darker colours indicate higher standard errors. Red lines indicate the 100 m and 200 m contour lines.

8.5.3 Length data

The length data were restricted to the targeted fish species outlined in the previous section and the mean length per BRUV drop analysed. A density plot of the lengths shows that the target species observed were all 20 cm or greater with the mean length approximately the same in both Take and No Take zones but a few larger fish recorded in the No Take zones (Figure 16). However, the distributions are quite similar.

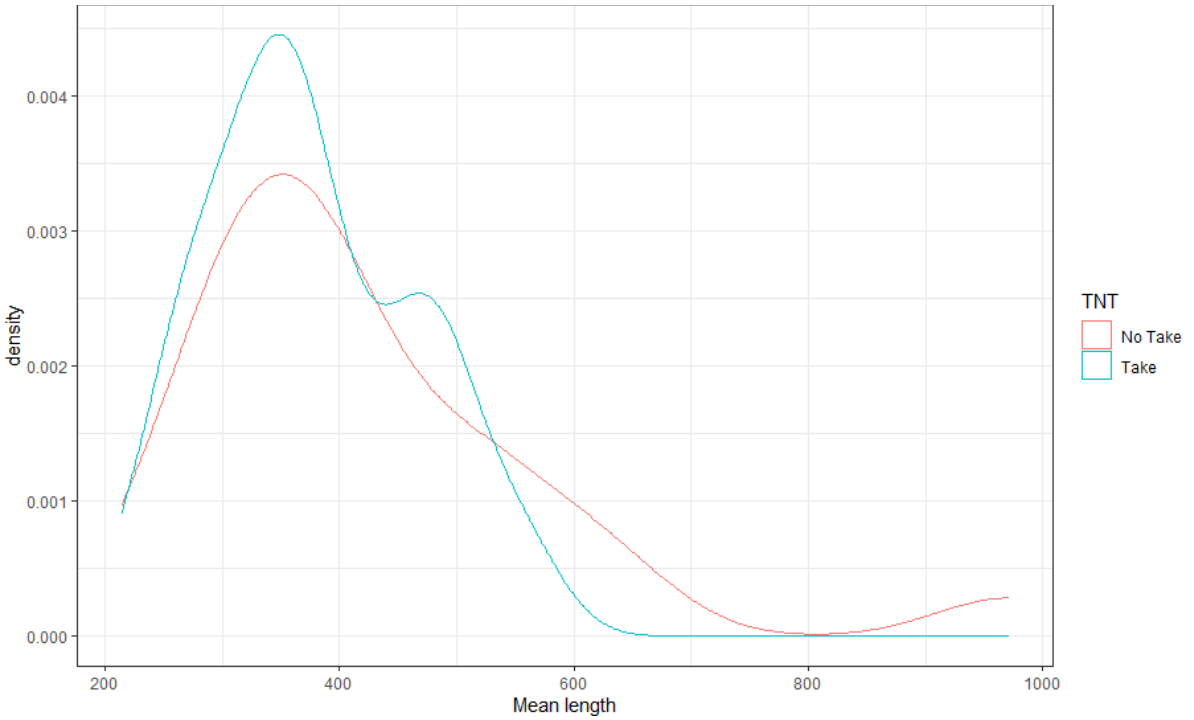

Figure 83 Plot of mean length of target fish species per BRUV drop in Take (BLUE) vs No take (RED) zones.

Table 29 Summary of final model for total MaxN for target fish species using 2019 survey data. Deviance explained = 16.4%, number of observations = 77.

	Estimate	**p-value**
(Intercept)	6.0874	<0.0001
TNT: Take	-0.0367	0.5615
Type: New	-0.17446	0.0107
	edf (estimated degrees of freedom)	**p-value**
s(tpi2)	1	0.1509
s(bathy)	1	0.0353

We fitted a lognormal GAM to the mean length data to determine the effects of protection and habitat. The terms considered in the model were the same as those previously described for the MaxN models and the same model fitting process was followed. However, despite the lognormal distribution being appropriate for the data, even the 'best' model (based on BIC) only explained approximately 16% of deviance in the data It may be that the data are too aggregated to adequately describe the length patterns in the region (i.e. they may be different for different fish and the signals may be distorted) or we may be missing important environmental covariates that explain the length distributions. There was no significant difference in the mean length in the Take and No Take areas.

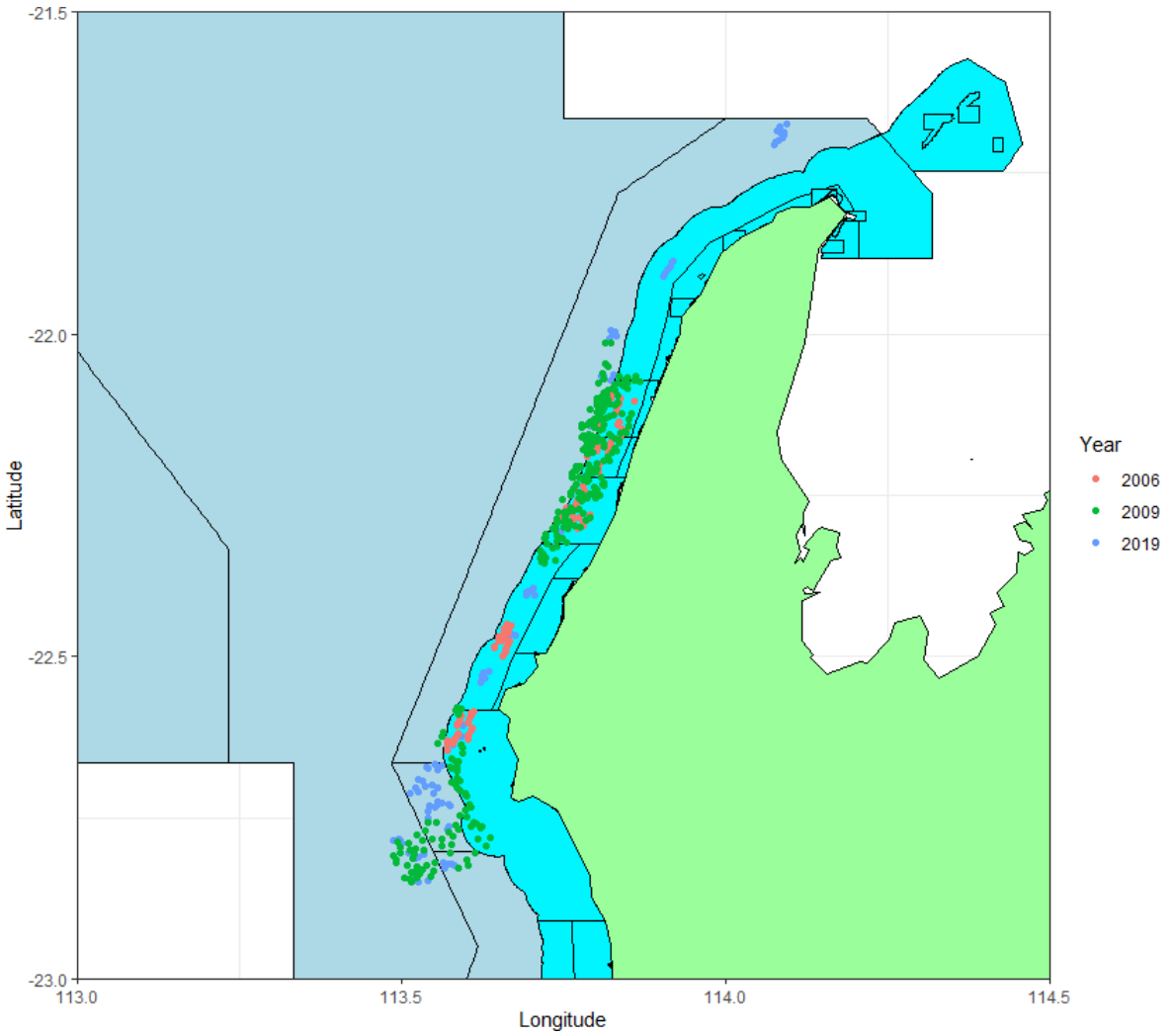

Figure 84 Sites visited in 2006, 2009 and 2019 that fall within the bathymetry layer.

8.6 Temporal data analysis

When the 2019 survey was designed, some sites that had been visited in 2006 and 2009 were selected. These sites make up approximately a quarter of the data. However, we can also make use of the information collected at the sites previously sampled even if they weren't revisited in 2019, provided the sites are from a similar spatial area (Figure 84). To ensure approximately the same spatial footprint between the historical and current data, we originally restricted the data to those sites that lie within the bathymetry layer we used to plan the 2019 survey.

Table 30 Summary of final model for *P. multidens* using 2006, 2009 and 2019 survey data. Deviance explained = 61.7%, AIC= 1035.5, number of observations = 447.

	Estimate	**p-value**
(Intercept)	-1.3767	0.0011
TNT:Take	-0.7401	0.0016
Year: 2009	0.0977	0.8396
Year 2019	2.4903	<0.0001
	edf (estimated degrees of freedom)	**p-value**
s(Distance to ramp)	2.457	0.0002
s(tpi2)	1.000	0.0733
s(bathy)	3.629	<0.0001
te(x,y):Year2006	3.000	0.0002
te(x,y):Year2009	3.000	0.0004
te(x,y):Year2019	4.238	<0.0001

A similar model was fitted to the data as the *P.multidens* model based on 2019 data only. However, a Year main effect term was added and a separate spatial tensor spline for each year. While the model fitted the data well, the predictions onto the grid in the north-western corner were very unrealistic (Max N values greater than 1000). Further investigation of the model revealed that this was due to only having 2019 data in that area and so the sample data was reduced to only those sites below -22.1 Latitude. A Take/No-Take by Year interaction term was included but subsequently dropped due to not being significant, the term for aspect was again dropped resulting in the model in Table 30.

The model shows a significant effect of MNP zones with less *P. multidens* in Take areas compared to No Take. The Year term is also significant with more fish observed in 2019 compared to 2006 and 2009. As with the model based on 2019 data only, distance to nearest boat ramp and bathymetry are again significant.

Spatial predictions were produced for 2006, 2009, 2019 using a similar process to the previous models but with a spatially restricted grid (Figure 85, Figure 86, Figure 87). The areas with the highest predicted values are fairly consistent from year to year despite the

separate annual spatial prediction terms. The standard errors are only shown for 2019 (Figure 88) but were similar for the years prior.

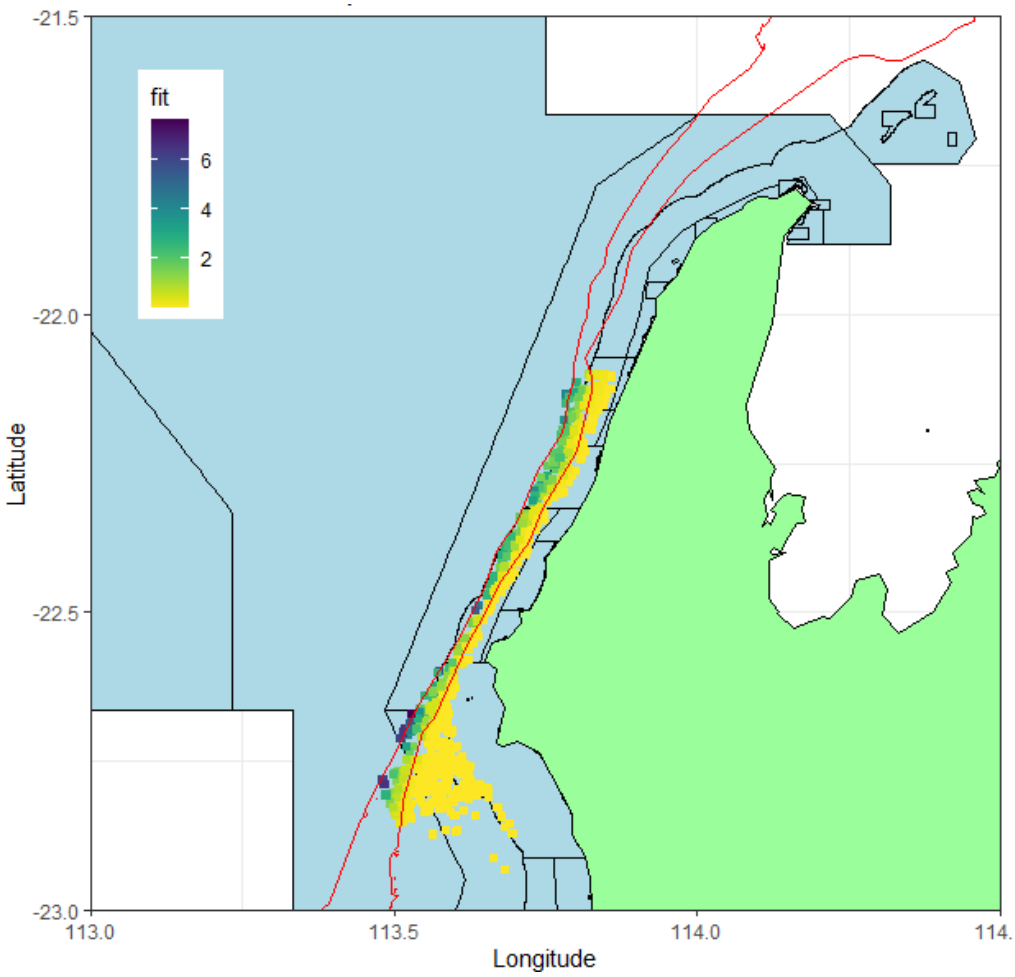

Figure 85 Model predictions for *P. multidens* for 2006. Red lines indicate the 100 m and 200 m contour lines.

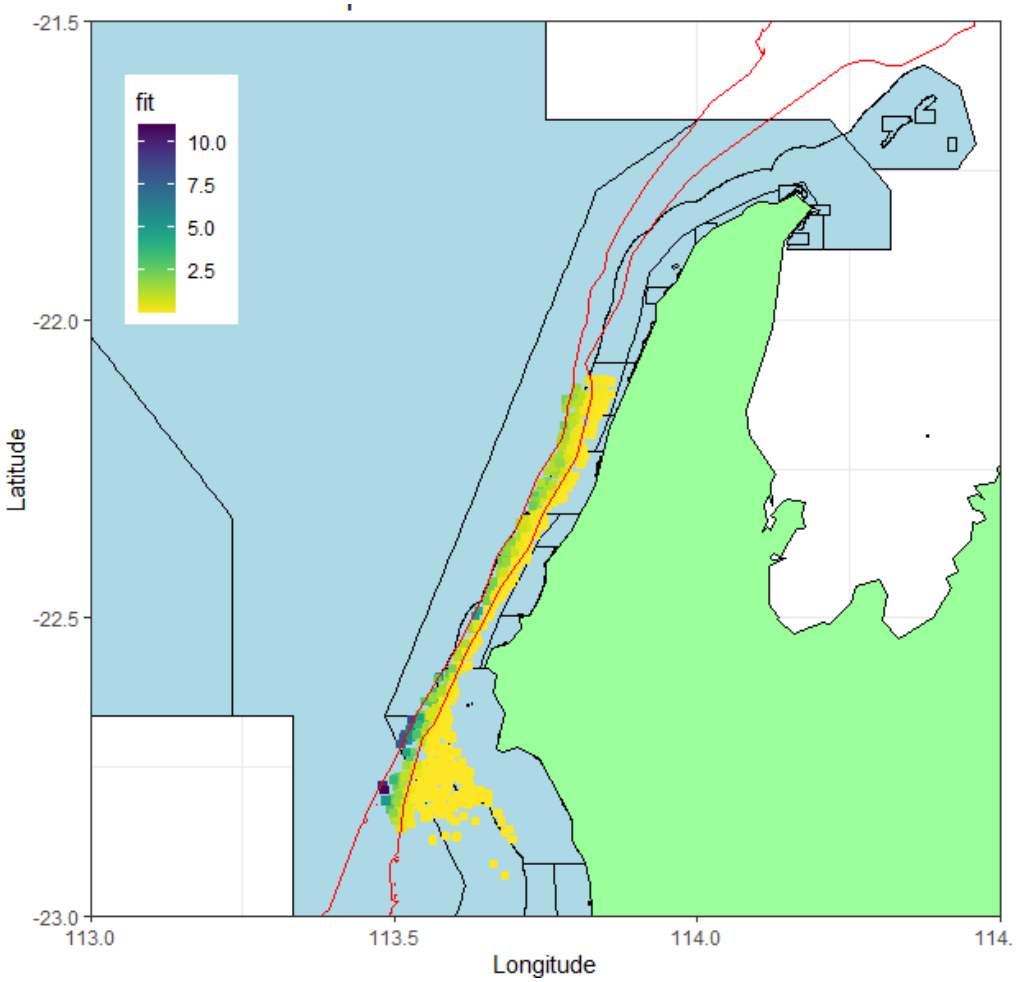

Figure 86 Model predictions for *P. multidens* for 2009. Red lines indicate the 100 m and 200 m contour lines.

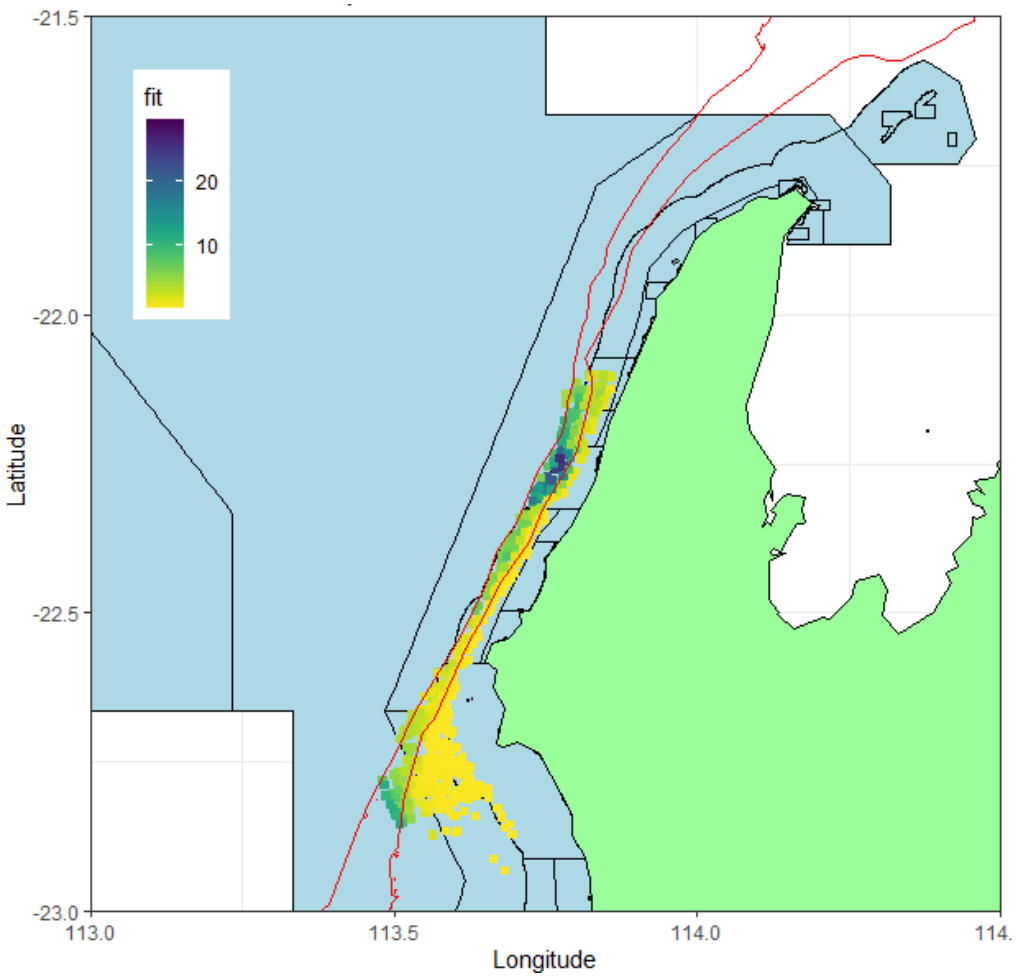

Figure 87 Model predictions for *P. multidens* for 2019. Red lines indicate the 100 m and 200 m contour lines.

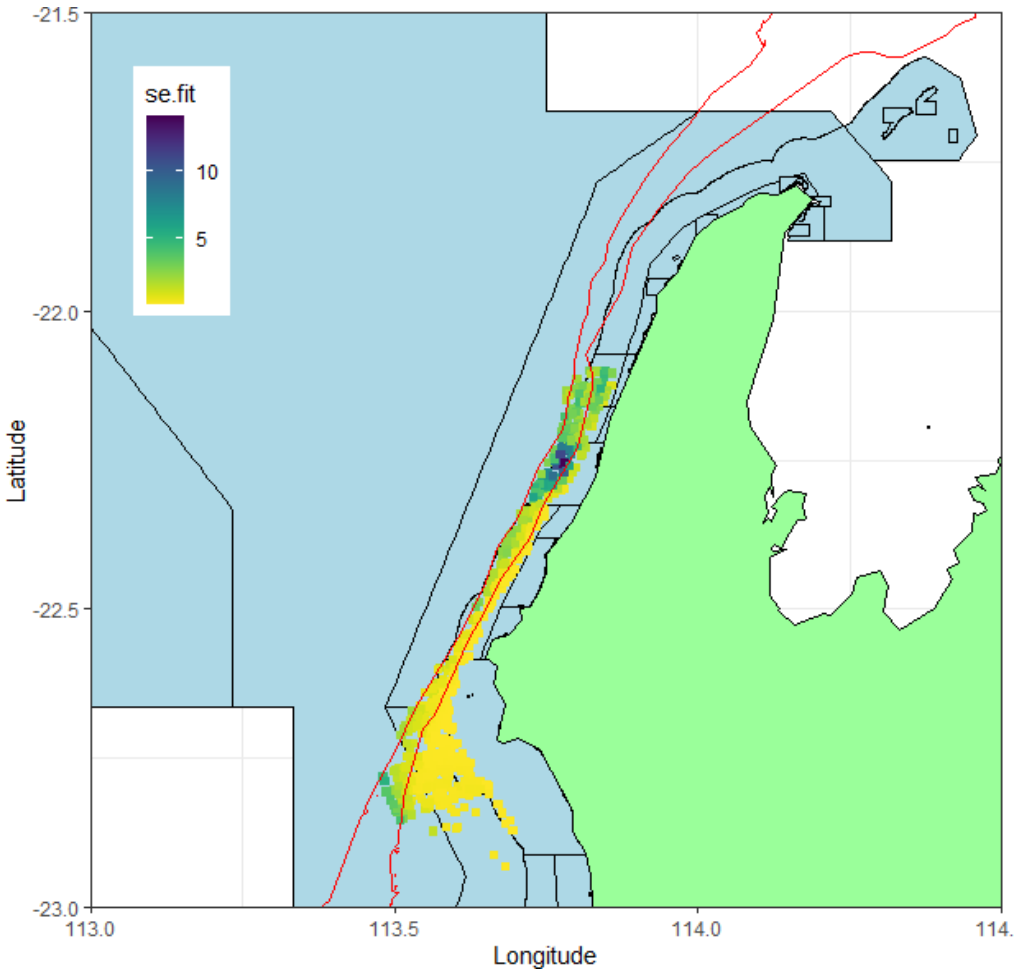

Figure 88 Standard error estimates for model predictions for *P. multidens* for 2019. Red lines indicate the 100 m and 200 m contour lines.

8.7 References

Wood, S.N. (2017) Generalized Additive Models: An Introduction with R (2nd edition). Chapman and Hall/CRC.

Przeslawski, R. and Foster, S. (2018) Field manuals for marine sampling to monitor Australian waters, National Environmental Science Programme, Marine Biodiversity Hub, Canberra, A.C.T., doi: 10.11636/9781925297669.

8.8 Appendix – Mean MaxN for each species by Take/No Take area

Name (Family, Genus, Species)	Take	No Take
Acanthuridae_Acanthurus_grammoptilus	0.014	0.027
Acanthuridae_Acanthurus_mata	0.000	0.081
Acanthuridae_Naso_hexacanthus	0.081	0.270
Apogonidae_Cheilodipterus_quinquelineatus	0.000	0.054
Apogonidae_Ostorhinchus_fasciatus	0.000	0.000
Ariidae_Netuma_thalassina	0.027	0.027
Balistidae_Abalistes_filamentosus	0.351	0.378
Balistidae_Abalistes_stellatus	0.122	0.135
Balistidae_Pseudobalistes_flavimarginatus	0.000	0.027
Balistidae_Pseudobalistes_fuscus	0.000	0.054
Balistidae_Sufflamen_fraenatum	0.189	0.135
Balistidae_Xanthichthys_lineopunctatus	0.135	0.108
Blenniidae_Unknown_sp1	0.000	0.027
Bothidae_Unknown_spp	0.095	0.000
Caesionidae_Caesio_cuning	0.054	0.000
Caesionidae_Caesio_teres	0.000	0.595
Caesionidae_Pterocaesio_chrysozona	0.000	1.135
Caesionidae_Pterocaesio_digramma	0.000	1.946
Callionymidae_Unknown_sp1	0.014	0.000
Carangidae_Carangoides_caeruleopinnatus	0.297	0.297
Carangidae_Carangoides_chrysophrys	1.162	0.946
Carangidae_Carangoides_equula	0.243	0.027
Carangidae_Carangoides_fulvoguttatus	0.041	0.378
Carangidae_Carangoides_gymnostethus	0.514	1.405
Carangidae_Caranx_ignobilis	0.027	0.000
Carangidae_Caranx_papuensis	0.014	0.000
Carangidae_Decapterus_spp	3.811	10.162
Carangidae_Gnathanodon_speciosus	0.081	0.919
Carangidae_Seriola_dumerili	0.365	0.135
Carangidae_Seriola_rivoliana	0.041	0.054
Carangidae_Seriolina_nigrofasciata	0.095	0.027
Carangidae_Unknown_sp1	0.000	0.135
Carcharhinidae_Carcharhinus_albimarginatus	0.027	0.108
Carcharhinidae_Carcharhinus_limbatus	0.000	0.027
Carcharhinidae_Carcharhinus_plumbeus	0.122	0.189
Carcharhinidae_Carcharhinus_sp10	0.041	0.000
Carcharhinidae_Carcharhinus_tilstoni	0.014	0.000
Carcharhinidae_Galeocerdo_cuvier	0.054	0.027

Name (Family, Genus, Species)	Take	No Take
Carcharhinidae_Loxodon_macrorhinus	0.054	0.081
Carcharhinidae_Prionace_glauca	0.000	0.000
Carcharhinidae_Rhizoprionodon_acutus	0.014	0.000
Carcharhinidae_Triaenodon_obesus	0.014	0.000
Carcharhinidae_Unknown_sp10	0.014	0.000
Chaetodontidae_Chaetodon_assarius	0.000	0.108
Chaetodontidae_Heniochus_acuminatus	0.054	0.054
Cirrhitidae_Cirrhitichthys_falco	0.027	0.000
Cirrhitidae_Cyprinocirrhites_polyactis	0.027	0.027
Congridae_Conger_spp	0.014	0.000
Echeneidae_Echeneis_naucrates	0.108	0.189
Fistulariidae_Fistularia_commersonii	0.041	0.000
Glaucosomatidae_Glaucosoma_buergeri	0.000	0.000
Gobiidae_Amblyeleotris_sp10	0.000	0.081
Haemulidae_Diagramma_pictum labiosum	0.041	0.027
Haemulidae_Plectorhinchus_gibbosus	0.000	0.000
Holocentridae_Myripristis_botche	0.000	0.081
Labridae_Bodianus_bilunulatus	0.000	0.081
Labridae_Bodianus_solatus	0.068	0.486
Labridae_Choerodon_cauteroma	0.000	0.000
Labridae_Choerodon_jordani	0.068	0.000
Labridae_Choerodon_sp1	0.000	0.027
Labridae_Choerodon_vitta	0.014	0.000
Labridae_Choerodon_zamboangae	0.068	0.189
Labridae_Coris_caudimacula	0.027	0.027
Labridae_Labroides_dimidiatus	0.000	0.081
Labridae_Novaculichthys_taeniourus	0.000	0.027
Labridae_Pseudojuloides_sp1	0.000	0.135
Labridae_Suezichthys_cyanolaemus	0.000	0.054
Labridae_Unknown_sp1	0.014	0.027
Labridae_Unknown_sp7	0.014	0.000
Labridae_Unknown_sp8	0.041	0.000
Lethrinidae_Gymnocranius_euanus	0.095	0.216
Lethrinidae_Gymnocranius_grandoculis	1.297	1.649
Lethrinidae_Gymnocranius_griseus	0.351	0.297
Lethrinidae_Gymnocranius_sp1	0.027	0.000
Lethrinidae_Lethrinus_miniatus	0.581	2.270
Lethrinidae_Lethrinus_nebulosus	0.243	0.162
Lethrinidae_Lethrinus_olivaceus	0.027	0.108
Lethrinidae_Lethrinus_punctulatus	0.014	0.027
Lethrinidae_Lethrinus_ravus	0.027	0.081

Name (Family, Genus, Species)	Take	No Take
Lethrinidae_Lethrinus_rubrioperculatus	0.473	1.270
Lutjanidae_Aphareus_furca	0.027	0.000
Lutjanidae_Aprion_virescens	0.000	0.027
Lutjanidae_Lutjanus_gibbus	0.000	0.135
Lutjanidae_Lutjanus_quinquelineatus	0.000	1.135
Lutjanidae_Lutjanus_sebae	0.203	0.324
Lutjanidae_Lutjanus_vitta	0.027	0.162
Lutjanidae_Pristipomoides_filamentosus	0.027	0.054
Lutjanidae_Pristipomoides_multidens	3.716	1.865
Lutjanidae_Pristipomoides_spp	0.041	0.000
Lutjanidae_Pristipomoides_typus	0.662	0.216
Lutjanidae_Symphorus_nematophorus	0.000	0.000
Malacanthidae_Hoplolatilus_sp1	0.014	0.000
Malacanthidae_Malacanthus_brevirostris	0.014	0.000
Microdesmidae_Gunnellichthys_monostigma	0.014	0.000
Microdesmidae_Ptereleotris_sp1	0.189	0.081
Microdesmidae_Ptereleotris_sp2	0.000	0.027
Monacanthidae_Aluterus_monoceros	0.041	0.108
Monacanthidae_Eubalichthys_caeruleoguttatus	0.014	0.000
Monacanthidae_Nelusetta_ayraud	0.041	0.000
Monacanthidae_Paramonacanthus_choirocephalus	0.000	0.027
Mullidae_Parupeneus_chrysopleuron	0.041	0.378
Mullidae_Parupeneus_cyclostomus	0.000	0.054
Mullidae_Parupeneus_heptacanthus	0.081	0.108
Mullidae_Parupeneus_indicus	0.000	0.027
Mullidae_Parupeneus_spilurus	0.054	0.514
Muraenidae_Gymnothorax_nudivomer	0.027	0.000
Muraenidae_Gymnothorax_prionodon	0.014	0.000
Muraenidae_Gymnothorax_sp1	0.014	0.027
Muraenidae_Gymnothorax_sp3	0.014	0.000
Muraenidae_Gymnothorax_sp4	0.014	0.000
Muraenidae_Gymnothorax_sp5	0.000	0.027
Muraenidae_Gymnothorax_thyrsoideus	0.000	0.054
Muraenidae_Gymnothorax_undulatus	0.014	0.027
Muraenidae_Uropterygius_concolor	0.000	0.000
Nemipteridae_Nemipterus_spp	0.108	0.243
Nemipteridae_Parascolopsis_eriomma	0.122	0.000
Nemipteridae_Parascolopsis_inermis	0.041	0.054
Nemipteridae_Pentapodus_nagasakiensis	0.324	0.162
Nemipteridae_Scolopsis_affinis	0.000	0.081
Nemipteridae_Scolopsis_monogramma	0.000	0.000

Name (Family, Genus, Species)	Take	No Take
Orectolobidae_Orectolobus_sp1	0.014	0.000
Pinguipedidae_Parapercis_clathrata	0.000	0.000
Pinguipedidae_Parapercis_nebulosa	0.365	0.351
Pinguipedidae_Parapercis_sp1	0.081	0.000
Pinguipedidae_Parapercis_sp10	0.014	0.027
Pomacanthidae_Apolemichthys_trimaculatus	0.095	0.000
Pomacanthidae_Chaetodontoplus_personifer	0.122	0.189
Pomacanthidae_Genicanthus_lamarck	0.000	0.054
Pomacanthidae_Pomacanthus_imperator	0.014	0.000
Pomacanthidae_Pomacanthus_semicirculatus	0.014	0.027
Pomacentridae_Pristotis_obtusirostris	0.000	0.027
Priacanthidae_Priacanthus_blochii	0.041	0.000
Priacanthidae_Priacanthus_hamrur	0.000	0.054
Priacanthidae_Priacanthus_sp1	0.014	0.000
Priacanthidae_Priacanthus_sp10	0.027	0.000
Rachycentridae_Rachycentron_canadum	0.014	0.000
Rhinidae_Rhynchobatus_australiae	0.014	0.000
Scaridae_Scarus_ghobban	0.041	0.162
Scaridae_Scarus_sp3	0.000	0.054
Scombridae_Scomberomorus_commerson	0.014	0.000
Scombridae_Scomberomorus_spp	0.027	0.000
Serranidae_Cephalopholis_sonnerati	0.027	0.054
Serranidae_Cephalopholis_spiloparaea	0.000	0.000
Serranidae_Epinephelus_areolatus	0.378	0.297
Serranidae_Epinephelus_coioides	0.000	0.000
Serranidae_Epinephelus_morrhua	0.054	0.000
Serranidae_Epinephelus_multinotatus	0.000	0.054
Serranidae_Epinephelus_rivulatus	0.054	0.054
Serranidae_Epinephelus_tukula	0.000	0.027
Serranidae_Pseudanthias_cooperi	0.014	0.054
Serranidae_Pseudanthias_georgei	0.230	0.054
Serranidae_Variola_louti	0.027	0.054
Sparidae_Argyrops_spinifer	1.014	0.486
Sparidae_Chrysophrys_auratus	0.014	0.000
Sparidae_Dentex_carpenteri	0.365	0.405
Sphyraenidae_Sphyraena_qenie	0.189	0.027
Sphyraenidae_Sphyraena_sp10	0.027	0.000
Sphyrnidae_Sphyrna_lewini	0.041	0.000
Sphyrnidae_Sphyrna_mokarran	0.000	0.054
Synodontidae_Saurida_undosquamis	0.216	0.216
Synodontidae_Synodus_sp10	0.014	0.000

Name (Family, Genus, Species)	Take	No Take
Tetraodontidae_Arothron_stellatus	0.000	0.000
Tetraodontidae_Canthigaster_rivulata	0.014	0.027
Tetraodontidae_Lagocephalus_lunaris	0.095	0.000
Tetraodontidae_Lagocephalus_sceleratus	0.338	0.973
Triakidae_Hemitriakis_falcata	0.068	0.162
Triakidae_Hypogaleus_hyugaensis	0.000	0.027
Triakidae_Mustelus_ravidus	0.041	0.000
Veliferidae_Velifer_hypselopterus	0.000	0.162

APPENDIX A – CHARLOTTE ASTON'S MASTERS THESIS

Recreational fishing impacts in an offshore and deep-water marine park:
establishing robust benchmarks of fished species using hybrid frequentist model selection and Bayesian inference

Charlotte Lovisa Aston | 22291142

Supervised by:

Dr Tim Langlois, School of Biological Science,
The University of Western Australia
Dr Renae Hovey, School of Biological Science,
The University of Western Australia
Dr Jacquomo Monk, Institute of Marine and Arctic Studies,
The University of Tasmania

Formatted in the style of Marine Ecology Progress Series

This thesis is submitted in partial fulfilment of the requirements for a
Master of Biological Science
BIOL5552-5 Masters in Biological Science Research Dissertation
School of Biological Sciences
Faculty of Science
The University of Western Australia
October 2020

Word Count: 7090

1

Abstract

Throughout Australia's Commonwealth network of marine parks (MPs), compromise with extractive users has frequently resulted in the placement of many No-Take Zones (NTZs) in remote locations, far away from human activity, limiting perceived impact on extractive users but also limiting their use for investigating impacts of fishing. This study aimed to establish a benchmark in the distribution of fished species across the Ningaloo Marine Park – Commonwealth (NMP-Commonwealth) to test if there was any evidence of an effect of recreational fishing and to examine if the remote location of the newly established NTZ limits it use to study the effects of fishing. Throughout the NMP-Commonwealth, where only recreational fishing is permitted, we expected the abundance of fished species to increase with increasing distance to the nearest boat ramp, as a proxy of recreational fishing effort, but we did not expect the abundance of non-fished species, and overall species richness to vary systematically across the marine park. Using data collected using baited stereo-video cameras, a hybrid frequentist-Bayesian modelling framework was developed to disentangle the effect of fishing effort from the newly established NTZ and the influence of fine-scale bathymetry, and its derivatives, and habitat composition data obtained from the field of view. Distance to boat ramp was found to be a strong predictor of fished species abundance, indicating that the effect of recreational fishing can be detected across the NMP-Commonwealth. A weak positive effect of the NTZ on fished species abundance was found and it is expected that this difference across the NTZ boundary will increase over time. Habitat composition predictors were found to be unimportant for predicting fished species abundance, but strongly influenced species richness and non-fished species abundance. This study found clear a footprint of recreational fishing across the NMP-Commonwealth and as a result the new NTZ, despite its remote location, can still act as a control in future studies of recreational fishing effects.

Table of Contents

Acknowledgements

I would first like to thank my supervisors; Tim, Jac and Renae for their wonderful support over the last year and a half, it has been my absolute honour to work with you. Not only have I learnt a great deal throughout this experience, but you have all helped me become so much more confident in myself and my skills as a researcher. Secondly, I would like to thank all the people who have helped me along the way to complete this project. In particular Todd Bond and Brooke Gibbons, if not for them (and their seemingly endless patience) I would have been hopelessly lost under a mountain of video footage with no clue what fish species I was looking at or even the faintest idea of how to get all my data into a useable form. I would not have been able to do this without you. Thank you to Sam, Michali and Andy of Keshi Mer II, and Andrea and Matthew for their assistance in the field. Finally, thank you to Rebecca Fisher (Australian Institute of Marine Science) and Scott Foster (Commonwealth Scientific and Industrial Research Organisation) who took the time to explain some rather complicated statistics to me. This research is supported by the Australian Government's National Environmental Science Program Marine Biodiversity Hub, with additional funding from CSIRO, UWA, Parks Australia and the Keith Sheard Travel Scholarship.

Introduction

Globally, No-Take Zones (NTZs) are being established in order to conserve biodiversity and further our understanding of marine ecosystem processes by acting as a control for the effects of fishing (Langlois & Ballantine 2005, Costello 2014). As of 2018, Australia had declared 44% of Commonwealth waters (between 5 km and 370 km offshore) as marine parks (MPs), with the objectives of protecting and conserving biodiversity, cultural and heritage values, whilst maintaining sustainable use and enjoyment (Marine Division - DSEWPC 2012, Parks Australia 2019). Approximately, 20% of the Commonwealth MP network is currently designated as NTZs (Phillips 2017).

The broad aim of the Australian Marine Park (AMP) network was to create a *"comprehensive, adequate and representative system of marine reserves"* that will protect ecological processes and biodiversity at all levels (Beeton et al. 2015). Amongst extractive uses, both commercial and recreational fishing are recognised as important socio-economic values of Australia's MPs (Young et al. 2014, Director of National Parks 2018). During the AMP planning process, compromises were made to reduce the overlap of restrictive zoning (e.g. NTZs) with extractive activities such as commercial and recreational fishing, resulting in AMPs where the newly established NTZs are remote from human activity (Buxton & Cochrane 2015, Moore et al. 2016, Edgar et al. 2018). This is a common narrative in both NTZ and MP planning around Australia. Many of the NTZs within State waters (within 5 km of the coast) are either very remote or for those located in high human use areas, are either very small or have shore fishing zones which likely undermine their potential benefits to biodiversity conservation and science (Wescott 2006, Kellner et al. 2007, McLaren et al. 2015).

Whilst recreational fishing is an important socioeconomic value for Australia's MPs, recreational effort and its impacts are not easily measured, especially compared to commercial fishing where detailed metrics from established sources are available (Young et al. 2014, Director of National Parks 2018). Where both commercial and recreational fishing occur, disentangling their effects is complex and typically requires consistent data collection over large spatial scales (Brooker et al. 2020). Commercial fishing has been absent from the Ningaloo Marine Park (Commonwealth [NMP-Commonwealth]) since 1987 and so fishing pressure within the MP is almost exclusively

recreational (Department of Biodiversity Conservation and Attractions, 2017). The establishment of the no-take National Park Zone within the NMP-Commonwealth provides an opportunity to investigate the impact of recreational fishing in isolation. A variety of proxies have been suggested for recreational fishing effort, with the two most prevalent being 1) distance to boat ramp (Stuart-Smith et al. 2008) and 2) human gravity, where the local human population density (Cinner et al. 2018) or rate of visitation (Brooker et al. 2020) decays with increasing distance from access points. Within the Ningaloo region, which is a popular but seasonal tourist destination, the transient nature of the human population (Smallwood et al. 2011) and lack of consistent visitation data means that any gravity metric is likely to be ineffective as a proxy for recreational fishing effort within NMP-Commonwealth. Instead, we chose to use the more conservative but equally robust metric of distance to boat ramp as proxy for recreational fishing pressure. As with the majority of no-take National Park Zones within the AMP network, the new NTZ within the NMP-Commonwealth is distant from existing access points for recreational fishing (Figure 1), potentially confounding its role to act as a control for the effects of fishing.

Underwood (1995) argued that treating management actions as testable hypotheses will improve the ability of ecological research to inform management decisions. The new NTZ in the NMP-Commonwealth provides a control for the experiment that is fishing, allowing us to test its effects (Langlois & Ballantine 2005). Like any well-designed experiment, factors that may confound the results must be accounted for. In this case, the NTZ is situated at the furthest location from the main access points for boat based recreational fishing (Figure 1). This study aims to determine whether the role of the new NTZ to act as a control for the effects of fishing is in fact confounded by its remote location within the NMP-Commonwealth. Or, whether we are likely to be able to disentangle location effects (e.g. the new but remote NTZ) from recreational fishing pressure, using distance to boat ramp as a proxy for fishing effort. The abundance of fished demersal fish species greater than legal size, obtained from baited stereo-video was used to investigate the effect of recreational fishing, as it has been successfully used to understand the impacts of NTZ's within the shallow waters of the Ningaloo Marine Park (State waters, Haberstroh et al. *in review*) and as an indicator of fishing effects within other MPs (Evans & Russ 2004, McLaren et al. 2015). To distinguish trends in fish abundance and composition not associated with recreational fishing

pressure across the NMP-Commonwealth, we also investigated the abundance of non-fished species and species richness.

Habitat is highly influential on the abundance, distribution and assemblage structure of demersal fish species across both NTZs and fished areas (Wilson et al. 2010). Only very coarse (>250 m grid size) bathymetry data was available to most of the planning for the AMP network and unknown strong habitat gradients may exist across the newly established NTZ (Bax 2011, Devillers et al. 2015). To determine whether habitat availability may also be confounding the effect of the NTZ, we explored habitat information as covariates at different spatial scales. In this study we contrasted the ability of available detailed bathymetry derivatives (5m grid size) from multi-beam data with and without habitat composition data from field of view classification (Langlois et al. 2020). We hypothesized that the habitat composition data from field of view classification would be the most useful predictor of fish abundance and species richness (Collins et al. 2017).

For biodiversity monitoring to provide relevant information for MP management, e.g. through an evidence based decision making framework (Hayes et al. 2019), it is not sufficient to say that fishing or the implementation of a NTZ is having an effect. This influence must be quantified and described, typically through the use of effect sizes (Rouphael et al. 2011). To improve the robustness of effect size estimates, we employed Bayesian methods to calculate posterior distributions for the size of any effects detected. The use of Bayesian models for ecological inference has multiple advantages, including model validity at any sample size and no requirement of normally distributed model parameters (van de Schoot et al. 2014). Using robust estimates of effect sizes to inform management is important for MPs to achieve their overall conservation goals, as they enable managers, via monitoring and improvement frameworks, to consider what changes or trends are ecologically and socially acceptable (Underwood 2000). The use of Bayesian methods to calculate posterior distributions for effect sizes will also enable the importance of competing predictors (e.g. distance to boat ramp and NTZ status) to be compared.

Compared to near-shore MPs, there are fewer studies exploring how to effectively assess and monitor human impacts in offshore MPs that are often both expansive and remote (Alemany et al. 2013, Lawrence et al. 2015, Perkins et al. 2017, Hill et al. 2018, Sagar et al. 2020). In the case of

Australia's remote Commonwealth MPs, the isolated location of many of the NTZs, often far away from human activity, may hinder our ability to use them as a control for fishing or determine biodiversity benefits. By establishing a benchmark of fish biodiversity across the newly established NMP-Commonwealth, we will determine if recreational fishing, a key socio-economic value in this MP, has the expected impact of decreasing the abundance of greater than legal sized fished species. As the NTZ within the NMP-Commonwealth has only recently been established we would not predict that fished species would have increased within its boundaries (Babcock et al 2010). Despite the remote location of the NTZ, we hypothesised that distance from boat ramp will be a more important predictor than NTZ status, and therefore that the NTZ will still be able to provide an effective control for recreational fishing into the future.

Materials and Methods

Study Site

The Ningaloo coastline is located in the subtropics of north-western Western Australia (WA). It is approximately 260km long, extending from Red Bluff in the south to the North West Cape in the north and includes the largest fringing coral reef in Australia (Ningaloo Coast: World Heritage nomination 2010). Two MPs were gazetted in 1987 to protect the region's significant biodiversity, with all waters between three nautical miles and the high-water mark managed as part of the State Ningaloo Marine Park (NMP), and water seaward of this up to 200 nautical miles managed by the Commonwealth. Commercial fishing has been heavily restricted within both the State and Commonwealth MPs, with effectively no commercial fishing since 1987 (Department of Biodiversity Conservation and Attractions, 2017). All of the NMP-Commonwealth was designated a recreational use zone until 2018, when the park was rezoned to include a 116km^2 no-take National Park Zone (Director of National Parks 2018). The NTZ follows the IUCN's guidelines for zoning, prohibiting all extractive activities including recreational fishing (Day et al. 2012).

Sampling Design

Data collection occurred between the 12th-17th of August 2019 with samples taken from the northern area of the NMP-Commonwealth, from the MP's most northern edge to Point Cloates in

the south. A total of 122 sites were sampled and included a combination of new locations chosen for this study (75%) and legacy sites that have been sampled in 2006, 2009, 2013 and 2015 (Figure 1).

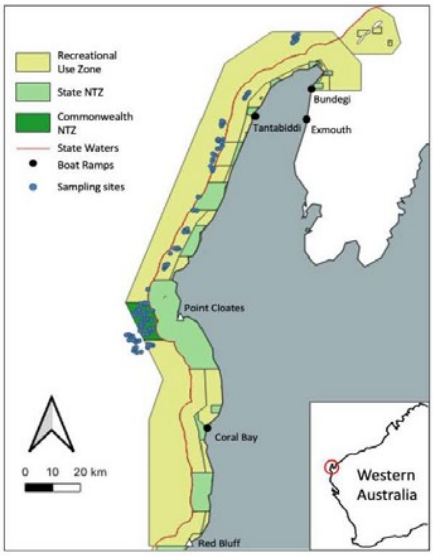

Figure 1. Map of sampling design for the NMP-Commonwealth showing the location of the 122 sampling points (blue dots), the no-take zone and the recreational use zone where recreational fishing is permitted. The black dots indicate boat ramps likely to be used by recreational fishers for access to the NMP-Commonwealth.

A probabilistic design-based approach was used to choose the sampling locations, where the probability of a site being selected for sampling was weighted according to several factors, whilst still maintaining adequate spatial representation (after Foster et al. 2018). As fish biodiversity was expected to be higher where bathymetric features such as ridges or reef platforms were present, existing bathymetry data was used to create a Terrain Position Index (TPI) which stratified the study area into eight groups following methods set out in Monk et al. (2016). An equal number of samples were selected from each of these eight groups, ensuring that the samples selected from each group covered a range of depths (60-190m). In order to capture any effect of recreational fishing in the NMP-Commonwealth, samples were taken from both inside (n=35) and outside the NTZ (n=36), as well as from comparable areas outside the MP including from the recreational use zone of the NMP (State waters, n=51).

Sampling technique

Data on fish diversity, abundance and length was collected using baited remote underwater stereo video camera (stereo-BRUV) systems. Each stereo-BRUV consisted of two Canon 4K HG25 cameras in plastic housings, mounted 0.7m apart and angled towards each other at 7° degrees. The angled camera allows determination of the distance and angle of the fish relative to the camera, as well as precise measurement of fish length. A wire mesh bait bag containing 800-1000g of pilchards was suspended approximately 1.2m in front of the cameras to attract fish to the stereo-BRUV. Each system also contained a backwards facing camera to collect additional habitat information which was combined with data from the front facing cameras. Samples were clustered in groups of six allowing multiple stereo-BRUV systems to be deployed and retrieved simultaneously, maximising cost and time effectiveness.

Data Analysis

Video Analysis

Stereo footage from the 122 sampling sites were analysed using EventMeasure software (www.seagis.com.au/event.html). All fish were identified to the lowest taxonomic level. An estimate of abundance was determined by recording the maximum number of individuals of a species seen in a single frame (MaxN) and is a relative estimate due to different species being attracted to the bait from different distances (Cappo et al. 2007). Length measurements were also calculated for each individual fish, measured from the tip of the snout to the fork of the tail.

Characterising broad scale seabed features from existing data

Multibeam echosounder (MBES) derived bathymetry and backscatter variables collected between 2005-2018 were used to characterise depth and seafloor geomorphology in the region. The processed bathymetry and backscatter were then used to derive additional variables of the seafloor including aspect (radians), slope (degrees) and roughness (Figure 2a, 2b). These variables capture the main seafloor characteristics as well as being known to be highly influential on demersal fish habitat (Friedlander & Parrish 1998, Pittman et al. 2007, Monk et al. 2012). Predictors such as these were used as proxies for habitat distribution in the initial zoning of the Commonwealth MPs (Bax 2011, Devillers et al. 2015).

Field of View Habitat Characterisation

Habitat analysis was carried out in TransectMeasure (https://www.seagis.com.au/transect.html) using high definition images taken from the forward and backward cameras attached to the stereo-BRUV. Three Field of View (FoV) predictors were estimated using the method outlined in Langlois et al. (2020). Each image was overlain with a 4x5 grid and the dominant habitat type (by percentage) in each cell was classified using the CATAMI classification scheme (Althaus et al. 2015), with grid cells covering open water excluded from further analysis. Due to the rarity of some habitat types, classifications were collated to give a percent cover of reef for each sample. The percent cover for the forwards and backwards images from each stereo-BRUV were then summed and an overall percent cover of reef was calculated for each sample. Relief for each cell was also assessed using a 0-5 scale, with 0 indicating a flat surface and 5 indicating exceptional structural complexity in the environment. For each sample, the values for relief in each cell from both forwards and backwards camera images were averaged and the standard deviation (SD Relief) was calculated (Figure 2c).

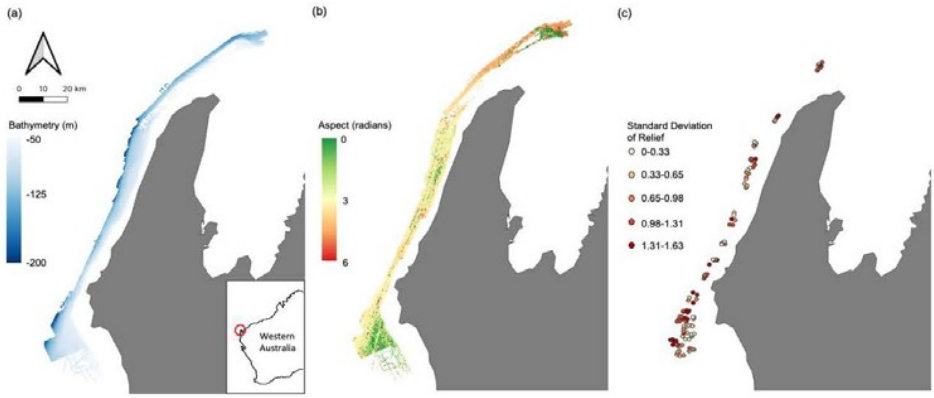

Figure 2. Examples of both broad scale seabed characteristics – (a) bathymetry (m), (b) aspect (radians cubed) – and site-specific field of view habitat characteristics – (c) standard deviation of relief – used as predictors in the models.

Assemblage Metrics

Three fish assemblage metrics were selected for analysis: abundance of recreationally fished fish species greater than legal length, species richness and abundance of non-fished species. Eighteen

species were used for analysis as recreationally fished at Ningaloo and length measurements were used to classify individuals as greater or less than the legal minimum catch size (Supplementary Material One). If no legal minimum catch size was specified, then all fish observed were considered legal size. Of the remaining non-recreationally fished species, small-bodied species that form large schools were removed from the analysis due to their disproportionately large effect on the outcomes of statistical testing. These species are also not site attached and are likely to move in and out of the NTZ and across habitat patches. As a result, MaxN for 126 species were used as non-fished species for analysis.

Statistical Analysis

The R language for statistical computing 4.0.2 (R Core Team 2018) was used for all data manipulation (dplyr, Wickham et al. 2020), analysis and graphing (ggplot2, Wickham 2016). A hybrid frequentist and Bayesian workflow was used for model selection and analysis. Initially, a generalised additive mixed effects (GAMM) and full subsets modelling approach (Fisher et al. 2018) was used to select models that best explained patterns in fish assemblages in the NMP-Commonwealth. The model selection procedure was carried out with and without FoV predictors to determine whether information on site specific habitat composition improved our ability to explain patterns in fish assemblage metrics, when compared to using fine scale bathymetry data and its derivatives. The stereo-BRUV cluster from which each sample was taken was modelled as a random effect which allows correlation within clusters, as similar species are likely to be found together by stochastic chance. The top two models selected by the frequentist GAM approach were then modelled within a Bayesian framework. For a full workflow of the model selection process see Supplementary Material Two.

Model Selection

Data was initially assessed for outliers and collinearity of predictor variables using Pearson's correlation index and variables that were greater than 95% correlated were removed from the analysis. Sites with missing data for any predictor variables were also removed from the data. Predictor variables were plotted, and transformations were chosen to ensure an even distribution across each variable's range and to minimise skew. The data was also assessed for spatial autocorrelation using a variogram.

In total nine predictor variables were included in the model selection process (Table 1). The effect of recreational fishing in the NMP-Commonwealth was assessed using the distance from each sample to the nearest boat ramp as a proxy. The status of each sample was also assigned according to whether the sample was taken from within the NTZ or comparable fished sites both inside and outside of the NMP-Commonwealth.

Table 1. Predictor variables for fish assemblage metrics used in the model selection process

Predictor Variable	Description
Distance to boat ramp (km)	Proxy for the effect of recreational fishing
Status	Designated based on whether the sample was taken inside or outside the No-Take Zone
Bathymetry	Broad scale ecological features
Aspect (radians cubed)	Broad scale ecological features
Slope (square root degrees)	Broad scale ecological features
Roughness (log)	Broad scale ecological features
Percent cover reef (square root)	Field of view predictor
Mean relief	Field of view predictor
Standard deviation of relief	Field of view predictor

The model selection process was completed separately for each of the three assemblage metrics. A full subsets generalised additive modelling approach was used for model selection using the FSSgam package for R (Fisher et al. 2018). The package constructs models for all possible combinations of predictor variables, but excludes models where variables have a correlation of greater than 0.28 (Graham 2003). Continuous variables were fitted with smoothing splines with the number of knots limited to 5. The gamm4 package, based on the lme4 package, was used within the FSSgam() function to generate the models, due to its ability to effectively model random factors. The models were ranked according to the Akaike Information Criterion for small sample sizes (AICc) with models that had a lower AICc ranked higher. The top two models were selected for use in further analyses providing that the second ranked model was within 2 AICc of the top model, otherwise only the highest ranked model was used. If the null model was within 2 AICc of the top model the null was selected regardless of rank, as per the principle of parsimony.

The FSSgam() function also produces a summary of the relative importance of each predictor variable across all fitted models. The importance score is calculated by summing the weight of all valid models that were fit using that predictor variable (Burnham & Anderson 2004).

A value for predicted response (±SE) was generated using the predict.gam() function in the mgcv package (Wood, 2011). A regular grid was generated composed of all unique combinations of 20 values for each predictor variable included in the model being predicted from, with these combinations used to calculate a predicted response.

The data was then modelled within a Bayesian framework using the stan_gamm4() function in the rstanarm package (Gabry & Goodrich 2020). An equivalent bayesian model was run for the top two models for each assemblage metric selected using the full subsets approach, and posterior distributions were produced for each predictor variable included in the models. A total of 41000 sampling iterations were completed but these were thinned to produce a final distribution composed of 1003 separate samples. The target average proposal probability for the No-U-Turn sampler variant of Hamiltonian Monte Carlo was increased to 0.99 to reduce the number of divergent transitions during sampling.

Response values were predicted for each Bayesian model by sampling from the posterior distribution of the predictor variables using the posterior_predict() function. The same grid was used as with the frequentist approach but rather than producing one predicted value for each combination of predictor variables, 1003 predicted responses were calculated, one for each simulation in the initial model.

Effect Size

Both frequentist and Bayesian effect sizes were calculated. Due to the curvilinear nature of GAMMs, effect sizes cannot be calculated using simple coefficients of the linear predictors, as can be done using standardised predictors with linear models. Instead, effect size for each predictor was calculated as the difference between the maximum and minimum values obtained for that predictor when the response across all other predictor values were averaged. This produces a single value for the effect size of each predictor variable in the model.

The Bayesian estimates of effect sizes for each predictor variable included in the top models were calculated in a similar way to the frequentist approach, except that this process was repeated for each of the 1003 simulations generated by sampling from the posterior distribution. This resulted in 1003 values for the effect size, allowing for the creation of a density plot for effect size of each predictor variable and calculation of credible intervals associated with effect size estimates and the 95% highest density interval.

Results

A total of 3689 individual fish were identified from 45 families, representing 92 genera and 166 species. The full subsets model selection produced the top ten models ranked by AICc with and without FoV variables for each assemblage metric, and the top two models were chosen for further analyses (Table 2). Overall, R^2 for the models is fairly low, ranging from 0.01 to 0.20, but models that included FoV variables consistently explained more variation in the data.

Table 2. Top two models ordered by parsimony for each assemblage metric, with and without field of view variables included. Bathymetry was included in the null and is therefore present as a predictor in all models.

Assemblage Metric	Field of View Variables Included	Best models (ordered by parsimony)	ΔAICc	ΔBICc	ωAICc	ωBIC	R2	EDF
Abundance of Fished Species Greater than Legal Size	N	Aspect + Distance to Boat Ramp	0.00	3.58	0.33	0.04	0.01	13.00
		Aspect + Status	1.60	2.67	0.15	0.07	0.02	10.00
	Y	Aspect + Distance to Boat Ramp	0.00	3.58	0.33	0.04	0.01	13.00
		Aspect + Status	1.60	2.67	0.15	0.07	0.02	10.00
Species Richness	N	Aspect	0.82	0.00	0.34	0.57	0.10	9.00
		Aspect + Status	0.00	1.73	0.51	0.24	0.14	10.00
	Y	SD Relief	0.00	0.00	0.49	0.88	0.17	9.00
Abundance of Non-fished species	N	Null	1.96	0.00	0.16	0.68	0.01	5.00
	Y	SD Relief	0.00	1.59	0.15	0.17	0.20	9.01
		Percent Reef Cover	0.05	1.65	0.14	0.17	0.11	9.00

Importance Scores

Although different predictor variables were of different importance across the three assemblage metrics, some general trends emerged (Figure 3). As bathymetry was included in the null it was present in every model examined and so it's importance score was not calculated. Aspect (radians cubed) shows high importance across all three sets of models, however, decreases in importance when FoV variables are included in the model selection procedure. Status shows a consistent intermediate importance across all models with little difference between models with and without FoV variables. Distance to boat ramp is important only in models predicting the abundance of fished species greater than legal size, showing high importance regardless of whether FoV variables were included.

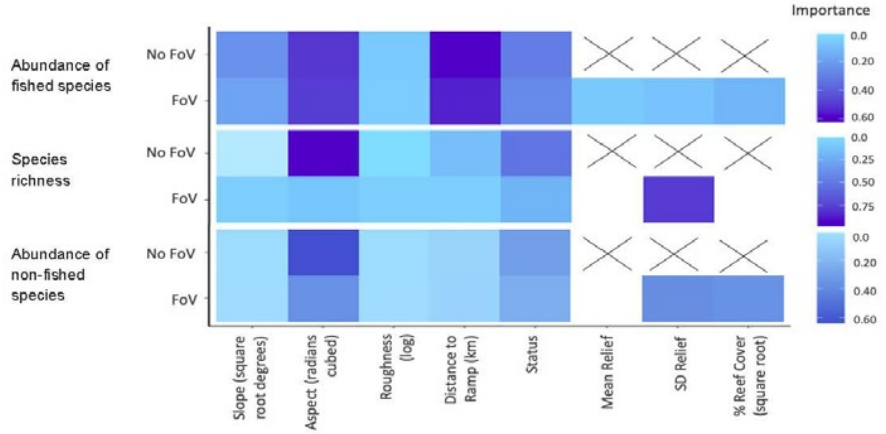

Figure 2. Importance scores for each predictor across all valid models. No field of view (FoV) indicates models which only considered fine scale bathymetry and its derivatives compared to FoV where habitat characteristics classified from images of habitat at the sample sites were considered.

Of the FoV variables the standard deviation of relief (SD relief) shows the greatest importance across all models, in particular for models predicting species richness and non-fished species abundance. FoV variables show minimal importance in predicting fished species abundance and both mean relief and the percent reef cover (square root) had importance scores of 0 for species richness models. Percent reef cover (square root) was only important in models predicting the abundance of non-fished species.

The top ranked model for each fish assemblage metric with and without FoV variables was plotted. Plots for the second ranked models and frequentist model predictions for each fish assemblage metric can be found in Supplementary Material Three.

Abundance of Fished Species Greater than Legal Size

Model selection produced the same top models for predicting the abundance of fished species greater than legal size with and without FoV variables. The 1003 posterior predicted values from the Bayesian model are displayed as paler lines around the darker mean line and represent a measure of uncertainty in the predictions. The relationship between mean predicted fished species shows abundance remaining fairly constant in shallow water before dropping off past approximately 120m depth (Figure 3a). There is greater certainty about the model predictions at deeper depths than shallow, as indicated by the width of the lines surrounding the mean. Aspect (radians cubed) shows a distinctly humped relationship to mean fished species abundance across both models, peaking at 150 radians (cubed), however the wide range of values produced by each simulation indicates there is some degree of uncertainty in the model predictions (Figure 3b). The model predicts a gradual decrease in fished species abundance as proximity (km) to boat to ramp increases (Figure 3c). Fished species abundance also shows a steep decline beyond 60 km, which may coincide with the 120m bathome. The posterior predicted values show a variable predicted response of mean fished species abundance, suggesting fairly large uncertainty particularly at the extremes.

Bathymetry has the biggest effect on the predicted mean abundance of fished species (Figure 3d), followed by aspect (radians cubed, Figure 3e). Effect sizes for both these variables show fairly narrow density plots indicating a high degree of certainty around these estimates. Distance to boat ramp has the smallest effect size as well as the widest distribution, suggesting greater uncertainty in the estimate of this effect (Figure 3f).

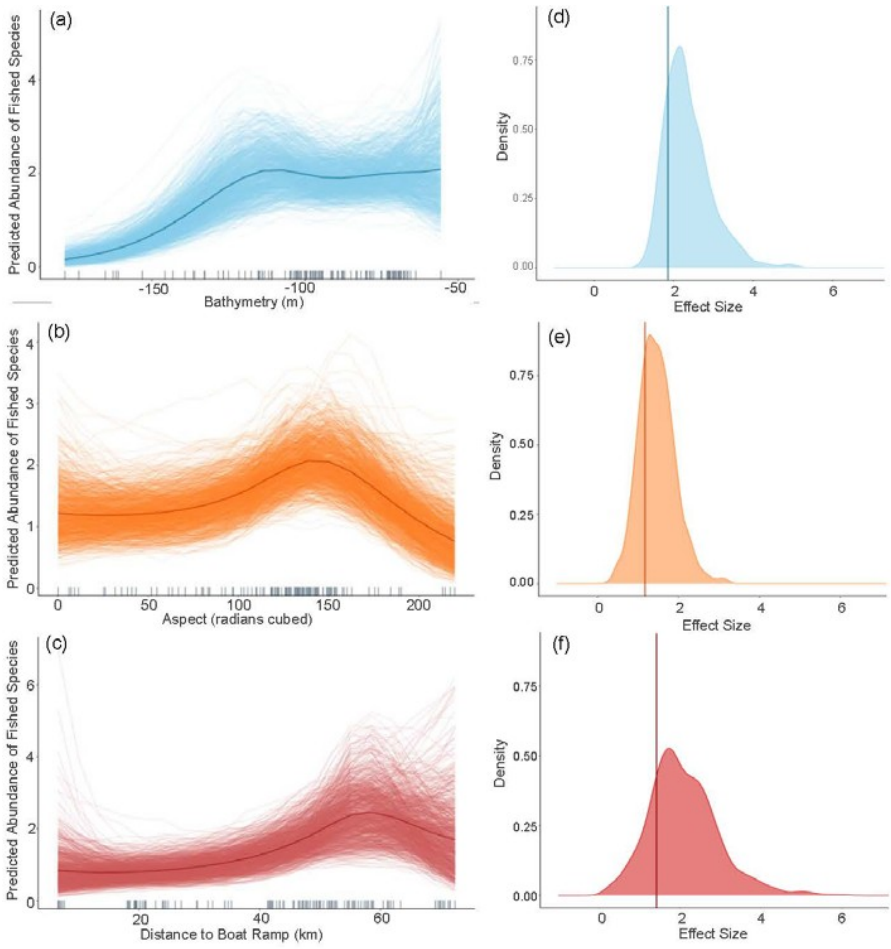

Figure 3. Predicted values for the top ranked model for abundance of fished species when field of view variables were not included - (a) bathymetry (m), (b) aspect (radians cubed), (c) distance to boat ramp (km). Density plots of effect size are also plotted for each aforementioned predictor – (d), (e), (f) respectively – with a vertical line indicating the frequentist effect size estimate.

The second top model for fished species abundance is also presented here (rather than in Supplementary Material Two) as it contains status as a predictor and is therefore relevant for

answering the question of whether the NTZ can act as a control for the effects of recreational fishing. Bathymetry (Figure 4a) and aspect (radians cubed, Figure 4b) show a highly similar relationship to fished species abundance as described in the top ranked model. The model also predicts increased fished species abundance inside the NTZ when compared to the fished areas, however the predicted response is highly variable (Figure 4c). Again, bathymetry has the largest effect size (Figure 4d) with aspect (radians cubed, Figure 4e) and status (Figure 4f) having similar estimated effects. As seen with species richness, the 95% credible bounds of the effect size estimate for status cross 0, indicating a limited effect.

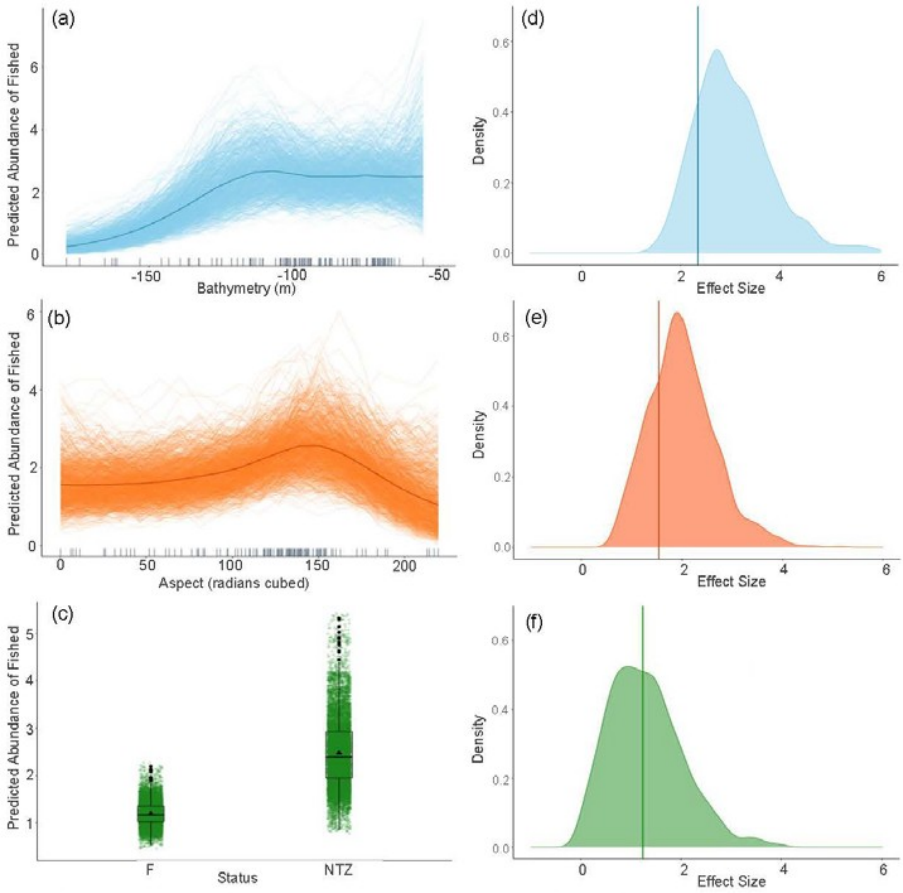

Figure 4. Predicted values for the second ranked model for abundance of fished species when field of view variables were not included - (a) bathymetry (m), (b) aspect (radians cubed), (c) status. Density plots of effect size are also plotted for each aforementioned predictor – (d), (e), (f) respectively – with a vertical line indicating the frequentist effect size estimate.

The relationship between status and all three assemblage metrics must be interpreted with caution as there is only one NTZ in the NMP-Commonwealth. The results from this one area may not be representative of the effect that limiting fishing pressure may have in other areas of the park.

Species Richness

The top model without FoV variables predicts that species richness remains fairly constant in shallow water up to approximately 80m depth, before declining steeply with increasing depth (Figure 5a). The variation in predictions for the model without FoV variables is higher for shallow depths and decreases as depth increases, indicating higher confidence in predictions in deeper water. High mean species richness is predicted at low aspect before declining until about 90 radians (cubed) and peaking again at approximately 150 radians (cubed) (Figure 5b). The posterior predictions show relatively small variation from the mean predicted species richness for aspect, indicating a high degree of certainty in the predictions. Species richness is predicted to be greater in the NTZ than in the fished areas (Figure 5c). Although there is a clear difference in means, there is a high degree of variability in the predictions of mean species richness in both NTZ and fished zones, however variability is greater in the NTZ.

Bathymetry had the greatest effect size both with and without FoV variables but with a fairly wide distribution, indicating a high degree of uncertainty around the effect size estimate (Figure 5d). Aspect (radians cubed) has a similarly wide effect size distribution but a smaller effect size overall (Figure 5e). The effect size for status is small but comparatively narrower and therefore less uncertain, however the 95% credible bounds cross 0 indicating a limited effect (Figure 4f).

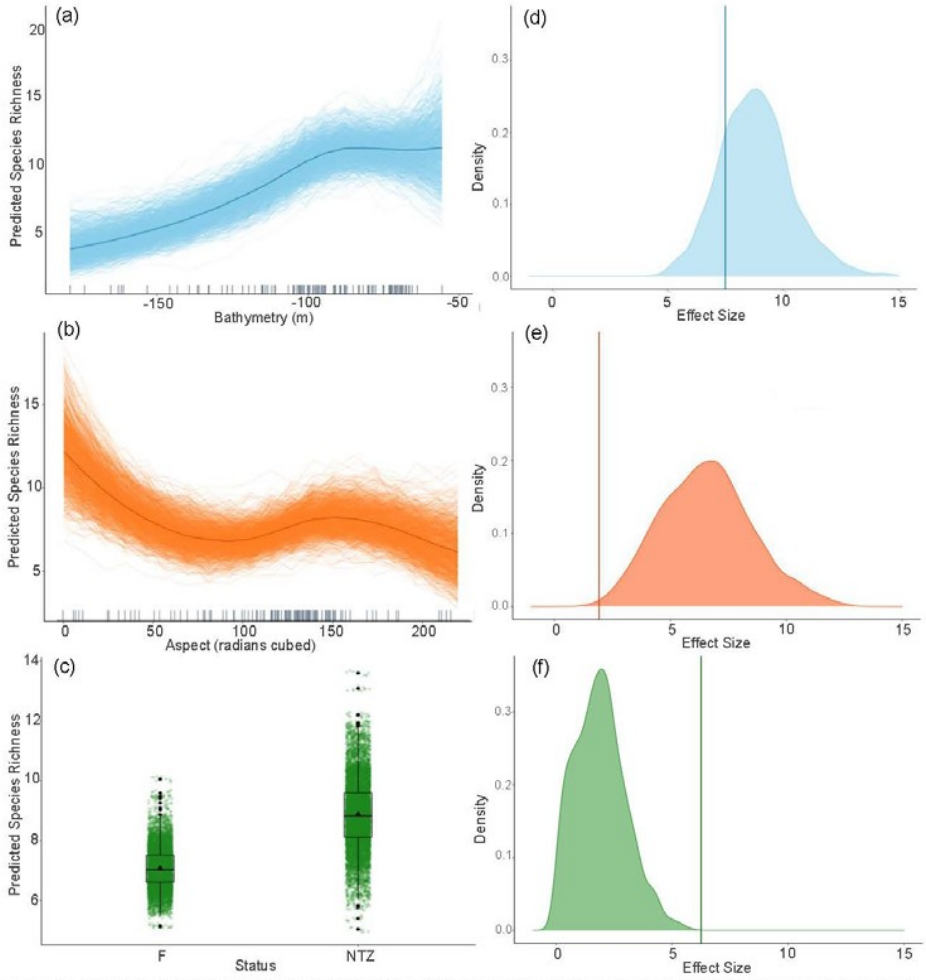

Figure 5. Predicted values for the top ranked model for species richness when field of view variables were not included - (a) bathymetry (m), (b) aspect (radians cubed), (c) status. Density plots of effect size are also plotted for each aforementioned predictor – (d), (e), (f) respectively – with a vertical line indicating the frequentist effect size estimate.

When FoV variables were considered, aspect (radians cubed) and status were no longer included in the top model. The predicted relationship between bathymetry and species richness remained

20

the same as when FoV variables were not considered, however uncertainty increased in predictions across all depths (Figure 6a). SD relief has a positive effect on species richness with increasing species richness at higher SD relief (Figure 6b). The variation in posterior predicted values is fairly small, with all posterior predictions close to the mean predicted species richness across all models. SD relief had the greatest effect size but also the widest distribution of either variable, indicating a high degree of uncertainty in the estimate (Figure 6c).

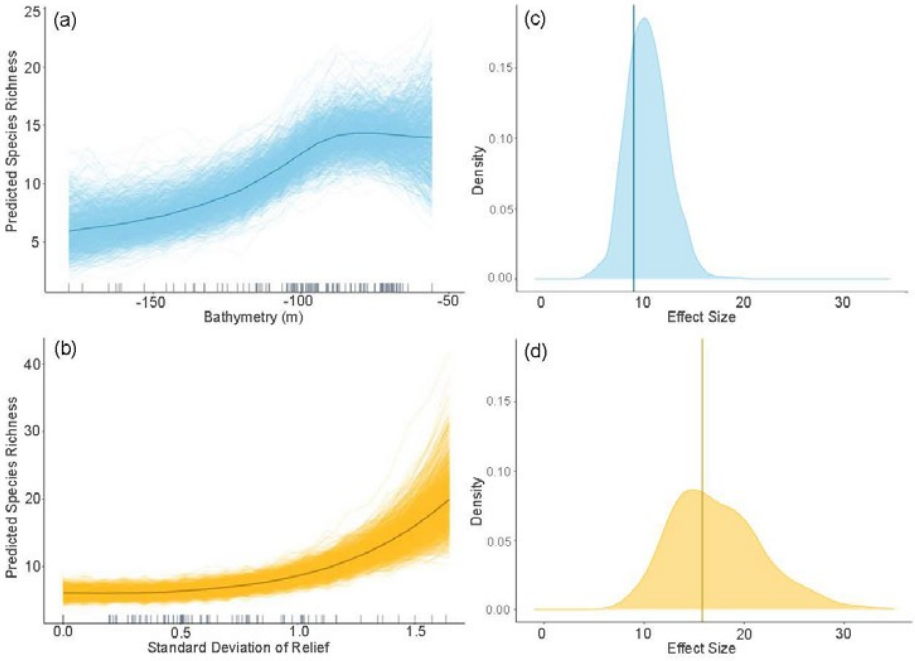

Figure 6. Predicted values for the top ranked model for species richness when field of view variables were not included - (a) bathymetry (m), (b) standard deviation of relief. Density plots of effect size are also plotted for each aforementioned predictor – (c) and (d) respectively – with a vertical line indicating the frequentist effect size estimate.

Abundance of Non-fished Species

When FoV variables were not included in the model selection process the null model was the most parsimonious model within 2 AICc of the top model. In models where FoV variables were considered, the top model included SD relief and bathymetry. The relationship between bathymetry

and non-fished species richness shows the same general trend as with the other assemblage metrics however the change in fish abundance across depths is much smaller (Figure 7a). Variation in posterior predicted values for abundance is large indicating a high degree of uncertainty. SD relief also shows the same relationship as seen with species abundance with very low abundance at low SD and rapidly increasing at high SD relief (Figure 7b).

There is a high degree of certainty around the effect size for bathymetry as shown by the narrow density plot (Figure 7c). The effect size for SD relief is larger than for bathymetry but is considerably wider and therefore less certain (Figure 7d).

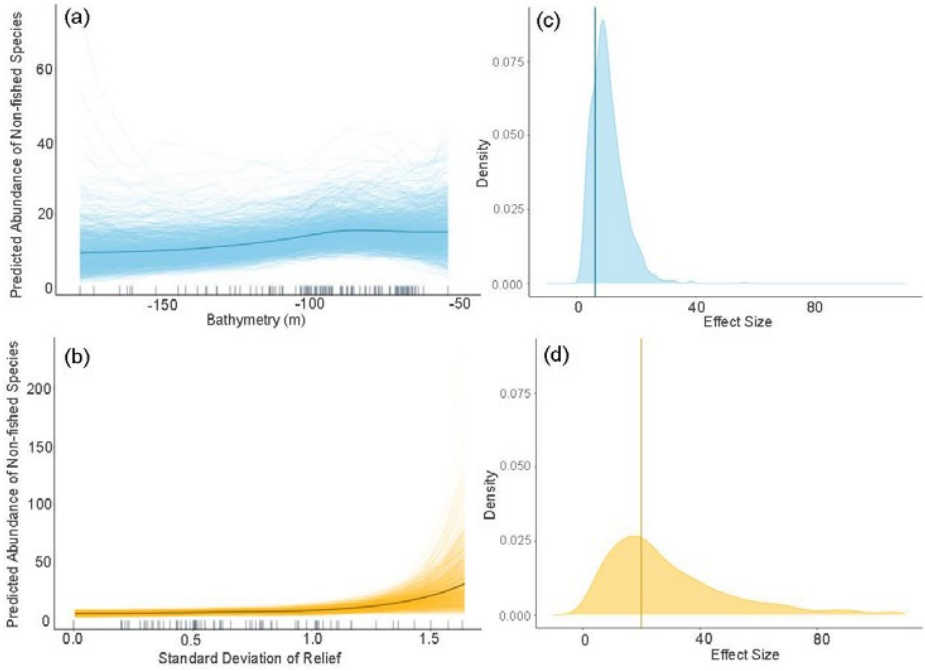

Figure 7. Predicted values for the top ranked model for the abundance of non-fished species when field of view variables were included - (a) bathymetry (m), (b) standard deviation of relief. Density plots of effect size are also plotted for each aforementioned predictor – (c) and (d) respectively – with a vertical line indicating the frequentist effect size estimate.

Discussion

This study contributes to a larger body of evidence that in the absence of commercial harvesting, recreational fishing can on its own have significant impacts on fish populations (Denny et al. 2004, Cooke & Cowx 2004, Cresswell et al. 2019). Distance to boat ramp was found to be a strong predictor for the abundance of fished species indicating a clear footprint of recreational fishing across the NMP-Commonwealth. Generally, recreational fishing in deeper, offshore waters is poorly understood in Australia, with much of the recreational fishing and research effort concentrated in estuaries and inshore areas (McPhee 2011). In particular, the way in which data is collected for recreational fishing in WA makes it difficult to disaggregate recreational catch estimates at the scale of either State or Commonwealth MPs, presenting difficulties for estimating its impact on fish populations in Commonwealth waters (Lynch et al. 2020). The proximity of the deep NMP-Commonwealth waters to boat ramps makes it highly accessible to recreational fishers, and studies have indicated a recent shift towards increased fishing activity in the offshore waters (Lynch 2006, Fowles et al. 2011, Mitchell et al. 2018). As a result, it is unsurprising that we should see a decrease in the abundance of large bodied fished species along a gradient of a proxy for fishing pressure. Cinner et al. (2018) showed a similar relationship to human gravity, which uses distance to and size of nearby population centres as a proxy for human use. We find distance to boat ramps to be a robust proxy for the effect of recreational fishing, correlating strongly with the abundance of fished species across the NMP-Commonwealth.

Sustainable use of marine resources including recreational (and commercial) fishing is a key socio-economic value of Australia's MPs (Young et al. 2014, Director of National Parks 2018). In an effort to balance extractive uses with biodiversity conservation, compromises were made when planning the MPs to minimise overlap between NTZs and areas of high use for extractive activities (Lynch 2006, Buxton & Cochrane 2015). This resulted in many of the newly established NTZs in the AMP network being located in areas far from human activity, limiting their use for studying the effects of recreational fishing. Despite the remote location of the newly established no-take National Park Zone within the NMP-Commonwealth, we demonstrate here that distance from boat ramps is a more important predictor of the distribution in the abundance of fished species than No-Take Zone status. We expect that in the future, as the NTZ becomes established and fished species increase in abundance within it, NTZ status will become an increasingly important predictor in

future monitoring data (Babcock et al. 2010). The recent establishment of the NTZ in the NMP-Commonwealth provides an opportunity to collect long-term data required to further investigate the effects of fishing within this region, with the benchmark presented in this study as a starting point. When investigating the effects of fishing, using NTZs, changes in fished populations and other ecosystem components can take decades to materialise (Babcock et al. 2010, Cresswell et al 2019). NTZ implementation can reveal surprising changes as ecosystems recover from the effects of fishing, which may allow us to investigate previously unrecognised emergent ecological processes (Jackson & Sala 2001, Langlois & Ballantine 2005, Ballantine 2014).

Due to the remote and offshore location of many of the Commonwealth MPs, there was a lack of fine scale information about species distribution and habitats for use when determining the initial spatial zoning (Lawrence et al. 2015). As a result, physical proxies for diversity (e.g. bathymetry or substrate) were the primary data used for the planning of the NTZs, which may not have captured unknown gradients in habitat that could affect demersal fish distribution (Bax 2011, Devillers et al. 2015). Contrary to our predictions, habitat composition data from FoV classification was not an overly important predictor to explain the abundance of large bodied fished species. Instead the larger-scale bathymetry derivatives provided adequate predictors. Conversely, non-fished species abundance and species richness were strongly correlated with habitat composition data from FoV classification. In particular SD relief showed strong importance and is a measure of habitat complexity which has been found to be critical for the maintenance of high species richness and abundance in deep reef communities (Andradi-Brown et al. 2016). In contrast to larger-bodied fished species abundance, non-fished species abundance is likely to be dominated by smaller bodied species, potentially more reliant on the small scale habitat complexity captured in the FoV (Collins et al. 2017). High complexity provides a variety of niches to support a greater number of species than would be found in a less complex habitat (Gratwicke & Speight 2005, Lingo & Szedlmayer 2006). Furthermore, small-bodied fish are often greater in abundance in complex environments as they are commonly prey species and use complexity in the environment as refuge from predators (Werner et al. 1983, Scharf et al. 2006, Andradi-Brown et al. 2016).

A similar relationship with bathymetry was seen across all three fish assemblage metrics, with the highest values for each metric observed at approximately 100m depth. The effect of bathymetry on demersal fish communities is well documented, and is strongly associated with the abundance of

benthic habitat forming species which generally decrease with increasing depth (Brown & Thatje 2014, Wellington et al. 2018). A consistent relationship was also seen with aspect (radians cubed) with a peak in species richness and fished species abundance at an approximately north west (NW) direction. These peaks observed in our fish assemblage metrics are likely associated with a relict shoreline, which is a Key Ecological Feature (KEF) for the north-west marine region (Australia. Department of the Environment, Water, Heritage and the Arts. 2008). The Carnarvon Shelf, which extends underneath the entirety of the Ningaloo Reef, has several rocky ridges and scoured areas seaward of Point Cloates, inside and outside the no-take National Park Zone, which form part of this historic coastline (Brooke et al. 2009, Nichol et al. 2012). In particular, localised scouring of the sand may have helped expose hard substrate and has allowed the development of a biodiversity hotspot for sponges and other benthic fauna, providing highly complex habitat that supports a wide range of fish species (Nichol et al. 2012, Schönberg & Fromont 2012). Many of these highly diverse habitats found on the edge of this shelf would likely have a NW aspect, contributing to the peaks seen in the fish assemblage metrics. NW facing habitats would be exposed to the south flowing Leeuwin Current, creating optimal conditions for filter feeding organisms, small-bodied planktivorous fish and subsequently their predators which are likely large-bodied fished species (Hanson & McKinnon 2009, Xu et al. 2015, Turner et al. 2018). The combination of exposed substrate and strong currents has likely contributed to the creation of ideal conditions for the development of diverse benthic habitats and prey assemblages that can support a wide range of demersal fish species.

The effect that seafloor characteristics have on fish assemblages is often linked to the scale at which the characteristics have been considered (Kendall et al. 2011). Here we show that different aspects of demersal fish assemblages are correlated with characteristics of the seafloor at different spatial scales. What was not explored in this study is the effect of varying the spatial scale of the same predictor on the relationship to fish assemblage metrics. Calculations of bathymetry derived seafloor characteristics such as slope or aspect often use a focal neighbourhood method, whereby the value for the characteristic in a cell is calculated based on values in a grid of neighbouring cells (Wilson et al. 2007). This grid can be increased to broaden the spatial scale at which the characteristic is calculated, in turn decreasing the detail that is captured. Studies examining the effect of changing the grid size have shown that while finer grid sizes are often more accurate when compared to *in situ* measurements, broad scale measurements can still be of ecological relevance

to demersal fish communities (Wedding et al. 2008, Pittman & Brown 2011). It is likely that both small- and large-scale seafloor characteristics contribute to patterns in fish assemblage metrics but that the relationship between any one characteristic and metric is likely to change across spatial scales (Kendall et al. 2011). As a result, understanding these relationships allows seafloor characteristics to be calculated at functionally meaningful scales than can inform management objectives.

This study used both frequentist and Bayesian methods for model selection, prediction and calculation of effect sizes. Frequentist approaches have historically been the statistical method of choice for ecologists due to their ability to answer a range of different questions with the computing power available (e.g. hypothesis testing and model selection, Dorazio 2015). With recent advances in computer technology, Bayesian methods have become increasingly popular within ecology and offer a variety of advantages over frequentist techniques. In particular, Bayesian frameworks offer a clear expression of uncertainty around estimates or predictions (van de Schoot et al. 2014). In this study, we utilised this advantage to calculate robust estimates of effect size with ceasily interpreted measures of uncertainty. In the context of MPs, management decisions may be made based on the results of statistical estimates of effect sizes which come with an inherent level of uncertainty (Agardy et al. 2003). The clear communication of this uncertainty to managers/stakeholders, who may not be scientists, is important as it can inform the allocation of resources for monitoring or management (Halpern et al. 2006). The biggest disadvantage of the Bayesian approach is that typically model selection procedures become computationally expensive. Here, the use of a hybrid approach with frequentist model selection followed by a Bayesian inference approach overcomes this issue and allows the generation of robust estimates of effect sizes. The hybrid model selection and inference procedures developed in this study may help to streamline future studies of NTZs and spatial zoning in offshore, deep water MPs.

Conclusion

Targets for protecting a percentage of the world's oceans have contributed to an increase in the use of marine parks and No-Take Zones as a key tool for biodiversity conservation and studying the effects of fishing (Gray 2010, Strain et al. 2019). Although aiming to follow the principles comprehensiveness, adequacy, and representativeness, the diverse range of users involved in the creation of MPs often leads to compromise, particularly in the placement of NTZs that prevent all

extractive activities (Lynch 2006). This study has found that a clear footprint of recreational fishing was found across the NMP-Commonwealth and so, despite its remote location the NTZ can act as a control for recreational fishing. We expect that over time, the difference in fished species abundance inside and outside the NTZ will increase, informing monitoring about the effect of recreational fishing in the MP. Whilst high resolution information about the habitats present in the park is not essential for predicting the abundance of fished species, this knowledge would aid in maximising biodiversity conservation, another key aim of the NMP-Commonwealth (Director of National Parks 2018). We have also demonstrated a hybrid model selection and inference framework which helps overcome the lack of model selection options for Bayesian modelling whilst also taking advantage of the ability to clearly represent uncertainty in resultant top models. It is hoped that this hybrid statistical approach will help with the creation of similar benchmarks in other remote, offshore MPs. The newly created NTZ and long-term absence of commercial fishing in the NMP-Commonwealth has provided a unique opportunity to understand the effects of recreational fishing in isolation. It is hoped that the benchmarks established here will enable a demonstration of how NTZs can be used to their fullest potential to control for the effects of fishing and better understand and conserve biodiversity.

References

Agardy T, Bridgewater P, Crosby MP, Day J, Dayton PK, Kenchington R, Laffoley D, McConney P, Murray PA, Parks JE, Peau L (2003) Dangerous targets? Unresolved issues and ideological clashes around marine protected areas. Aquat Conserv 13:353–367.

Alemany D, Iribarne OO, Acha EM (2013) Effects of a large-scale and offshore marine protected area on the demersal fish assemblage in the Southwest Atlantic. ICES J Mar Sci 70:123–134.

Althaus F, Hill N, Ferrari R, Edwards L, Przeslawski R, Schönberg CHL, Stuart-Smith R, Barrett N, Edgar G, Colquhoun J, Tran M, Jordan A, Rees T, Gowlett-Holmes K (2015) A Standardised Vocabulary for Identifying Benthic Biota and Substrata from Underwater Imagery: The CATAMI Classification Scheme. PLoS One 10:e0141039.

Andradi-Brown DA, Gress E, Wright G, Exton DA, Rogers AD (2016) Reef Fish Community Biomass and Trophic Structure Changes across Shallow to Upper-Mesophotic Reefs in the Mesoamerican Barrier Reef, Caribbean. PLoS One 11:e0156641.

Australia. Department of the Environment, Water, Heritage and the Arts. (2008) The North-west marine bioregional plan: bioregional profile - a description of the ecosystems, conservation values and uses of the North-west marine region / Australian Government, Department of the Environment, Water, Heritage and the Arts. The Dept Parkes, ACT.

Babcock RC, Shears NT, Alcala AC, Barrett NS, Edgar GJ, Lafferty KD, McClanahan TR, Russ GR (2010) Decadal trends in marine reserves reveal differential rates of change in direct and indirect effects. Proc Natl Acad Sci U S A 107:18256–18261.

Ballantine B (2014) Fifty years on: Lessons from marine reserves in New Zealand and principles

for a worldwide network. Biol Conserv 176:297–307.
Bax NJ (ed) (2011) Marine Biodiversity Hub, Commonwealth Environment Research Facilities, Final report 2007-2010. Department of Sustainability, Environment, Water, Population and Communities. Canberra, Australia.
Beeton RJS, Buxton CD, Cochrane P, Dittmann S, Pepperell JG (2015) Commonwealth Marine Reserves Review: Report of the Expert Scientific Panel. Department of the Environment, Canberra.
Brooke B, Nichol SL, Hughes MG, Doherty PJ (2009) Carnarvon Shelf Survey Post-Survey Report. Geoscience Australia, Canberra.
Brooker MA, de Lestang S, Fairclough DV, McLean D, Slawinski D, Pember MB, Langlois TJ (2020) Environmental and Anthropogenic Factors Affect Fish Abundance: Relationships Revealed by Automated Cameras Deployed by Fishers. Frontiers in Marine Science 7:279.
Brown A, Thatje S (2014) Explaining bathymetric diversity patterns in marine benthic invertebrates and demersal fishes: physiological contributions to adaptation of life at depth. Biol Rev Camb Philos Soc 89:406–426.
Burnham KP, Anderson DR (2004) Multimodel Inference: Understanding AIC and BIC in Model Selection. Sociol Methods Res 33:261–304.
Buxton CD, Cochrane P (2015) Commonwealth Marine Reserves Review: Report of the Bioregional Advisory Panel. Department of the Environment, Canberra.
Cappo M, Harvey E, Shortis M (2007) Counting and measuring fish with baited video techniques - an overview. In: Cutting-edge technologies in fish and fisheries science. Lyle J, Furlani D, Buxton C (eds) Australian Society for Fish Biology, p 233
Cinner JE, Maire E, Huchery C, MacNeil MA, Graham NAJ, Mora C, McClanahan TR, Barnes ML, Kittinger JN, Hicks CC, D'Agata S, Hoey AS, Gurney GG, Feary DA, Williams ID, Kulbicki M, Vigliola L, Wantiez L, Edgar GJ, Stuart-Smith RD, Sandin SA, Green A, Hardt MJ, Beger M, Friedlander AM, Wilson SK, Brokovich E, Brooks AJ, Cruz-Motta JJ, Booth DJ, Chabanet P, Gough C, Tupper M, Ferse SCA, Sumaila UR, Pardede S, Mouillot D (2018) Gravity of human impacts mediates coral reef conservation gains. Proc Natl Acad Sci USA 115:E6116–E6125.
Collins DL, Langlois TJ, Bond T, Holmes TH, Harvey ES, Fisher R, McLean DL (2017) A novel stereo-video method to investigate fish–habitat relationships. Methods Ecol Evol 8:116–125.
Cooke SJ, Cowx IG (2004) The Role of Recreational Fishing in Global Fish Crises. Bioscience 54:857–859.
Costello MJ (2014) Long live Marine Reserves: A review of experiences and benefits. Biol Conserv 176:289–296.
Cresswell AK, Langlois TJ, Wilson SK, Claudet J, Thomson DP, Renton M, Fulton CJ, Fisher R, Vanderklift MA, Babcock RC, Stuart-Smith RD, Haywood MDE, Depczynski M, Westera M, Ayling AM, Fitzpatrick B, Halford AR, McLean DL, Pillans RD, Cheal AJ, Tinkler P, Edgar GJ, Graham NAJ, Harvey ES, Holmes TH (2019) Disentangling the response of fishes to recreational fishing over 30 years within a fringing coral reef reserve network. Biol Conserv 237:514–524.
Day J, Dudley N, Hockings M, Holmes G, Laffoley D, Stolton S, Wells S (2012) Guidelines for applying the IUCN protected area management categories to marine protected areas. IUCN, Gland, Switzerland.
Denny CM, Willis TJ, Babcock RC (2004) Rapid recolonisation of snapper *Pagrus auratus*: Sparidae within an offshore island marine reserve after implementation of no-take status. Mar Ecol Prog Ser 272:183–190.

Department of Biodiversity, Conservation and Attractions (2017) Ecological Monitoring in the Ningaloo Marine Reserves 2017. Department of Biodiversity Conservation and Attractions, Perth.
Devillers R, Pressey RL, Grech A, Kittinger JN, Edgar GJ, Ward T, Watson R (2015) Reinventing residual reserves in the sea: are we favouring ease of establishment over need for protection? Aquatic Conservation: Marine and Freshwater Ecosystems 25:480–504.
Director of National Parks (2018) North-west Marine Parks Network Management Plan 2018. Director of National Parks, Canberra.
Dorazio RM (2015) Bayesian data analysis in population ecology: motivations, methods, and benefits. Popul Ecol 58:31–44.
Edgar GJ, Ward TJ, Stuart-Smith RD (2018) Rapid declines across Australian fishery stocks indicate global sustainability targets will not be achieved without an expanded network of 'no-fishing' reserves. Aquat Conserv 28:1337–1350.
Evans RD, Russ GR (2004) Larger biomass of targeted reef fish in no-take marine reserves on the Great Barrier Reef, Australia. Aquat Conserv 14:505–519.
Fisher R, Wilson SK, Sin TM, Lee AC, Langlois TJ (2018) A simple function for full-subsets multiple regression in ecology with R. Ecol Evol 8:6104–6113.
Foster SD, Monk J, Lawrence E, Hayes KR, Hosack GR, Przeslawski R (2018) Statistical Consideration for Monitoring and Sampling. In: *Field Manuals for Marine Sampling to Monitor Australian Waters*. Przeslawski R, Foster S (eds) National Environmental Science Programme (NESP), p 23–41
Fowles B, Gaynor A, Others (2011) The challenge of creating a scientifically-robust historical description of changing finfish populations in the Ningaloo Marine Park. Studies in Western Australian History:99.
Friedlander AM, Parrish JD (1998) Habitat characteristics affecting fish assemblages on a Hawaiian coral reef. J Exp Mar Bio Ecol 224:1–30.
Gabry J, Goodrich B (2020) Rstanarm: Bayesian Applied Regression Modelling via Stan.
Graham MH (2003) Confronting Multicollinearity in Ecological Multiple Regression. Ecology 84:2809–2815.
Gratwicke B, Speight MR (2005) The relationship between fish species richness, abundance and habitat complexity in a range of shallow tropical marine habitats. J Fish Biol 66:650–667.
Gray NJ (2010) Exploring the International Effort to Promote Marine Protected Areas. Conservation and Society 8:331–338.
Haberstroh AJ, McLean D, Holmes TH, Langlois T (in review) Baited video, but not diver video, detects a greater contrast in the abundance of legal-size target species between no-take zones and fished sites. Submitted to Mar Ecol Prog Ser.
Halpern BS, Regan HM, Possingham HP, McCarthy MA (2006) Accounting for uncertainty in marine reserve design. Ecol Lett 9:2–11; discussion 11–4.
Hanson CE, McKinnon AD (2009) Pelagic ecology of the Ningaloo region, Western Australia: influence of the Leeuwin Current. J R Soc West Aust 92:129.
Hayes KR, Hosack GR, Lawrence E, Hedge P, Barrett NS, Przeslawski R, Caley MJ, Foster SD (2019) Designing Monitoring Programs for Marine Protected Areas Within an Evidence Based Decision Making Paradigm. Frontiers in Marine Science 6:746.
Hill N, Barrett N, Ford J, Peel D, Foster S, Lawrence E, Monk J, Althaus F, Hayes K (2018) Developing indicators and a baseline for monitoring demersal fish in data-poor, offshore Marine Parks using probabilistic sampling. Ecol Indic 89:610–621.

Jackson JBC, Sala E (2001) Unnatural Oceans. Sci Mar 65:273–281.
Kellner JB, Tetreault I, Gaines SD, Nisbet RM (2007) Fishing the line near marine reserves in single and multispecies fisheries. Ecol Appl 17:1039–1054.
Kendall MS, Miller TJ, Pittman SJ (2011) Patterns of scale-dependency and the influence of map resolution on the seascape ecology of reef fish. Mar Ecol Prog Ser 427:259–274.
Langlois T, Goetze J, Bond T, Monk J, Abesamis RA, Asher J, Barrett N, Bernard ATF, Bouchet PJ, Birt MJ, Cappo M, Currey-Randall LM, Driessen D, Fairclough DV, Fullwood LAF, Gibbons BA, Harasti D, Heupel MR, Hicks J, Holmes TH, Huveneers C, Ierodiaconou D, Jordan A, Knott NA, Lindfield S, Malcolm HA, McLean D, Meekan M, Miller D, Mitchell PJ, Newman SJ, Radford B, Rolim FA, Saunders BJ, Stowar M, Smith ANH, Travers MJ, Wakefield CB, Whitmarsh SK, Williams J, Harvey ES (2020) A field and video annotation guide for baited remote underwater stereo-video surveys of demersal fish assemblages. Methods Ecol Evol 166:154.
Langlois TJ, Ballantine WJ (2005) Marine Ecological Research in New Zealand: Developing Predictive Models through the Study of No-Take Marine Reserves. Conserv Biol 19:1763–1770.
Lawrence E, Hayes KR, Lucieer VL, Nichol SL, Dambacher JM, Hill NA, Barrett N, Kool J, Siwabessy J (2015) Mapping Habitats and Developing Baselines in Offshore Marine Reserves with Little Prior Knowledge: A Critical Evaluation of a New Approach. PLoS One 10:e0141051.
Lingo ME, Szedlmayer ST (2006) The Influence of Habitat Complexity on Reef Fish Communities in the Northeastern Gulf of Mexico. Environ Biol Fishes 76:71–80.
Lynch TP (2006) Incorporation of recreational fishing effort into design of marine protected areas. Conserv Biol 20:1466–1476.
Lynch TP, Smallwood CB, Ochwada-Doyle FA, Lyle J, Williams J, Ryan KL, Devine C, Gibson B, Jordan A (2020) A cross continental scale comparison of Australian offshore recreational fisheries research and its applications to Marine Park and fisheries management. ICES J Mar Sci 77:1190–1205.
Marine Division - DSEWPC (2012) Completing the Commonwealth Marine Reserves Network: Regulatory Impact Statement. Department of Sustainability, Environment, Water, Population and Communities.
McLaren BW, Langlois TJ, Harvey ES, Shortland-Jones H, Stevens R (2015) A small no-take marine sanctuary provides consistent protection for small-bodied by-catch species, but not for large-bodied, high-risk species. J Exp Mar Bio Ecol 471:153–163.
McPhee D (2011) Marine Park Planning and Recreational Fishing: Is the Science Lost at Sea? Case Studies from Australia. The International Journal of Science and Society 2.
Mitchell JD, McLean DL, Collin SP, Taylor S, Jackson G, Fisher R, Langlois TJ (2018) Quantifying shark depredation in a recreational fishery in the Ningaloo Marine Park and Exmouth Gulf, Western Australia. Mar Ecol Prog Ser 587:141–157.
Monk J, Barrett NS, Hill NA, Lucieer VL, Nichol SL, Siwabessy PJW, Williams SB (2016) Outcropping reef ledges drive patterns of epibenthic assemblage diversity on cross-shelf habitats. Biodivers Conserv 25:485–502.
Monk J, Ierodiaconou D, Harvey E, Rattray A, Versace VL (2012) Are we predicting the actual or apparent distribution of temperate marine fishes? PLoS One 7:e34558.
Moore CH, Radford BT, Possingham HP, Heyward AJ, Stewart RR, Watts ME, Prescott J, Newman SJ, Harvey ES, Fisher R, Bryce CW, Lowe RJ, Berry O, Espinosa-Gayosso A, Sporer E, Saunders T (2016) Improving spatial prioritisation for remote marine regions:

optimising biodiversity conservation and sustainable development trade-offs. Sci Rep 6:32029.
Nichol SL, Anderson TJ, Battershill C, Brooke B (2012) Submerged Reefs and Aeolian Dunes as Inherited Habitats, Point Cloates, Carnarvon Shelf, Western Australia. In: Seafloor Geomorphology as Benthic Habitat. Harris P, Baker E (eds) Elsevier, Amsterdam, Netherlands, p 397–407
Ningaloo Coast: World Heritage nomination (2010) Department of the Environment, Water, Heritage and the Arts.
Parks Australia (2019) Australian Marine Parks. https://parksaustralia.gov.au/marine/parks/ (accessed 30 September 2019)
Perkins NR, Foster SD, Hill NA, Marzloff MP, Barrett NS (2017) Temporal and spatial variability in the cover of deep reef species: Implications for monitoring. Ecol Indic 77:337–347.
Phillips N (2017) Australia cuts conservation protections in marine parks. Nature.
Pittman SJ, Brown KA (2011) Multi-scale approach for predicting fish species distributions across coral reef seascapes. PLoS One 6:e20583.
Pittman SJ, Christensen JD, Caldow C, Menza C, Monaco ME (2007) Predictive mapping of fish species richness across shallow-water seascapes in the Caribbean. Ecol Modell 204:9–21.
R Core Team (2018) R: A language and environment for statistical computing. R Foundation for Statistical Computing, Vienna, Austria.
Rouphael AB, Abdulla A, Said Y (2011) A framework for practical and rigorous impact monitoring by field managers of marine protected areas. Environ Monit Assess 180:557–572.
Sagar S, Falkner I, Dekker AG, Huang Z, Przeslawski R (2020) Earth Observation for monitoring of Australian Marine Parks and other off-shore Marine Protected Areas. Geoscience Australia.
Scharf FS, Manderson JP, Fabrizio MC (2006) The effects of seafloor habitat complexity on survival of juvenile fishes: Species-specific interactions with structural refuge. J Exp Mar Bio Ecol 335:167–176.
Schönberg CHL, Fromont J (2012) Sponge gardens of Ningaloo Reef (Carnarvon Shelf, Western Australia) are biodiversity hotspots. Hydrobiologia 687:143–161.
Smallwood CB, Beckley LE, Moore SA, Kobryn HT (2011) Assessing patterns of recreational use in large marine parks: A case study from Ningaloo Marine Park, Australia. Ocean Coast Manag 54:330–340.
Strain EMA, Edgar GJ, Ceccarelli D, Stuart-Smith RD, Hosack GR, Thomson RJ (2019) A global assessment of the direct and indirect benefits of marine protected areas for coral reef conservation. Divers Distrib 25:9–20.
Stuart-Smith RD, Barrett NS, Crawford CM, Frusher SD, Stevenson DG, Edgar GJ (2008) Spatial patterns in impacts of fishing on temperate rocky reefs: Are fish abundance and mean size related to proximity to fisher access points? J Exp Mar Bio Ecol 365:116–125.
Turner JA, Babcock RC, Hovey R, Kendrick GA (2018) AUV-based classification of benthic communities of the Ningaloo shelf and mesophotic areas. Coral Reefs 37:763–778.
Underwood AJ (1995) Ecological Research and (and Research into) Environmental Management. Ecol Appl 5:232–247.
Underwood AJ (2000) Importance of experimental design in detecting and measuring stresses in marine populations. J Aquat Ecosyst Stress Recovery 7:3–24.
van de Schoot R, Kaplan D, Denissen J, Asendorpf JB, Neyer FJ, van Aken MAG (2014) A

gentle introduction to bayesian analysis: applications to developmental research. Child Dev 85:842–860.
Wedding LM, Friedlander AM, McGranaghan M, Yost RS, Monaco ME (2008) Using bathymetric lidar to define nearshore benthic habitat complexity: Implications for management of reef fish assemblages in Hawaii. Remote Sens Environ 112:4159–4165.
Wellington CM, Harvey ES, Wakefield CB, Langlois TJ, Williams A, White WT, Newman SJ (2018) Peak in biomass driven by larger-bodied meso-predators in demersal fish communities between shelf and slope habitats at the head of a submarine canyon in the south-eastern Indian Ocean. Cont Shelf Res 167:55–64.
Werner EE, Gilliam JF, Hall DJ, Mittelbach GG (1983) An Experimental Test of the Effects of Predation Risk on Habitat Use in Fish. Ecology 64:1540–1548.
Wescott G (2006) The long and winding road: The development of a comprehensive, adequate and representative system of highly protected marine protected areas in Victoria, Australia. Ocean Coast Manag 49:905–922.
Wickham H (2016) Ggplot2: Elegant Graphics for Data Analysis. Springer-Verlag, New York.
Wickham H, François R, L Henry, Müller K (2020) Dplyr: A Grammar of Data Manipulation.
Wilson MFJ, O'Connell B, Brown C, Guinan JC, Grehan AJ (2007) Multiscale Terrain Analysis of Multibeam Bathymetry Data for Habitat Mapping on the Continental Slope. Mar Geod 30:3–35.
Wilson SK, Fisher R, Pratchett MS, Graham NAJ, Dulvy NK, Turner RA, Cakacaka A, Polunin NVC (2010) Habitat degradation and fishing effects on the size structure of coral reef fish communities. Ecol Appl 20:442–451.
Wood SN (2011) Fast stable restricted maximum likelihood and marginal likelihood estimation of semiparametric generalized linear models. J R Stat Soc 73:3–36.
Xu J, Lowe RJ, Ivey GN, Jones NL, Brinkman R (2015) Observations of the shelf circulation dynamics along Ningaloo Reef, Western Australia during the austral spring and summer. Cont Shelf Res 95:54–73.
Young MAL, Foale S, Bellwood DR (2014) Impacts of recreational fishing in Australia: historical declines, self-regulation and evidence of an early warning system. Environ Conserv 41:350–356.

Supplementary Material One

Table 1. List of species classified as recreationally targeted within the Ningaloo Marine Park - Commonwealth.

Family	Genus	Species
Lethrinidae	*Gymnocranius*	*grandoculis*
Lethrinidae	*Lenthrinus*	*miniatus*
Lutjanidae	*Pristipomoides*	*filamentosus*
Scombridae	*Scomberomorus*	*commerson*
Lutjanidae	*Lutjanus*	*sebae*
Lethrinidae	*Gymnocranius*	*griseus*
Serranidae	*Epinephelus*	*rivulatus*
Serranidae	*Epinephelus*	*multinotatus*
Serranidae	*Variola*	*louti*
Carcharhinidae	*Loxodon*	*macrorhinus*
Lethrinidae	*Lethrinus*	*olivaceus*
Lutjanidae	*Symphorus*	*nematophorus*
Lethrinidae	*Lethrinus*	*nebulosus*
Carcharhinidae	*Carcharhinus*	*albimarginatus*
Lethrinidae	*Lethrinus*	*punctulatus*
Sparidae	*Chrysophrys*	*auratus*
Pomacanthidae	*Genicanthus*	*lamarck*
Lutjanidae	*Aprion*	*virescens*

33

Supplementary Material Two

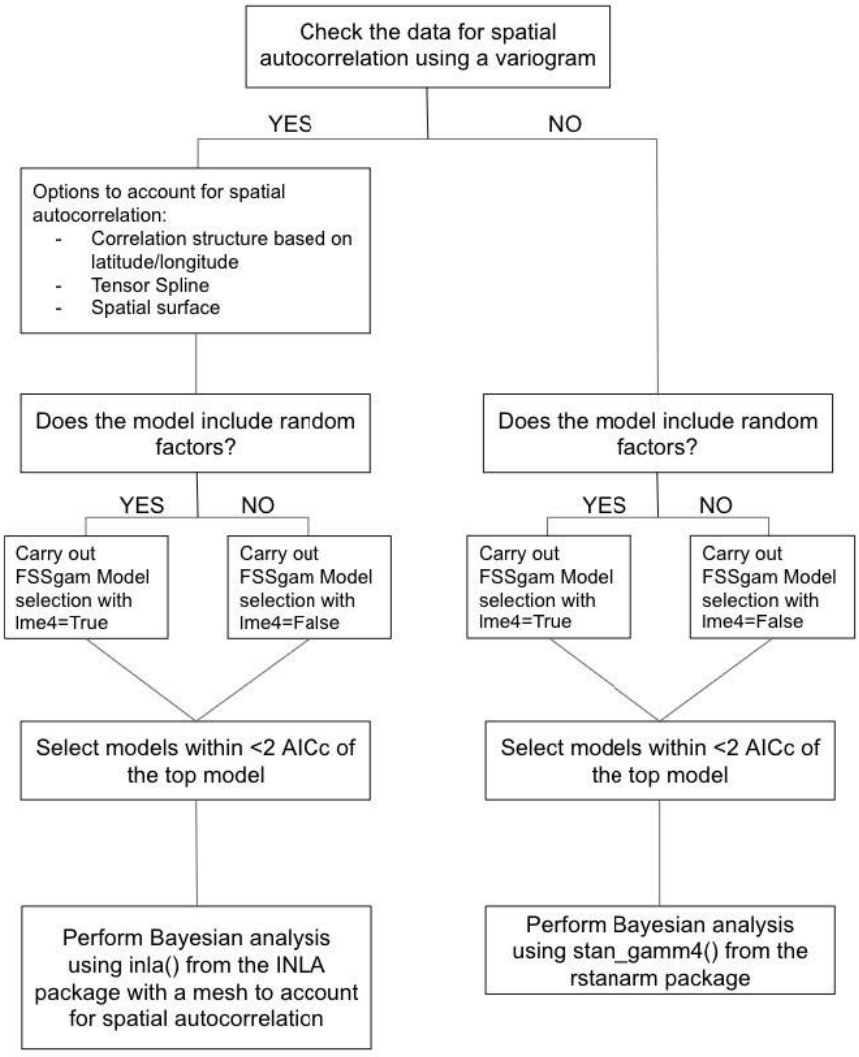

Figure 1. Workflow for model selection used in this study.

Supplementary Material Three

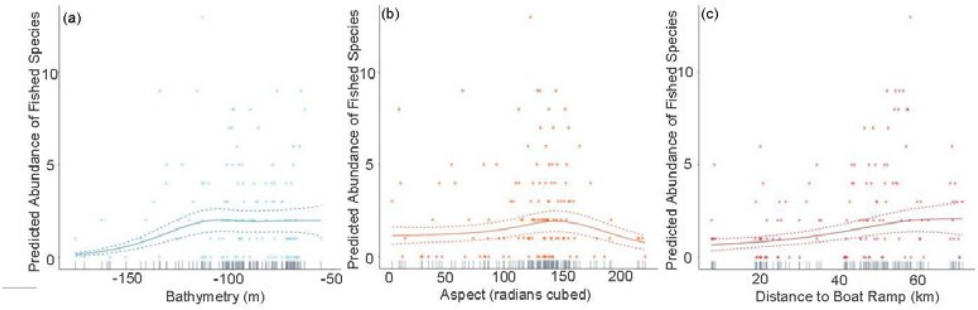

Figure 1. Predicted values from the top ranked frequentist generalised additive mixed effects model for fished species abundance when field of view variables were not included - (a) bathymetry (m), (b) aspect (radians cubed), (c) distance to boat ramp (km). The points represent the observed values, with the dashed lines representing the standard error of the prediction.

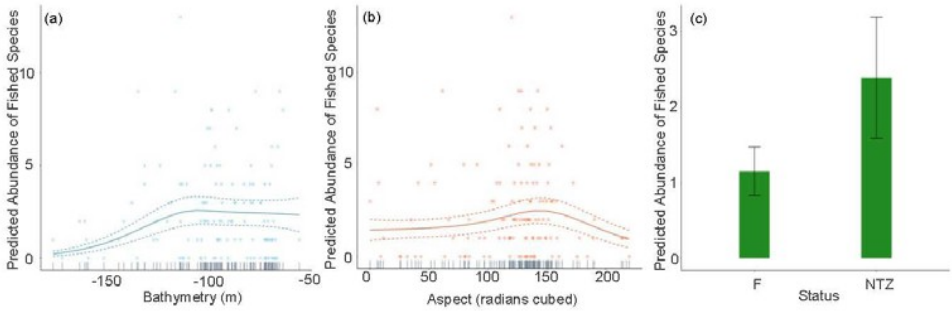

Figure 2. Predicted values from the second ranked frequentist generalised additive mixed effects model for fished species abundance when field of view variables were not included - (a) bathymetry (m), (b) aspect (radians cubed), (c) status. The points represent the observed values, with the dashed lines/error bars representing the standard error of the prediction.

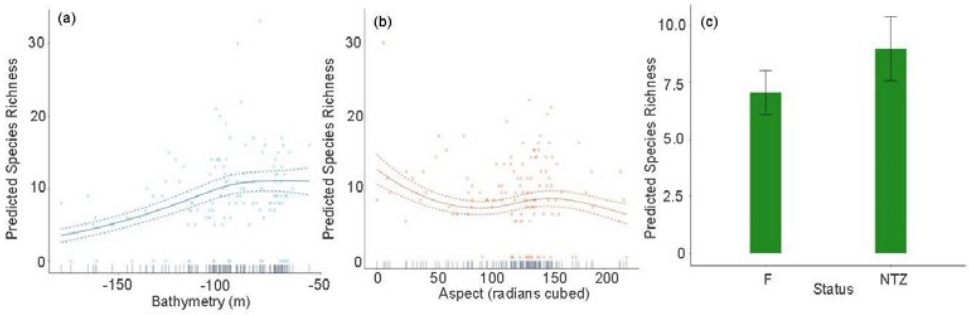

Figure 3. Predicted values from the top ranked frequentist generalised additive mixed effects model for species richness when field of view variables were not included - (a) bathymetry (m), (b) aspect (radians cubed), (c) status. The points represent the observed values, with the dashed lines representing the standard error of the prediction.

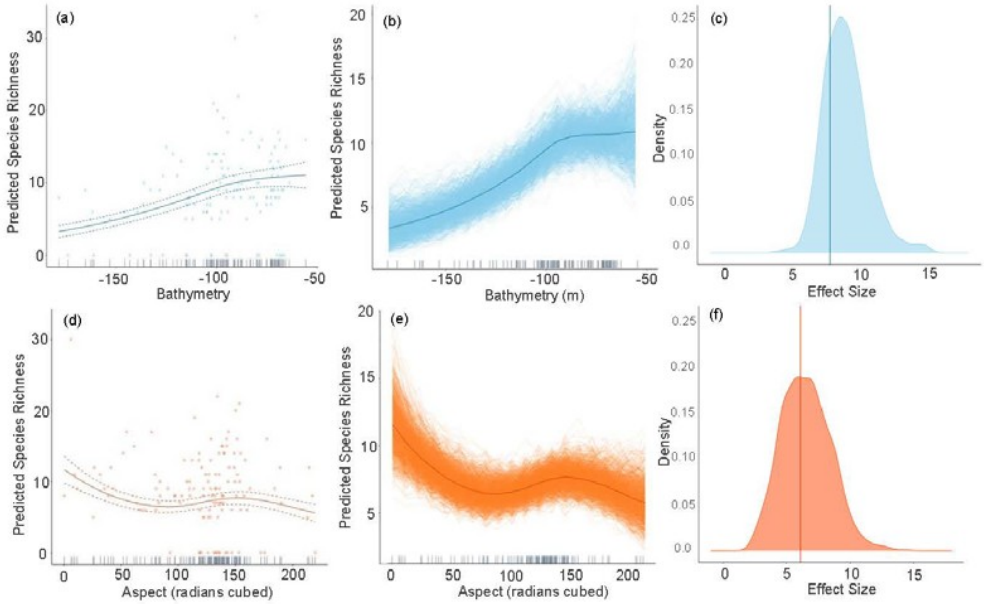

Figure 4. Predicted values from the second ranked frequentist generalised additive mixed effects model and Bayesian models for species richness when field of view variables were not included - (a) and (b) bathymetry (m), (d) and (e) aspect (radians cubed). Density plots of effect size are also plotted for each aforementioned predictor – (c) and (f) respectively – with a vertical line indicating the frequentist effect size estimate. Points on frequentist plots (a) and (d) indicate observed values and with dashed line representing standard error of the predictions.

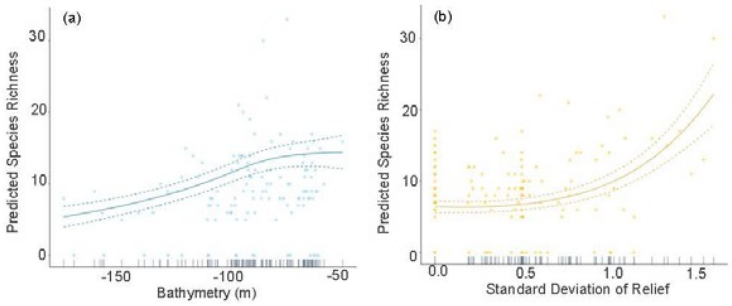

Figure 5. Predicted values from the top ranked frequentist generalised additive mixed effects model for species richness when field of view variables were included - (a) bathymetry (m), (b) standard deviation of relief. The points represent the observed values, with the dashed lines representing the standard error of the prediction.

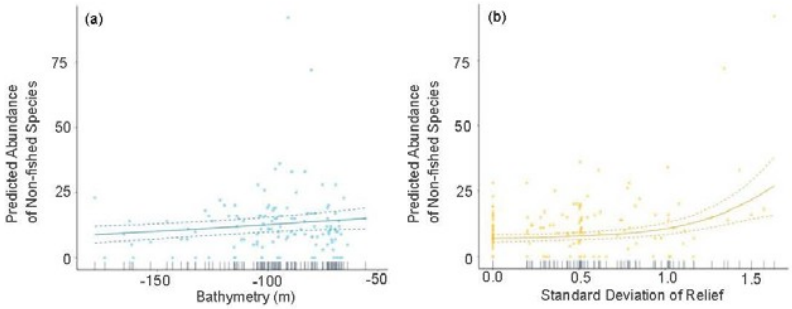

Figure 6. Predicted values from the top ranked frequentist generalised additive mixed effects model for non-fished species abundance when field of view variables were included - (a) bathymetry (m), (b) standard deviation of relief. The points represent the observed values, with the dashed lines representing the standard error of the prediction.

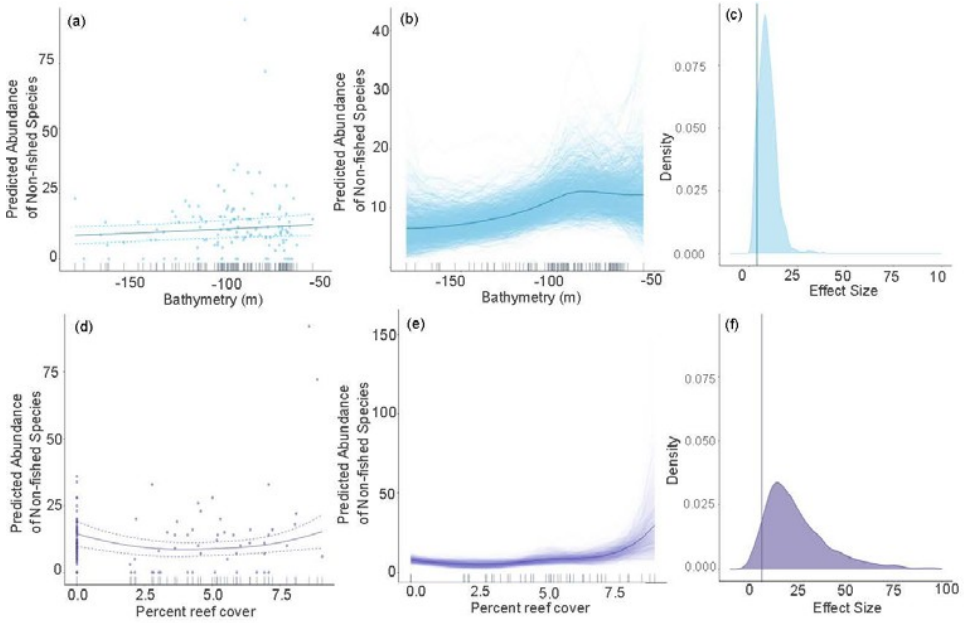

Figure 7. Predicted values from the second ranked frequentist generalised additive mixed effects model and Bayesian models for non-fished species abundance when field of view variables were included - (a) and (b) bathymetry (m), (d) and (e) percent reef cover (square root). Density plots of effect size are also plotted for each aforementioned predictor – (c) and (f) respectively – with a vertical line indicating the frequentist effect size estimate. Points on frequentist plots (a) and (d) indicate observed values and with dashed line representing standard error of the predictions.

Australian Government
Geoscience Australia

Australian Institute of Marine Science

Marine Biodiversity Hub
National Environmental Science Programme

CSIRO

IMOS
Integrated Marine Observing System

Charles Darwin University

University of Tasmania

NSW Government

The University of Western Australia

Museums Victoria

www.nespmarine.edu.au

Contact:
John Keesing
CSIRO

Address | Indian Ocean Marine Research Centre, 64 Fairway, Crawley WA 6009
email | john.keesing@csiro.au
tel | +61 8 9333 6500